

**A biodegradable system for the tailored
delivery of growth factors and its application
to bone morphogenetic protein-2 delivery for
bone repair**

Helen C. Cox, BSc.

Tissue Engineering Group

School of Pharmacy, University of Nottingham

Thesis submitted to the University of Nottingham for the
Degree of Doctor of Philosophy

August 2013



The University of
Nottingham

UNITED KINGDOM • CHINA • MALAYSIA

Abstract

The repair of bone defects and fracture non-unions remain a substantial challenge for clinicians. The current materials used to treat these injuries have limitations with regard to quality, availability and there are also long-term complications associated with them. This has resulted in research efforts to identify alternative graft materials that are able to aid tissue regeneration. Many of these tissue engineered materials include the use of growth factors to induce cell migration, proliferation, differentiation and matrix production. However, current delivery methods are limited by poor retention of growth factors upon implantation due to short plasma half lives resulting in low bioactivity. These limiting factors have lead to the clinical use of high doses and/or frequent injections, putting the patient at risk of adverse effects.

The aim of the work presented in this thesis was to develop and evaluate a controlled bone morphogenetic protein-2 (BMP-2) delivery system based on poly(lactide-co-glycolide) (PLGA) that would improve current therapies by controlling the dose and the localisation of BMP-2 at the treatment site as well as providing biodegradable scaffold to support the newly formed tissue.

Reproducible procedures were developed to manufacture spherical PLGA microparticles of defined sizes within a 1-100 μm range by a double emulsion, solvent evaporation method. Lysozyme was used as model protein for the growth factor BMP-2 and it was successfully encapsulated within the microparticles. The entrapment efficiency positively correlated with microparticle size with the largest microparticles regularly achieving greater than 70% entrapment efficiency. The optimal total protein loading was 1% _(w/w) and as loading increased, the entrapment efficiency decreased.

Lysozyme released from PLGA microparticles retained its activity *in-vitro*. The rate of release was manipulated by the novel use of a PLGA-polyethylene glycol-PLGA triblock copolymer added at the point of microparticle manufacture to achieve a number of distinctly different but reproducible cumulative release curves. The common problem of tri-phasic release from PLGA systems was overcome and the rate of release was accelerated over the rate of polymer degradation.

The release profiles achieved were applicable to the delivery of different growth factors to mimic *in-vivo* kinetics. A sustained release profile over a one month period was chosen for translation to recombinant human BMP-2 (rhBMP-2) delivery and the growth factor was shown to remain active throughout its incorporation into the microparticles and after its subsequent release. *In-vitro* studies demonstrated that released rhBMP-2 could up regulate alkaline phosphatase expression in murine C2C12 myoblast cells and human mesenchymal stem cells, as well as causing murine primary calvarial cells to produce a mineralised matrix. The rhBMP-2 loaded microparticles were used in an *ex-vivo* embryonic chick femur model of bone repair and caused localised ossification by chondrogenic cells in the epiphysis as determined by positive picosirius red staining.

The results presented in this thesis build on published data regarding PLGA delivery systems for growth factors by demonstrating a robust, novel method of tailoring their release. Work was focussed on rhBMP-2 but it is feasible that the technology could be transferred to different growth factors. These microparticles would therefore be valuable tools not only in pre-clinical studies of bone repair but could also be applied to the regeneration of other tissues.

Declaration

Name: Helen Cox

Student number: 4113921

Registration: 01-Feb-2010 to 30-Sep-2013 (includes thesis pending period)

Initial submission: March 2013

Viva voce examination: May 2013

Final submission: August 2013

DECLARATION:

I declare that this thesis is the result of my own work except where indicated by referencing and acknowledgements and has been mainly undertaken during my period of registration for the degree of Doctor of Philosophy at the University of Nottingham.

Signed:

Date:

Acknowledgements

First and foremost I would like to thank my husband Stuart, my daughter Alison and my son James for giving me the support and freedom to complete this PhD project.

I would like to thank Professor Kevin Shakesheff for giving me the idea, the inspiration and motivation to embark on this period of study and Dr Felicity Rose for her helpful and insightful input throughout.

I have appreciated the respect and encouragement that I have received from the members of the Tissue Engineering group in Nottingham. In particular, I would like to thank Dr Lisa White for being a mentor during the first phase and Dr Hassan Rashidi providing training during the second phase of the project.

I would like to acknowledge Dr Yvonne Reinwald, Dr Roozbeh Qodratnama and Dr Omar Qutachi for their invaluable help and advice. As fellow students, I would like to thank Mike Sawkins and Giles Kirby for being excellent travelling companions to national and international conferences.

The project was both self funded and formed part of a Biotechnology and Biological Sciences Research Council grant (BB/G010617/1).

The last three years have been challenging, frustrating, enjoyable and satisfying. I'm sure if my parents were still alive, they would have been proud.

“Education is the best provision for old age”

(Aristotle)

Publications (2011-2013)

“PLGA-based microparticles for the sustained release of BMP-2”

GTS Kirby, LJ White, CV Rahman, HC Cox, O Qutachi, FRAJ Rose, DW Hutmacher, KM Shakesheff and MA Woodruff. *Polymers* 2011, 3, 571-586

*“Biofilm eradication with biodegradable modified-release antibiotic pellets
A potential treatment for glue ear”*

M Daniel, R Chessman, S Al-Zahid, B Richards, CV Rahman, W Ashraf, JS McLaren, HC Cox, O Qutachi, H Fortnum, N Fergie, K Shakesheff, JP Birchall and RR Bayston. *Arch Otolaryngol Head Neck Surgery* 2012, 138 (10) 942-9

“PLGA/PEG-hydrogel composite scaffolds with controllable mechanical properties”

CV Rahman, G Kuhn, LJ White, GTS Kirby, OP Varghese, JS McLaren, HC Cox, FRAJ Rose, R Muller, J Hilborn and KM Shakesheff. *J Biomedical Materials Research Part B* 2013, 101 (4) 648-55

“Accelerating protein release from microparticles for regenerative medicine applications”

LJ White, GTS Kirby, HC Cox, R Qodratnama, O Qutachi, FRA J. Rose, KM Shakesheff *Materials Science and Engineering* 2013, 33 (5) 2578-83

“A biodegradable antibiotic-impregnated scaffold to prevent osteomyelitis and encourage new bone growth”

JS McLaren, KM Shakesheff, R Bayston, RA Quirk, LJ White, HC. Cox, CV Rahman, GW Blunn, AE Goodship and BE Scammell.

E Cell Materials Journal: in review

Selected poster presentations (2011-2012)

“Temporal control of model protein release from biodegradable microspheres”

HC Cox, LJ White, GTS Kirby, R Qodratnama, O Qutachi, FRAJ Rose and KM Shakesheff

Presented at the United Kingdom and Ireland Controlled Release Society (UKICRS) annual symposium 2011 Queens University, Belfast, Northern Ireland.

“A novel injectable scaffold for bone repair applications”

HC Cox, AS Dhillon, LG Hamilton, JS McLaren, CV Rahman, RA Quirk, AE Goodship, FRAJ Rose, KM Shakesheff.

Presented at the Tissue Engineering and Regenerative Medicine International Society North American conference (TERMIS-NA) 2011 Houston, Texas, USA

“Sustained delivery of active BMP-2 from PLGA microspheres for bone regeneration applications”

HC Cox, LJ White, Y Reinwald, GTS Kirby, FRAJ Rose and KM Shakesheff
Presented at the United Kingdom and Ireland Controlled Release Society (UKICRS) annual symposium 2012 Aston University, Birmingham, England

“Sustained delivery of active rhBMP-2 for bone regeneration applications”

HC Cox, H Rashidi, LJ White, Y Reinwald, GTS Kirby, FRAJ Rose and KM Shakesheff

Presented at the Academy of Pharmaceutical Sciences (APS Pharmsci) annual conference. 2012 East Midlands Conference Centre, Nottingham, England. Commended and received poster award

Table of contents

Abstract	II
Declaration	IV
Acknowledgements	V
Publications and presentations	VI
Table of contents	VIII
List of figures	XV
List of tables	XXII
Abbreviations	XXIII

Chapter 1: Introduction to the field of regenerative medicine and bone tissue engineering

	1
1.1 The growth of regenerative medicine and tissue engineering	1
1.2 Orthopaedic applications for regenerative medicine	3
1.3 Structure and natural growth of bone	4
1.3.1 Bone structure	4
1.3.2 Bone development, growth and remodelling	6
1.3.3 Normal bone repair	9
1.3.4 Problems with bone repair mechanisms	11
1.4 Biomaterials for orthopaedic regenerative applications	12
1.4.1 Inorganic materials	12
1.4.2 Organic materials	15
1.4.3 Synthetic polymers	18
1.4.3.1 Poly (alpha hydroxy acid) polymers	21
1.5 Parameters to control PLGA degradation	22
1.6 Fabrication of polymeric MPs and scaffolds as delivery devices	23
1.6.1 Fabrication techniques without organic solvents	24
1.6.2 Fabrication techniques with organic solvents	24

1.7	Emulsion techniques for PLGA MP manufacture	25
	1.7.1 The principle of emulsion formation	25
	1.7.2 MP manufacture by emulsion and solvent evaporation	26
1.8	Injectable and non-injectable systems	29
1.9	Surface modifications to improve cell attachment	30
1.10	Model protein and growth factors	30
	1.10.1 Model proteins	30
	1.10.2 Growth factors	31
	1.10.2.1 The BMP-2 signalling pathway	32
1.11	Release kinetics	35
	1.11.1 Cumulative release profiles	35
	1.11.2 Reducing burst and creating a sustained release profile	38
1.12	Determining the efficacy of microparticulate delivery systems by <i>in-vitro</i> , <i>ex-vivo</i> and <i>in-vivo</i> models of bone regeneration	39
1.13	Summary of introduction and future aims	41

Chapter 2: Development of techniques to fabricate protein loaded

PLGA microparticles with control over size, morphology and entrapment efficiency

2.1	Introduction	43
2.2	Materials and methods	47
	2.2.1 Equipment, consumables and materials	47
	2.2.2 Micronisation of lysozyme and HSA with PEG6000	48
	2.2.3 Preparation of lysozyme in HSA	49
	2.2.4 MP manufacture	49
	2.2.4.1 Solid in oil in water emulsion method (S/O/W)	49
	2.2.4.2 Water in oil in water emulsion method (W/O/W)	50
	2.2.4.3 Oil in water emulsion method (O/W)	51

2.2.5	MP sizing: Laser diffraction	54
2.2.6	MP imaging: Scanning electron microscopy	54
2.2.7	PLGA degradation studies	55
	2.2.7.1 pH study	55
	2.2.7.2 Mass loss study:	55
	2.2.7.3 Morphology study:	56
2.2.8	Total protein detection: Bicinchoninic acid (BCA) assay	56
	2.2.8.1 Measurement of entrapment efficiency	56
2.2.9	Lysozyme activity: <i>Micrococcus lysodeikticus</i> assay	57
2.2.10	Statistical analysis	58
2.3	Results and Discussion	59
2.3.1	Control of MP size	59
2.3.2	MP morphology	74
2.3.3	PLGA degradation	78
	2.3.3.1 Measurement of pH	78
	2.3.3.2 Measurement of mass loss	79
	2.3.3.3 Changes in MP morphology	82
2.3.4	Optimisation of total protein and lysozyme assays	84
	2.3.4.1 The bincinchoninic acid assay	84
	2.3.4.2 The <i>Micrococcus lysodeikticus</i> assay	86
2.3.5	Entrapment efficiency of HSA/lysozyme in PLGA MPs	89
	2.3.5.1 Solid in oil in water emulsion (S/O/W)	89
	2.3.5.2 Water in oil in water emulsion (W/O/W)	91
2.4	Conclusions	95

Chapter 3: Control of protein delivery from PLGA MPs by the novel use of a triblock copolymer to uncouple protein release from polymer degradation	96
3.1 Introduction	96
3.2 Materials and Methods	101
3.2.1 Preparation and characterisation of PLGA-PEG-PLGA triblock copolymer	101
3.2.2 MP manufacture incorporating PLGA-PEG-PLGA triblock copolymer	103
3.2.3 Manufacture of self assembling thermo-sensitive scaffolds directly loaded with lysozyme by hot melt fabrication	103
3.2.4 Determination of glass transition temperature of polymers by rheology	106
3.2.5 Degradation of PLGA ± triblock copolymer through mass loss	106
3.2.6 Protein release studies	107
3.2.6.1 Release of HSA/lysozyme from MPs	107
3.2.6.2 Release of lysozyme from PLGA/PEG scaffolds	108
3.2.7 Detection of lysozyme activity: <i>M lysodeiktus</i> assay	110
3.2.8 Statistical analysis	110
3.3 Results and Discussion	111
3.3.1 Characterisation of PLGA-PEG-PLGA triblock copolymer	111
3.3.2 The effect of PLGA-PEG-PLGA triblock copolymer on the viscoelastic properties of PLGA	112
3.3.3 The effect of PLGA-PEG-PLGA triblock copolymer on the degradation rate of PLGA	118
3.3.4 HSA/lysozyme release from PLGA MPs	120

3.3.4.1	Effect of PLGA-PEG-PLGA triblock copolymer content on protein release from MPs fabricated with PLGA 50 50 and PLGA 85 15	120
3.3.4.2	Reproducibility of release profiles	131
3.3.4.3	The influence of MP size on protein release profile	138
3.3.5	Lysozyme release from thermosensitive PLGA/PEG scaffolds	140
3.3.6	Detection of lysozyme activity in release supernatants	143
3.3.7	Lowering total protein loading improves short term release profiles from sub 30 micron PLGA MPs	147
3.4	Conclusions	150

Chapter 4:	Tailored release of biologically active rhBMP-2 from biodegradable microparticles	152
4.1	Introduction	152
4.2	Materials and Methods	156
4.2.1	Reconstitution of rhBMP-2, addition of HSA and storage	156
4.2.2	Manufacture of HSA/rhBMP-2 loaded PLGA MPs formulated with PLGA-PEG-PLGA triblock copolymer	157
4.2.3	Incorporating HSA/rhBMP-2 loaded MPs into PLGA/PEG thermosensitive scaffolds	158
4.2.4	Release assays	158
4.2.4.1	Indirect release assays (supernatant collection)	158
4.2.4.2	Direct release (co-culture)	159
4.2.5	Detection of rhBMP-2 in release supernatants by ELISA	161
4.2.6	Culture of C2C12 myoblasts and immortalised human mesenchymal stem cells	161

4.2.7	Measurement of rhBMP-2 in release supernatants by alkaline phosphatase expression in C2C12 myoblasts and immortalised human mesenchymal stem cells	162
4.2.8	Co-culture of HSA/rhBMP-2 loaded MPs with C2C12 cells as a method for detecting rhBMP-2 activity and measuring rhBMP-2 release	163
4.2.9	Von Kossa staining to detect mineralisation <i>in-vitro</i>	164
4.2.10	Imaging of cells, cells with MPs and scaffolds	165
4.3	Results and Discussion	166
4.3.1	Comparison of model protein and growth factor release	166
4.3.2	Effect of PLGA-PEG-PLGA triblock copolymer and MP mass on rate of protein release from PLGA MPs	169
4.3.3	Incorporation of HSA/rhBMP-2 loaded PLGA MPs with thermosensitive scaffolds and the effect on release	173
4.3.4	Detection of rhBMP-2 and rhBMP-2 activity in release supernatants	176
	4.3.4.1 rhBMP-2 detection: ELISA	176
	4.3.4.2 rhBMP-2 activity: Alkaline phosphatase assay	178
4.3.5	ALP expression by human mesenchymal stem cells	183
4.3.6	Direct effect of rhBMP-2 loaded MPs on C2C12 cells	185
4.3.7	Sustained rhBMP-2 release determined by direct co-culture of HSA.rhBMP-s loaded MPs with C2C12 cells	189
4.3.8	Von Kossa staining for calcium deposits	192
4.4	Conclusions	195

Chapter 5: The development of an ex-ovo chick femur as a model		
to investigate the effects of rhBMP-2 loaded		
microparticles on bone regeneration and repair		196
5.1	Introduction	196
5.2	Materials and Methods	201
5.2.1	Dissection of embryonic chick femur	201
5.2.2	Creating critical sized defect in diaphysis and epiphysis.	203
5.2.2.1	Wedge defects	203
5.2.2.2	Drill defects	203
5.2.2.3	Non-union defects	203
5.2.3	Filling defects with HSA/rhBMP-2 loaded MPs	204
5.2.3.1	Defect filling using femtojet injector	204
5.2.3.2	Defect filling using microspatulas	204
5.2.4	Filling the non-union defect with mesenchymal stem cells in alginate	204
5.2.5	Organotypic culture of chick femurs	205
5.2.6	Tissue processing and sectioning	205
5.2.7	Histological staining: picosirius red and alcian blue	206
5.3	Results and Discussion	206
5.3.1	Normal chick femur growth	206
5.3.2	Chick femur growth during organotypic culture	212
5.3.3	Critical sized defects in chick femur	215
5.3.3.1	Wedge defects	215
5.3.3.2	Drill defects	217
5.3.3.3	Non-union defects	222
5.3.4	Filling the defects with MPs	225
5.3.4.1	Injection method	225
5.3.4.2	Microspatula method	227

5.3.4.3	Filling the non-union defect	231
5.3.5	Potential pitfalls in histological analysis	233
5.3.6	Effect of rhBMP-2 loaded MPs on chick femur growth and repair	235
5.4	Conclusions	241
Chapter 6: Summary and future direction		243
Chapter 7: References		248
Appendices:		266
Appendix I:	Equipment, consumables and materials	266
Appendix II:	Microparticle batch manufacturing record	272
Appendix III:	Reagents tissue processing histological staining	276
Appendix IV:	Optimisation of MP size analysis (Coulter L5M)	277
Appendix V:	GPC and NMR data for triblock copolymers	279
List of Figures:		
Chapter 1		
Figure 1.1	Schematic of long bone showing the structure of both cortical and cancellous bone	5
Figure 1.2	Bone remodelling by the action of osteoblasts and osteoclasts	7
Figure 1.3	Schematic showing main processes during endochondral ossification	9
Figure 1.4	Schematic showing normal bone fracture repair	11
Figure 1.5	Synthesis of poly(lactic-co-glycolic acid) (PLGA)	21
Figure 1.6	Principle of oil in water emulsion	26

Figure 1.7	Schematic showing the water-in-oil-in-water emulsion method of polymer MP manufacture	28
Figure 1.8	The main components of the smad signalling pathways and role of BMP-2 in osteogenesis	34
Figure1.9	Typical cumulative release traces	37
 Chapter 2		
Figure 2.1	Representative MP size distribution from previous work	45
Figure 2.2	Schematic showing [A] the solid in oil in water (S/O/W) and [B] the water in oil in water (W/O/W) emulsion method for PLGA MP manufacture	53
Figure 2.3	MP size distribution comparing manufacture by vortex mixer and manufacture by homogeniser	61
Figure 2.4	Optimisation of MP manufacture process comparing homogeniser speed, rotor height and time	63
Figure 2.5	MP size distribution comparing the S/O/W method of manufacture with the W/O/W method of manufacture	65
Figure 2.6	Control of MP size based on PLGA concentration	67
Figure 2.7	Comparison of PLGA 85 15 MPs collected by centrifugation or filtration	70
Figure 2.8	Size distribution traces for nine batches of PLGA 50 50 MPs made under three different conditions	72
Figure 2.9	SEM comparing PLGA MPs manufactured by the W/O/W and the S/O/W emulsion method	76
Figure 2.10	SEM images of PLGA MPs fabricated in three different size ranges	77

Figure 2.11	Comparison of pH values over time for PLGA 85 15 and PLGA 50 50 both formulated with 30% (w/w) PLGA-PEG-PLGA triblock copolymer and incubated at 37°C in PBS	80
Figure 2.12	Mass loss of PLGA 50 50 MPs through degradation at 37°C and at 45°C after incubation at 37°C in PBS	81
Figure 2.13	SEM of PLGA 50 50 MPs with 10% (w/w) PLGA-PEG-PLGA triblock copolymer after incubation at 37°C in PBS for [A] 0 days, [B] 9 days, [C] 14 days, [D] 20 days, [E] 28 days and [F] 36 days	83
Figure 2.14	The bicinchoninic acid assay standard curve at a pH range of 2 to 12 to determine the effect of pH on the assay	85
Figure 2.15	The <i>Micrococcus lysodeikticus</i> assay standard curve at a pH range of 2 to 12 to determine the effect of pH on the assay	87
Figure 2.16	Typical standard curves for [A] bicinchoninic acid assay and [B] <i>Micrococcus lysodeikticus</i> assay in PBS at pH 7.4	88
Figure 2.17	Effect of HSA/lysozyme loading on the entrapment efficiency of using the W/O/W emulsion method and a comparison of the entrapment efficiency a 5% (w/w) protein loading using the S/O/W method of manufacture	92
Figure 2.18	The relationship between MP size and entrapment efficiency using the W/O/W method of MP manufacture	94
 Chapter 3		
Figure 3.1	Schematic of in-situ setting of thermosensitive MPs	100
Figure 3.2	Manufacture of PLGA/PEG temperature sensitive MPs	105
Figure 3.3	Schematic of MPs tested in release studies 1 and 2	109

Figure 3.4	Rheological traces of 50 50 PLGA MPs with [A] 0%, [B] 10% and [C] 30% _(w/w) PLGA-PEG-PLGA triblock [D] Glass transition temperature of the polymers	116
Figure 3.5	Rheological traces of 85 15 PLGA MPs with [A] 0%, [B] 10% and [C] 30% _(w/w) PLGA-PEG-PLGA triblock [D] Glass transition temperature of the polymers	117
Figure 3.6	Mass loss of PLGA 50 50 in PBS through degradation at 37°C and 45°C. MPs formulated with 0%, 10%, 20%, and 30% _(w/w) PLGA-PEG-PLGA triblock copolymer	119
Figure 3.7	Effect on morphology of the incorporation of PLGA-PEG-PLGA triblock copolymer into PLGA MPs	122
Figure 3.8	Cumulative release of HSA/lysozyme (1% _(w/w) loading) from PLGA 50 50 MPs (50-100 µm) formulated with 30%, 10% or 0% _(w/w) PLGA-PEG-PLGA triblock copolymer	126
Figure 3.9	Comparison of cumulative protein release from PLGA 50 50 and PLGA 85 15 MPs (50-100 µm) loaded with 1% HSA/lysozyme and formulated with 10% and 30% _(w/w) PLGA/PEG/PLGA triblock copolymer	128
Figure 3.10	Summary of release profiles achieved in study 1 the effect of PLGA-PEG-PLGA concentration and L:G ratio	129
Figure 3.11	Reproducibility of cumulative protein release profiles	133
Figure 3.12	Comparison of protein release from study 1 and study 2	134
Figure 3.13	Individual cumulative protein release profiles from PLGA 50 50 MPs with either 10 % or 30% _(w/w) PLGA-PEG- PLGA as well as a 1:1 mix of both batches	137
Figure 3.14	Cumulative protein released from different sizes of PLGA 50 50 MPs loaded with 1% _(w/w) HSA/lysozyme with no PLGA-PEG-PLGA triblock modification	139

Figure 3.15	[A] Total protein release of lysozyme from PLGA/PEG scaffold. [B] Typical PLGA/PEG scaffold [C] SEM showing surface of scaffold prior to start of study [D] SEM showing surface of scaffold after 56 days in PBS [E] SEM showing the interior of a scaffold after 56 days in PBS	142
Figure 3.16	Lysozyme activity released from PLGA 50 50 and 85 15 MPs with a range of PLGA-PEG-PLGA Concentrations	145
Figure 3.17	Activity of lysozyme from PLGA/PEG scaffolds	146
Figure 3.18	Cumulative total protein release profiles from 1-5 μm , 20-30 μm PLGA 50 50 MPs with three protein loadings	149
 Chapter 4		
Figure 4.1	The main signalling molecules in the transforming growth factor beta super family	153
Figure 4.2	Schematic for release study of HSA/rhBMP-2 from PLGA MPs by direct co-culture with C2C12 cells	160
Figure 4.3	Release profiles from [A] 100 mg of 50 -100 μm MPs and [B] 50 mg of 20 – 30 μm MPs comparing HSA/rhBMP2 and HSA/lysozyme	168
Figure 4.4	Cumulative total protein released from HSA/rhBMP-2 loaded 20 -30 μm PLGA 50 50 MPs with 10% or 30% _(w/w) PLGA-PEG-PEG triblock under two conditions.	170
Figure 4.5	Release from 50 mg HSA/bmp-2 loaded PLGA 50 50 MPs incorporated in a PLGA 85 15/6.5% _(w/w) PEG400 scaffold compared to release from 50 mg HSA/bmp-2 loaded MPs alone. Imaging of MPs and scaffold	175

Figure 4.6	Detection of rh-BMP-2 by ELISA from PLGA 50 50 MPs formulated with 30% _(w/w) TB loaded with 1% HSA/rhBMP-2 over 40 days	177
Figure 4.7	Dose dependent response of rhBMP-2 on morphology and alkaline phosphatase expression by C2C12 cells	180
Figure 4.8	Release from PLGA MPs with HSA/rhBMP-2 and 10% _(w/w) PLGA-PEG-PLGA triblock copolymer	182
Figure 4.9	rhBMP-2 activity measured by ALP expression in Immortalised huMSCs compared to C2C12 cells	184
Figure 4.10	Co-Culture of C2C12 cells with blank PLGA 50 50 MPs and HSA/rhBMP-2 loaded PLGA 50 50 MPs	186
Figure 4.11	Effect of HSA/rhBMP-2 loaded PLGA 50 50 10% _(w/w) PLGA-PEG-PLGA MPs on ALP expression in C2C12 cells	187
Figure 4.12	Effect of C2C12 cell number when cultured with 2 mg of HSA/rhBMP-2 loaded PLGA 50 50 MPs	188
Figure 4.13	Morphology of C2C12 cells after 5 days of culture with and without PLGA MPs loaded with 1% HSA/rhBMP-2 having pre-released their protein for 1 to 12 days	191
Figure 4.14	Von Kossa staining for mineralisation	194
 Chapter 5		
Figure 5.1	Normal chick development during the gestational period	200
Figure 5.2	Schematic showing the technique to dissect femurs from 11 day chick embryos	202
Figure 5.3	Chick embryo after 12 days of incubation at 37°C	207
Figure 5.4	Images of chick femurs dissected each day between days 8 and day 15 of incubation at 37°C	210

Figure 5.5	Alcian blue and picosirius red staining of embryonic chick femurs after days 8 to 15 days of incubation at 37°C	211
Figure 5.6	Growth of a chick femur over a 10 day organotypic culture period and effect of poor handling	214
Figure 5.7	Wedge defects, bone collar off and partially intact	216
Figure 5.8	Drill defects in diaphysis	219
Figure 5.9	Diaphyseal defects and staining of the same femurs after 10 days of organotypic culture	220
Figure 5.10	Epiphyseal defects and staining of the same femurs after 10 days of organotypic culture	221
Figure 5.11	Non union defect model day 1 and day 10	223
Figure 5.12	Alcian blue/picosirius red staining of the non union defect model after 10 days of organotypic culture	224
Figure 5.13	Injection of blank PLGA MPs into day 11 diaphyseal drill defects	226
Figure 5.14	MPs applied to the defect by microspatula	228
Figure 5.15	Cross sections through drill defect filled with blank PLGA MPs using a microspatula.	230
Figure 5.16	Non-union defect in a day 11 ex-ovo chick femur filled with mesenchymal stem cells seeded in alginate	232
Figure 5.17	Representation showing how identical shapes can give different results due to their orientation.	234
Figure 5.18	The effect of filling PLGA MPs into a diaphyseal drill defect in a day 11 embryonic chick femur	236
Figure 5.19	The effect of filling PLGA MPs into an epiphyseal drill defect in a day 11 embryonic chick femur	239
Figure 6.20	A drill defect was made prior to culture and filled with rhBMP-2 loaded PLGA MPs	240

List of Tables

Chapter 2

Table 2.1	Complete range of achievable MPs sizes using the W/O/W emulsion method of manufacture and Silverson homogeniser	73
Table 2.2	Effect of solvent evaporation time on the entrapment Efficiency of lysozyme ± human serum albumin in PLGA microspheres using the S/O/W emulsion method	90

Chapter 3

Table 3.1	Table of PLGA-PEG-PLGA triblock copolymer parameters	112
Table 3.2	Average size distribution of PLGA microparticles formulated with PLGA-PEG-PLGA triblock copolymer (TBII-B)	124
Table 3.3	Entrapment efficiency of PLGA microparticles formulated with PLGA-PEG-PLGA triblock copolymer (TBII-B)	124

Chapter 4

Table 4.1	Estimated average daily release of rhBMP-2 (ng) calculated from total protein release curves	172
Table 4.2	ALP expression by C2C12 cells after incubation HSA/rhBMP-2 MPs that had pre-released their protein for different time periods	192

List of abbreviations

ALP	alkaline phosphatase
ATCC	American type culture collection
BBSRC	biotechnology and biological sciences research council
BCA	bicinchoninic acid
BSA	bovine serum albumin
CAM	chorioallantoic membrane
CMC	carboxymethylcellulose
CPC	calcium based phosphate cements
DCM	dichloromethane
DMEM	Dulbecco's modification of Eagle's medium
DMSO	dimethyl sulphoxide
EDTA	ethylenediamine tetra acetic acid
EGF	epidermal growth factor
ELISA	enzyme linked immunosorbent assay
FCS	foetal calf serum
FDA	food and drug administration
FGF	fibroblast growth factor
g	gram
G'	storage modulus
G''	loss modulus
GDNF	glial derived neurotrophic factor
GPC	gel permeation chromatography
Hz	Hertz
HIF2- α	hypoxia inducible factor 2 alpha
HSA	human serum albumin
huMSC	human mesenchymal stem cells
IGF 1/2	insulin-like growth factor 1/2
IMS	Industrial methylated spirits
kDa	kilodalton
L:G	lactide:glycolide ratio
mg	milligram
mL	millilitre
mM	millimolar
MP	microparticle
mPCCs	mouse primary calvarial cells

Mwt	molecular weight
nm	nanometer
O/W	oil in water emulsion
PBS	phosphate buffered saline
PDGF	platelet derived growth factor
PEG	polyethylene glycol
pH	measurement of acidity/alkalinity
PLGA	poly(lactide-co-glycolide)
pNPP	para nitrophenyl phosphate
pNP	Para nitrophenol
PTFE	polytetrafluoroethylene
PVA	polyvinyl alcohol
RGD	arginine-glycine-aspartine
rhBMP-2	recombinant human bone morphogenetic protein -2
S/O/W	solid in oil in water emulsion
SDS	sodium dodecyl sulphate
SEM	scanning electron microscopy
TBII-B, C, F	PLGA-PEG-PLGA triblock copolymer B, C and F
Tg	glass transition temperature
TGF β	transforming growth factor β
UV	ultraviolet light
VEGF	vascular endothelial growth factor
W/O/W	water in oil in water emulsion
Wnt 3/3a	wingless&int 3/3a
α MEM	alpha minimal essential medium
% _(w/v)	percentage weight/volume
% _(w/w)	percentage weight/weight
μ g	microgram
μ l	microlitre
μ m	micrometer (micron)

Chapter 1: Introduction to the field of regenerative medicine and bone tissue engineering

1.1 The growth of regenerative medicine and tissue engineering

Regenerative medicine is defined as the process of replacing or regenerating human cells, tissues or organs to restore or establish normal function. In the early twentieth century, transplants of bone, soft tissue and corneas were developed leading to the first successful kidney transplant being performed in 1954 (Merrill, 1954, Merrill, 1984). Transplant surgery gained pace with successful pancreas and liver transplants in the 1960s and by the 1980s the first heart and lung transplants were performed. However, the high doses of immunosuppressant drugs that were required to prevent graft rejection meant that the risk of infection was high. But, the aging post war 'baby boom' generation fuelled the demand for donor organs which far exceeded the supply and many patients died before surgical intervention (Kemp, 2006). There was a need to search for alternatives to donor organs and the field of tissue engineering emerged in the late 20th century. One of the first breakthroughs was to expand and grow the patient's own skin cells in the laboratory to form constructs. These were used to treat burns and ulcers, thus overcoming immunocompatibility issues (Munster, 1996). Other autologous tissues (for example bone chips) were used in regenerative applications but these often had variable levels of success due to poor quality tissue, low tissue yield, infection and required two surgical procedures which added to potential pain and side effects (Arrington 1996).

The development of biomaterials for regenerative medicine gained importance and one of the first non human materials, pioneered by Dr Stephen Badylak,

was porcine small intestinal submucosa. This was prepared by removing the mucosal, serosal and muscular layers of the intestine, isolating the collagenous matrix then, after decellularisation and sterilisation, the resulting extracellular matrix based biomaterial would provide a rich environment for tissue repair and could be used for a number of structural applications from repairing ligaments and vasculature to closing severe wounds (Sandusky, 1995, Lindberg, 2001). Continued research led to the discovery of synthetic and naturally occurring polymers as scaffolds to encourage three-dimensional growth of tissue. The work of Professor Robert Langer was at the forefront of this field and has provided the foundations for further research (Langer, 1990, Cohen, 1991, Kumar, 2002, Sokolsky-Papkov, 2007, Zimmermann, 2011).

The discovery and isolation of stem cells was of major importance and human embryonic stem cells were isolated in 1998 (Thomson, 1998). The differentiation pathway of stem cells can be directed by *in-vitro* manipulation to form a number of tissues which has obvious benefit for regenerative applications (Pountos, 2005). In addition to cells and a three dimensional scaffold, the cytokines and growth factors that orchestrate the complex signalling pathways within tissues are essential components to successful tissue regeneration. Manufacture of these molecules through bacterial genetic engineering has pushed forward tissue engineering research (Terpe, 2006). The importance of mechanical stimulation on regenerating tissue to recreate the *in-vivo* environment has resulted in the creation of bioreactors to mimic *in-vivo* forces to improve the tissue construct (El Haj, 2010). More recently, computer controlled three-dimensional printing devices have been developed with the potential to create 'made to measure' biomaterials with incorporated cells and growth factors for implantation (Seitz, 2005, Butscher, 2012, Ozbolat, 2013).

The long term goal of tissue engineering and regenerative medicine is to combine stem cells and biomaterials to transform the treatment of human disease through the development of innovative new therapies that offer a faster, more complete recovery with significantly fewer side effects or risk of complications (Murphy, 2012, Mallick, 2013).

1.2 Orthopaedic applications for regenerative medicine

The orthopaedic sector of the biomaterials market is large and is expanding due to the demographics of an increasingly ageing population as well as bone loss through trauma and disease. The cost of treatment for osteoporotic fractures alone in the United States alone exceeded \$17 billion in 2005 and is estimated to increase to \$25 billion per year by 2025 (Burge, 2007). New surgical techniques and medical devices have emerged and biomaterials have been developed for use as fixative devices such as pins, screws and plates as well as bone cements. Biomaterials for bone filling applications are being used to provide an alternative to autograft (harvested from the patient) and allograft (obtained from donor), as both of these types of material have their limitations. Autografts despite having high immunocompatibility require major surgery and often the availability and yield is low with risk of infection and recurrent pain. Allografts including demineralised bone matrices run the risk of graft rejection by the immune system and transmission of donor pathogens (Braun, 1992, Arrington 1996).

Many synthetic bone void fillers have been developed but for them to be completely successful they need to be able to i): provide mechanical support, ii): act as a substrate for osteoid deposition, iii): have a porous architecture, iv): encourage bone cell migration into the scaffold, v): support and promote

osteinduction, vi): support and promote osseointegration, vii): degrade in a controlled manner viii): produce non-toxic degradation products, ix): not cause an inflammatory response x): be sterilised without loss of bioactivity and xi): deliver bioactive molecules or drugs in a controlled manner to accelerate healing (Porter, 2009).

As yet no synthetic bone filler is available that meets all these criteria but work by many groups is focussed on integrating biomaterials with stem cells and growth factors to facilitate tissue regeneration (Jain, 2000, Dawson, 2008, Howard, 2008, Martino, 2012, Mehta, 2012).

1.3 Structure and natural growth of bone

1.3.1 Bone structure

Bone is a complex tissue which provides structural support for the body for movement and also provides protection for internal organs. It plays a role in regulating calcium levels, storing fat and producing red blood cells. Bone is a strong composite material consisting of collagen fibres and hydroxyapatite crystals and has a porous structure with the pores being mostly interconnected to allow infusion of body fluids. The periosteum is the fibrous membrane found on the outer surface of the bone.

There are two types of bone with distinct structures (Figure 1.1). Cortical bone is compact and dense consisting of parallel concentric columns (osteons) which house the Haversian canal system linked by Volkmann's canals. This type of bone is mainly found in the shafts of long bones where they play a load bearing role. Cancellous bone is more lightweight and porous and consists of

a network of randomly arranged fine plates of lamellar bone called trabeculae that are separated by interconnecting pores up to 1mm in size. Cancellous bone is highly vascularised and houses two types of bone marrow, yellow that acts as a fat storage and red which is the site of erythropoiesis.

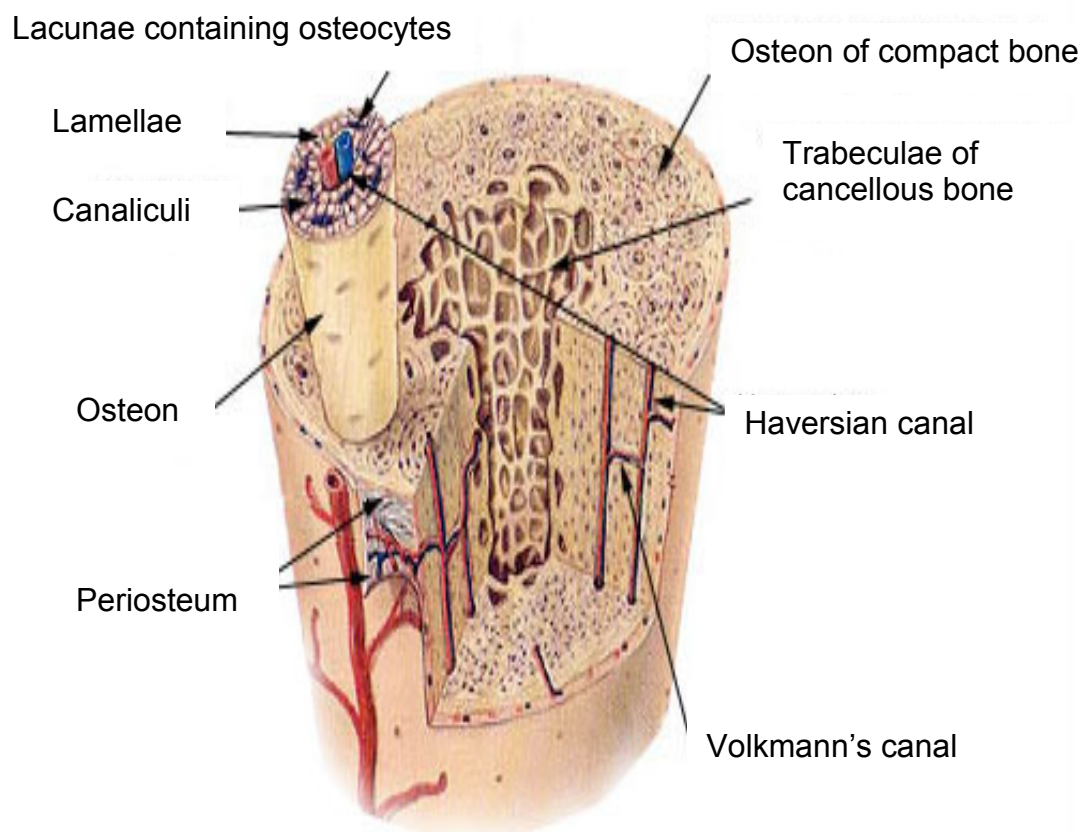


Figure 1.1 A schematic showing the typical structure of a long bone. The cortical or compact bone structure is shown at the circumference with the more porous cancellous or spongy bone structure within the centre of the long bone (Flint, 2007)

1.3.2 Bone development, growth and remodelling

Bone has a number of inherent cell types and these play an important role in development, growth and maintenance. Osteoblasts are formed from osteoprogenitor cells and lay down osteoid and mineralised matrix. Once osteoblasts become trapped in the bone matrix they either differentiate into osteocytes and have a paracrine role on active osteoblasts or undergo apoptosis. Osteoclasts play a role in bone resorption by secreting acids and proteolytic enzymes which dissolve crystalline hydroxyapatite and degrade bone matrix rich in collagen fibres. This bone remodelling is a constant process which is controlled by complex signalling pathways (Crockett, 2011). A simplified cartoon of the process is shown in Figure 1.2

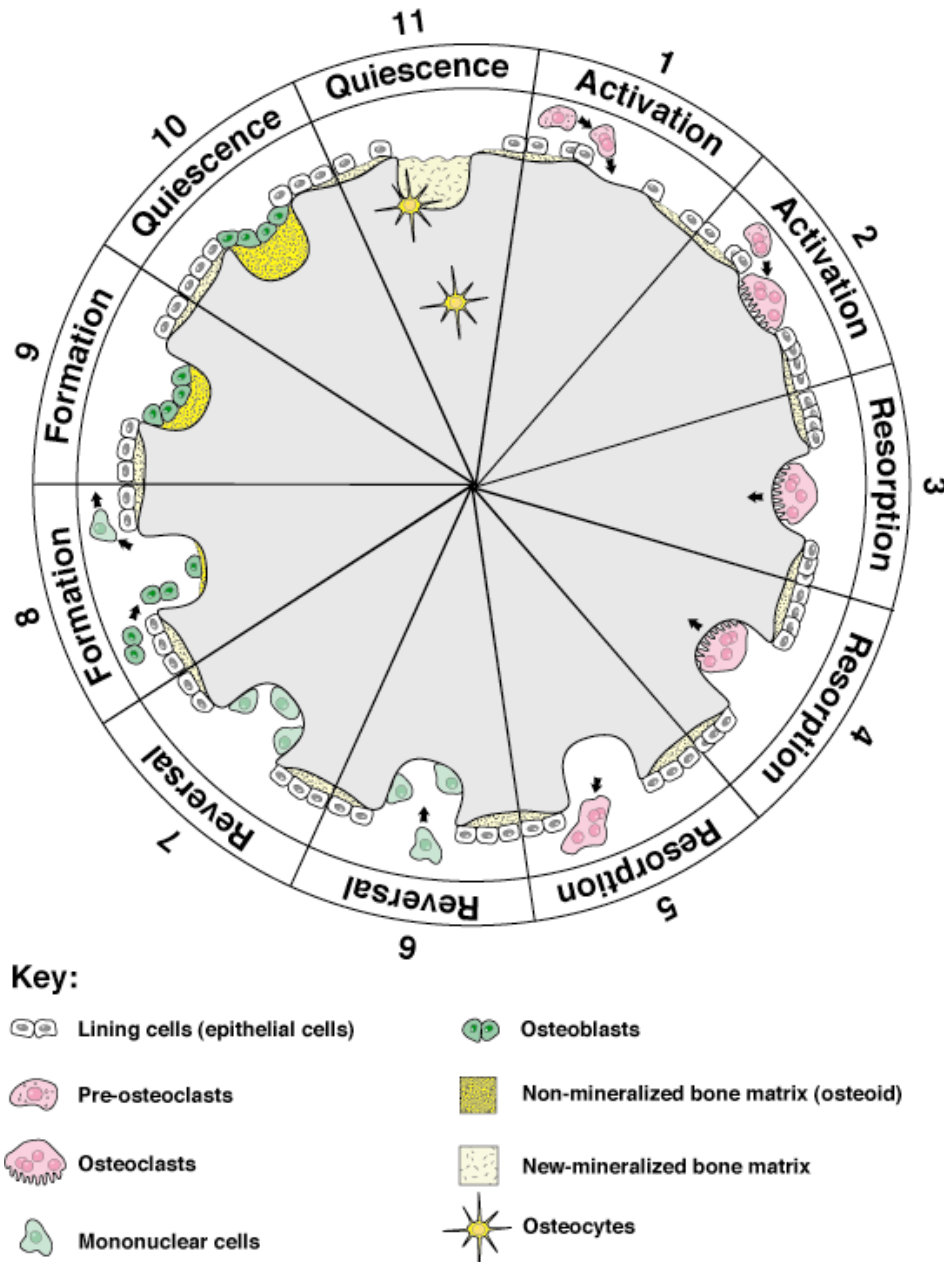


Figure 1.2 A schematic to demonstrate the processes involved in bone remodelling. Pre-osteoclasts are activated and form the osteoclasts that initiate bone resorption. The reversal of this occurs by the action of osteoblasts which deposit osteoid that becomes mineralised over time. Osteocytes which have a paracrine role in osteogenesis become embedded in the matrix. (Crockett, 2011)

In the early developing foetus, most of the skeleton is composed of hyaline cartilage, a tough, flexible connective tissue that has no minerals or salts. As the foetus grows, osteoblasts and osteoclasts slowly replace cartilage cells through endochondral ossification (Mackie, 2008). Calcium compounds must be present in the blood for ossification to take place. The primary ossification centre is in the bone diaphysis where initially, a bone collar forms followed by cavity formation and vascularisation. As blood vessels, osteoclasts, and osteocytes continue to invade, the medullary cavity is formed and the diaphysis slowly continues to lengthen during embryonic development. Vessels also bud into the hyaline cartilage at the epiphysis of the long bones forming secondary ossification centres (Figure 1.3)(Flint, 2007).

Cartilage remains at the epiphyseal plates (growth plates) and at the end of the bones. This cartilage is the only remains of the original hyaline cartilage model. The epiphyseal plates allow continued growth of the bones into adulthood and the articular cartilage at the end of the bone facilitates movement. In humans the epiphyseal growth plate has a distinct zonal arrangement of cells, resting, proliferative, hypertrophic cartilage, calcified cartilage and the ossification zone (Burdan, 2009). By adulthood the epiphyseal plates close to form an epiphyseal line.

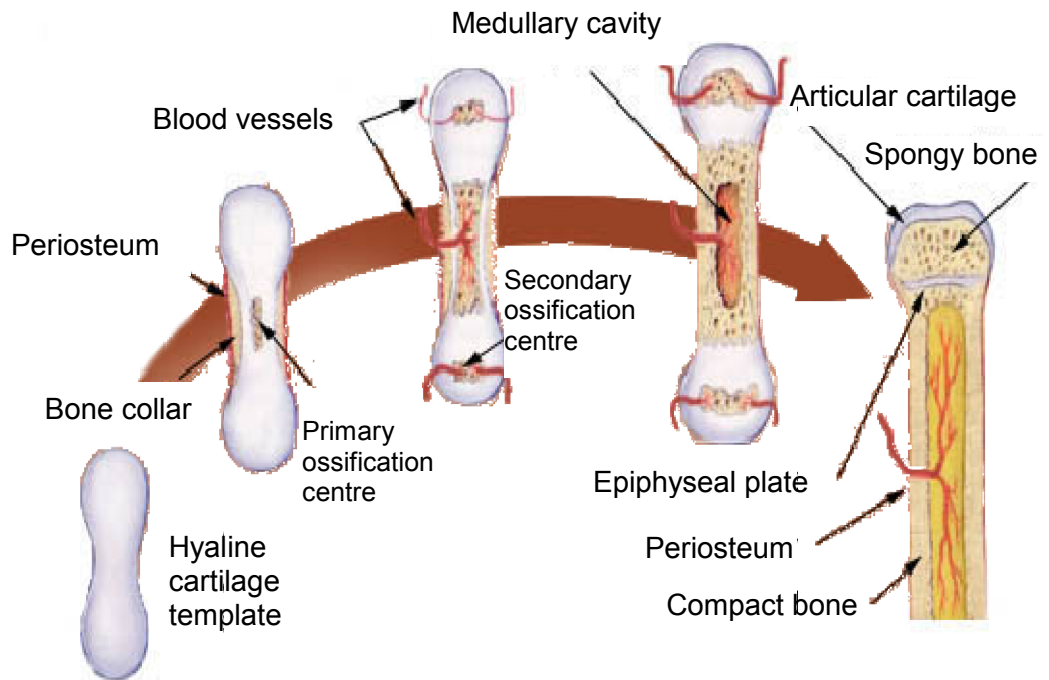


Figure 1.3 A schematic to demonstrate the main processes that occur during endochondral ossification. A non mineralised cartilage template is converted to bone firstly at the diaphysis (primary ossification centre) and then at the epiphyses (secondary ossification centres) after the invasion of blood vessels. Leading to the recognised long bone structure. Adapted from (Flint, 2007)

1.3.3 Normal bone repair

There are four main stages of bone healing that overlap but occur sequentially, the first three are shown in Figure 1.4 with the fourth stage being the process of bone remodelling (Jahagirdar, 2009). Firstly, after trauma, there is haematoma formation, a blood clot of insoluble fibrin is formed which provides a framework for the influx of cells which leads to the second stage of repair, inflammation. Various growth factors and inflammatory cytokines are released (transforming growth factor β , platelet derived growth factor, fibroblastic growth factor, interleukin-1 and interleukin-6) and endothelial cells along with

fibroblasts form granulation tissue. The inflammation stage lasts for around seven days. The damaged bone tissue at the edges of the fracture fragments die back and osteoclasts work to remove the dead bone cells and phagocytes ingest the necrotic tissue. However, osteoblasts are unable to work to lay down new bone tissue at this stage because of the movement of the fracture fragments. Thirdly, the repair stage, soft callous formation occurs as fibroblasts begin to lay down cartilage to form a 'scaffold' between the two fragments. Despite being quite fragile, the soft callus provides sufficient stability at the fracture site for new blood vessels to form and for osteoblasts at the periosteum to begin laying down 'woven bone' at the margins of the fracture. The bone has a disorganised structure, but it's the first bone contact between the two fracture fragments. A hard callous forms from two to three weeks after the fracture by endochondral ossification and is encouraged by gentle mechanical loading. The resulting union of the bones restores cortical continuity but the callous is often enlarged. The fourth stage is therefore bone remodelling and can occur over many weeks. The remodelling process as described in Section 1.3.2 ensures that the woven osteoid bone is remodelled into lamellar bone and restores full functional integrity.

Clinical intervention is required to stabilise the damaged bone and often mechanical fixings are used in conjunction with biomaterials such as cements. It is not only trauma that requires intervention. Other conditions such as vertebral disc degeneration causing extreme lower back pain can be alleviated by spinal fusion using bone graft and/or biomaterials to fuse adjacent vertebrae together often in conjunction with a spinal cage. The inclusion of bioactive growth factors into the procedure has also been cited (Even, 2012). Other specialised applications such as kyphoplasty is minimally invasive and would lend itself to a load bearing microparticulate therapy (Bornemann, 2013).

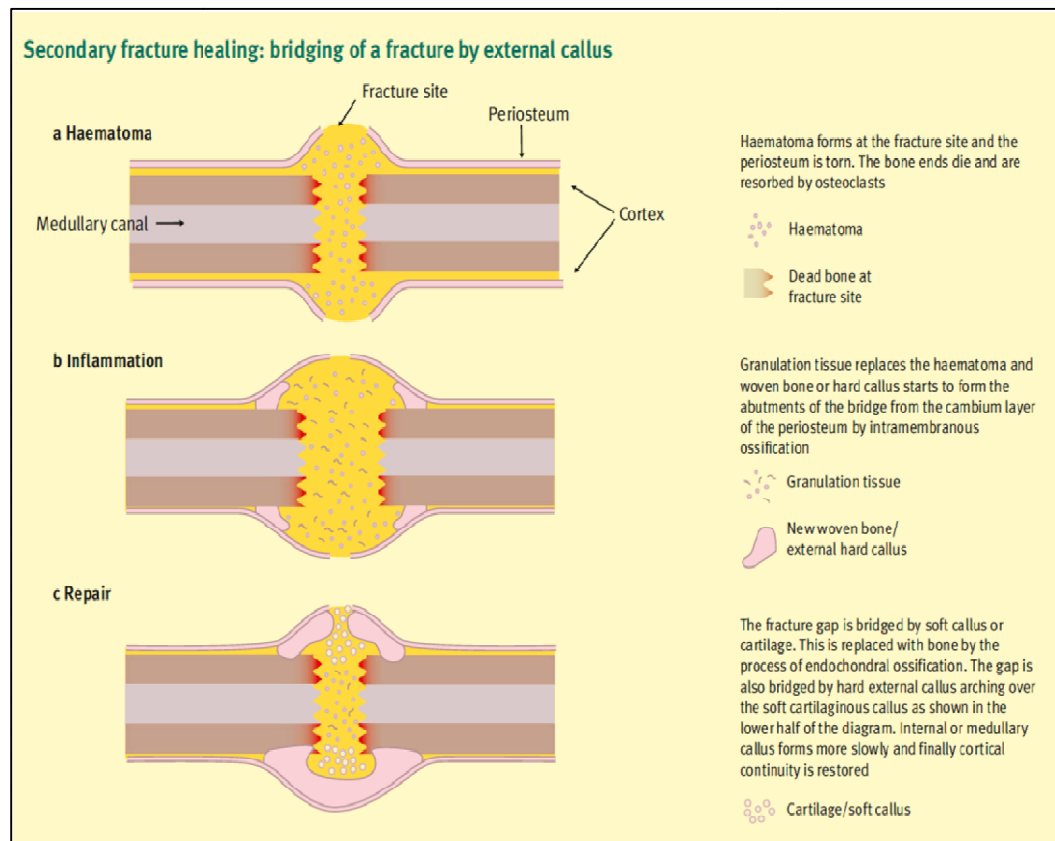


Figure 1.4 Schematic showing the stages of normal bone fracture repair (Jahagirdar, 2009)

1.3.4 Problems with bone repair mechanisms

With medical intervention, most bone fractures heal satisfactorily to restore full function. However, in some cases the healing process can be hindered and is often due either to insufficient quantity of osteoprogenitor cells or an inability of the cells to recognise and respond to cellular cues (Bajada, 2007). The lifestyle of the patient can play a role with smoking and obesity being prominent factors in poor bone repair (Kung, 2012). In addition, patients with underlying medical conditions such as diabetes are also prone to poor bone healing (Kayal, 2007). Patients taking immunosuppressant medications may

suffer from delayed bone healing and be susceptible to infections which can cause further complications.

Swift medical intervention after trauma is important and if not available, this could lead to a poor blood supply to the area or insufficient stabilisation of the fracture which would be detrimental to healing. This can result in a non-union or mal-union and bone graft materials along with medical fixation devices are often needed. Another main detractor to bone healing is the advancing age of the patient and can often result in many people being confined to wheelchairs as mobility is lost after osteoporotic fractures which are slow or unable to heal.

1.4 Biomaterials for orthopaedic regenerative applications

To improve the prognosis of the patient, a number of biomaterials have been used clinically to augment bone healing. The biomaterials have different origins and are described briefly in the following Sections.

1.4.1 Inorganic materials

There are many inorganic materials that have been used for bone tissue engineering applications each having their own advantages and drawbacks. A lot of research has focussed on combining materials to produce composites to improve the overall performance of the material (Rezwan, 2006). Some of the main component materials are described below.

Hydroxyapatite is chemically similar to the mineral component of bones and is a complex phosphate of calcium with a chemical formula of $\text{Ca}_{10}(\text{PO}_4)_6(\text{OH})_2$. It is classed as bioactive because osteoblasts will adhere to it and therefore it

is often used as a coating for orthopaedic implants promoting osseointegration between bone and the medical device so allowing for cement-less implants (Akizuki, 2003). A disadvantage is that hydroxyapatite will only degrade very slowly by dissolution or fragmentation followed by phagocytosis by macrophages and/or by the action of osteoclasts (Rumpel, 2006). A slow degradation rate may inhibit the developing tissue.

Beta-tricalcium phosphate ($\text{Ca}_3(\text{PO}_4)_2$) like hydroxyapatite, is biocompatible, non-toxic and resorbable but it degrades much faster mainly by the action of osteoclasts and has also been used in many bone substitute materials (Horowitz, 2009). The drawback with these materials is that they are not macroporous and have a low porosity which does not encourage cell in-growth nor do they mimic the mechanical properties of bone.

Calcium based phosphate cements (CPCs) are another class of biomaterials often used in bone augmentation. These mainly consist of tetra-calcium phosphate ($\text{Ca}_4(\text{PO}_4)_2\text{O}$) combined with anhydrous di-calcium phosphate (CaHPO_4) which when mixed with water will create a workable paste that will harden quickly producing nanocrystalline hydroxyapatite. CPCs were approved by the Federal Drug Administration of the United States for use in non-load bearing bone defects in 1996 (Larsson, 2002). The potential for use as an injectable treatment is advantageous but they are not macroporous in structure and can produce heat during the hardening process and have handling problems (Oda, 2006).

Calcium sulphates have been used for many years and are used in bone tissue engineering where faster resorption of the material is an advantage over and above providing structural support (Larsson, 2011). They do not

have good mechanical properties, but, have been used in conjunction with antibiotics where control of infection was more important than structural support (Bajada, 2007, Kluin, 2013).

Bioactive glasses were discovered as long ago as 1969 (Hench, 2006) and have been in clinical use since 1985 (45S5Bioglass[®]) for interfacial bonding of implant with host tissue. The first bioactive glasses consisted of a combination of SiO₂, Na₂O, CaO and P₂O₅ and these developed hydroxyapatite crystals *in-vivo* which bonded to layers of collagen fibres produced by osteoblasts. Further research into bioactive glasses has resulted in more sophisticated formulations which can bond to both soft and hard tissues and play a role in regulating gene expression in osteoprogenitor cells (Hench, 2009). The disadvantages of some bioglasses is their mechanical weakness but this can be overcome by high temperature (>950 °C) thermal treatment which crystallises the glass (Bellucci, 2011). In addition, the porosity of the bioglass is problematic but a foaming step during manufacture can overcome this problem (Sepulveda, 2001, Jones, 2006).

Metals such as titanium, stainless steel and cobalt-chromium alloys are used by orthopaedic surgeons in the form of plates, pins and screws to aid bone reconstruction. Metals are also used total joint replacements (for example hip replacements) often with osteoinduction coatings for better integration. The company Zimmer introduced 'trabecular metal[™]' in 2010 for dental application and for knee replacement surgery in 2011 (Collins, 2012). This material was constructed from the metal tantalum and resembles the structure and strength of cancellous bone being 80% porous. However, it only has limited application and is not biodegradable.

1.4.2 Organic materials

Collagen is an obvious candidate for bone graft applications due to its abundance in natural bone although, in isolation, it has limited mechanical properties and is often used in conjunction with inorganic materials (Zimmer Collagraft®) or growth fractures such as bone morphogenetic protein-2 (Medtronic Infuse®) for non-load bearing applications. Growth factors tend to have a low affinity for collagen which results in a low loading and a fast release from the scaffold. This can be addressed by cross-linking the collagen fibres and has shown some success in proving a more sustained release rate (Zhang, 2012).

Gelatin is material derived from partial hydrolysis of collagen and is widely used in the food industry but also been used in research into bone graft materials. Alone, gelatin is not osteoconductive, osteoinductive nor does it have great mechanical strength but can be used as an inert material in conjunction with other materials. For example, calcium silicate-gelatin composites demonstrated high compressive strength (141 MPa) and provided a favourable environment for cell growth (Ding, 2011). Recently, gelatin has been conjugated with heparin to improve growth factor immobilisation with some success (Nakamura, 2012).

Hyaluronic acid is a high molecular weight polysaccharide and an essential component of extracellular matrix. It has extensively used as a dermal filler but it has been reported that it increases osteoblastic bone formation *in-vivo* through increased mesenchymal stem cell differentiation and migration (Sasaki, 1995). It is therefore an interesting candidate for bone graft applications. Hyaluronic acid has been successfully used to augment bone

graft material to promote callous formation. A study in 2006 (Aslan, 2006) showed bone allograft material (Tutoplast[®] cancellous particles) performed better when administered with hyaluronic acid than when used in isolation in a rabbit tibial defect model. However, alone hyaluronic acid has poor mechanical strength for a bone void filler, but its viscoelastic properties may be of more use as a treatment to relieve osteoarthritis by direct injection into the joint (Iannitti, 2012).

Fibrin is formed from fibrinogen by the protease thrombin and polymerises to form a mesh which is the basis of the blood clotting mechanism. The administration of fibrinogen and thrombin is the basis of a 'fibrin glue' which acts as a tissue adhesive and has been used in conjunction with bone graft materials, although there have been conflicting reports as to its effect on osseointegration (Le Guehennec, 2004). Fibrin is often used in conjunction with other materials such as calcium phosphate cements to improve its functional and physical properties (Lopez-Heredia, 2013).

Alginates, extracted from seaweed and brown algae, are hydrogels and have many uses in bioengineering because of their biocompatibility and controlled stiffness. Alginate is a linear polysaccharide consisting of β -D-mannuronic acid (M) and α -L-guluronic acid (G) monomers. The monomers are ionically crosslinked with a non-toxic divalent cation such as calcium chloride and the consistency of the gel can be manipulated for the required application (Jeong, 2012). In particular, they are good cell delivery vehicles as they can be manufactured to form microspheres (Zhai, 2013) but in isolation they are not osteoconductive. If required for bone graft applications they tend to be used with other biomaterials due to their poor mechanical strength and rapid degradation.

Agarose is another gelling polysaccharide, extracted from red algae, which has similar advantages and disadvantages to those of alginate. Its stiffness can be controlled, but it is not osteoconductive. It is mainly used for soft tissue engineering applications. However it has been used in bone-grafting studies as a component in a composite material. For example, hydroxyapatite/agarose gels have been identified as good candidates for bone graft material (Tabata, 2003) and chitosan/agarose/gelatin scaffolds show promise for scaffolds in general tissue engineering applications (Bhat, 2012).

Chitin is a polysaccharide and a component of the exoskeleton of insects and the outer shell of crustaceans. The removal of its acetyl group results in chitosan which has a positive charge and is more biocompatible and is also osteoconductive (Di Martino, 2005). It also has the advantage of being intrinsically antibacterial and biocompatible (Venkatesan, 2010). To improve its physical characteristics, chitosan has been used in conjunction with calcium sulphate and BMP-2 in a rabbit segmental defect model (Cui, 2009) as well as with hydroxyapatite (Danilchenko, 2011) and has showed encouraging results for bone regeneration.

Corals have been investigated as bone graft substitutes in particular the coral *Porites* which has a structure and strength similar to that of cancellous bone. The coral is biocompatible, osteoconductive and biodegradable at different rates depending on the porosity (Demers, 2002). However, coral is not osteoinductive nor osteogenic and showed no advantage over hydroxyapatite when compared directly in conjunction with platelet rich plasma in a rabbit study (Shafiei-Sarvestani, 2012).

Finally, silk is a naturally occurring material with good tensile strength which has interested scientists working in bone graft research. Recently, protein isolated from silkworms has been combined with silk fibres to create scaffolds which are biodegradable with high compressive strength (Mandal, 2012). The material has also been used to develop a more realistic model of lamella bone by growing mesenchymal stem cells on patterned silk films (Tien, 2012). Research is ongoing at Oxford Biomaterials to develop silkbone™ which is a load bearing bone graft material.

The main disadvantage of all naturally occurring polymers is that the batch to batch variation is generally high and the yields achieved can be quite variable.

1.4.3 Synthetic polymers

Although, naturally occurring inorganic and organic materials have been the basis of much research into bone graft substitutes, synthetic materials have also grown in importance due to the ability to tailor their degradation rates and cut down on batch to batch and processing variability. Research has concentrated on a number of different polymer types, many of which have been developed as drug delivery devices as well as bone graft substitutes (Gunatillake, 2006).

Polyanhydrides are attractive as a biomaterial for short term delivery of bioactive agents although they do not possess great mechanical strength (Kumar, 2002). However, if they are synthesised with methacrylate end groups that readily photopolymerise then they will produce highly cross-linked polyanhydrous networks with significant mechanical strength (Muggli, 1999). Polyanhydrides are biodegradable and are not affected by gamma irradiation.

The main disadvantage of this material is its hydrolytic instability and it therefore requires low temperature dry storage in order to avoid molecular weight loss (Kumar, 2002).

Biodegradable polyphosphazenes have been identified as materials for drug delivery matrices and scaffolds for tissue engineering. The most common being aminated polyphosphazenes and alkoxy-substituted phosphazenes (Lakshmi, 2003). The degradation products of ammonia and phosphates are non-toxic at low doses, but are likely to cause toxicity at higher concentrations. The rate of degradation can be altered by substituting different side-groups and this is advantageous both for use as a delivery device as well as a scaffold matrix. Polyphosphazenes have been used in composite materials for bone tissue engineering, for example with polyesters where they can buffer their acidic degradation products (Deng, 2010).

Polyphosphate polymers have a phosphodiester backbone which remains anionic over a wide range of pH and thus when it degrades, the local environment is less susceptible to pH change. Polyphosphates have been synthesised to deliver rh-osteogenic protein-1 to stimulate osteoblast proliferation *in-vitro* and have the potential for use in bone graft materials (Renier, 1997). Calcium polyphosphate was successfully used as a delivery vehicle for cultured articular chondrocytes in a sheep femoral defect model. The degradation products from this porous material were calcium and phosphate which elicited no inflammatory responses (Kandel, 2006). Recently, this group has shown the potential for this material in high load bearing applications but the scaffolds must be pre-sintered and are therefore could not be delivered as an injectable product (Pilliar, 2013).

Polypropylene fumarate is an unsaturated linear polyester that can be modified or cross-linked through its fumarate double bonds to give it strength and it degrades by hydrolysis of the ester bonds. Fine tuning of physical parameters during synthesis will result in a candidate material for bone grafting (Wang, 2006) and it has been used for craniofacial applications where the disadvantage of heat generation by exothermic crosslinking was overcome by the addition of crosslinked microparticles (Henslee, 2012).

Acrylic polymers such as poly(methylmethacrylate) have been widely used as bone cements for decades and are still an important material today. The viscosity of poly(methylmethacrylate) can be controlled by a number of methods during manufacture and this gives surgeons flexibility to use different delivery systems (Webb, 2007). The enduring problem with this biomaterial is that polymerisation of the monomers is exothermic with temperatures over 70°C recorded, the temperature rise is not always consistent, but can be sufficient to cause thermal necrosis which can compromise tissue repair (Reckling, 1977). However, this material hardens quickly (working time of 10-15 minutes), exhibits high compressive strength and is still commonly used as a bone cement.

Poly(ϵ -caprolactone) which is a hydrophobic aliphatic polyester and has a very slow degradation rate and so it is useful as a long term orthopaedic implantable devices (Lam, 2009). As well as being used alone as either electrospun scaffolds or as microparticles for drug delivery (Balmayor, 2009, Cirillo, 2012), it is also often used as a composite material for example with calcium sulphate or tricalcium phosphate to improve its physical properties and osteoconduction (Zhou, 2007, Liu, 2011). Poly(ϵ -caprolactone) has also been used in conjunction with growth factors such as bone morphogenetic

growth factor -2 where the growth factor was attached to the polymer by a crosslinking conjugation method to encourage osteogenic activity in bone marrow stromal cells (Zhang, 2010).

1.4.3.1 Poly (α - hydroxy acid) polymers

Poly (α - hydroxy acid) polymers are thermoplastic poly(α - esters) and have emerged as the most prominent candidates in the field of bone regeneration especially where glycolide and lactide are the monomers used. Polyglycolide (poly(glycolic acid)) has high crystallinity (45 -55 %), good mechanical strength and stiffness but, it degrades quickly and is not soluble in a number of organic solvents (Middleton, 2000). Polylactide (poly(lactic acid)) is more amorphous in structure and exists as both D- and L- enantiomers. Poly(L)-lactide has a much lower crystallinity and slower degradation profile and has good tensile strength. Poly[DL]-lactide has an amorphous structure and a much lower strength and a higher degradation rate (Middleton, 2000). To achieve the best qualities of both polymers, their monomers can be combined by random ring-opening copolymerisation in the presence of a catalyst to create poly(lactide-co-glycolide) also known as poly(lactic-co-glycolic acid) or PLGA (Figure 1.5).

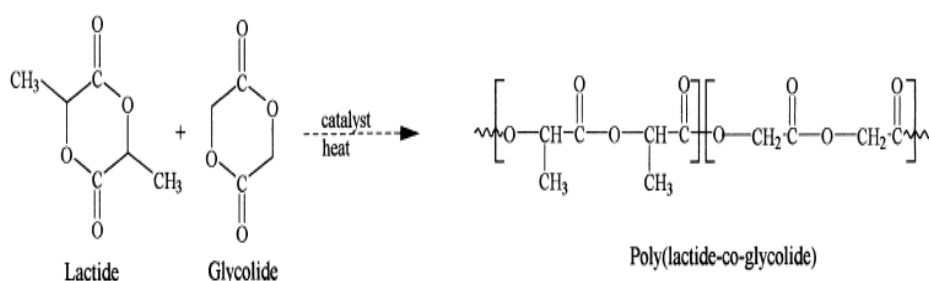


Figure 1.5 Synthesis of poly(lactic-co-glycolic acid) (PLGA) (Middleton, 2000)

PLGA has been used extensively for research into controlled release as it can be tailored to degrade at different rates by altering factors such as the lactide:glycolide monomer ratio, molecular weight and end-group chemistry (Makadia, 2011). The degradation products of PLGA (lactic and glycolic acid), are metabolised naturally by the tri-carboxylic acid cycle and are ultimately excreted as water and carbon dioxide. PLGA is therefore considered biocompatible, non-toxic and is approved by the Food and Drug Administration for certain applications.

1.5 Parameters to control PLGA degradation

The general mechanism of PLGA degradation is by hydrolysis of its ester linkages into shorter oligomers and finally into the monomers lactic and glycolic acid (Korber, 2010). The degradation is described as bulk erosion as it takes place throughout the whole of the sample and the rate at which water penetrates exceeds the rate at which the polymer is converted into water soluble materials. However, initially degradation will occur more rapidly at the polymer surface due to the greater availability of water (Middleton, 2000).

As already suggested, altering the chemical composition of the polymer will alter its degradation rate. Having higher lactide content will result in a slower degradation rate due to its higher hydrophobicity and lower crystallinity. For example, PLGA with an L:G ratio of 50:50 will degrade in the order of weeks but PLGA with an L:G ratio of 85:15 will take months to degrade (Anderson, 1997, Wu, 2001). The molecular weight of PLGA will also affect the degradation rate as the initial drop in molecular weight (a measure of degradation) is greater for higher molecular weight PLGA than for lower molecular weight PLGA (Wu, 2001). The end group chemistry plays a role as

PLGA, a carboxylic acid end group will degrade faster than an ester end group and degradation products may autocatalyse further degradation (Sokolosky-Papkov, 2007, Yu, 2010).

In addition to the above, other important factors affecting the degradation rate of PLGA were summarised by Anderson in 1997 as follows: i) water permeability and solubility (hydrophobicity), ii) chemical composition, iii) mechanism of hydrolysis, (necatalytic, autocatalytic, enzymatic), iv) additives (acids, bases, monomers, solvents, drugs), v) morphology (crystalline or amorphous), vi) device dimension (size, shape, surface to volume ratio), vii) porosity, viii) glass transition temperature, ix) molecular weight and molecular weight distribution, x) physico-chemical factors (ion exchange, ionic strength, pH), xi) sterilisation and xii) site of implantation (Anderson, 1997).

Although all of these parameters should be considered when developing a new biodegradable medical device, in practice they cannot all be addressed and the required application may influence the prioritisation of the parameters.

1.6 Fabrication of polymeric microparticles and scaffolds as delivery devices

PLGA is clearly a potentially useful material for tissue engineering applications but, it needs to be fabricated into a workable product. This could be an injection moulded device (e.g. an interference screw or stent), a three dimensional porous scaffold to support tissue growth or drug loaded microparticles for targeted release of a therapeutic. The following Sections briefly introduce some of the current manufacturing methods.

1.6.1 Fabrication techniques without organic solvents

Many different fabrication techniques are available to create workable scaffolds from PLGA that are suitable for bone tissue engineering. Amongst these are hot melt extrusion (Singhal, 2011) and jet milling (Nykamp, 2002). The advantage of these is that there is no aqueous interface for potential degradation of the bioactive (especially important for water soluble proteins) and no solvents are required. But, the temperature may be detrimental to many biological molecules. Nevertheless, it has been shown that lysozyme will remain active using this method (Ghalanbor, 2010).

Supercritical fluid technology has also been exploited to manufacture foamed polymer scaffolds for orthopaedic applications using supercritical carbon dioxide (Tai, 2007, Kang, 2008). An advantage is that these scaffolds tend to have an open porous architecture which is an important factor for cell growth and transfer of nutrients across the scaffold.

1.6.2 Fabrication techniques with organic solvents

Most fabrication techniques to manufacture scaffolds or microparticles do require the use of organic solvents. During electrospinning, the dissolved polymer is subjected to an electrical charge whilst being ejected from a syringe. The jet of polymer solution is attracted to a collector plate where it solidifies to leave polymer fibres which will form a scaffold mesh on which cells can be seeded (Kenawy, 2002, Huber, 2007).

Spray drying is a popular technique for the production of microparticles. The polymer solution is fed into a chamber through an atomiser where it is rapidly

dried by a hot gas (Patel, 2009). The resulting microparticles are of a consistent size but the cost of spray drying equipment is prohibitive for research use. In order to encapsulate active molecules, emulsions can also be successfully spray dried (Giunchedi, 2001).

Microfluidic and solvent exchange techniques have resulted in the manufacture of polymer microparticles of uniform size both in the research and commercial sector (Yeo, 2004a) but generally, despite producing good monodispersed microparticles, these techniques are very slow to produce a workable yield (Zhu, 2009).

The most popular method of manufacturing polymer microparticles is by using a variety of emulsion techniques and these will be discussed in detail in the next Section.

1.7 Emulsion techniques for PLGA microparticle manufacture

The use of biodegradable microparticles as a drug delivery system has grown in importance over the last few years and using different emulsion techniques, both hydrophilic and hydrophobic molecules can be encapsulated. A microparticulate system has the potential to be minimally invasive and deliver the bioactive to the desired site within the body.

1.7.1 The principle of emulsion formation

An emulsion is formed when two immiscible liquids (e.g. an oil and water) are mixed together to disperse one liquid into the other in the form of drops (Figure 1.6). Emulsions can either be oil-in-water (O/W) or water-in-oil (W/O),

depending on whether the continuous phase is the water or the oil. Once mixing stops, the drops may coalesce and the two phases can therefore separate and destabilise the emulsion. To form a stable emulsion, an emulsifying agent must be added into the system. This is usually in the form of a surfactant which forms a film at the interface of the droplet and resists coalescence. The stability of an emulsion is dependent on interfacial viscosity, electric charge on drops, droplet size and concentration, and viscosity of the continuous phase. Walstra gave a detailed review of the principles of emulsion formation (Walstra, 1993).

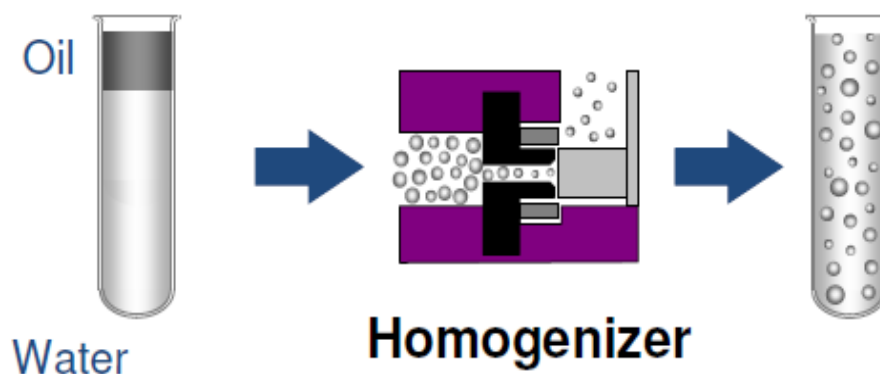


Figure 1.6 The principle of oil in water emulsion

<http://people.umass.edu/mcclemen/FoodEmulsions2008/Presentations>

1.7.2 Microparticle manufacture by emulsion and solvent evaporation

The principle of emulsion formation has been exploited to manufacture drug encapsulated polymer microparticles for use in drug delivery and tissue engineering applications. This section will focus primarily on encapsulation of proteins as these have complex structures which are directly related to their

function and thus pose challenges to avoid denaturation and loss of bioactivity during the encapsulation process.

There are two major methods developed to encapsulate proteins into polymer microparticles, solid-in-oil-in-water (S/O/W) emulsion and water-in-oil-in-water emulsion (W/O/W) (Morita, 2000a, Castellanos, 2001, Wischke, 2008, Dawes, 2009, Bible, 2009). Proteins tend to adsorb at water/organic solvent interfaces and this is thought not only to disturb the delicate conformation of proteins but also to trigger various physico-chemical transformations leading to protein destabilization reactions (Sah, 1999, Fu, 2000). Therefore the S/O/W method which maintains proteins in their solid state and only subjects them to one oil-water interface would therefore seem more appropriate to maintain protein function. A novel method of protein micronisation with polyethylene glycol by lyophilisation was suggested by Morita to improve protein encapsulation and stability (Morita, 2000b).

The W/O/W method of microparticle production is widely used and involves dissolving the required drug or protein in a small volume of water then creating a primary water-in-oil emulsion by homogenising the protein solution with a solution of the required polymer in an organic solvent such as dichloromethane. The primary emulsion is then transferred into another aqueous solution comprising of an emulsion stabiliser such as polyvinyl alcohol where it is homogenised for a second time. The organic solvent must then be removed by solvent extraction or evaporation to leave protein loaded microparticles (Figure 1.7).

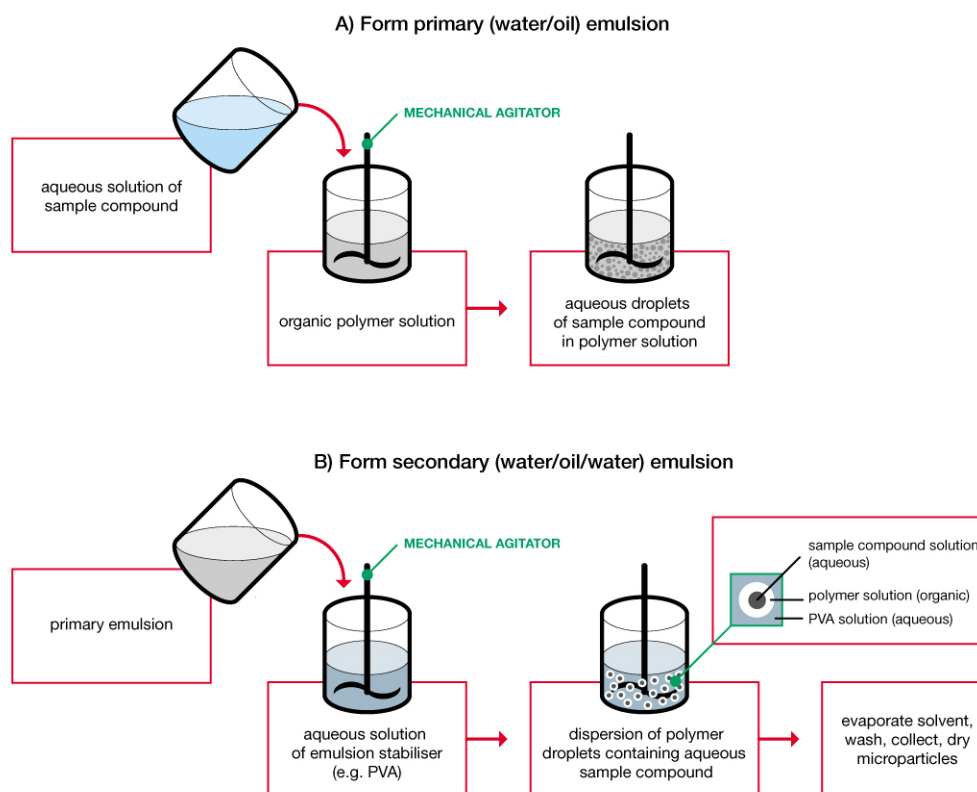


Figure 1.7 Schematic showing the water-in-oil-in-water double emulsion method of polymer microparticle manufacture (Bible, 2009)

Although the double emulsion is relative simple, it encompasses a number of variables all of which will affect the parameters of the resulting microparticles. Without tight control of the method the microparticles will have a broad size distribution and variable protein content (Ye, 2010). The challenge would be to develop reproducible and robust protocols to manufacture microparticles in defined size ranges for different applications with good entrapment efficiencies and no loss of biological activity of the entrapped molecule by adapting and optimising the parameters in the double emulsion protocol.

1.8 Injectable and non-injectable systems

The great advantage of a microparticulate system is that it has the potential to be injectable and can therefore be used for minimally invasive surgical procedures which would improve patient recovery times. A recent review describes the chemistry behind many of the current injectable scaffold systems in development (Rahman, 2012b). Most injectable bone fillers available on the market are cement based and so must be prepared at the point of use and generally need a high force for delivery, often requiring specialist delivery devices (e.g Depuy, Confidence spinal cement system®). Other polymer based products are usually supplied in specialist syringes and as such they rarely pass through a typically sized syringe bore of 2 mm (Smith and Nephew, Trugraft®). A product with properties that improve injectability would be advantageous for a number of orthopaedic applications (for example kyphoplasty).

Bone graft products are available as a malleable formulation which although not minimally invasive, gives the surgeon the opportunity to mould the graft to exactly fit the the defect (Novabone, Nova bone putty® and Apatech, Actifuse™Shape). Other bone graft materials are pre-formed into rigid porous scaffolds prior to use. These can infer maximum strength to the defect immediately but drawbacks involve shaping the scaffold to the correct size during surgery (Smith and Nephew Truwedge®). The number of different systems available both injectable and non-injectable gives the surgeon a choice for the required application.

1.9 Surface modifications to improve cell attachment

Although PLGA is a widely used material for tissue engineering, its surface chemistry is not ideal for cell attachment. The surface of untreated PLGA microparticles is hydrophobic, negatively charged and with very few functional carboxyl groups. But, the surface chemistry can be modified to encourage receptor-mediated cellular interactions which will further promote tissue regeneration. Plasma polymerisation followed by allylamine deposition and attachment of extracellular matrix components such as RGD-peptides or by covalent grafting of poly(N-vinylpyrrolidone) are some methods to achieve this aim (Verrier, 2002, Kallrot, 2006, Guerrouani, 2007, Bible, 2009). Improved osteoblast attachment to PLGA scaffolds and cell differentiation was also demonstrated by modifying the polymer surface with a thin layer of natural biomaterials such as collagen (Wu, 2006).

Cells will more readily attach to a roughened surface and a simple treatment to etch the surface for example with sodium hydroxide is reported (Park, 2005). However, the disadvantage of this is that the treatment will open up surface pores allowing entrapped protein to be released prematurely. It therefore may only be pertinent to methods to create porous microparticles.

1.10 Model Protein and Growth Factors

1.10.1 Model proteins

Model proteins are often used for preliminary research to represent the molecule of interest as closely as possible. Model proteins are usually chosen based on molecular weight and electric charge and are used as they tend to

be readily available and cost effective for the researcher for use in optimisation assays.

A number of different model proteins have been cited in the literature as being used in studies to determine release rates from polymeric microparticles. In particular, those that have been used with regard to bone regeneration are ovalbumin for transforming growth factor β 3 (TGF β 3), horseradish peroxidase for vascular endothelial growth factor (VEGF), ribonuclease A for insulin-like growth factor 1 and 2 (IGF 1/2) and lysozyme for fibroblast growth factor 8 (FGF8), platelet derived growth factor (PDGF) and BMP-2 (Simon, 1999, Hiemstra, 2007, Wells, 2007, Yilgor, 2010).

The water/oil interface during microparticle manufacture by emulsion techniques can be detrimental to maintaining structure and function of the protein being encapsulated. A number of studies have endeavoured to improve the entrapment efficiency and retain the structure/function relationship of the protein (Yeo, 2004b, Giteau, 2008). Serum albumins have been shown to limit the emulsification induced aggregation of several different proteins, including lysozyme, ovalbumin and recombinant human erythropoietin. (van de Weert, 2000a, Perez, 2002). Human serum albumin has also been used in a similar way (Kang, 2002).

1.10.2 Growth factors

The term growth factor is a broad description for several families of intracellular signalling proteins which have a number of different defined roles involving cell recruitment, migration and differentiation (Blackwood, 2012). Bone regeneration and repair is a complex process which is regulated by a

large number of bioactive molecules. Both growth factors and cytokines are involved in natural bone healing and some molecules have been identified as candidates to enhance the repair process. The key players in angiogenesis and osteoinduction have been identified as bone morphogenetic proteins (BMPs), transforming growth factor β (TGF β), fibroblast growth factor (FGF), insulin-like growth factor (IGF), vascular endothelial growth factor (VEGF), platelet-derived growth factor (PDGF), epidermal growth factor (EGF), parathyroid hormone (PTH), interleukins (IL), hypoxia inducible factor-2-alpha (HIF2- α) and Wingless/int 3/3a (wint 3/3a) (Kelpke, 2004, Kanczler, 2007, Kousteni, 2008, McMahon, 2008, Yang, 2010, Tamura, 2010).

A review by Kempen highlighted that to be successful in stimulating the auto-inductive capacity of bone, multiple growth factors should be delivered with temporal control to allow molecular interactions but successful research in this area is limited due to inconsistent or unknown pharmacokinetic release profiles from the delivery device (Kempen, 2010).

1.10.2.1 The BMP-2 signalling pathway

BMP-2 induces osteoblast differentiation via SMAD proteins which are intracellular proteins that transduce extracellular signals from ligand binding at the cell membrane to the nucleus where they activate gene transcription (Figure 1.8). In brief, initiation of the BMP-2 signalling pathway occurs at the cell surface by the binding of BMP-2 to a BMP type II receptor resulting in the phosphorylation and activation of the BMP type I receptor. This in turn, propagates the signal by phosphorylating a family of proteins known as SMAD proteins (Yamamoto, 1997). These proteins are intracellular proteins that transduce extracellular signals from ligand binding to the nucleus where gene transcription is activated. The type I receptor will firstly phosphorylate the

receptor-regulated SMADs (R-SMADs) which then bind the coSMAD SMAD4. R-SMAD/coSMAD complexes accumulate in the nucleus where they act as transcription factors and participate in the regulation of target gene expression. A number of transcription factors Runx2/Cbfa1, Osx, Dlx5 and Msx2 work synergistically to regulate the gene expression of downstream proteins to induce several types of osteoblasts and therefore play a prominent role in skeletal development. The system is regulated by antagonist to BMP-2 blocking binding at the cell surface as well as anti-smad proteins which inhibit smad signaling. The main components of the BMP-2 signalling system are shown in Figure 1.8.

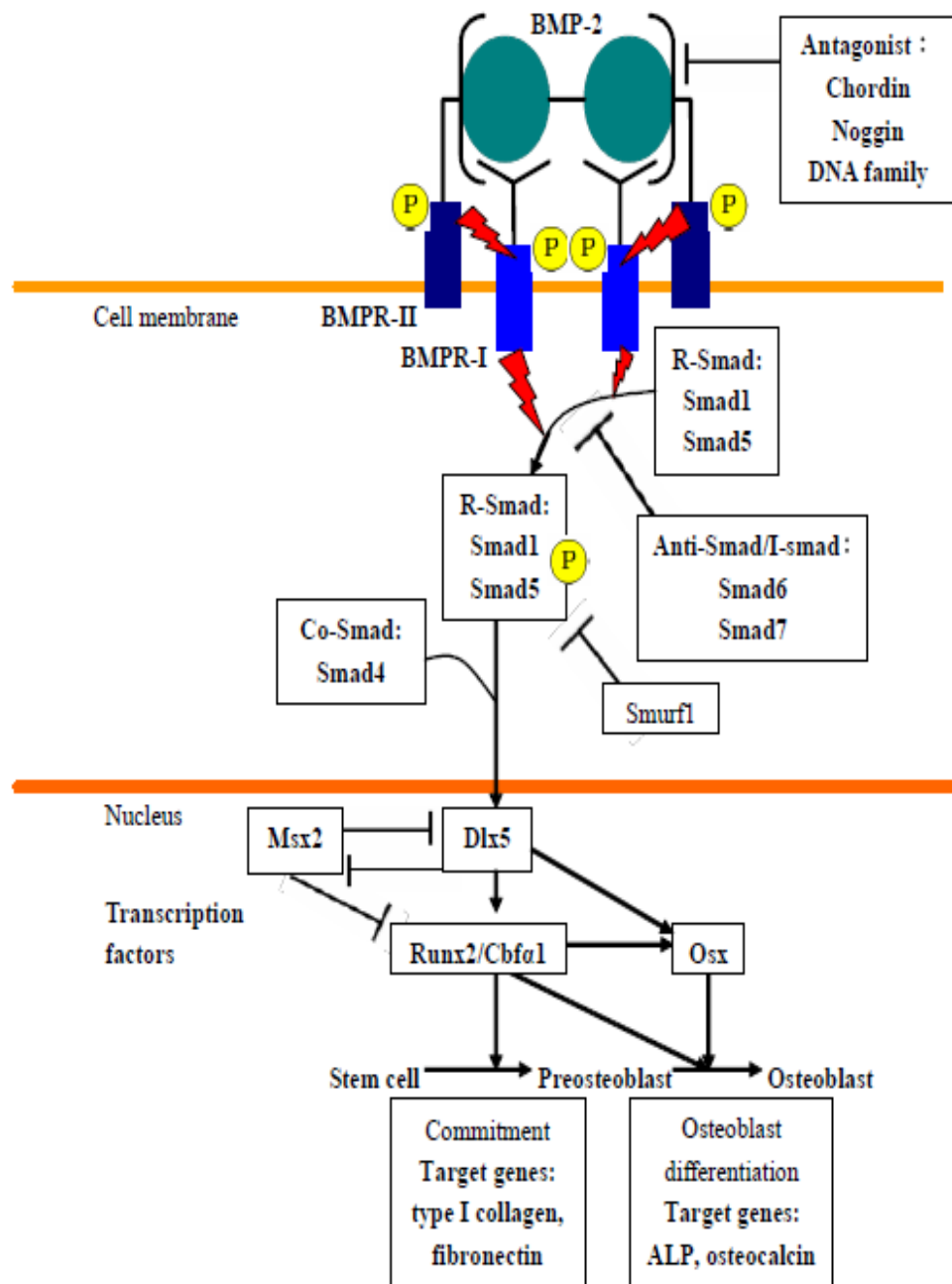


Figure 1.8 The main components of the smad signalling pathways of BMP-2 in osteogenesis. Phosphorylation steps are highlighted by [🔪] (Wu, 2008).

1.11 Release kinetics

If tissue engineering of bone is to be successful, the bioactive molecules required to orchestrate its regeneration and repair must be presented in a manner similar to the *in-vivo* kinetics. It is therefore of utmost importance that the release of growth factors from the delivery device can be temporally controlled.

1.11.1 Cumulative release profiles

There are a number of mathematical models of drug release kinetics including zero order (release independent of concentration), first order (release dependent on concentration), Hixson-Crowell (release by dissolution) and Higuchi (release by diffusion) amongst others (Kalam, 2007). However, it is well documented that drug release from PLGA microparticles follows a tri-phasic profile involving both diffusion and erosion (Cohen, 1991, Jiang, 2002, Ye, 2010, Dawes, 2010). Firstly, there is a burst release followed by a lag phase with little or no drug release and then a second release phase. In the early burst and lag phase, protein release is governed by diffusion through a network of water filled pores and channels.

The burst is caused by the rapid diffusion of surface bound and near surface entrapped protein and the lag is caused by the inability of entrapped protein to diffuse out due to being protected by hydrophobic PLGA. The lag phase continues until erosion of the polymer matrix by hydrolysis of the ester backbone occurs releasing more protein from the structure (Li, 2001, Paillard-Giteau, 2010). The tri-phasic profile is not optimum for drug delivery as

therapeutic levels may be too high during the burst and will not be maintained during the lag phase.

An alternative method of using PLGA microparticles for drug delivery is to add the drug within a carrier solution to 'empty' PLGA microparticles to form a paste. They can then be sintered at their glass transition temperature to produce scaffolds of defined size from which the active will leach after implantation. This approach has been effective at delivering antibiotics to combat otitis media with effusion (Daniel, 2012).

Cumulative release profiles are often plotted showing the percentage of drug released against time as this highlights different rates of release. Figure 1.9 shows some of the typical traces seen. The most common traces achieved from polymeric systems are diminishing profiles, tri-phasic or bi-phasic profiles. For some applications such as arthritis, a pulsatile release is more applicable and there are ways to achieve this by developing a biomaterial in which the active is layered or a biomaterial that is sensitive to for example, pH or temperature (Sharma, 2010). For many drugs or growth factors the optimal release would be linear zero order with the option of different rates of release. For example, it would be advantageous for angiogenic growth factors to be delivered in a sustained manner but quicker than osteogenic growth factors for optimal tissue repair (Kempen, 2009).

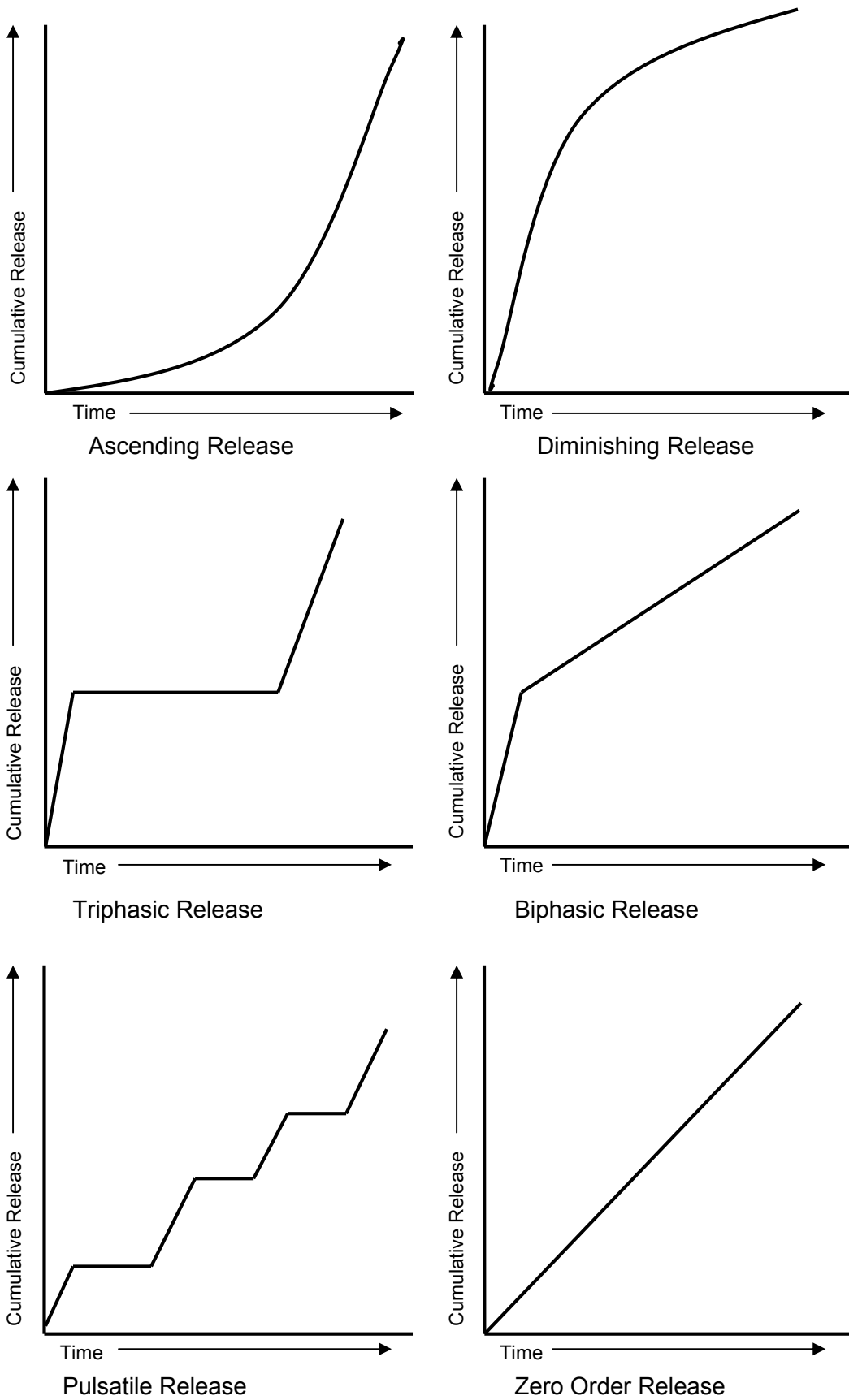


Figure 1.9 Typical cumulative release traces from delivery systems

1.11.2 Reducing burst and creating a sustained release profile

The avoidance of a high burst release is important and especially so for the delivery of rhBMP-2, as recently, complications have been highlighted with the clinical use of rhBMP-2 and these are mainly due to poorly controlled doses leading to overgrowth and uncontrolled bone formation, soft tissue swelling, pain, bladder retention, male infertility and osteolysis (Perri, 2007, Zara, 2011, Carragee, 2011, Helgeson, 2011).

Strategies adopted to reduce the initial burst have involved altering microparticle manufacture procedures to modify internal morphology (Igartua, 1997, Mao, 2007), altering the protein molecular weight and/or loading (Sandor, 2001, Boerckel, 2011), modifying protein with additives to improve stability (Diwan, 2001, Morita, 2001) or modifying the PLGA with the addition of a hydrophilic component (Cleek, 1997, Kirby, 2011). There are two review papers written in 2004 and 2008 which summarise all of the above strategies to reduce burst release and improve protein release profiles (Yeo, 2004b, Giteau, 2008).

Creating a sustained release profile which is linear with time is often the ideal *for in-vivo* delivery of growth factors but it is rarely reported and incomplete protein release is often cited as a problem (Giteau, 2008, Wischke, 2008). Different strategies have been applied to further understand profiles ranging from the use of continuous flow systems (Hernandez, 1998, Aubert-Pouessel, 2002), the comparison of static and dynamic systems (Hernandez, 1998), the effect of release medium and embedding PLGA spheres in hydrogel composites (Galeska, 2005). Progress has also been made in releasing

multiple growth factors simultaneously from a single scaffold (Raiche, 2004, Jaklenec, 2008, Saif, 2010).

The understanding of the processes involved in encapsulation and releasing proteins from microspheres for sustained delivery has improved over the years but there is no standard protocol that can be applied to all proteins due to their unique structure, molecular weight and charge and so substantial development is required to achieve successful delivery systems for a number of therapeutic proteins.

1.12 Determining the efficacy of microparticulate delivery systems by *in-vitro*, *ex-vivo* and *in-vivo* models for bone regeneration.

The discovery and development of new biomaterials for drug or growth factor delivery requires extensive research to determine the chemistry and the release profiles of the delivery device. It is then important to ensure that the bioactivity of growth factor is retained post release. Most *in-vitro* growth factor bioassays rely on cell proliferation, for example, commercial assays are available to detect various forms of FGF and PDGF which utilise the proliferation potential of the NR6R-3T3 mouse fibroblast cell line to respond to the growth factors (Rizzino, 1988).

The advantage of rhBMP-2 is that it will inhibit the differentiation pathway of the C2C12 myoblast cell line into myotubes and drive the differentiation into an osteoblast lineage (Katagiri, 1994). C2C12 cells exposed to rhBMP-2 will express alkaline phosphatase (ALP) activity with the levels of activity being directly proportional to rhBMP-2 concentration (Kim, 2004) and can be measured by changes in absorbance at 405 nm.

Although the enzyme linked immunosorbent assay (ELISA) is often used to detect released growth factors, it is a technique that can only quantify the presence of the active molecule and is not a measure of its biological function.

The middle ground between *in-vitro* assays and animal studies is usually *ex-vivo* assays and the fertile chicken egg has become a useful tool in this research area. Once the chorioallantoic membrane (CAM) has developed, its blood vessel network provides an optimal environment for research. Since the lymphoid system is not fully developed, the CAM can sustain tissues being grafted onto it without rejection. Researchers have used the CAM model to assess bone repair and the effect of biomaterials on repair using the CAM assay (Vargas, 2009, Wei, 2011). The assay is very labour intensive and often gives variable results but it provides a useful tool for screening formulations prior to animal studies.

Although studies on small animal models to determine bone repair have been performed (Lee, 1994, Rahman, 2012a), there are issues with self healing and therefore most animal models of bone repair involve the use of large animals such as sheep to investigate the repair of critical sized defects (Pilliar, 2007) or spinal fusion (Khan, 2004). The nature and the cost of such studies is prohibitive for screening a large number of formulations and therefore, it is essential that the early laboratory research and development is performed to the highest standard to give value to pre-clinical studies.

1.13 Summary of introduction and future aims

Regenerative medicine has gained prominence in recent years leading to innovative approaches to many aspects of tissue engineering. In particular, there is a high clinical need within the orthopaedic market for bone void fillers. Improvements over products currently available would potentially give the surgeon the chance deliver growth factors or even stem cells to the patient within a scaffold to improve their prognosis. This introduction has highlighted the wide range of naturally occurring and synthetic materials available for use in bone tissue engineering as well as discussing different methods of fabricating them into potential medical devices.

The thrust of the project described within this thesis, is to create novel microparticulate scaffolds to deliver selected growth factors in a controlled manner with the potential to serve as injectable biomaterials for skeletal repair.

The aims of the following results Chapters are as follows:

Chapter 2

- To develop a protocol to create biodegradable microparticles
- To control microparticle size and morphology
- To investigate PLGA degradation
- To optimise the entrapment efficiency of model protein

Chapter 3

- To characterise a PLGA-PEG-PLGA triblock copolymer
- To assess the degradation of PLGA/copolymer blends
- To control the release of model protein from microspheres
- To determine reproducibility of the release profiles
- To ensure that the model protein remains biologically active throughout

Chapter 4

- To translate the technology from model protein to rhBMP-2 delivery
- To use a thermosensitive scaffold to support to the microparticles
- To determine that biological activity of rhBMP-2 is retained post release from microparticles.

Chapter 5

- To investigate chick embryonic bone growth both *in-ovo* and *in-vitro*
- To develop an *ex-vivo* model of bone repair using the chick embryo
- To determine to effect of growth factor loaded microparticles on the chick femur defect model.

The key theme that will run throughout the course of the work within this thesis will be the need to produce high quality results that are reproducible from one study to the next to give confidence in the data and added value to future studies. If successful, the biomaterials developed during the course of this work will go forward to a large animal critical sized defect model of bone regeneration and repair.

Chapter 2: Development of techniques to fabricate protein loaded PLGA microparticles with control over size, morphology and entrapment efficiency

2.1 Introduction

Biodegradable polymer microspheres have been used for many years in the field of tissue engineering as three dimensional scaffolds for tissue support as well as for drug delivery devices. However, despite extensive research, there still remains a requirement for an efficient tissue-engineered substitute for autologous bone grafting that will provide an adequate environment for successful new tissue growth.

The method for fabricating spherical polymer microparticles (MPs) via emulsion is a relatively straightforward procedure but, there are a number of variables which are inter-related and these will have an impact on the MPs with regard to their size distribution and the encapsulation efficiency of the loaded drug all of which will in turn, impact on the efficiency of the biomaterial. Some research groups that have investigated a few of the formulation variables involved within the emulsion process such as, the continuous and dispersed phase volumes, the stabiliser concentration, the freeze drying process and amongst others, the fabrication temperature (Igartua, 1997, Yang and Chung, 2000, Mao, 2007). But, most of the research has been related to the subsequent release profile of loaded molecule and the fine control of MP size within the 1 to 100 micron size range is not well documented even though this parameter may be paramount to understanding the release profiles (Namur, 2006).

Being able to finely tune the MP size range would be of considerable benefit. A tight microparticle population would be more likely to release the loaded growth factor or drug in a predictable and reproducible manner and would therefore give more confidence that the correct dose is being delivered to the patient. Also, having a tighter control over the size range would also improve the efficiency of new injectable devices allowing the localised administration of MPs in a minimally invasive manner (Hou, 2004). The narrowly defined MP size would also cut down wastage as post manufacture processing such as sieving would not be required thus the manufacturing process would be more cost effective.

Researchers at the University of Nottingham had previously used PLGA MPs for *in-vitro* studies of drug release but the MPs that were used had a population range from 50 to 500 μm (Figure 3.1). The procedures to manufacture the MPs were not standardised or tightly controlled, thus, the size of the resulting MPs was variable. This method employed a vortex mixer to create emulsions and was very user dependent and therefore a difficult process to control. The quality of emulsion was influenced by how the tube was held on the vortex mixer and the speed at which the mixer was set. Sieving the MPs post manufacture to the desired size could result in up to 50% loss of yield. Clearly, this method required investigation and improvement to optimise the MP yield.

Although, the control of size had not been the main goal for this previous work, having robust protocols in place for MP production would not only potentially improve work on growth factor release but, also give added value to other projects within the Tissue Engineering group at Nottingham by minimising time spent on development. The acquisition of a Silverson L5M homogeniser was

the chief driver for this work, the advantage of this machine over other homogenisers was the fine control over speed and its ability to operate at speeds as low as 500 rpm.

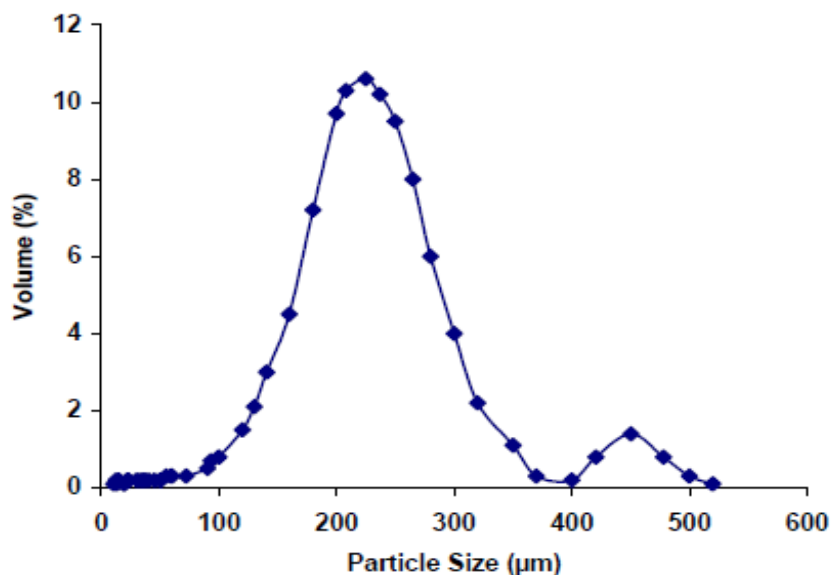


*Figure 2.1 Representative particle size distribution of MPs
(taken from A. Olaye thesis submitted February 2009)*

Many other groups have worked with PLGA MPs as tools for drug delivery but although nearly all characterise them by size often only the average size is stated rather than the complete size range of the MPs. Amongst others, typical sizes that have been reported are 26.6 µm (Jiang, 2002), 23 -31 µm (Morlock, 1996) or 35-40 µm (Morita, 2000b). Other groups have manufactured larger MPs for example 266 ± 100 µm (Friess, 2002) or 89.38 ± 28.05 µm (Chun, 2004). However, in each case the MP size had not been tailored for the application but seemed to be merely a result of the adopted protocol. A published protocol using the double emulsion method to create MPs specifically in the size range of 50 – 100 µm required a sieving step post manufacture. This would have been detrimental to final yield which is

especially important to avoid if the MPs have an expensive growth factor as cargo (Bible, 2009).

The objectives for the first part of this Chapter were therefore to thoroughly interrogate the double emulsion process to enable the reproducible production of spherical MPs with defined size ranges. The use of a homogeniser rather than vortex mixer will be investigated for the production of all the size ranges required for planned studies. The aim was to cut down both inter-batch and intra-batch variability by standardising the protocol wherever possible.

As well as standardising MP size, the method of protein loading required optimisation. It is reported that protein denaturation occurs at a water oil interface and therefore single emulsion techniques are potentially better than double emulsion techniques (Sah, 1999, van de Weert, 2000b). Although, a wide range of entrapment efficiencies have been reported using both techniques. Diwan and Park used the W/O/W method and recorded an entrapment efficiency of lysozyme in PLGA MPs of 39% but this was improved with pegylation of the molecule to 76% (Diwan, 2001). Work by Kang reported entrapment efficiency values for bovine serum albumin (BSA) into PLGA MPs of 40-50% (Kang, 2001). Yang showed that encapsulation efficiency increased as BSA concentration was reduced but values of around 50% for encapsulation efficiency were typical (Yang, 2001). The S/O/W emulsion technique is reported to improve the entrapment efficiency over W/O/W techniques (Morita, 2000b). In addition, S/O/O techniques along with pegylation of the protein have been reported to give entrapment efficiencies of 73 - 98% (Al-Azzam, 2002). An MP manufacture technique that does not require pre-treatment of the active molecule and has good entrapment

efficiency will ensure that any loss of the active ingredient during processing is kept to a minimum.

Therefore, the aim of the second part of this Chapter was to achieve entrapment efficiencies of a model protein that were as high as possible and above values reported in the literature. We aimed to achieve entrapment efficiencies of greater than 50% and hypothesised a higher entrapment efficiency could be achieved by altering manufacture parameters.

To achieve this firstly, a bulk carrier protein was added to the model protein to shield it from the water/oil interface (He, 2011) and secondly, manufacturing parameters were controlled and standardised for optimisation of entrapment efficiency.

Lysozyme is a common model protein for cytokine and growth factor research and it was selected for this work to model the growth factor recombinant human bone morphogenetic protein -2 (rhBMP-2) due to the similarity of isoelectric points (lysozyme: 9, BMP-2: >8.5) and molecular weights (lysozyme: 14 kD, BMP-2: 26 kD). It is widely available and cheap to purchase but importantly, its activity and therefore stability can be detected *in-vitro* by using a *Micrococcus lysodeikticus* bioassay (Saint-Blancard, 1970, Sah, 1997).

2.2 Materials and methods

2.2.1 Equipment, consumables and materials

All the laboratory equipment, consumables and chemicals used during the work for this Chapter can be sourced in Appendix I, tables A1, A2 and A3 where the manufacture, model, catalogue number and supplier are stated.

Where microparticle (MP) batch numbers are stated, the details of the manufacturing parameters can be found in Appendix II.

2.2.2 Micronisation of lysozyme and human serum albumin (HSA) with PEG6000

This method was adapted from that of Morita (Morita, 2000a) and was used to manufacture MPs containing lysozyme alone, HSA alone and a combination of lysozyme and HSA. Twenty batches of micronised protein were made at one time to reduce batch to batch variability with the intention of using this for a 5% total protein loading into 1 g of PLGA. A 40% _(w/v) PEG6000 solution was made by weighing 40g of PEG6000 and adding 100 ml of distilled water. This was kept under magnetic stirring at a gentle speed for 2 hours. Lysozyme (1 g), HSA (1 g) or a combination of lysozyme (0.02 g) and HSA (0.98 g) was weighed into a 50 ml volumetric flask and 20 ml of the 40% PEG6000 solution was added. Distilled water was then added up to a volume of 50 ml and the solution was stirred for 1 hour. The _(w/v) 40% PEG6000/protein solution was added (2.5 ml) to twenty glass scintillation vials and these were covered, snap frozen in liquid nitrogen and freeze dried overnight. The vials were vacuum packed and stored frozen until required. Each vial contained 50 mg of protein sample in 400 mg of PEG6000. Batches of PEG6000 alone were prepared for loading into MPs to act as blank controls. Acknowledgement goes to Giles Kirby (PhD student, School of Pharmacy, University of Nottingham) for preparing the batches.

2.2.3 Preparation of lysozyme in human serum albumin (HSA)

Ten batches of lysozyme/HSA were made at one time to reduce batch to batch variation. For a 5% _(w/w) total loading into 1 g of PLGA, 450 mg of HSA was weighed into a microcentrifuge tube followed by 50 mg of lysozyme to which 1 ml of distilled water was added. The tube was gently rocked until all the protein was dissolved, the contents were then stored frozen in 100 μ l aliquots each containing 45 mg HSA and 5 mg lysozyme.

For a 1% _(w/w) total loading into 1 g of PLGA, 90 mg of HSA and 10 mg of lysozyme were weighed and stored in the same way.

2.2.4 Microparticle manufacture

2.2.4.1 Solid in oil in water emulsion method (S/O/W)

Previously prepared batches of micronized lysozyme were used for the S/O/W emulsion method of MP manufacture (Section 2.2.2) and the method was modified from Morita (Morita, 2000b) and a schematic of the method is shown in Figure 2.2A. An aqueous solution of polyvinyl alcohol (PVA) at 0.3% _(w/v) was prepared by adding 3 g of PVA to 1 litre of distilled water and gently stirring overnight. Generally, MP batch sizes of 1 g were prepared and so 1 g of PLGA of the required Lactide: Glycolide (L: G) ratio and molecular weight was weighed into a glass vial. If any PLGA-PEG-PLGA was to be added to PLGA then the mass was reduced to accommodate the triblock copolymer (e.g. 10% _(w/w) triblock would be 100 mg triblock and 900 mg of PLGA) and the organic solvent dichloromethane (DCM) added.

The volume of DCM affected the resulting MP size but generally for most batches 5 ml was added (PLGA concentration 20% _(w/v)) where other volumes are used it will be stated in the results. Once dissolved (approximately 30 minutes on an orbital shaker), the PLGA/DCM was added to the lyophilised PEG/lysozyme and placed on a vortex mixer set at 2,200 rpm for 45 seconds to thoroughly disperse the protein within the oil phase. The 0.3% _(w/v) aqueous solution of PVA was passed through a 0.2 µm filter unit under vacuum and 200 ml was measured into a 250 ml beaker.

The PLGA/DCM/Lysozyme/PEG6000 solution was transferred to the PVA solution and mixed using a Silverson L5M homogeniser fitted with a square hole high shear screen for 2 minutes at 2,000 rpm. A 50 mm glass magnetic follower was added and the beaker was stirred at 300 rpm for 4 hours on a magnetic stirring plate to allow the solvent to evaporate. The MPs poured into a Nalgene 0.2 µm filter unit and were washed with 1 litre of distilled water, before being collected in a small volume using a Pastette. The tubes were covered then snap frozen in liquid nitrogen and freeze dried. For storage, the tubes were vacuum packed and kept frozen until required.

2.2.4.2 Water in oil in water emulsion method (W/O/W)

This method was adapted from that of Bible (Bible, 2009) and a schematic of the process is shown in Figure 2.2B. Previously prepared protein solution was supplied in 100 µl aliquots used for MP manufacture (Section 2.2.3). PVA solution (0.3% _(w/v)) was prepared by adding 3 g of PVA to 1 litre of distilled water and stirring gently overnight. The PVA solution was then passed through a 0.2 µm filter and 200 ml measured into a 250 ml beaker (one per batch).

The required polymer composition (e.g. PLGA ± PLGA-PEG-PLGA triblock copolymer) was weighed, to give a total of 1 g, into a PTFE screw top jar and DCM added. The volume of DCM affected the resulting MP size but in general, 5 ml was added (PLGA concentration 20% _(w/v)) where other volumes are used it will be stated in the results. The jars were placed on an orbital shaker for 30 minutes for the polymer to dissolve. The 100 µl aliquot of prepared protein (HSA/lysozyme) was added to the PLGA/DCM and homogenised using the Silverson L5M for 2 minutes. The speed would affect the MP size but in most cases 4,000 rpm was used for the primary emulsion. This emulsion was then transferred to 200 ml of 0.3% _(w/v) PVA and further homogenised for 2 minutes to produce a secondary emulsion. The speed was set at either 2,000 or 9,000 rpm depending on MP size required. A 50 mm glass magnetic follower was added and the beaker was stirred at 300 rpm on a magnetic stirring plate for 4 hours to allow the solvent to evaporate.

Depending on the expected size of the MPs they were collected by filtration (for >30 µm MPs) or by centrifugation (for <30 µm MPs). The filtration method is described in Section 2.2.4.1 and for centrifugation, the beaker contents were split into four 50 ml centrifuge tubes, spun at 3,000 rpm (MSE Mistral 1000) for 3 minutes and washed 5 times with 50 ml distilled water, eventually transferring the MPs into just one tube where they were covered, snap frozen in liquid nitrogen and freeze dried. For storage, the tubes were vacuum packed and kept frozen until required.

2.2.4.3 Oil in water emulsion method (O/W)

The oil in water method of MP manufacture can be used if the active to be encapsulated is soluble in oil phase or, as in this case, it can be used to

prepare PLGA MPs that have no protein loading. For a single batch, 1 g of PLGA was weighed into a glass vial and the required amount of DCM added (usually 5 ml). Once the polymer had dissolved, it could be added to a 200 ml bath of 0.3% _(w/v) PVA and homogenised at 2,000 rpm for 2 minutes. The resulting emulsion was then stirred at 300 rpm on a magnetic stirrer for 4 hours to allow the DCM to evaporate. The MPs were then washed and collected by either centrifugation or filtration and freeze dried (as described above).

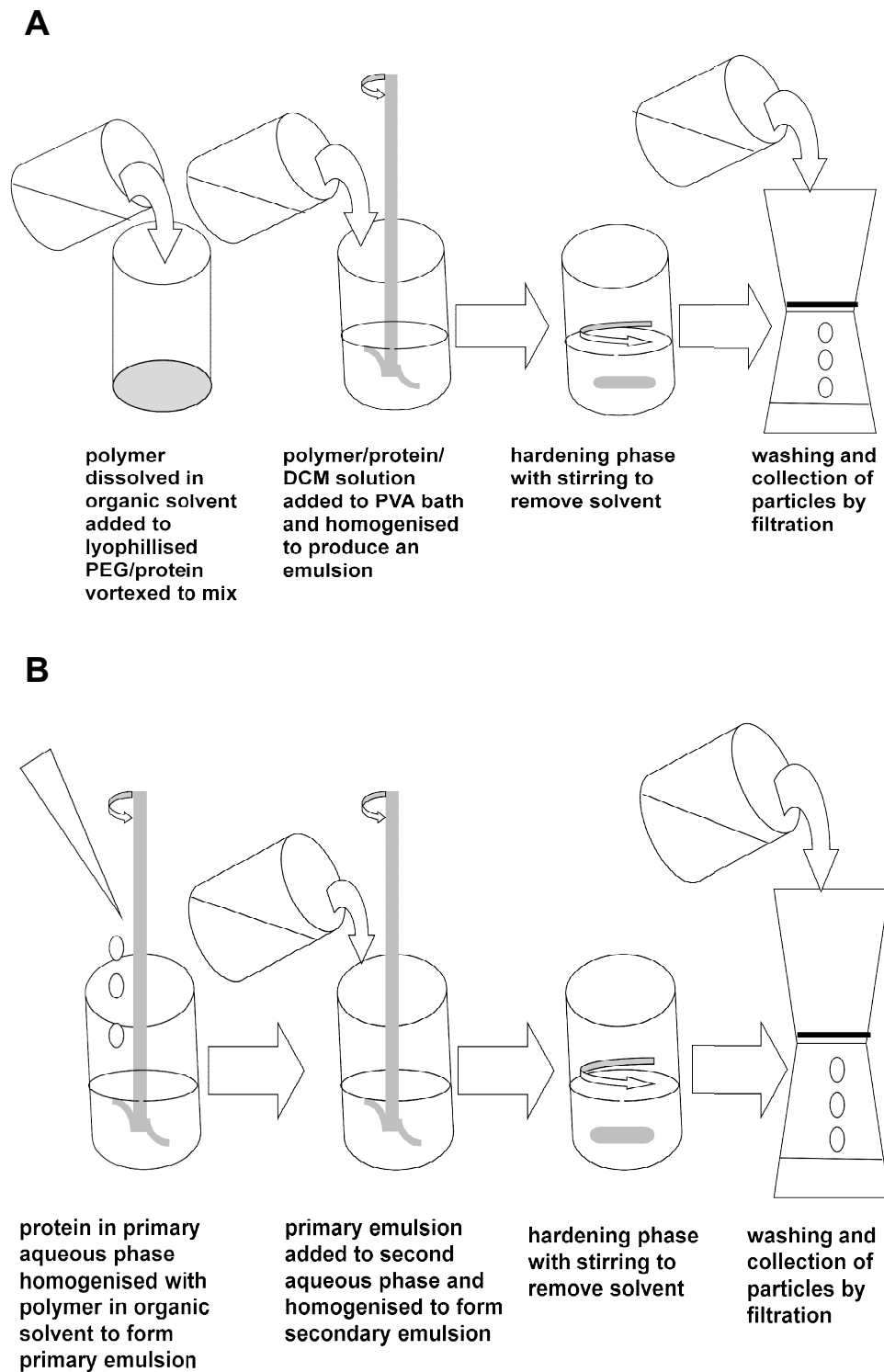


Figure 2.2 Schematic showing [A] the solid in oil in water (S/O/W) emulsion method of PLGA microparticle manufacture and [B] the water in oil in water (W/O/W) emulsion method of PLGA MP manufacturing.

2.2.5 Microparticle sizing: Laser diffraction

MPs were sized using a Coulter LS230 machine by suspending a representative population of MPs in water in a micro volume cell under stirring. MPs were added until the optimal amount was achieved which was indicated by the obscuration value which must be between 8 and 12 %. Obscuration is a measure of the percentage of light that is attenuated due to extinction (scattering and/or absorption) by the particles. A broadened beam of laser light was then passed through the MPs, the scattered light was focussed by a Fourier lens onto a detector array and, using an inversion algorithm, a particle size distribution was inferred from the collected diffracted light data using a garnet optical model (Micromeritics, 2000).

A number of tests were performed to determine the length of the run required and whether repeat runs on the same sample were necessary. This data is shown in Appendix IV. As a result, runs were measured for 30 seconds with just one reading for each batch. Traces of MP diameter were plotted against the diffraction percentage as a function of volume.

2.2.6 Microparticle imaging: Scanning electron microscopy

Thin layers of MPs were attached to an adhesive stub and gold sputter coated for six minutes at 30 mA using a Balzers SCD 030 sputter coater. MPs were imaged at a range of magnifications using a JSM 6060LV Scanning Electron Microscope (SEM) (JEOL, Welwyn Garden City, UK) with the accelerating voltage set to 10 kV. Acknowledgement goes to Dr Lisa White for performing some of the imaging.

2.2.7 PLGA degradation studies

2.2.7.1 pH study: Comparison of PLGA lactide: glycolide ratio

MPs in the size range of 50-100 μm were manufactured from PLGA 85 15 (56 KDa) and PLGA 50 50 (59 KDa) with the incorporation of 30% $_{(w/w)}$ PLGA-PEG-PLGA triblock copolymer (TBII-C). The MPs (100 mg) were suspended in 3 ml of PBS in a 15 ml tube and allowed to rock at 5 rpm on a 3D rocker. At various time-points over a 60 day period, the PBS was collected and replaced with fresh. The pH of these supernatants was determined using a calibrated pH meter. A scatter-plot of pH against time was prepared for both batches of MPs.

2.2.7.2 Mass loss study: Effect of temperature and PLGA-PEG-PLGA content on degradation

MPs were manufactured using PLGA 5:50 (59 KDa) in the 20-30 μm size range without and modification with triblock copolymer (10, 20 and 30% $_{(w/w)}$). MPs (20 mg) were weighed (in triplicate) into microcentrifuge tubes and 1.5 ml of PBS was added. The MPs were thoroughly re-suspended and the tubes were placed on their side at either 37°C or 45°C. At weekly intervals, the tubes were centrifuged at 3000 rpm (MSE Mistral 1000) for 3 minutes and the supernatants removed. The MPs were dried overnight on a freeze drier and the tubes were then re-weighed. Once weighed, fresh PBS was added, the MPs re-suspended and replaced in their incubation conditions. Mass loss over time was determined by calculating the remaining mass in each tube as follows:

(Mass of tube + MPs at each time-point) – (original mass of tube)

The remaining mass of MPs was plotted against time for both temperatures

2.2.7.3 Morphology study: Effect of degradation on microparticle morphology

MPs were manufactured using PLGA 5:50 (56 KDa) in the 20-30 μm size range with the incorporation of 10% $_{(w/w)}$ PLGA-PEG-PLGA triblock copolymer (TBII-C). A number of replicates of MPs (25 mg) were suspended in 1.5 ml PBS in microcentrifuge tubes and placed on a 3-D rocker set at 5 rpm in a 37°C humidified incubator. After 3, 9, 14, 20 and 28 days, some of the PBS was removed and the remainder was removed by drying the MPs overnight on a freeze drier. The MPs were then imaged using a JSM 6060LV SEM to determine any changes in their morphology.

2.2.8 Total protein detection: Bicinchoninic acid assay (BCA)

The BCA assay was used to assess the entrapment efficiency of MPs as described below as well as measuring total protein release from MPs which is described in the following Chapter.

2.2.8.1 Assessment of encapsulation efficiency of microparticles

Measurement of the protein encapsulation efficiency was adapted from the method by Sah (Sah, 1997) and determined by dissolving 10 mg of protein loaded PLGA microspheres in 750 μl DMSO followed by the addition of 2150 μl of 0.02 % $_{(w/v)}$ SDS in 0.2M NaOH. The micro BCA protein assay kit which

detects protein by the reduction of Cu^{2+} to Cu^{1+} and subsequent chelation of Cu^{1+} with BCA to give a colourmetric response, was used. The BCA working solution (150 μl) was plated out with 150 μl of the dissolved MP solution with appropriate calibration standards (i.e HSA/lysozyme in a range of 1-40 $\mu\text{g}/\text{ml}$) using DMSO/NaOH/SDS solution as the diluent. Absorbance was measured after 2 hours of incubation at 37°C at 562 nm on a plate reader (Tecan, Infinite M200). The total protein was calculated from the polynomial equation of the standard curve. Entrapment efficiency can then be calculated as follows:

$$\left(\frac{\text{Actual mass of protein in a 10 mg sample of MPs}}{\text{Expected mass of protein in 10 mg sample based on loading}} \right) \times 100$$

2.2.9 Lysozyme activity: *Micrococcus lysodeikticus* assay

The determination of lysozyme activity was based on the fact that lysozyme would preferentially hydrolyze the β -1,4 glycosidic linkages between N-acetylmuramic acid and N-acetylglucosamine which occur in the mucopeptide cell wall structure of the bacterium *Micrococcus lysodeikticus*. Therefore, a turbid bacterial solution will become clear upon bacterial cell lysis and the reduction in the absorbance measurement at 450 nm would be directly proportional to lysozyme concentration (Saint-Blancard, 1970). Each test sample in triplicate (150 μl) was added to 100 μl of an aqueous solution of *M. lysodeikticus* at 2.3 mg/ml and the absorbance at 450 nm was measured at 0 and 1 minute. The difference between the two readings indicated lysozyme activity. A standard curve was drawn (linear between 0.1-10 $\mu\text{g}/\text{ml}$) and the concentration of the lysozyme in the test samples was calculated from the equation of the straight line.

2.2.10 Statistical analysis

Where error bars are presented on figures, they were calculated from the standard deviation of the mean with a minimum replicate number of three.

Values for protein concentration were calculated from either the polynomial equation or the straight line equation of the appropriate standard curve as stated.

Where statistical analysis was stated, unpaired, two-tailed *t*-tests were performed using Graphpad 'quickcalcs' software. The probability value of *P* denotes the likelihood that the results were achieved by chance (e.g. $p < 0.05$ equates to a probability of the results being obtained by chance being less than one in twenty). Significant was apportioned as follows: * equals $P < 0.05$, ** equals $P < 0.01$ and *** $P < 0.0001$ and > 0.05 is not significant (ns).

2.3 Results and Discussion

2.3.1 Control of microparticle size

The initial investigation into MP size was to manufacture PLGA MPs without any drug or protein loading by using the oil in water (O/W) emulsion technique. Three batches were made with a 20%_(w/v) PLGA 85 15 solution in DCM and were mixed using the homogeniser set at 9,000 rpm in a 0.3%_(w/v) polyvinyl alcohol solution (PVA). DCM was the chosen organic solvent as it is widely used and has been shown to produce MPs with good entrapment efficiencies (Birnbaum, 2000). The DCM was allowed to evaporate overnight under continuous stirring. The only difference between the three batches was the magnetic stirring speed which were attributed as 'fast', 'medium' or 'slow' as the stirrers used did not have an rpm readout. The difference in stirring speed during evaporation had a profound effect on the MP size. The 'fast' group had a mean diameter of 31 μm , the 'medium' group were 44 μm and the 'slow' group had a mean diameter of 59 μm . This parameter was soon standardised to 300 rpm for all subsequent MPs manufactured by the acquisition of a multiway stirrer plate with controlled stirring speed. It was also necessary to standardise the method to measure MP size at an early stage of the project to ensure that all future size distributions were comparable. The administration of sample, the run time and the settings on the Coulter LS230 were optimised through experimentation, written up as a standard protocol and used for all future size analysis.

As discussed earlier (Chapter 1 Section 1.7.2), the S/O/W emulsion method of protein encapsulation was predicted to be the best method for MP manufacture due to there being only one aqueous interface and therefore this

method was initially chosen to make MPs that were used for size distribution comparisons. The original vortex mixer method was directly compared to a method developed using a Silverson homogeniser both set at 2,000 rpm and the size distribution results are shown in Figure 2.3. Upon visual inspection, there was a clear difference between the size distribution profiles with the vortex prepared batch having a much wider distribution. The deviation about the mean for the vortex mixer batch was 36% compared to 23% for the homogeniser made MP batch. The mean MP size for the homogeniser batch was $111 \pm 33 \mu\text{m}$ with the median being $114 \mu\text{m}$ (data direct from Coulter L5M). The mean MP size for the vortex mixer batch was $84 \pm 47 \mu\text{m}$ with the median being much lower at $68 \mu\text{m}$. The MPs manufactured using the homogeniser demonstrated a mathematically more normal size distribution.

A further advantage of the homogeniser is that the rotor can be set and left to run without intervention, therefore potentially cutting down on batch to batch variation as well as improving the size distribution of MPs within each batch.

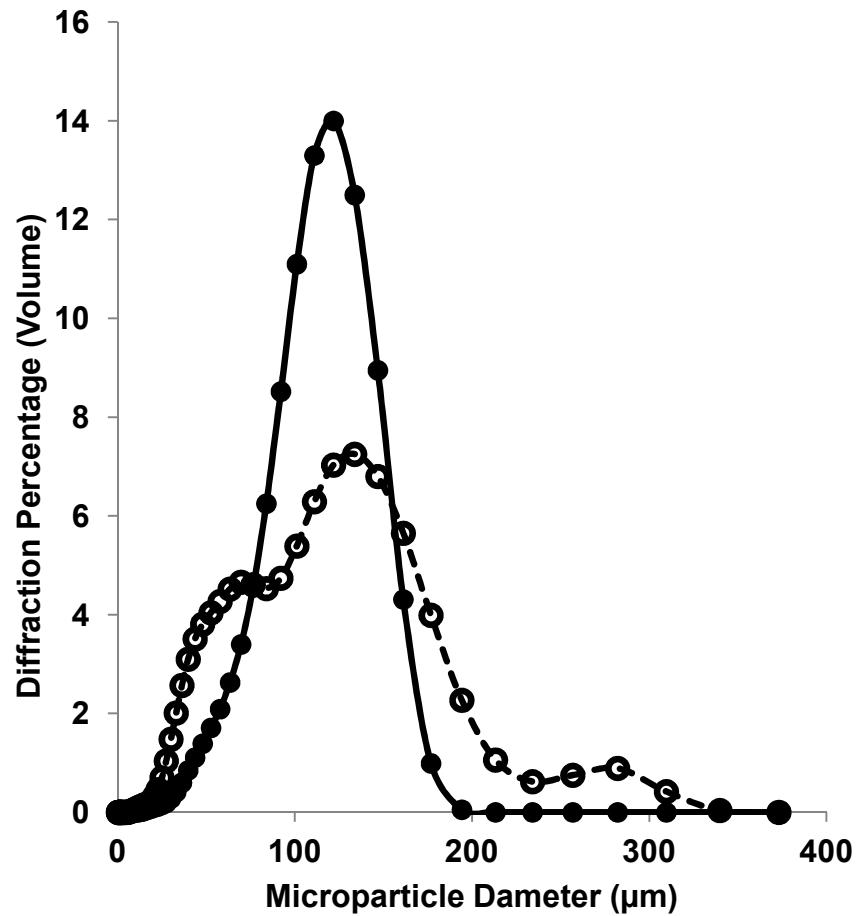


Figure 2.3: MP size distribution comparing manufacture by vortex mixer (○) and manufacture by homogeniser (●). The mean MP size for the vortex mixer batch was $83 \pm 47 \mu\text{m}$ and for the homogenised batch $112 \pm 33 \mu\text{m}$. Both batches were loaded with 5% lysozyme/PEG6000 following S/O/W method and manufactured from PLGA 50 50 Mwt 59KDa

Batches: BN 81 and 83

These results meant that the manufacture of MPs using the Silverson L5M homogeniser was now the preferred method over the vortex mixer and further studies were performed to standardise the protocol. This work was part of a mini-project by MPharm students performed under my joint supervision and investigated the effect of rotor speed, rotor position and mixing time on the size distribution of the resulting MPs. Figure 2.4 shows the main findings of this work. In short, the homogeniser speed setting has an effect on the MPs size with the fastest speed resulting in the smallest MPs (Figure 2.4A) when a 2 cm rotor height and a 2 minute homogenisation time was used. This is a logical result as the increased shear forces involved with higher rotor speed will result in smaller W/O droplets being formed (Walstra, 1993) and therefore this parameter would be important to control in future studies of MP size.

The height of the rotor in the emulsifying bath did not affect the MP size at all when a speed of 2,000 rpm and a time of 2 minutes were used (Figure 2.4B). However, this is not to say that rotor height should not be controlled as other speeds and times may have had an effect on MP size. The rotor height was therefore fixed at 2 cm for all future batches.

Finally, the time of homogenisation was tested against a 2 cm rotor height and a 2,000 rpm rotor speed (Figure 2.4C). The results showed that this did have an effect on MP size. MPs produced after 3 minutes of mixing were less than half the size ($40 \pm 16 \mu\text{m}$) than those produced after 2 minutes of mixing ($100 \pm 42 \mu\text{m}$). Although, just 1 minute of mixing did not produce any larger MPs, the distribution was wider ($93 \pm 46 \mu\text{m}$). This was obviously a key parameter to control and therefore a 2 minute homogenisation time was adopted for all future batches.

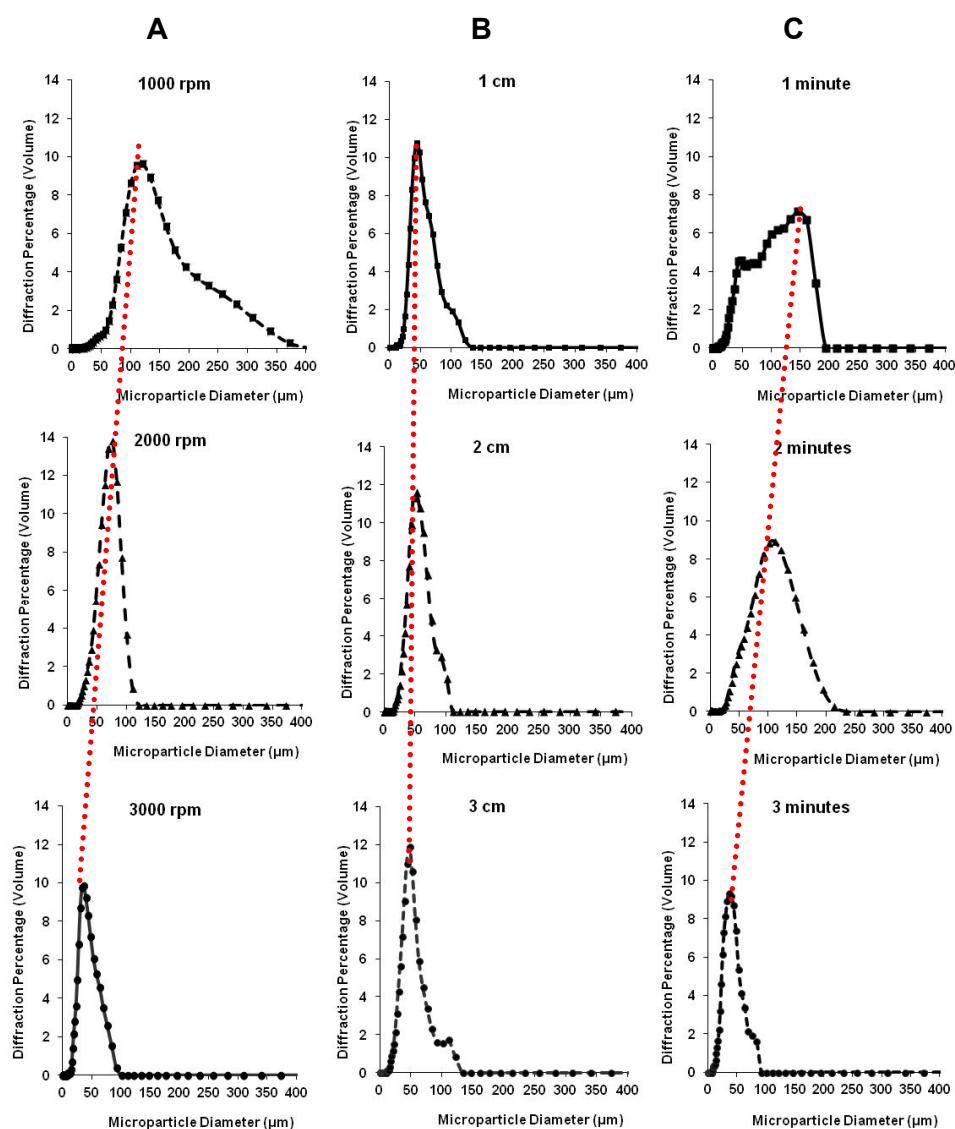


Figure 2.4: Optimisation of MP manufacture process. [A] shows the effect of homogeniser speed [B] shows the effect of rotor height and [C] shows the effect of homogenisation time. The red dashed line crosses through the peak values and highlights the effect on size due to the variable tested. All MPs were manufactured with PLGA 50/50 Mw 62 KDa and were loaded with 5% HSA/lysozyme following the S/O/W method.

(Batches from MPharm student project 2010 courtesy of Charlotte Walker, Annette Chen and Ria Godhania)

Data that will be discussed later in Section 2.3.5 will show that despite the literature citations, the S/O/W method of MP manufacture in our hands, did not give the best entrapment efficiencies and as a result the W/O/W emulsion method for entrapment of lysozyme was adopted and so MPs made by the two different methods were compared.

Triplicate batches of MPs were manufactured using the S/O/W and the W/O/W method to investigate the MPs size and the batch to batch variability of the protocols. The data for MPs loaded with 5% _(w/w) lysozyme is shown in Figure 2.5. The average size of the MPs manufactured using the S/O/W method was larger than those manufactured using the W/O/W method ($118 \pm 34 \mu\text{m}$ compared to $93 \pm 28 \mu\text{m}$) when a homogeniser speed of 2,000 rpm was used. This was not unexpected as the micronized lysozyme would have a particle size of around $5 \mu\text{m}$ (Morita, 2000a) and this would bulk out the MP during manufacture, whereas in the W/O/W method, the lysozyme is fully dissolved in an aqueous solution (Giunchedi, 1998). However, there was no statistical significance between the sizes of the MPs manufactured by each of the two methods.

The variation between the batches was acceptable as indicated by the standard deviation. The variability between the W/O/W batches in this case appeared greater than the variation between the S/O/W batches but it is important to note that the S/O/W batches were all made on the same day and the W/O/W batches were made on different days which would be likely to introduce more error due to for example, different batches of polyvinyl alcohol being used to stabilise the emulsion.

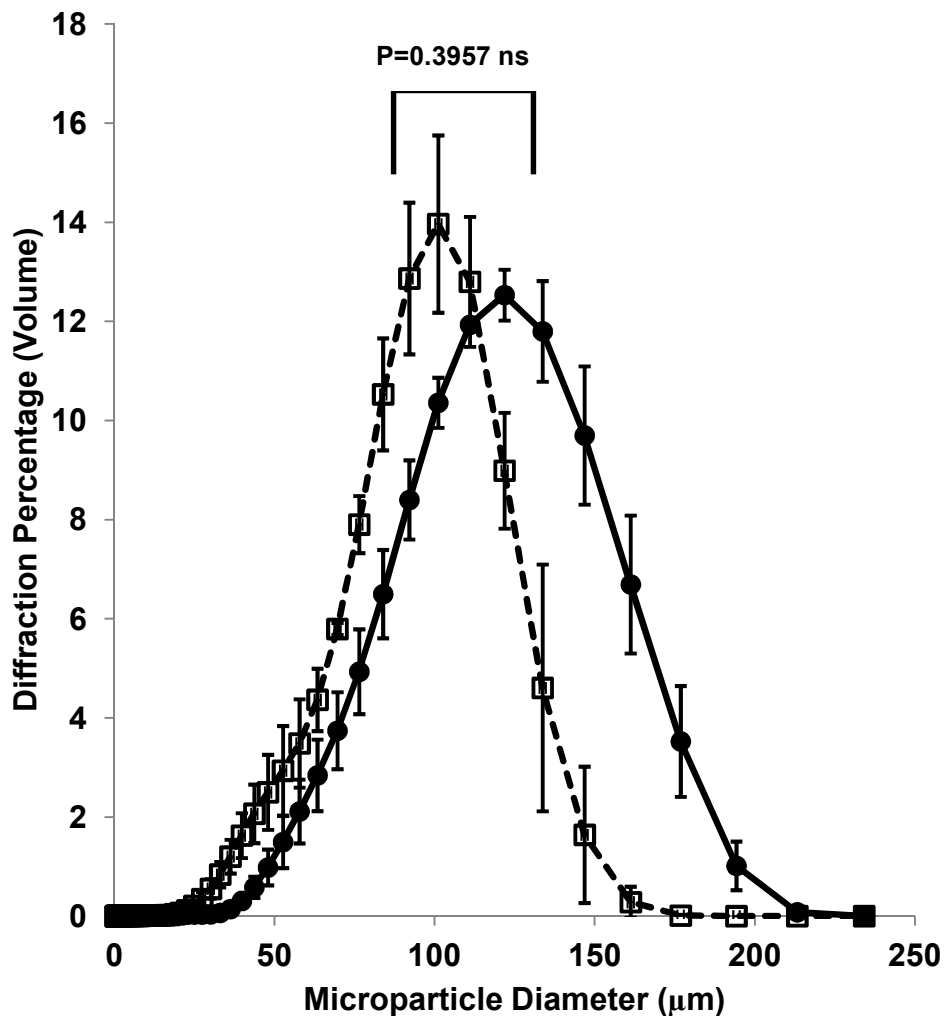


Figure 2.5: MP size distribution comparing the S/O/W method of manufacture (●) with the W/O/W method of manufacture (□). Each trace represents the mean of three separate MP batches (PLGA 50 50 59 or 62 KDa each with 5% total protein loading). The mean size distribution shifts from $118 \pm 34 \mu\text{m}$ for the S/O/W batch to $93 \pm 28 \mu\text{m}$ for the W/O/W batch.

(Batches: BN 69, 70 and 71 (SOW) and BN 117, 120, 96 (WOW))

The data has shown that the MP manufacture method and a number of parameters within the manufacture process will affect the outcome of the MP size. However until now, only a single PLGA concentration had been tested and it was thought that this variable would play a significant role in size distribution (Devrim, 2011). A comparative study was therefore carried out to look at the size distribution profiles of MPs manufactured with a number of PLGA concentrations but with all other manufacturing parameters kept constant. In this case the W/O/W method was used with a primary homogenisation speed of 4,000 rpm and a secondary homogenisation speed of 9,000 rpm both for 2 minutes duration. All of the MPs had a 1% _(w/w) total protein loading PLGA solutions of 2, 5, 10, 15 and 20% _(w/v) were used to manufacture MPs and their size distributions are shown in Figure 2.6.

As hypothesised, there was a clear effect on the MP size caused by PLGA concentration with the lowest PLGA concentration producing the smallest MPs (2.4 μm) and the highest PLGA concentration producing the MPs nearly ten times larger (21.6 μm). The effect is clearly shown by the trend line across the batches.

This can be explained by a number of factors, the higher PLGA concentration having a higher viscosity which in turn will require higher shear forces for droplet dispersion. If the energy input via the homogeniser remains the same and is not increased then the resulting MPs will be larger (Viswanathan, 1999, Hamishehkar, 2009). The resulting size may also be due to the maximum volume of a sphere that can be solidified as a function of polymer concentration. It was also concluded by Behrend that the viscosity of the dispersed phase has a more significant influence droplet size over the viscosity of the continuous phase provided coalescence is avoid by the addition of an emulsion stabiliser (Behrend, 2000).

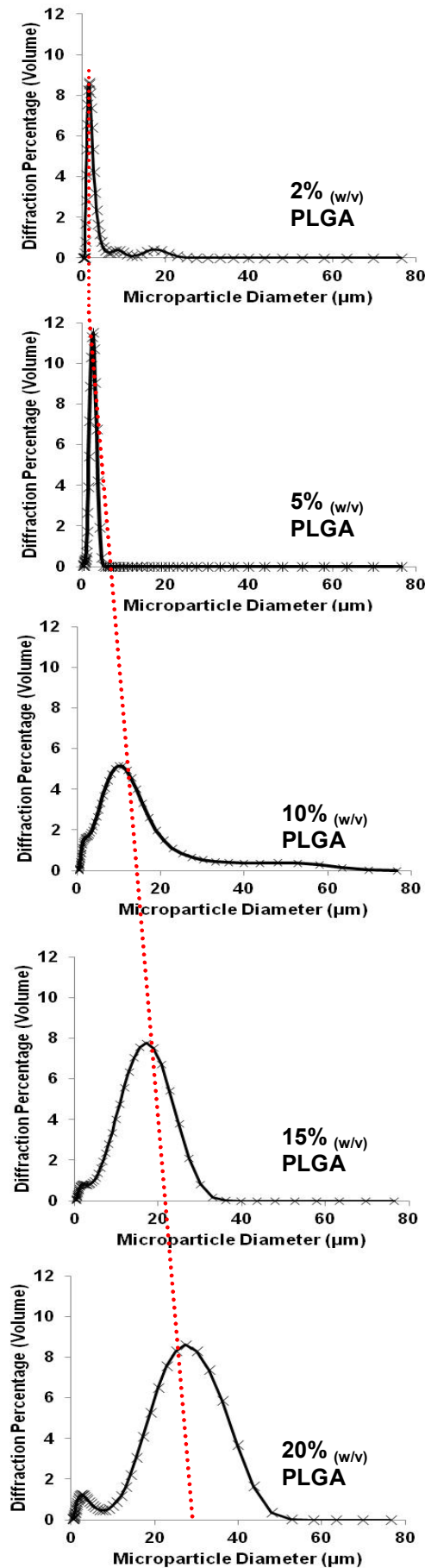


Figure 2.6: Control of MP size based on PLGA concentration.

The mean diameters were: 2% (w/v) PLGA 2.4 ± 2.5 µm, 5% (w/v) PLGA 2.5 ± 0.8 µm, 10% (w/v) PLGA 9.0 ± 8.9 µm, 15% (w/v) PLGA 13.8 ± 7.4 µm and 20% (w/v) PLGA 21.6 ± 7.4 µm.

All batches manufactured by W/O/W double emulsion with homogeniser speed set at 4,000 rpm for the primary emulsion and 9,000 rpm for the secondary

Batches: BN 48, 175, 43, 171 and 39

Through the data accumulated thus far, the impact of some of the process variables on MP size distribution was becoming clear. However, the optimum solvent evaporation time and MP collection method was still not determined. Data to be discussed in section 2.3.5 will argue that the shorter the solvent evaporation time, the better the entrapment efficiency of the MPs and therefore 4 hours was chosen as a standard parameter.

There are two main methods of retrieving and washing MPs prior to freeze drying, these being centrifugation and filtration. It is important to remove all traces of the PVA from the surface of the MPs but equally important not to damage the MPs during the process. Figure 2.7 shows the size distribution of two batches of MPs manufactured in exactly the same way with the only difference being the collection method. In this case, filter paper (pore size 2.7 μm) was used and whilst the size distribution profiles were expected to be similar, it was notable that the batch collected by centrifugation was slightly smaller. This was probably because the centrifugation method would collect all of the MPs in the sample whereas some of the smallest MPs may have passed through the filter paper. However, the two profiles did also not overlap exactly at the higher end of the size distribution with the centrifugation batch again presenting smaller MPs. It is unclear why this was and whether the perceived effect caused by centrifugation is significant. Although the MPs were manufactured under the same conditions they were not prepared together and potentially other variables (e.g. PVA batch) may have had a minor effect on the MPs.

A further improvement to the filtration method to cut down on variability between batches was to use commercially available filter units that had a 0.2 μm pore size. These would allow to retrieval of almost all of the MPs. However,

in some cases, if the smallest fraction ($< 5 \mu\text{m}$) was not required, the MPs could be allowed to settle for a few minutes leaving the smallest MPs suspended in the PVA which could then be removed by pipetting prior to the centrifugation or filtration step. This removal of the smallest MPs would improve the normal distribution of the size profile.

It appeared upon inspection of the SEM micrographs that neither of the washing and collection methods damaged the MPs (Figure 2.7B and C). The MPs in both batches were non porous and spherical. However, if MPs of less than $20 \mu\text{m}$ were to be prepared, the centrifugation method of MP collection was preferable and routinely used as the filtration of the MPs became very slow. The smallest MPs may have begun to clog the filter which in turn, may have led to insufficient washing off of the PVA from the MPs which could lead to agglomeration of the MPs post drying.

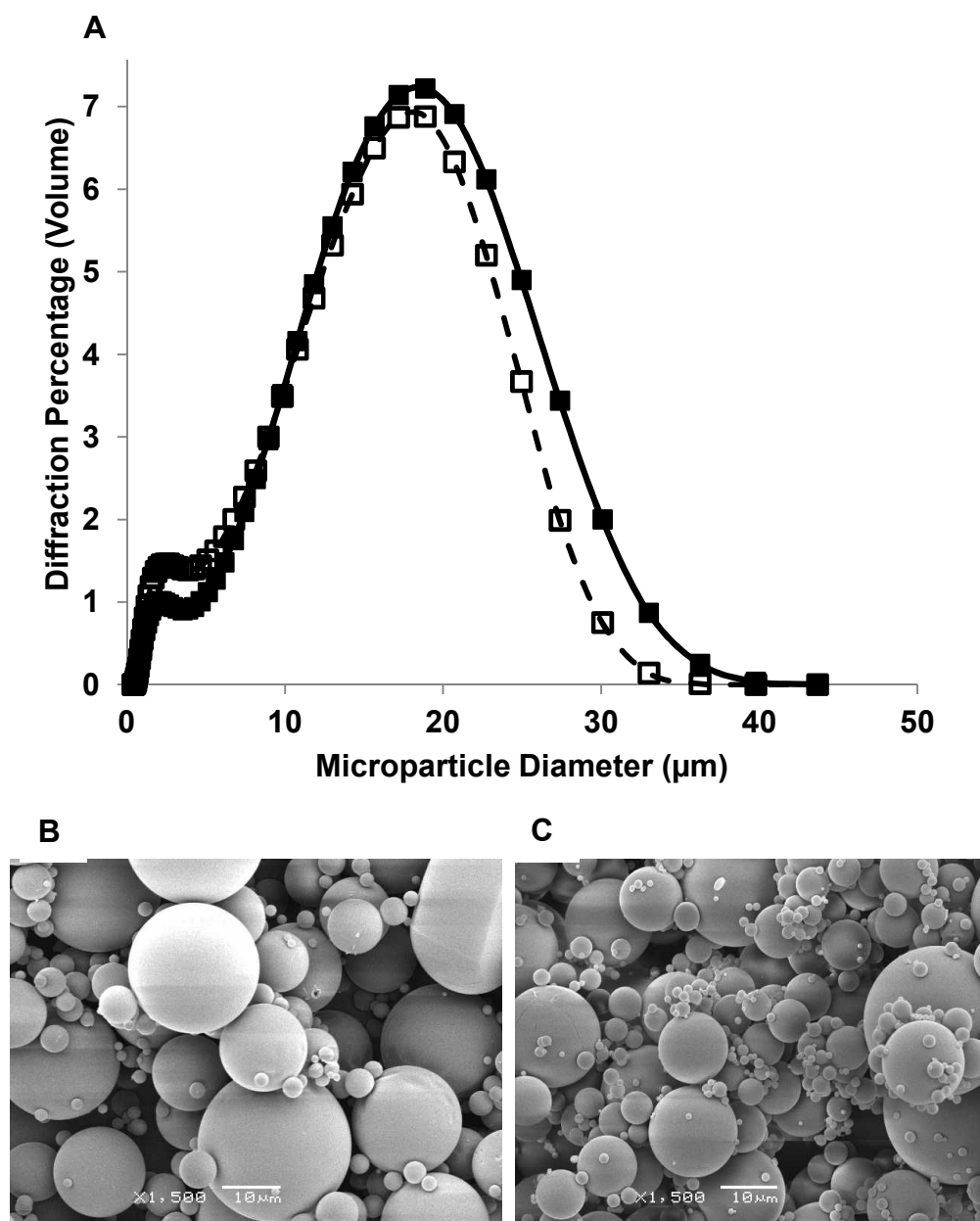


Figure 2.7: [A] Size distribution of PLGA 85 15 MPs manufactured by single emulsion (20% PLGA, 19,000 rpm) and collected by centrifugation (□) or filtration (■). The mean MP size for the centrifuged batch was $12.8 \pm 7.8 \mu\text{m}$ and for the filtration batch, $14.6 \pm 8.3 \mu\text{m}$. [B] Scanning electron micrograph of PLGA MPs collected by filtration (x1,500). [C] Scanning electron micrograph of PLGA MPs collected by centrifugation (x1,500).

Batches: BN 4 and 11

The processing method for the manufacture of MPs had been thoroughly investigated and using the knowledge gained by the above studies, a robust protocol could be written to highlight which parameters should remain constant and which parameters that could be altered to affect the size range of the MPs. The only parameter not to be investigated in these studies was the emulsion stabiliser (PVA) concentration. Although this parameter was also likely to affect MP size (Ye, 2010), a 0.3% _(w/v) solution was adopted from the start and used throughout as it was a commonly used concentration.

The MPs would be used to initially to investigate protein release profiles *in-vitro* (Chapter 3) and would go on to be used in *in-vitro* cell assays (Chapter 4) and *ex-vivo* models of bone regeneration (Chapter 5). Three distinct size ranges were chosen to further interrogate the reproducibility of the protocol and three batches of each size range were made. The size ranges of these MPs are shown in Figure 2.8 and will be referred to in the text as '1-5 μm ', '20-30 μm ' and '50-100 μm ' MPs. The distribution profiles of the three separate batches within each size range were similar (images of these MPs can be seen in the next Section in Figure 2.10), but there was statistical significance between the three different size distributions.

The reproducible fine tuning of MPs sized between 1 and 100 μm can be achieved by standardising the majority of the manufacturing parameters and only altering the PLGA concentration and/or the homogeniser speed at the primary and secondary emulsion. Table 2.1 shows the achievable size ranges using this processing method and to date no other groups have reported in the literature such control of MP size without post manufacture processing.

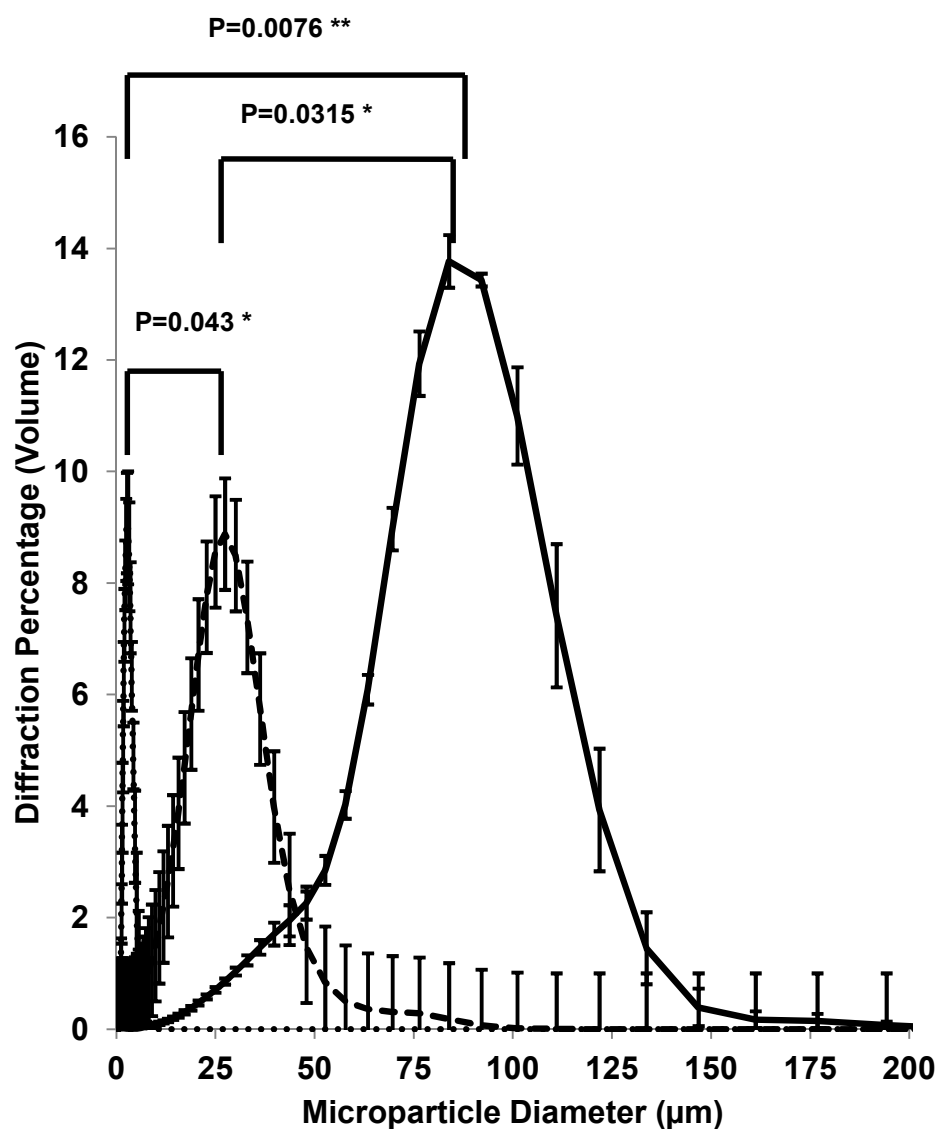


Figure 2.8 . Size distribution traces for three batches of PLGA 50/50 MPs. The average size of these MPs was $2.9 \pm 1.1 \mu\text{m}$ (5% PLGA homogeniser setting 4,000/9,000 rpm), $25.3 \pm 12.9 \mu\text{m}$ (20% PLGA homogeniser setting 4,000/9,000 rpm) and $82.8 \pm 27.8 \mu\text{m}$ (20% PLGA homogeniser setting 4,000/2,000 rpm).

Batches: BN 216, 217, 184, 179, 180, 181, 188, 191, 193

Table 2.1: Complete range of achievable MPs sizes using the W/O/W double emulsion method of manufacture and Silverson homogeniser between 1 and 100 μm .

Size Description	DCM Volume (PLGA % (w/w))	Primary rpm	Secondary rpm	Size Achieved:
1- 3 μm	50 ml (2%)	9000	9000	1.8 \pm 0.6 μm
1- 5 μm	20 ml (5%)	4000	9000	2.5 \pm 0.8 μm
5 – 10 μm	10 ml (10%)	4000	9000	6.8 \pm 5.6 μm
10 – 20 μm	6.67 ml (15%)	4000	9000	13.8 \pm 7.5 μm
20 – 30 μm	5 ml (20%)	4000	9000	26.2 \pm 13.5 μm
50 – 100 μm	5 ml (20%)	4000	2000	86.6 \pm 24.6 μm

2.3.2 Microparticle morphology

As discussed previously, two methods of MP manufacture were investigated (S/O/W and W/O/W). As well as determining the size distribution, it was also important to image the MPs to ensure that they had spherical morphology ensuring that a stable emulsion had been formed and to determine whether there were any surface pores on the MPs which could affect the outcome of future protein release studies.

Figure 2.9 shows the morphology of 50 – 100 μm MPs manufactured by each of the two methods at three different magnifications. The W/O/W MPs have very few surface pores and exhibit a smooth surface. On the other hand, the S/O/W MPs are more irregularly shaped they have more pores and a rough surface. The rough surface maybe due to the surface bound microparticles of lysozyme that were not encapsulated properly and the pores possibly due to the presence of hydrophylic PEG used in the micronisation process leaching out of the MP, this was confirmed by the recent work by Bhatt (Bhatt, 2012). Also, MPs yielding surface pores were also produced when the copolymer Poloxamer 407 was added during MP manufacture (Mahboubian, 2010). However, these detailed features were not highlighted in the literature by others (Morita, 2000b, Al-Azzam, 2002) and indeed it maybe that the speed of solvent evaporation or the freeze drying efficiency may have contributed to the different morphologies (Rosca, 2004, Allison, 2008b). Unfortunately, the freeze drying process was the least controllable process in the MP manufacture protocol due to multi-usage of two different freeze driers. However, wherever possible the same freeze drying conditions were employed for each batch of MPs manufactured.

The surface morphology of the S/O/W MPs may have contributed to loss of protein during the manufacturing process, therefore reducing entrapment efficiency which will be discussed later in Section 2.3.5. For long term protein release studies, the non-porous surface of the W/O/W MPs would be more advantageous to avoid a fast burst release (Allison, 2008a).

Figure 2.10 shows the morphology of the three distinct size ranges defined in Figure 2.8 at three different magnifications. In each case the MPs were non-porous, spherical and were expected to be good tools for localised protein delivery.

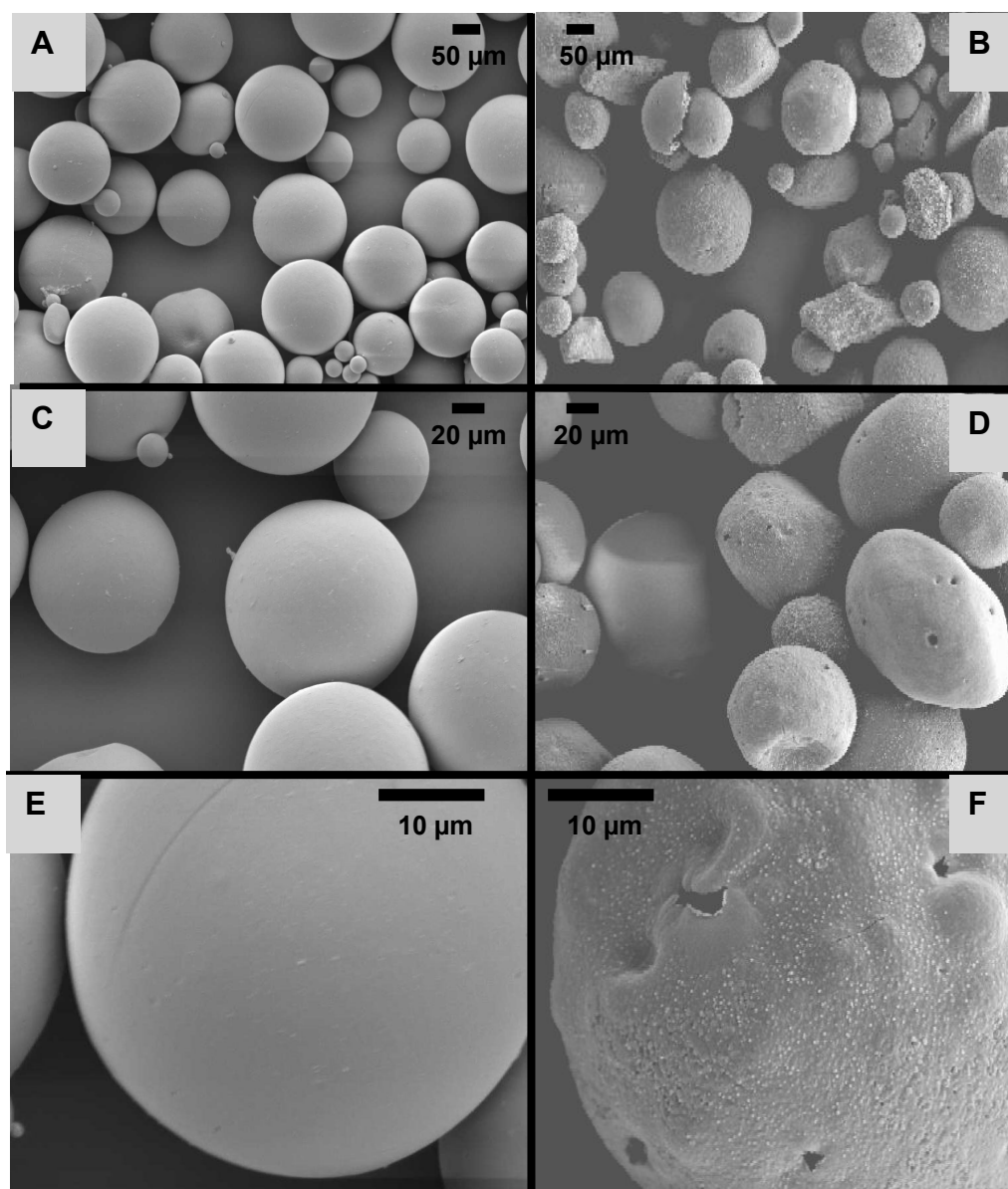


Figure 2.9: Scanning electron micrographs comparing PLGA MPs manufactured by the W/O/W emulsion method [A, C and E) and the S/O/W emulsion method [B, D and F]. The W/O/W MPs have a 1% _(w/w) HSA/lysozyme loading and the S/O/W MPs have a 5% _(w/w) HSA/lysozyme loading. Scale bars are as indicated

Images of S/O/W MPs courtesy of Giles Kirby (PhD student, School of Pharmacy, University of Nottingham)

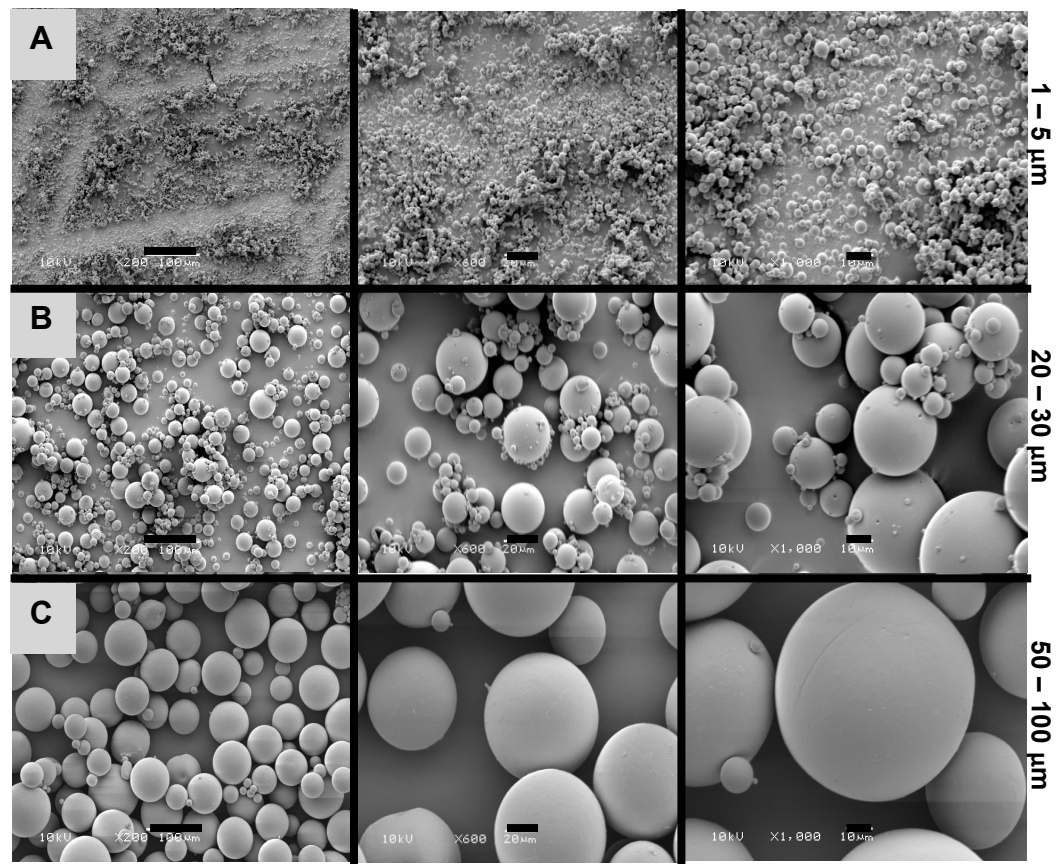


Figure 2.10: SEM images of PLGA MPs fabricated from 5% (w/v) [A] and 20% (w/v) [B] PLGA with homogeniser speeds set at 4,000/9,000 rpm and MPs fabricated from 20% (w/v) PLGA with homogeniser speed at 4,000/2,000 rpm [C] at magnifications of x200 (scale bar 100 μm), x600 (scale bar 20 μm) and x1000 (scale bar 10 μm).

Batches: BN 184, 343, 348

2.3.3 PLGA Degradation

2.3.3.1 Measurement of pH

An important aspect for using PLGA polymers for drug delivery applications is their controllable degradation rate. As the polymer degrades, it will begin to swell opening up micro-pores allowing the entrapped molecules to release (Dawes, 2010). Degradation of PLGA is by hydrolytic scission of the ester linkages of the polymer back bone and it is reported that PLGA polymers with different lactide:glycolide ratios will degrade at different rates with the higher lactide content slowing the rate due to the pendent (attached to polymer backbone) methyl group on the lactic acid sterically hindering the attack of water molecules thus the presence of lactic acid increases the hydrophobicity of the polymer (Anderson, 1997, Wu, 2001).

If PLGA were to degrade in a closed environment, then there would be a build up of degradation products (lactic and glycolic acid) which would reduce the pH of the surrounding media (Liu, 2012). This is a good tool to measure PLGA *in-vitro* but it is unlikely to mimic the *in-vivo* situation as i) the degradation products are not confined to the site of administration and ii) there are active metabolic processes within the body to remove and excrete the degradation products. To compare the degradation of PLGA 50 50 and PLGA 85 15 having similar molecular weights in PBS, the pH was monitored over 60 days, with fresh PBS being added at each time point. The data is shown in Figure 2.11 and shows that the pH drop was more rapid for the PLGA 50 50 than the PLGA 85 15 which only began to drop after 45 days, thus confirming the literature findings (Wu, 2001). Interestingly, beyond 40 days, the pH in the PLGA 50 50 test group began to rise. This was probably because from 15

days onwards, the polymer began to lose mass, the degradation products were removed with each replacement of PBS until eventually the effect of the pH drop was being diluted out by the addition of fresh PBS. This hypothesis could only be confirmed by setting up a mass loss degradation study.

2.3.3.2 Measurement of mass loss

A PLGA degradation study examining mass loss was set up by incubating a known mass of PLGA 50 50 MPs in PBS at 37°C and at defined time-points, removing the PBS, drying and reweighing the MPs. A similar study with the same PLGA was also set up at 45°C. The hypothesis was that this would accelerate the degradation rate and increase the mass loss. This aspect of PLGA degradation may have consequences on the use of these MPs as delivery devices as a faster degrading polymer is more likely release its contents quicker and potentially allow for control of release through manipulation of the glass transition temperature.

The results of the PLGA 50 50 mass loss study are shown in Figure 2.12. Despite a considerable level of error in the results due to the nature of the experiment, it was still quite evident that mass loss does occur over time as the polymer degrades and the mass loss is dramatically accelerated at higher temperatures. The glass transition temperature (T_g) of this polymer was reported as 49.0°C (measured by DSC) and it is stated that as the T_g is approached, the degradation rate will increase (Aso, 1994). This data confirms these findings.

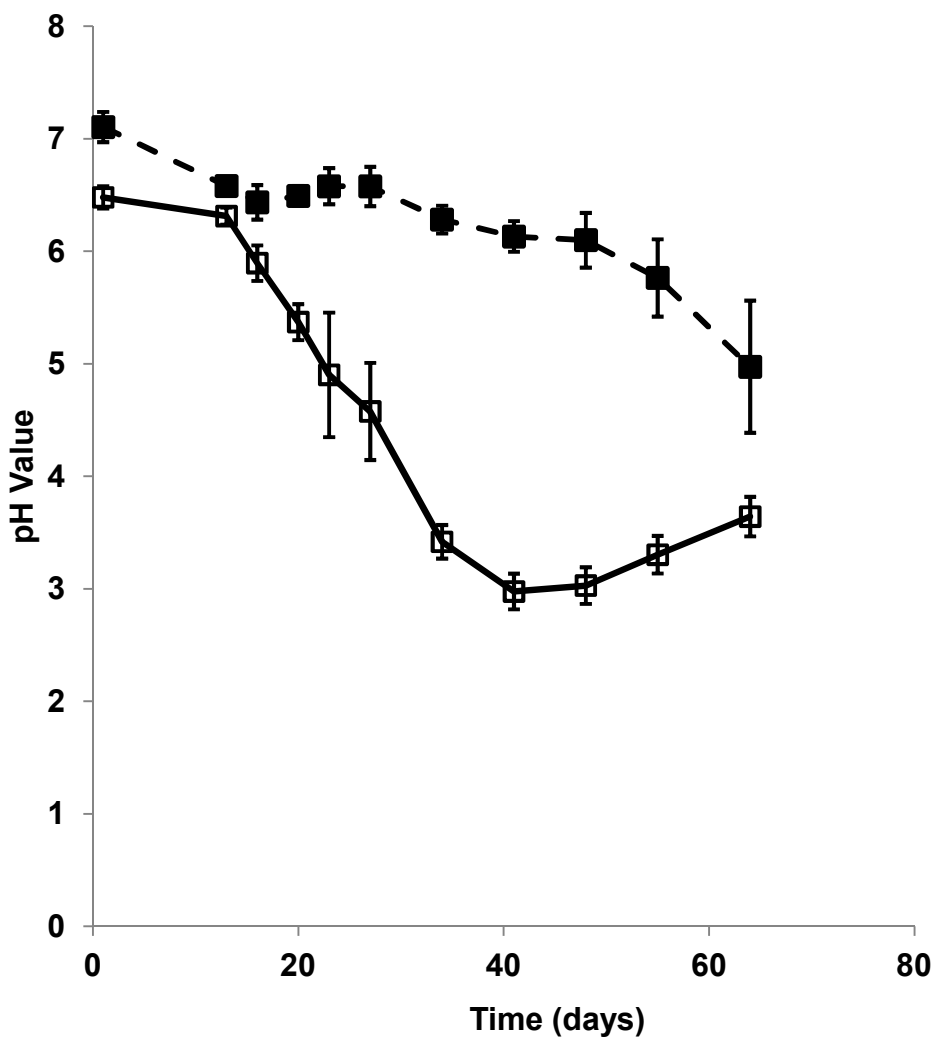


Figure 2.11: Comparison of pH values over time for PLGA 85 15 Mwt 56 kDa (■) and PLGA 50 50 Mwt 59 kDa (□) both formulated with 30% _(w/w) PLGA-PEG-PLGA triblock copolymer and incubated at 37°C in PBS. The PBS was replaced with fresh at each time-point.

Batches: BN 135, 142, 149 (PLGA 50 50) B140, 147, 154 (PLGA 85 15)

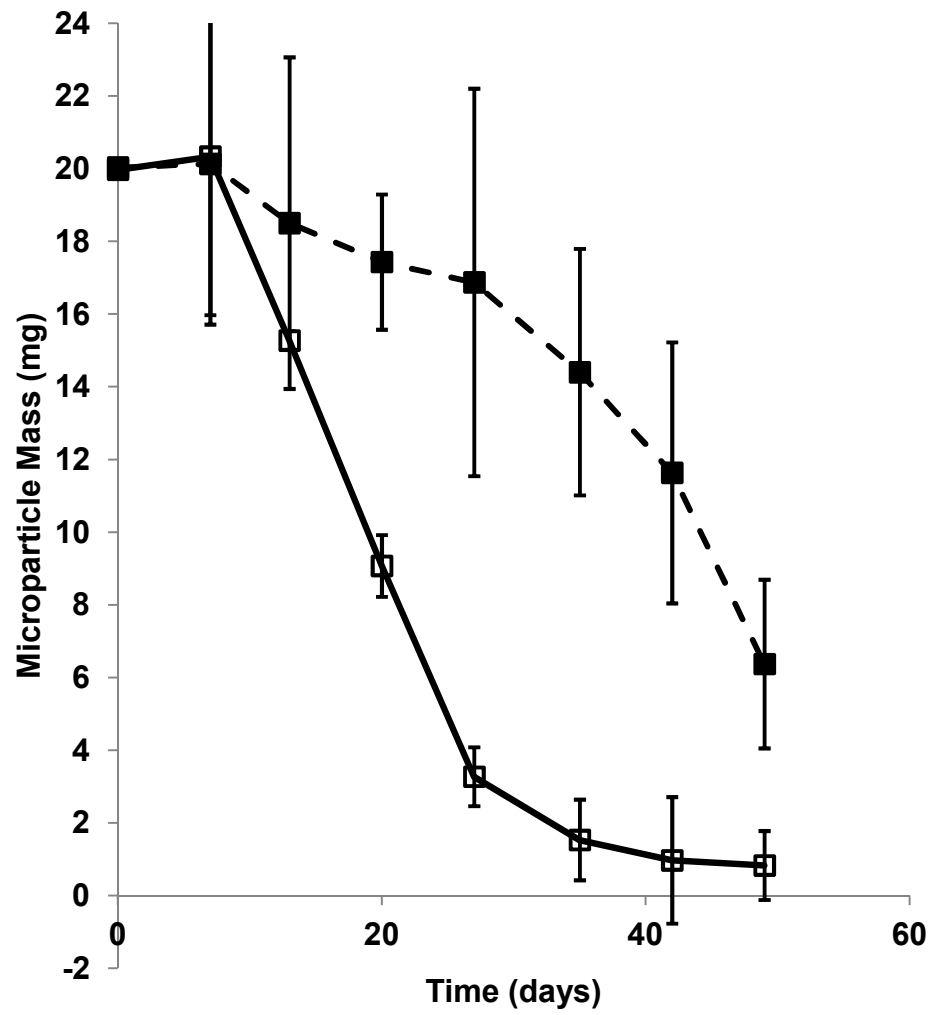


Figure 2.12: Mass loss of PLGA 50/50 MWt 56 KDa MPs through degradation at 37°C (....) and at 45°C (—) after incubation at 37°C in PBS. The PBS was replaced with fresh at each time-point.

Batch: BN 172

2.3.3.3 Change in MP morphology

A final investigation into the degradation of PLGA MPs was an attempt to image the MPs over time. PLGA 50 50 was used as it has the quickest degradation time and in addition a small amount (10% _(w/w)) of PLGA-PEG-PLGA triblock copolymer was added to increase the degradation rate (the copolymer will be introduced in detail in the following Chapter). This data on MP degradation was not as clear cut as pH and mass loss studies (Figure 2.13). During the first 9 days of incubation there was no change in the external morphology of the MPs. This was not unexpected as neither mass loss nor a pH drop had been detected over this time in other experiments. However, by day 14 the MPs had begun to fuse with each other rather than degrade as individual MPs which had been reported by other researchers (Dawes, 2010). It has also been reported that the macroporosity of individual MPs reduces as degradation occurs but microporosity increases (Mao, 2007).

The effect seen in Figure 2.13 was probably the result of bulk erosion occurring. By 20 days some MPs had blended into each other to form microporous plaques whilst other MPs still maintained their shape. This continued up to 28 days where most MPs had either become individual flat discs or had combined together. It was noted that by 28 days the total volume of the MPs had reduced and by day 36 all of the MPs had amalgamated into one structure approximately 3 mm in length which upon examination was pliable. This may have been a residue of the PLGA-PEG-PLGA triblock copolymer.

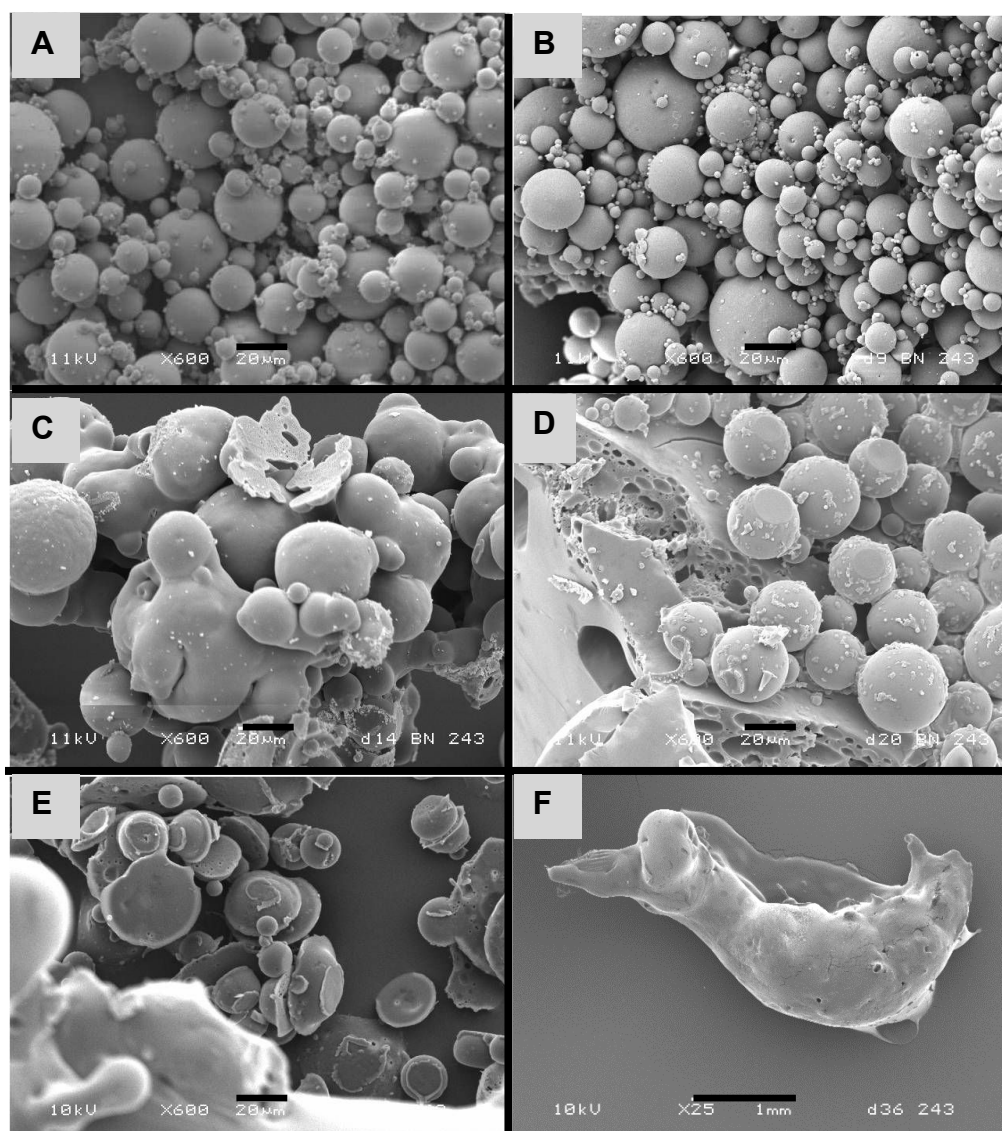


Figure 2.13: Scanning electron micrographs of PLGA 50/50 MPs formulated with 10% (w/w) PLGA-PEG-PLGA triblock copolymer after incubation at 37°C in phosphate buffered saline for [A] 0 days, [B] 9 days, [C] 14 days, [D] 20 days, [E] 28 days and [F] 36 days. Scale bar 20 μm x600 (A-E) and 1 mm x25 (F)

Batch: BN 243

2.3.4 Optimisation of total protein and lysozyme activity assays

2.3.4.1 The bincinchonic acid assay

There are a number of different methods to determine total protein content including, UV absorption spectroscopy (@ 280 nm), dye based assays (Bradford assay) and copper reduction assays (Lowry). The bincinchonic acid assay (BCA) is a well established assay and is also based on copper reduction but it has a higher tolerance against interference (Noble, 2009). Amino groups in proteins will reduce Cu^{2+} to Cu^{1+} in an alkaline environment which in turn will chelate with BCA and give a measurable colour change. The goal of this work is to be able to detect protein released from PLGA MPs but as has been demonstrated in the previous section, there is likely to be a drop in pH in the surrounding release media as the polymer degrades. Thus, it was important to ascertain whether this drop in pH would affect the sensitivity of the BCA assay. Also, the protein extraction method (Sah, 1997) uses sodium hydroxide which would have a high pH which may also affect the assay. Therefore BCA standard curves were prepared with HSA/lysozyme standards (ratio 9:1) from 3-100 $\mu\text{g/ml}$ in PBS adjusted to a range of pH values from 2 to 12.

As can be seen in Figure 2.14 the pH value of the diluent had little or no effect on the BCA standard curve. This was a surprising result as the assay is expected to work only in an alkaline environment. It may be that the pH of the working solution (pH 11.25) was enough to counteract the lower pH of the diluents. Nevertheless, this result gave confidence that the assay would give reliable results for both entrapment assays and release assays.

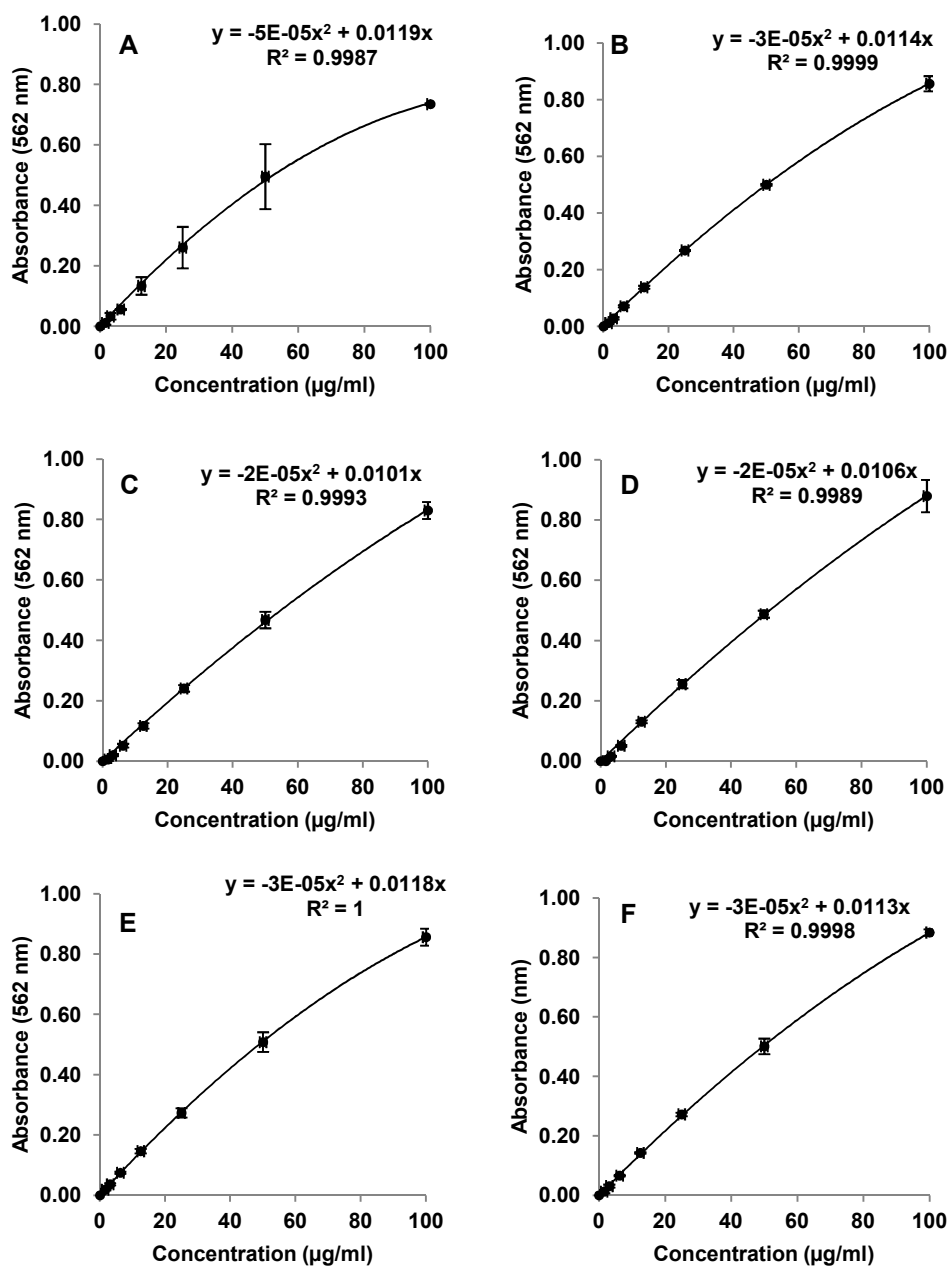


Figure 2.14: The bicinchoninic acid assay standard curve performed at [A] pH 2, [B] pH 4, [C] pH 6, [D] pH 8, [E] pH 10 and [F] pH 12 to determine the effect of pH on the assay $n=3$.

2.3.4.2 The *Micrococcus lysodeikticus* assay

The main driver for the use of lysozyme in optimisation studies was the fact that its biological activity can be measured *in-vitro* by its action on the bacterium *Micrococcus lysodeikticus*. This assay utilises the fact that lysozyme preferentially hydrolyzes the β -1,4 glycosidic linkages between N-acetylmuramic acid and N-acetylglucosamine which occur in the bacterial cell wall structure of *Micrococcus lysodeikticus* bacteria. The turbid solution of cells becomes less cloudy as the cells lyse and this can be measured over time at an absorbance of 450nm.

As for the BCA assay, it was important to determine whether the assay was affected by pH. Standard curves were set up with HSA/lysozyme standards (ratio 9:1) at 3-100 μ g/ml in PBS adjusted to a range of pH values from 2 to 12. The lysozyme component would be a tenth of the total protein and so the standard curves were constructed with a lysozyme concentration of 0.5-10 μ g/ml. Figure 2.15 shows that this assay is very sensitive to pH. Either the lysozyme was becoming denatured, (but this is unlikely for low pH values as it is reported to be most stable in acidic conditions such as glycine buffer (Jiang, 2002)) or more likely the bacteria are affected by pH and receptor binding in the cell wall was not possible. It was reported that in acid conditions that lysozyme still binds to the mucopolysaccharides of the cell wall but no lytic activity is evident (Gagliardi, 1986).

It was therefore concluded that although total protein can be measured at a range of pH values with confidence, results from the lysozyme activity assay will only be of value around neutral pH. Figure 2.16 shows a typical standard curve for both BCA and *Micrococcus lysodeikticus* assay in standard PBS buffer at pH 7.4. For each assay a new standard curve will be constructed.

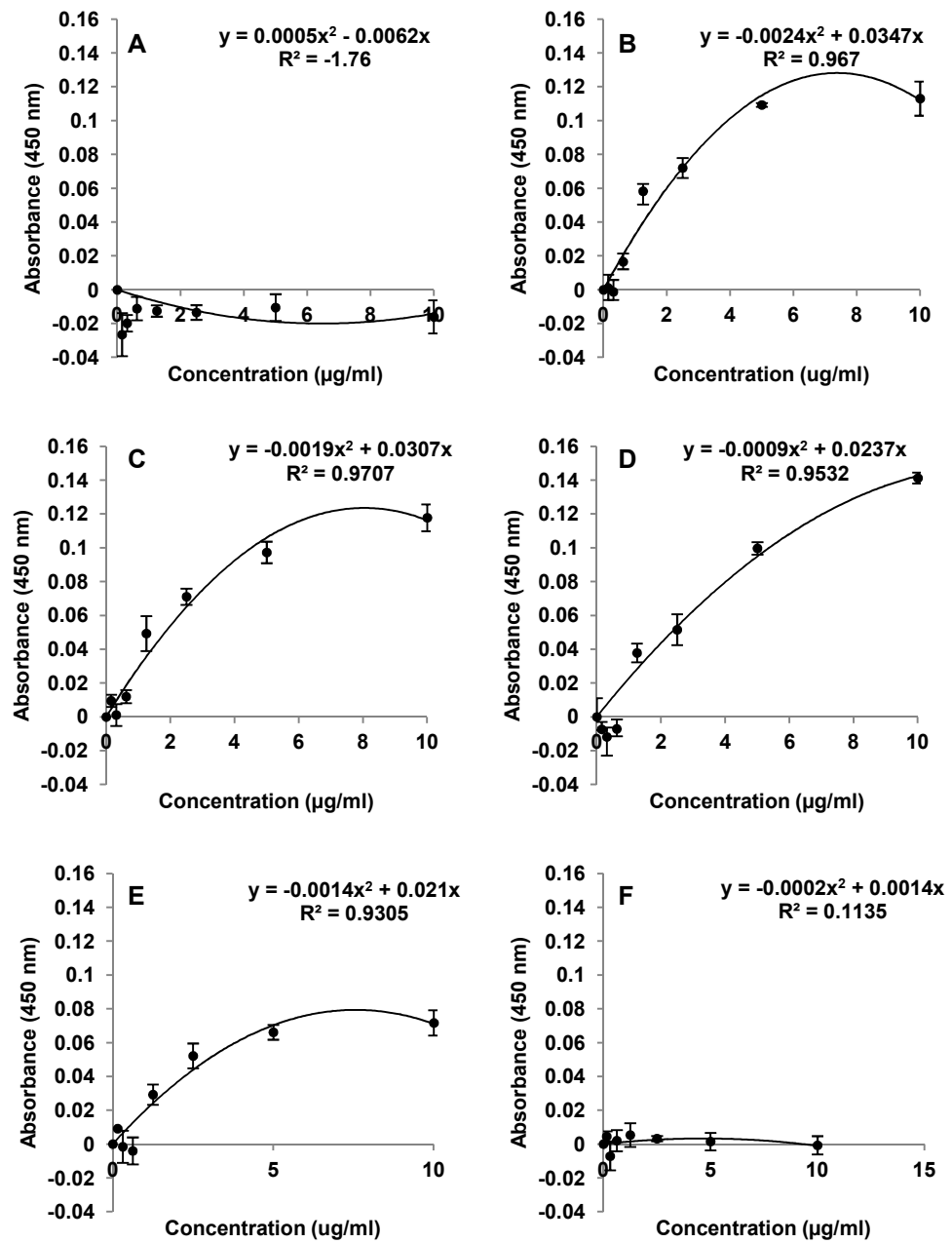


Figure 2.15: The *Micrococcus lysodeikticus* assay standard curve performed at [A] pH 2, [B] pH 4, [C] pH 6, [D] pH 8, [E] pH 10 and [F] pH 12 to determine the effect of pH on the assay $n=3$.

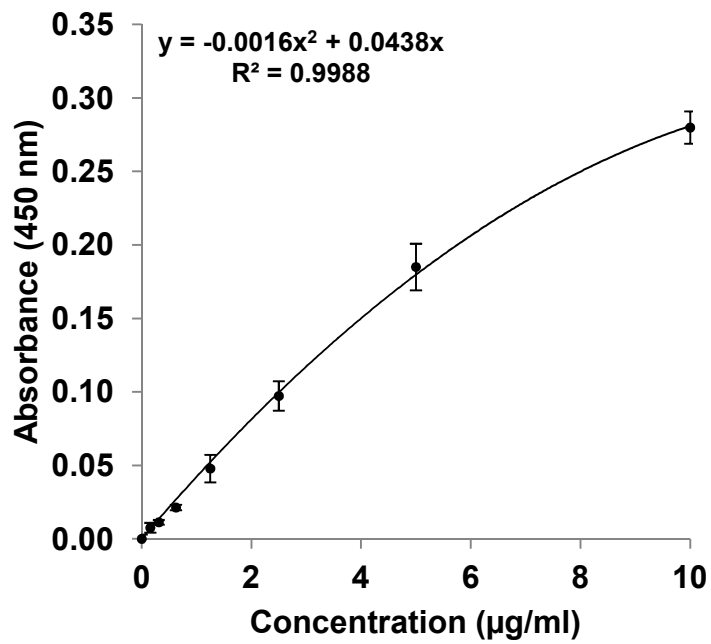
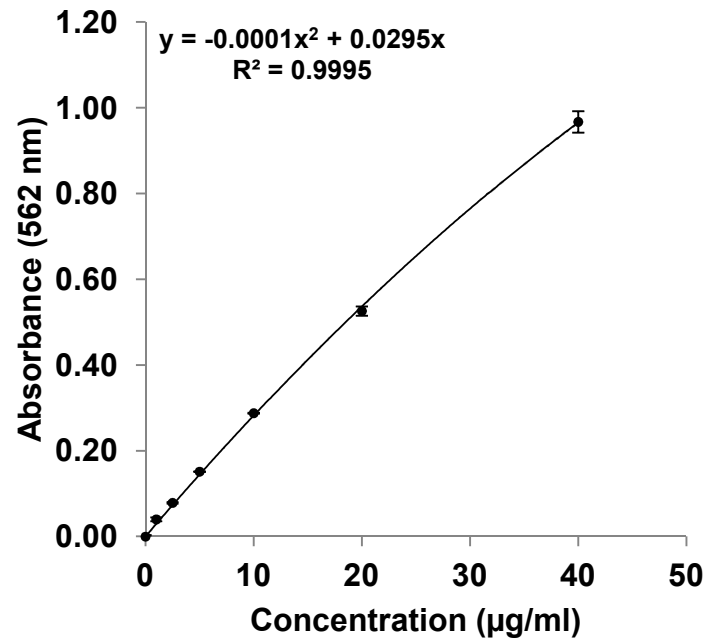


Figure 2.16: Typical standard curves for [A] bicinchoninic acid assay and [B] *Micrococcus lysodeikticus* assay in PBS at pH 7.4 n=3

2.3.5 Entrapment efficiency of HSA/lysozyme in PLGA MPs

2.3.5.1 Solid in oil in water emulsion

Lysozyme was used in conjunction with human serum albumin (HSA) as a bulk carrier and stabilising excipient (Morlock, 1996, He, 2011). The addition of the bulk carrier was to shield the active molecule from the water/oil interface during MP manufacture. The solid-in-oil-in-water (S/O/W) single emulsion method of protein entrapment required the lysozyme to be co-lyophilised with PEG6000 in an aqueous medium (Morita, 2000a). The action of freeze drying resulted in the protein being micronized in a continuous PEG phase and the proposed advantage of this method was that the protein can be directly mixed into the organic polymer phase and only one emulsion step was required, subjecting the protein to only one water/oil interface.

As well as the addition of bulk carrier and MP manufacture by S/O/W, the effect of solvent evaporation time on entrapment efficiency was investigated. It was reduced from 24 hours to 4 hours to minimise protein loss in the PVA stabilising bath. The results of this investigation are shown in Table 2.2. In each case the total protein loading was 5% (50 mg into 1 g PLGA 50 50) and it was micronized with 400 mg PEG6000. Lower masses of PEG6000 were also used to co-lyophilise the lysozyme and HSA but the entrapment efficiencies for these were generally below 20%.

Reducing the evaporation time had a clear effect on improving the entrapment efficiency for all three loading conditions (HSA/lysozyme, HSA alone and lysozyme alone) but, the values were not comparable. HSA loading alone provided the best entrapment efficiency with an improvement from 21.8% after 24 hours evaporation to 56.8% after 4 hours of evaporation. The shorter

time also improved the entrapment efficiency of the lysozyme alone batch by 91% but still the final value was only 13% meaning the vast majority of the lysozyme had been lost during the manufacturing process. The HSA/lysozyme batch after 4 hours of solvent evaporation returned an entrapment efficiency of 21.8% compared to 9.7% after a 24 hour solvent evaporation period.

Despite the clear advantages of reducing the evaporation time, the overall results for the entrapment efficiency were not encouraging and it would not be cost effective or efficient to transfer this method of manufacture to the entrapment of growth factors due to the high losses.

Table 2.2 Effect of solvent evaporation time on the entrapment efficiency of lysozyme \pm human serum albumin in PLGA MPs using the S/O/W emulsion method

<i>HSA/PEG/Lysozyme Content in 1 g PLGA 50 50</i>	<i>Evaporation Time (hrs)</i>	<i>Entrapment Efficiency (%) (n=3)</i>
49 mg HSA 1 mg Lyso 400 mg PEG6K	24	9.7 \pm 1.2
49 mg HSA 1 mg Lyso 400 mg PEG6K	4	21.9 \pm 0.7
50 mg HSA 400 mg PEG6K	24	21.8 \pm 14.6
50 mg HSA 400 mg PEG6K	4	56.8 \pm 14.9
50 mg lyso 400 mg PEG6K	24	6.8 \pm 1.0
50 mg lyso 400 mg PEG6K	4	13.0 \pm 1.6

2.3.5.2 Water in oil in water emulsion

Despite the predicted poor entrapment efficiency results expected with the W/O/W manufacture method, when tested the results were in fact, more encouraging. Batches of PLGA MPs were manufactured with a range of HSA/lysozyme loadings ranging from 0.05 to 5% _(w/w) and entrapment efficiency estimations by BCA assay were made for each batch in triplicate. There was a strong inverse relationship between loading and entrapment efficiency, as loading went up entrapment efficiency went down but even with 5% _(w/w) loading, the W/O/W method out-performed the S/O/W method (Figure 2.17). A similar result was reported in the literature by Trivedi who found that encapsulation efficiency of Aceclofenac in PLGA significantly increased as the drug:polymer ratio decreased and the same trend was reported for doxorubicin in PLGA nanospheres (Trivedi, 2008, Kalaria, 2009). The likely explanation for these results was that the more drug/protein that was available, the more that would be likely to be lost during solvent evaporation and this would be especially pertinent for lysozyme which is hydrophilic and likely to leach away. A total loading of 1% _(w/w) was chosen as a standard loading for the majority of future studies and the entrapment efficiency of this protein loading was highly significant when compared to the S/O/W result (Figure 2.17).

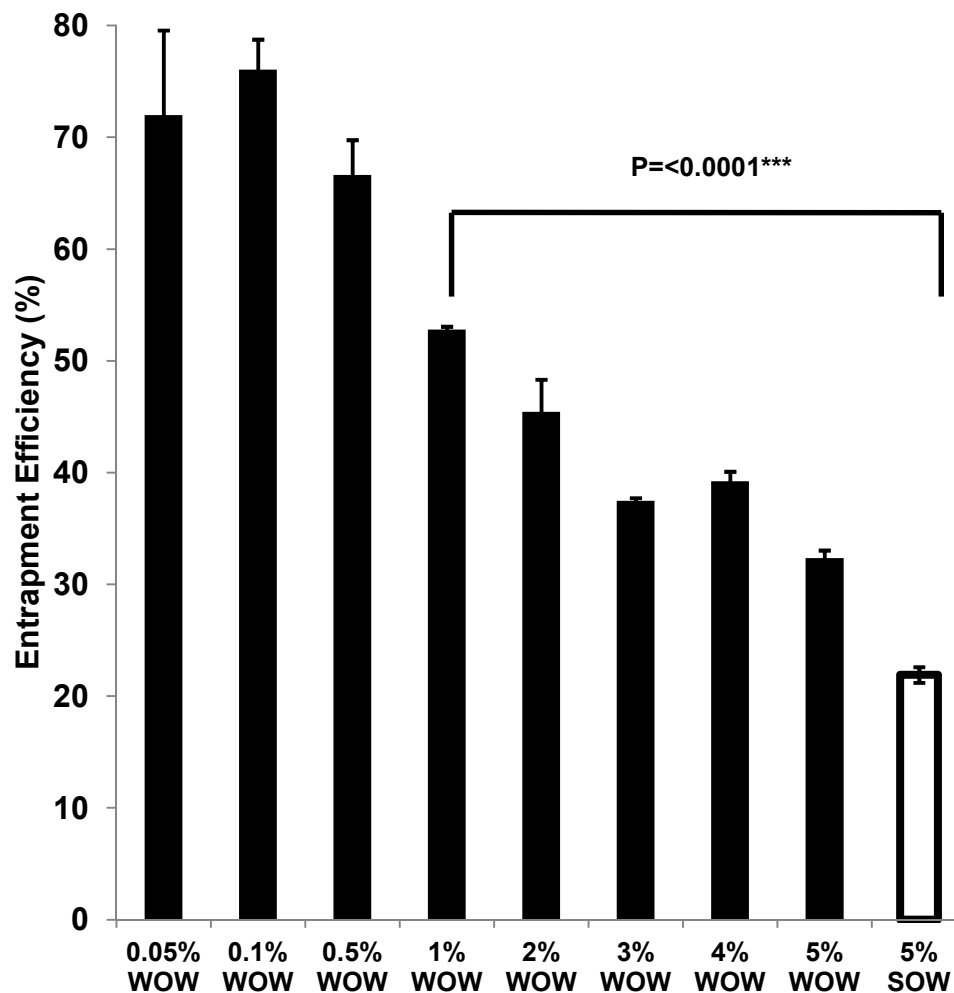


Figure 2.17: Effect of HSA/lysozyme loading on the entrapment efficiency of PLGA 50 50 MPs (50-100 μ m) using the W/O/W emulsion method (4 hour evaporation time) and a comparison of the entrapment efficiency a 5% (w/w) protein loading using the S/O/W method of manufacture. (For W/O/W PLGA Mwt was 56 KDa and for S/O/W PLGA Mwt was 58 KDa)

Batches: BN 101 (SOW) and BN 188-195 (WOW)

The work performed thus far on this project was to optimise the achievable size range of manufactured PLGA MPs but, the important studies on entrapment efficiency were only performed on 50-100 μm sized MPs and so entrapment efficiency measurements were performed on a range of MP sizes each loaded with a total of 1% protein (9 mg HSA with 1 mg lysozyme in 1 g of PLGA 50 50) and manufactured following the W/O/W method. The results are shown in Figure 2.18. For MPs above 2.5 μm , the entrapment efficiency was above 50% and increased with MP size. There was a discrepancy with the 20-30 μm size range in this study but further work with this size range has yielded MPs with typically 70-80% entrapment efficiency. The smallest MPs had the lowest loading efficiency and this was attributable to lower PLGA concentrations being used during manufacture resulting in MPs with thinner outer shells which would be more prone to hydrolytic attack during the solvent evaporation process during manufacture. The significance between the entrapments efficiencies of the 1-5 μm , 20-30 μm and 50-100 μm MPs is highlighted in Figure 2.18.

It was suggested by Dhakar and Colleagues that the polymer concentration affects entrapment efficiency in three ways: i) at high concentrations, the polymer precipitates faster on the surface of the aqueous dispersed phase preventing diffusion across the phase boundary, ii) the high concentration increases viscosity and delays diffusion within the polymer droplets and iii) a high polymer concentration results in larger MPs and loss from the surface is reduced. Therefore and as confirmed in Figure 2.18, MP size is directly related to entrapment efficiency (Dhakar, 2010).

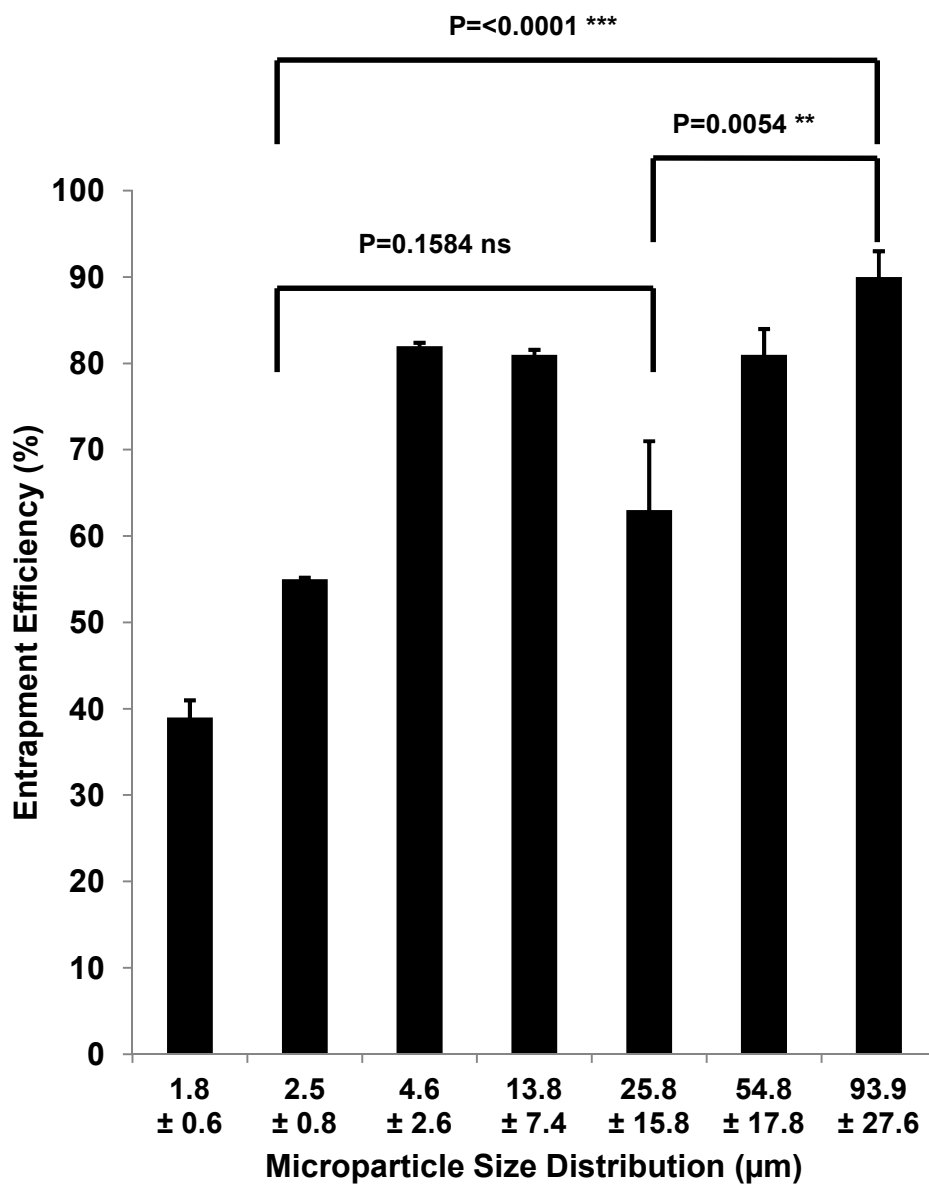


Figure 2.18: The relationship between MP size and entrapment efficiency using the W/O/W double emulsion method of MP manufacture. 1% _(w/w) loading PLGA 50 50 Mwt 58 KDa. n=3

Batches: BN 49, 175, 173, 171, 179, 39 and 191

2.4 Conclusions

This Chapter has highlighted the manufacture parameters that affect the size distribution and entrapment efficiency of biodegradable PLGA MPs. Although a lot of work has been cited in the literature regarding the use PLGA, no groups as yet have demonstrated the control over size distribution from 1 to 100 microns as reported in this Chapter. The variable parameters within the protocol for manufacturing these MPs have been thoroughly tested to produce a reproducible and robust method for producing the biodegradable MPs.

A range of different values for protein entrapment efficiencies have been reported in the literature and much of the data in this Chapter agreed with the trends in published data regarding MP size and drug loading. However, it was interesting to discover that the W/O/W method of manufacture was preferable to the S/O/W method despite there being two aqueous interfaces within the W/O/W method which were expected to be detrimental to encapsulation efficiency. The reason for this remains unclear but may relate to the addition of a stabilising excipient or bulk carrier to the bioactive model protein lysozyme. As yet the retention of biological activity of the protein within the MP was unknown but the *Micrococcus lysodeikticus* assay to determine lysozyme activity had been investigated and operating parameters were defined for sample testing.

The techniques described in this Chapter for MP manufacture will be used to make MPs for future studies to determine the typical rate of lysozyme release over time and further formulation of the MPs will attempt to tailor the release profiles to different rates which may have the potential for use with different growth factors.

Chapter 3: Control of protein delivery from PLGA microparticles by the novel use of a triblock copolymer to uncouple protein release from polymer degradation

3.1 Introduction

During bone and cartilage repair, there is a complex cascade of biological events controlled by growth factor signalling promoting progenitors and inflammatory cells to migrate and trigger healing processes. Although for some applications, therapeutic drugs can be delivered at supraphysiologic concentrations without any serious side effects (for example antibiotics), the delivery of growth factors must have much tighter control in order to be effective, mimic *in-vivo* kinetics and avoid unwanted biological effects. The aim of this Chapter is to describe the development of a novel microparticulate delivery system having controlled kinetics of release that are faster than the degradation of the scaffold. A system that combines control over the rate of growth factor delivery and provides support for the surrounding and newly formed tissue will be a considerable achievement in the field of tissue engineering.

The previous Chapter described the development and optimisation of a protocol to manufacture PLGA microparticles (MPs) reproducibly in defined size ranges. In addition, the MPs were successfully loaded with the model protein lysozyme in conjunction with human serum albumin (HSA) as a bulk carrier and investigations into the degradation of PLGA were performed. This Chapter will build on this work by investigating the profile of lysozyme release from PLGA MPs during *in-vitro* release assays and attempt different strategies to control the rate of protein release from the MPs.

Despite PLGA being cited as a valuable material for drug delivery applications due to its non-toxic degradation products and having FDA approval for use in certain medical devices and drug delivery applications, it is well documented that protein release from PLGA follows a triphasic profile (Cohen, 1991, Jiang, 2002, Ye, 2010). This release profile involves two mechanisms; diffusion and erosion. Firstly there is a burst release followed by a lag phase and then a second phase of release. In the early burst and lag phase, protein release is governed by diffusion through a network of water filled pores and channels. The burst is caused by the rapid diffusion of surface bound and near surface entrapped protein and the lag is caused by the inability of entrapped protein to diffuse out due to being protected by hydrophobic PLGA. The lag phase continues until erosion of the polymer matrix by hydrolysis occurs releasing more of the entrapped protein from the structure. The triphasic profile is not optimum for drug delivery as therapeutic levels may be too high during the burst and are not be maintained during the lag phase. The release profiles have been the subject of mathematical modelling (Batycky, 1996) and the size and porosity of the microspheres are highlighted as playing a key role in drug release mechanisms (Klose, 2006).

Many strategies have been adopted to improve the release profiles by reducing the initial burst which can account for a large percentage of protein loss in the first few hours. Studies have investigated altering MP manufacture procedures to modify internal morphology (Igartua, 1997, Mao, 2007), altering the protein molecular weight and/or loading (Sandor, 2001), modifying protein with additives to improve stability (Kang, 2001, Diwan, 2001) and comprehensive reviews have been written on these approaches (Yeo, 2004b, Giteau, 2008). As well as high burst, incomplete release of protein from PLGA has long been cited as a problem (Rosas, 2001, Giteau, 2008). The

combination of these two issues means that often the actual amount of therapeutic protein available for release over the optimum timescale is very low.

The strategy proposed for this thesis was to incorporate an 'in-house' manufactured PLGA-PEG-PLGA triblock copolymer into the PLGA at the point of MP manufacture to modulate the MPs release profiles. Although triblock copolymers have been used alone as drug delivery devices (Chen, 2005, Ghahremankhani, 2007), they have not been used incorporated into PLGA MPs. If MPs could be engineered to release their payload in specified time-frames ranging from a few days to a number of weeks then, it would give the flexibility to manufacture MPs loaded with different growth factors so mimicking the growth factor kinetics required during tissue repair and keep the delivery localised.

It was hypothesised, that introduction of PLGA-PEG-PLGA triblock copolymer into MPs would make them more hydrophilic and that this would modify release from the MP in two ways. Firstly, it would encourage the ingress of water to 'wash out' the surface and near surface bound protein and secondly, the ingress of water would accelerate the hydrolytic attack on PLGA and so increase the degradation rate allowing protein to be released gradually, through pores and channels, so avoiding the lag phase seen in MPs fabricated from PLGA alone (White, 2013) .

Before materials can be tested *in-vivo* they must first be thoroughly assessed *in-vitro* for both ethical and financial reasons. Many studies have been performed to investigate *in-vitro* release profiles from MPs but as yet no standard protocol has been determined to give a good *in-vitro/ in-vivo*

correlation. Researchers have compared static with dynamic release systems (Hernandez, 1998), continuous flow systems (Aubert-Pouessel, 2002) and looked at the importance of maintaining sink conditions (Klose, 2011). But, the important thing to note is that whatever *in-vitro* release system is used, it must be adequately controlled to minimise variables and error so that subsequent release assay results can be comparable.

Despite real progress being reported in releasing multiple growth factors simultaneously from a single scaffold to achieve multiple responses in the surrounding tissue (Raiche, 2004, Sohler, 2006, Suciati, 2006, Jaklenec, 2008), a MP based system with the potential to be delivered by microinjection has not yet been developed and there is no standard manufacturing procedures that can be applied to all proteins due to their unique structure, molecular weight and charge.

A further problem with using MPs as delivery tools is the potential for migration of the MPs away from the site of delivery. This could potentially lead to systemic side effects or cause an unwanted inflammatory response (Yoon, 2008, Wu, 2010). Incorporation of a second type of MP, one that is thermosensitive, could bind the protein loaded MPs in a porous matrix so avoiding migration and provide stability to the scaffold structure. This would give support to the surrounding tissue and provide a better environment for new tissue growth. PLGA and low molecular weight PEG have been blended together by hot melt techniques and can be milled to form irregular shaped MPs (Rahman, 2012a). The PEG acts as a plasticiser and by careful manipulation of the PEG concentration, the MPs can be tailored to become cohesive at body temperature. These temperature sensitive MPs will form bridging points between other temperature sensitive MPs as well as with the

protein loaded MPs forming a single solid structure and thus preventing migration of growth factor loaded MPs from the site. As the low molecular weight PEG is not chemically bonded to the PLGA, it can leach away in an aqueous environment due to its hydrophilicity and this will cause a rise in glass transition temperature of the polymer resulting in the bridging points strengthening and therefore the overall structure becoming stronger (Dhillon, 2011). A schematic depicting the mechanism of setting is shown in Figure 3.1

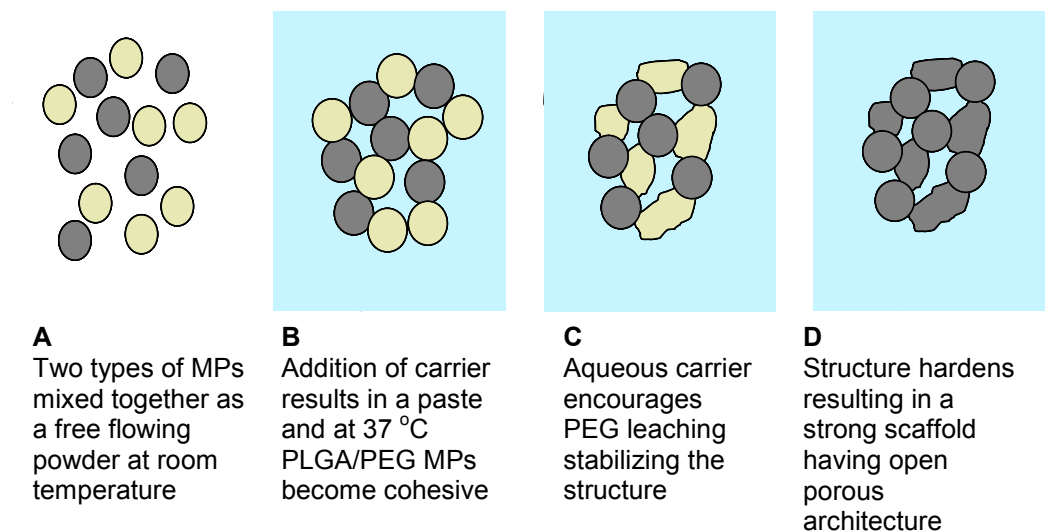


Figure 3.1 Schematic of in-situ setting mechanism of thermosensitive MPs and incorporation of a non-temperature sensitive component which could be either be an osteoconductive ceramic or a growth factor loaded MP

Adapted from (Rahman, 2013)

This project aims to address some of these issues to achieve a microparticulate delivery system with the potential to apply the technology to different growth factors to achieve profiles of release over different and clinically appropriate therapeutic time frames. An additional aim is to provide a three dimensional porous scaffold to support to the surrounding tissue and encourage cell proliferation and differentiation. The system would be most

effective if protein was released in advance of the polymer degradation so that there was a scaffold still present to host the new tissue growth.

Although the work in this project is aimed primarily at bone regeneration, the technology once developed, could potentially be applied to the repair of other damaged tissues such as cartilage, liver or nervous system (Schneider, 2012, Chistiakov, 2012, Xiong, 2012).

3.2 Materials and Methods

All the laboratory equipment, consumables and chemicals used during the work for this Chapter can be sourced in Appendix I, tables A1, A2 and A3. Where MP batch numbers are stated, the details of the manufacturing parameters can be found in Appendix II.

3.2.1 Preparation and characterisation of PLGA-PEG-PLGA triblock copolymer

Synthesis of the PLGA-PEG-PLGA triblock copolymer occurred by ring opening polymerisation of the DL-lactide and glycolide monomers in the presence of PEG1500 and a stannous octoate ($\text{Sn}(\text{Oct})_2$) catalyst under a dry nitrogen atmosphere using vacuum gas manifold or Schlenk line (Zentner, 2001). Prior to polymerisation, PEG was first dried in the reaction vessel under vacuum with stirring at 120°C for 3 hours. The temperature was then raised to 150°C, the monomers were added to the vessel and the reaction mixture was allowed to equilibrate under a dry nitrogen atmosphere. After 30 minutes, the $\text{Sn}(\text{Oct})_2$ was added and the reaction allowed to proceed for a further 8 hours. The resultant copolymer was dissolved and precipitated in water in order to remove un-reacted monomers. The triblock copolymer was

then dried under vacuum to remove residual water and stored frozen until required. Acknowledgement goes to Giles Kirby (PhD student, School of Pharmacy, University of Nottingham) for preparing the batches (Kirby, 2011).

The molecular weight and polydispersity index of the copolymer was determined using gel permeation chromatography (GPC) with differential refractometer detection. Tetrahydrofuran (THF) was employed as an eluent, with two columns (30 cm, PolarGel-M) in series calibrated against polystyrene standards.

Nuclear Magnetic Resonance (NMR) analysis of the copolymer was undertaken using a Bruker DPX-300 Spectrometer (300 MHz) with deuterated chloroform (CDCl₃) as the solvent. A tetramethylsilane (TMS) signal was taken as the zero chemical shift. The composition of the copolymer was determined by ¹H NMR by integrating the signals pertaining to each monomer (Hou, 2008).

Three batches of PLGA-PEG-PLGA triblock copolymer were used in this work and these were labelled as TBII-B, TBII-C and TBII-F.

Acknowledgement goes to Natasha Birkin (School of Chemistry, University of Nottingham) for performing the GPC and NMR

3.2.2 MP manufacture incorporating PLGA-PEG-PLGA triblock copolymer

PLGA MPs were formed using a water-in-oil-in-water (W/O/W) emulsion method as previously described in Chapter 2 with lysozyme and human serum albumin (HSA) being co-encapsulated together. But, in addition to the PLGA polymer, PLGA-PEG-PLGA triblock copolymer was introduced into the dichloromethane (DCM). The MP size range chosen for the work on optimisation of release profiles were in the 50-100 μm range and were manufactured using the following parameters. An aqueous solution of HSA and lysozyme (9 mg HSA, 1 mg lysozyme dissolved in 100 μl distilled water) was added to a solution of PLGA and PLGA-PEG-PLGA in DCM. In each case a 1 g batch was manufactured and the triblock copolymer was added to give weight percentages of 0, 10, 20 and 30% (w/w) . The phases were homogenised for two minutes at 4,000 rpm (Silverson L5M) to form the water-in-oil emulsion. This primary emulsion was transferred to 200 ml 0.3% (w/v) PVA solution and was homogenised for a second time at 2,000 rpm for a further two minutes. The resultant double emulsion was stirred at 300 rpm for a minimum of 4 hours to facilitate DCM evaporation. MPs were then collected by filtration, washed and lyophilized. Control MPs without protein (100 μl distilled water) were always manufactured alongside the test MPs.

3.2.3 Manufacture of self assembling thermosensitive scaffolds directly loaded with lysozyme by hot melt fabrication.

PLGA can be plasticised with low molecular weight PEG (PEG400) by hot melt blending to lower the glass transition temperature of PLGA. MPs manufactured with a glass transition temperature around 37°C will form a

scaffold at body temperature to provide support for the surrounding tissues. A blend of 93.5% PLGA_(w/w) with 6.5%_(w/w) PEG400 is ideal for such applications (Dhillon, 2011) and a schematic of the manufacturing process is shown in Figure 3.2. Briefly, PLGA (85 15, 56 KDa) was weighed (9.35 g) onto a PTFE sheet and 0.65 g of PEG400 was added directly. The sheet was transferred to a hotplate set at 120°C to allow the polymers to melt and the PEG400 was mixed in thoroughly using a PTFE spatula. The polymer sheet was allowed to cool, cut into small pieces and milled using a Krups 75 mill. The required size fraction (usually 100-200 micron) was collected by sieving through woven mesh sieves. Once collected, the MPs were stored vacuum packed and frozen until required

To directly melt blend lysozyme into the PLGA/PEG MPs, lysozyme was ground using a pestle and mortar to try to reduce its particle size. The PLGA/PEG MPs (4.95 g) were mixed with the ground lysozyme (50 mg) on a PTFE sheet to give a 1%_(w/w) total loading of lysozyme. The mix was transferred to a hotplate set at 70°C and the blend was allowed to melt before being thoroughly mixed with a PTFE spatula. MPs were manufactured by milling as described above.

To form scaffolds, PLGA/PEG/lysozyme particles (100 mg) were weighed and transferred to the barrel of a 1 ml syringe. The bore end of the syringe had been cut off and the plunger used to gently compress the particles against a gloved thumb. Syringes containing particles were prepared in triplicate. The syringes containing scaffolds were placed vertically into a 50 ml tube that contained dampened blue roll to keep the atmosphere moist. The scaffolds were sintered for 2 hours at 37°C then, removed from the syringe barrels and dried overnight in a freeze drier.

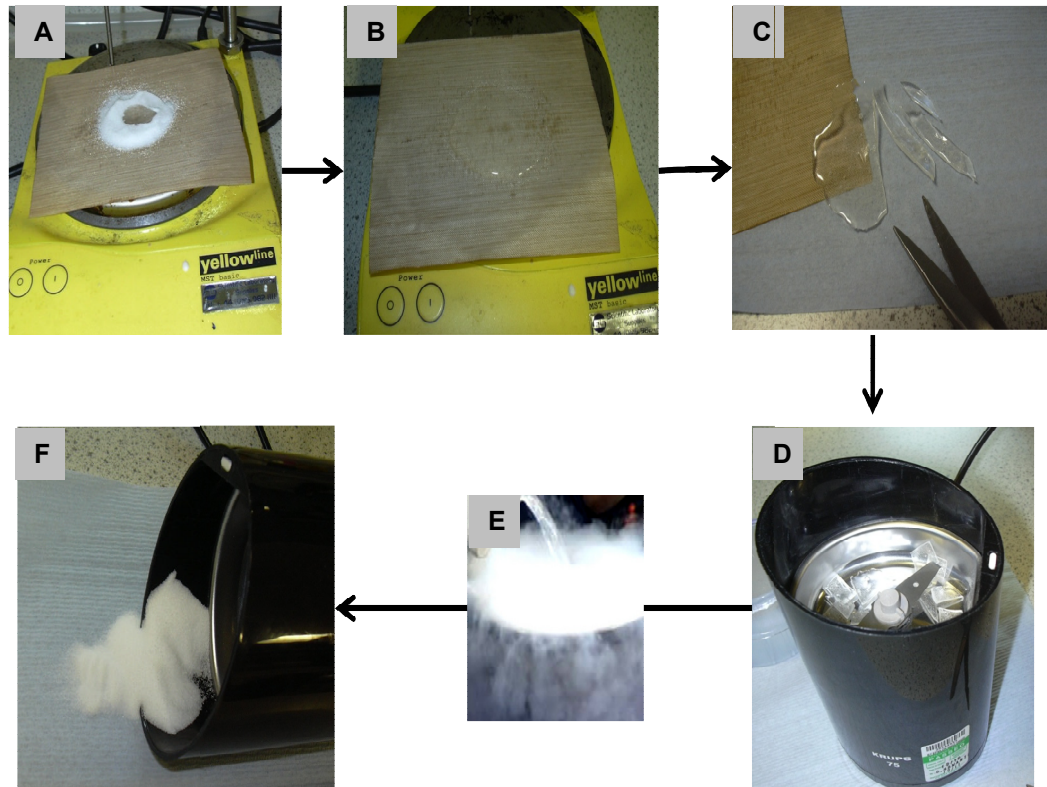


Figure 3.2 Schematic showing the manufacture of PLGA/PEG temperature sensitive MPs. [A] PLGA and PEG400 is weighed onto a PTFE sheet and [B] melted on a hotplate. Once mixed, the polymer is allowed to cool and [C] cut into pieces. The pieces are [D] added to the body of a mill which is [E] treated with a small amount of liquid nitrogen to cool. The polymer is [F] milled to produce individual MPs.

3.2.4 Determination of glass transition temperature by rheology

Rheology is the study of deformation and flow of materials and can be used to determine the glass transition temperature of polymers. A Physica MCR 301 rheometer fitted with 25 mm parallel plate geometry and an environmental hood was used to determine the rheological properties of PLGA MPs and PLGA MPs formulated with PLGA-PEG-PLGA triblock copolymer. Oscillatory measurements at a constant gap distance (0.5 mm) and a controlled strain (0.1%) were conducted under nitrogen gas flow to determine the change in the material with temperature as the dependant variable.

Each sample of MPs manufactured from PLGA 50 50 and PLGA 85 15 having either 0, 10 or 30% _(w/w) PLGA-PEG-PLGA triblock copolymer loading were in turn loaded onto the rheometer's Peltier plate and the environmental hood was lowered. Data was collected every 30 seconds with constant strain amplitude of 0.1% and a frequency of 1 Hz applied over a temperature ramp of 20°C to 70°C. Graphs of phase angle (δ), storage modulus (G') and loss modulus (G'') were plotted against temperature and the point at which the storage and loss modulus intercepted was deemed to be the glass transition temperature of the material.

3.2.5 Degradation of PLGA \pm triblock copolymer through mass loss

In order to assess the effect of PLGA-PEG-PLGA triblock copolymer on the degradation rate of PLGA, mass loss was measured over time following the method previously described in Section 2.2.7.2. The MPs were prepared with 0%, 10% and 30% _(w/w) and a defined mass (20 mg) of the MPs was incubated at either 37°C or 45°C (for accelerated degradation) in PBS. At defined time-

points, the MPs were dried and re-weighed before being re-suspended back in PBS. Traces of MP mass against time were prepared.

3.2.6 Protein release studies

3.2.6.1 Release of HSA/lysozyme from PLGA MPs

Release studies were set up by weighing a known mass of blank MPs and protein loaded MPs (e.g. 25 mg, 50 mg or 100 mg depending on the MP size) into labelled tubes (either 15 ml or 1.6 ml centrifuge tubes) in triplicate for each batch. Phosphate buffered saline (PBS) was then added (e.g. 1 ml, 1.5 ml or 3 ml) and the lids were secured. The tubes were then gently rocked on a 3-D shaker at 5 rpm in a humidified incubator set at 37°C.

At defined time-points, the tubes were removed from the rocker. For MPs >50 µm, the tubes were placed upright and left for at least 30 minutes for the MPs to settle at the bottom of the tube. For smaller MPs, the tubes were centrifuged at 3000 rpm (MSE, Mistral 1000) for 3 minutes to sediment the MPs. The supernatants were collected using either a plastic Pasteur pipette or Gilson pipette and were stored frozen until required. Fresh PBS to the same volume was returned to the tubes which were re-sealed and re-incubated on the rocker until the next collection time-point. The frozen supernatant samples could be tested in the BCA assay for total protein (Section 2.2.8.1) using PBS as the diluent.

At the end of the study, after the last collection point, the tubes were dried on a freeze drier and any remaining particles/protein were dissolved out in

DMSO/SDS/NaOH solution and a BCA protein assay performed (Section 2.2.8.1). The cumulative protein released was calculated as a percentage of the total protein measured (cumulative total released plus total remaining in tubes) for each time-point.

$$\frac{\text{cumulative release of protein at each time-point } (\mu\text{g})}{\text{cumulative release at end of study } (\mu\text{g}) + \text{protein in tube at end of study } (\mu\text{g})} \times 100 = \text{cumulative \%age released at each time-point}$$

A schematic of the main two studies set up is shown in Figure 3.3

3.2.6.2 Release of lysozyme from PLGA/PEG scaffolds

The PLGA/PEG/lysozyme scaffolds manufactured in Section 3.2.3 were placed in the wells of a 24 well plate and 2 ml of PBS added to each. As a control three PLGA/PEG particulate scaffolds without lysozyme were also placed in the plate which was placed on a 3D rocker set at 5 rpm. At specified time-points, the PBS was collected from each well and replaced with fresh. The collected sample was tested for total protein (BCA) and lysozyme activity (*M. lysodeketicus*) and cumulative release curves were constructed.

The scaffolds were imaged under SEM and a sample of the PLGA/PEG/lysozyme MPs were tested to determine their entrapment efficiency.

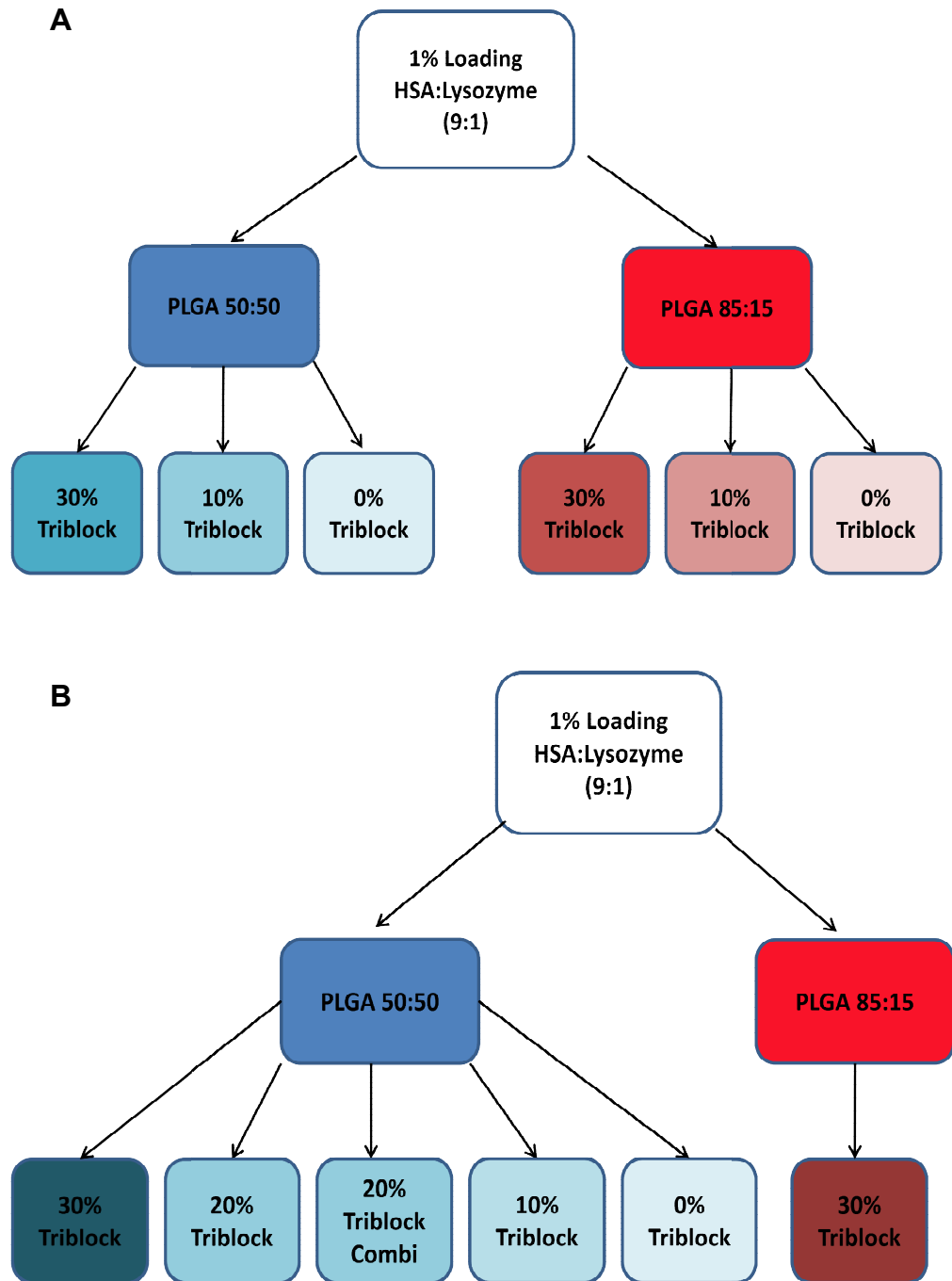


Figure 3.3 Schematic showing the MP formulations tested in [A] release study 1 and [B] release study 2. ‘20%_(w/w) triblock combi’ refers to a 1:1 mix of 30%_(w/w) triblock and 10%_(w/w) triblock microparticles

3.2.7 Detection of lysozyme activity: *Micrococcus lysodeketicus*

The *Micrococcus lysodeketicus* assay was used to measure lysozyme activity in the supernatants as described in Section 2.2.9.

3.2.8 Statistical analysis

Where error bars are presented on figures, they were calculated from the standard deviation of the mean with a minimum replicate number of three. For cumulative release profiles, cumulative error bars were calculated by squaring the standard deviation at each time-point, adding the values cumulatively then calculating the square root of the cumulative value for standard deviation at each time point.

Values for protein concentration or protein activity were calculated from either the polynomial equation or the straight line equation of the appropriate standard curve as stated.

3.3 Results and Discussion

3.3.1 Characterisation of PLGA-PEG-PLGA triblock copolymer

The studies performed to demonstrate release profiles from biodegradable MPs throughout this project necessitated the use of three different PLGA-PEG-PLGA triblock copolymer batches (TBII-B, TBII-C and TBII-F).

Unfortunately, the nature of the manufacturing technique rendered it difficult to produce polymers with exactly the same parameters. Molecular weight and molecular weight distribution of the copolymers was evaluated for each batch using gel permeation chromatography (GPC) and ^1H NMR analysis was also performed to characterise the material. The results of these analyses are shown in Appendix IV and acknowledgement goes to Natasha Birkin, School of Chemistry, University of Nottingham for performing the characterisation. The quantitative data obtained from the analysis of the copolymers is summarized in Table 3.1.

Despite the polydispersity indices being similar, the overall molecular weights varied from just under 4000 to just over 5000 Da. This discrepancy in molecular weights could influence the effect that the triblock copolymer would exert on protein release from MPs. Hence, it was important that the same triblock copolymer batch was used in comparative studies to ensure the effect seen is not due to different triblock batches. The three triblock copolymer batches were manufactured at different stages during the three year project and thus a direct comparative study was not performed. However, there was evidence that MPs made incorporating the lower molecular weight triblock copolymer released their cargo quicker than those manufactured with the higher molecular weight triblock copolymer. Preferred storage conditions

(frozen and vacuum packed) would help avoid degradation and the batches were dispensed into aliquots to avoid repeated freeze thaw cycles.

Table 3.1 Table of PLGA-PEG-PLGA triblock copolymer parameters

<i>Triblock copolymer batch</i>	<i>Molecular Weight (Da)</i>	<i>Poly Dispersity Index</i>
PLGA-PEG-PEG TBII-B	5202	1.56
PLGA-PEG-PEG TBII-C	4590	1.60
PLGA-PEG-PEG TBII-F	3960	1.53

3.3.2 The effect of PLGA-PEG-PLGA triblock copolymer on the viscoelastic properties of PLGA.

The viscoelastic property of a polymer can be determined by dynamic mechanical thermal analysis and is measured by applying a sinusoidal force (stress) and determining the resulting displacement (strain). Rheology is the study of deformation and flow of a material. If the material was perfectly elastic, the stress and strain would be in perfect phase. If it was purely viscous there would be a 90 degree phase lag. A viscoelastic material will result in phase lag in between 0 and 90 degrees which can be determined by a rheometer and is represented by the following equations.

Stress: $\sigma = \sigma_0 \sin(t\omega + \delta)$

Strain: $\varepsilon = \varepsilon_0 \sin(t\omega)$

Where

ω is the frequency of strain oscillation

t is the time

δ is the lag phase between stress and strain

The shear storage or elastic modulus (G') represents the deformation energy stored and the shear loss or viscous modulus (G'') represents the deformation energy dissipated as heat.

Storage modulus: $G' = \frac{\sigma_0}{\varepsilon_0} \cos \delta$

Loss modulus: $G'' = \frac{\sigma_0}{\varepsilon_0} \sin \delta$

Phase angle (tan delta): $\tan \delta = \frac{G''}{G'}$

The rheometer can therefore be used to determine the viscoelastic properties of PLGA and the effect of adding PLGA-PEG-PLGA triblock copolymer.

The rheology of the PLGA-PEG-PLGA block copolymers with polylactic acid MPs incorporated in the copolymer has been investigated (Hou, 2008) but, to date there is no published work on rheological analysis of PLGA MPs that have been formulated with triblock copolymer during the fabrication process.

As a polymer goes through its glass transition, the storage modulus will decrease significantly and the loss modulus will reach a maximum. Using data from the rheometer set at a constant strain amplitude of 0.1% and a frequency of 1 Hz applied over a temperature ramp of 20°C to 70°C, graphs of phase angle ($\tan \delta$), storage modulus (G') and loss modulus (G'') can be plotted against temperature (Santovena, 2004). Transition from a glassy state to a

rubbery state does not occur instantaneously at one temperature, but in order to define a glass transition temperature or T_g , the point where G' equals G'' was taken as this is also defined as the gelation point (Weng, 2007). This value usually relates closely to the peak in phase angle ($\tan \delta$) which is another value quoted but this often overestimates the T_g . The glass transition temperatures reported in the certificate of analysis for the two polymers used are 49°C for PLA 50 50 (Mwt 56 KDa) and 50.3°C for PLGA 85 15 (Mwt 52 KDa). These values were recorded by differential scanning calorimetry (DSC) rather than rheological analysis.

The data in Figures 3.4 and 3.5 show the dynamic mechanical thermal analysis traces for MPs made from PLGA 50 50 and PLGA 85 15 both alone and with the incorporation of 10% (w/w) and 30% (w/w) PLGA-PEG-PLGA triblock copolymer. The addition of PLGA-PEG-PLGA triblock copolymer had a direct and dose responsive effect on the T_g of both PLGA polymers. Regarding the PLGA 50 50, the polymer with no PLGA-PEG-PLGA had a glass transition temperature of 45.7°C which was reduced down to 33.6°C on the addition of 30% (w/w) PLGA-PEG-PLGA. The 10% (w/w) loading gave an intermediate T_g (Figure 3.4). The same analysis was performed on PLGA 85 15 fabricated with 10% and 30% (w/w) PLGA-PEG-PLGA triblock copolymer and this data is shown in Figure 3.5. Again the copolymer affected the glass transition temperature but the values were higher. The starting T_g was 57.8°C reducing down to 52.7°C (10% (w/w)) followed by 45.6°C (30% (w/w)).

The reason for this is that the PLGA-PEG-PLGA is acting as a plasticiser on the higher molecular weight PLGA. It interweaves between the tightly packed entangled polymer chains taking up space and acts like a lubricant enabling the chains to move more readily making the PLGA become more flexible. It

has been reported that the glass transition temperature of PLGA decreases with a decrease in lactide content and these results uphold these findings (Passerini, 2001).

The potential advantage of this for protein release is that as shown in the previous Chapter (Figure 2.12), polymer degradation occurs quicker as temperature increases. Increased degradation will result in faster protein release. If the polymeric matrix of the MP can be altered to have a lower T_g , then it should be possible to achieve faster degradation and therefore faster protein release at lower temperature such as body temperature.

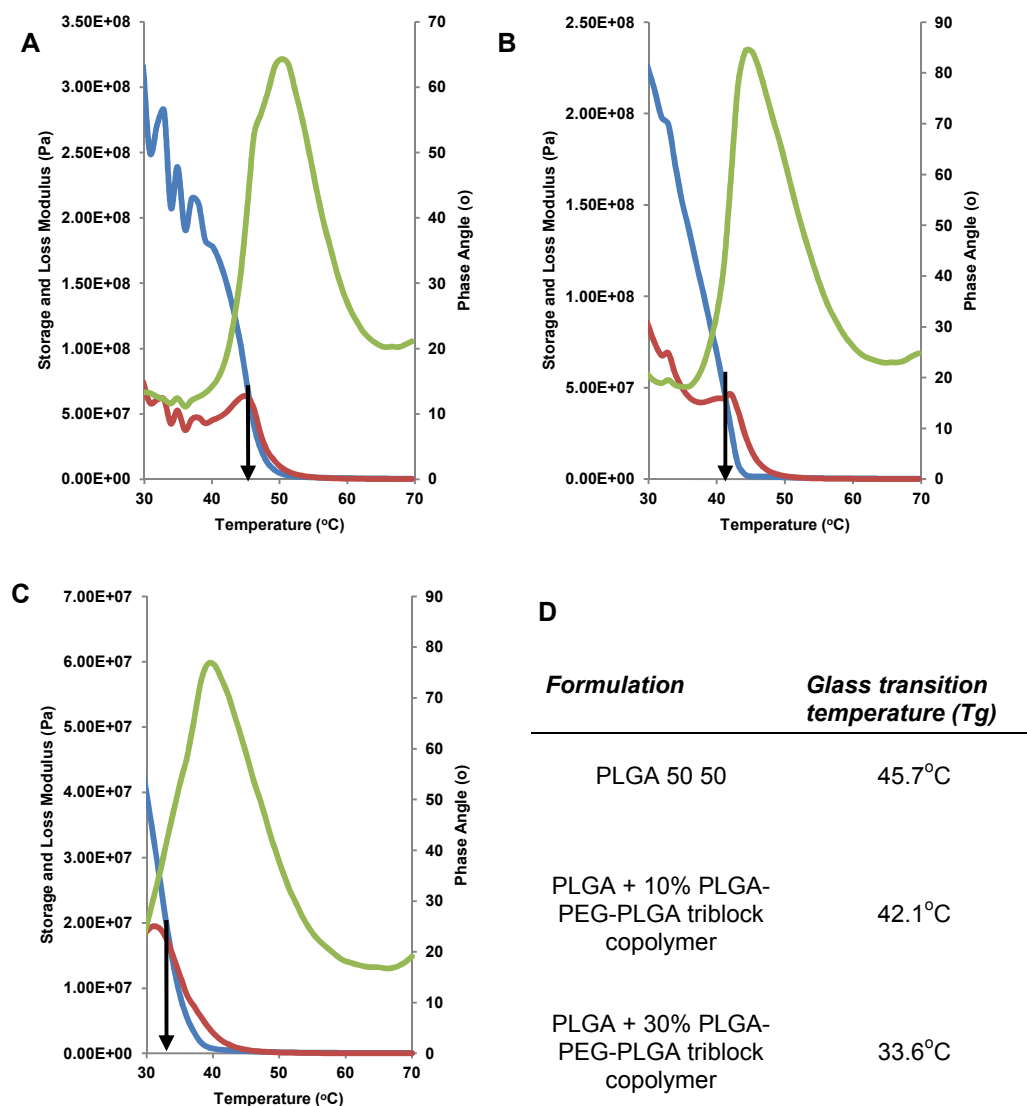


Figure 3.4: Rheological traces of [A] PLGA 50 50 Mwt 56 KDa and MPs formulated with [B] 10% and [C] 30% w/w PLGA-PEG-PLGA triblock copolymer. Storage modulus (blue), loss modulus (red) and phase angle (green). [D] Glass transition temperature of the polymers. Copolymer batch TBII-C was used

Batches: BN 231, 235 and PLGA 50 50

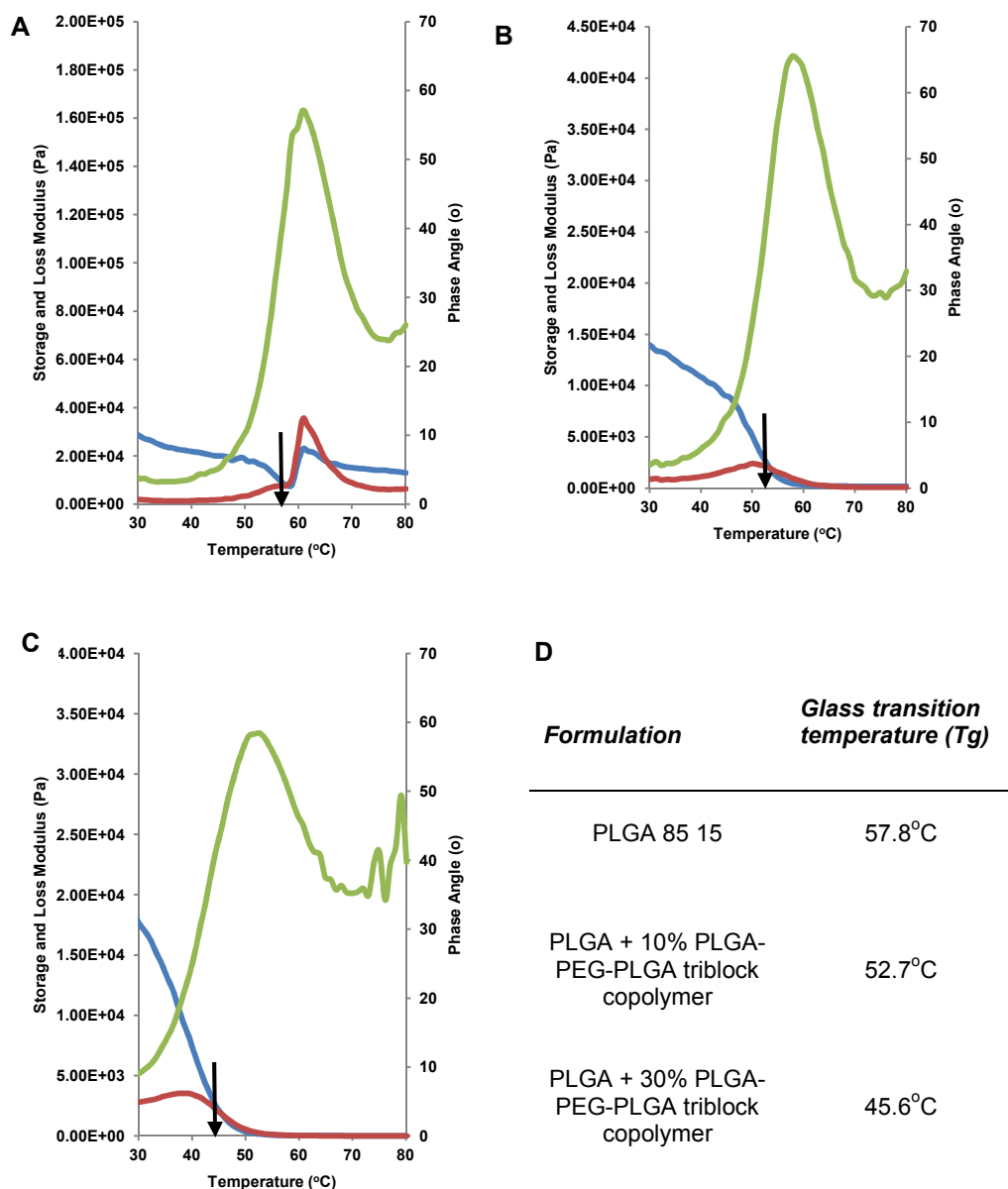


Figure 3.5 Rheological traces of PLGA 85 15 Mwt 52 KDa formulated with [A] 0%, [B] 10% and [C] 30% w/w PLGA-PEG-PLGA triblock copolymer. Storage modulus (blue), loss modulus (red) and phase angle (green). [D] Glass transition temperature of the polymers. Copolymer batch TBII-B was used

Batches: BN 128, 130 and 132

3.3.3 The effect of PLGA-PEG-PLGA triblock copolymer on the degradation rate of PLGA.

This project has established that the degradation rate of PLGA MPs is related to temperature with a higher temperature causing faster degradation. Also, the addition of a triblock copolymer lowered the glass transition temperature. It can therefore be hypothesised that the incorporation of PLGA-PEG-PLGA triblock copolymer may increase the overall degradation rate and that this will impact on future studies of protein release. This was tested by manufacturing PLGA 50 50 MPs with 0, 10, 20 and 30% _(w/w) triblock copolymer (TBII-C) and performing a mass loss study over 50 days at two different temperatures. The results are shown in Figure 3.6 where data is recorded at 37°C and at 45°C. Although the addition of triblock copolymer appeared to increase the PLGA degradation rate, there was not a great deal of difference between the formulations as due to the nature of the experiment, the error was relatively high. At 45°C the degradation was much faster in all groups with no obvious differentiation between the triblock concentrations but the MPs without triblock degraded the slowest.

It was now feasible that MPs loaded with a model protein could be manufactured with different degradation rates and therefore display different release rates. Although the degradation rate is likely to play a key role in protein release from these MPs, the increased hydrophilic nature of these MPs is also expected to play a positive role in accelerating the release above the degradation rate. In which case the PLGA MPs would still be able to provide structure after the protein had been released.

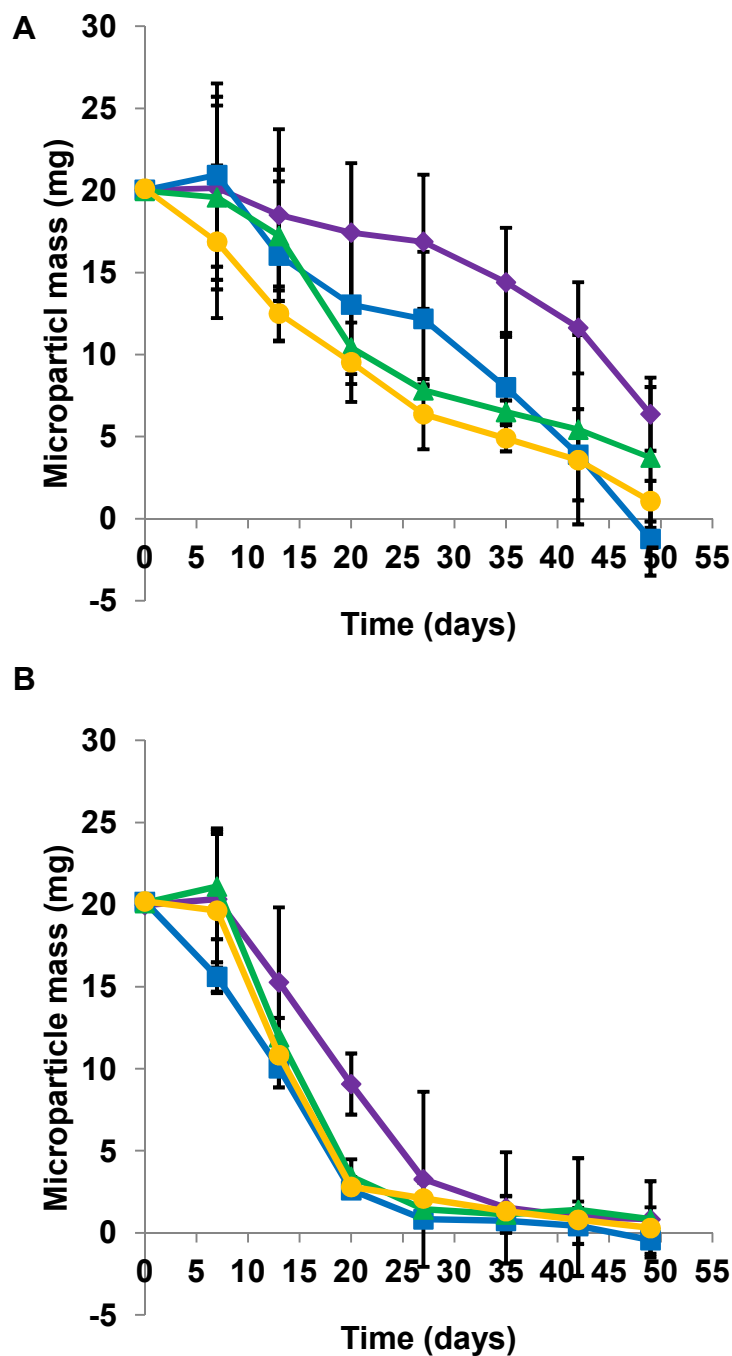


Figure 3.6: Mass loss of PLGA50 50 Mwt 56 KDa through degradation at [A] 37 °C and [B] 45 °C. Microparticles formulated with 0% (purple), 10% (blue), 20% (green) and 30% (orange) (w/w) PLGA-PEG-PLGA triblock copolymer and incubated in PBS. The MPs were dried before weighing at each time-point. Copolymer batch TBII-C was used

Batches: BN 172, 230, 232, and 234

3.3.4 HSA/Lysozyme release from PLGA MPs

3.3.4.1 Effect of PLGA-PEG-PLGA triblock copolymer content on protein release from MPs fabricated with PLGA 50 50 and PLGA 85 15

A release study was set up to determine both the effect of PLGA-PEG-PLGA triblock copolymer and the lactide: glycolide ratio on the release of HSA/lysozyme from PLGA MPs. The schematic depicting the organisation of the study is shown in Figure 3.3A. All MPs were fabricated following the standard protocol described in the previous Chapter using 20% _(w/v) PLGA with a 1% _(w/w) loading of HSA/lysozyme (9 mg and 1 mg) with a primary homogenisation speed of 4,000 rpm and a secondary homogenisation speed of 2,000 rpm.

All batches of MPs were imaged by scanning electron microscopy and were sized by laser diffraction. Figure 3.7 shows the morphology of these MPs. Some of the MPs had surface pores but this phenomenon did not relate to either the copolymer concentration or the lactide: glycolide ratio. Indeed, the most porous MPs were evident in the batches that contained no triblock copolymer (e.g PLGA 85 15 0% _(w/w) triblock copolymer). However, not all MPs exhibited pores and generally, the outer surface of the MPs was smooth. These surface pores may relate to pockets of entrapped protein that were very close to the MP surface which were lost during the solvent evaporation process resulting in a small pore. The creation of these pores is therefore a side effect of the emulsion process and may not be easily controlled but will be monitored for trends in the data. Conceivably, the burst release from MPs with surface pores may be reduced due to surface protein already being lost during the manufacturing process. However, in practice, using the PLGA 85 15 with no triblock copolymer as an example, the converse appeared to be true

(Figure 3.10 open circle) with a burst release of just over 30% from this formulation. No further protein release was detected from this formulation for the next 30 days indicating that the remaining protein remained entrapped within the polymer matrix. This formulation was allowed to release up to 70 days and a second phase of release occurred after 47 days (data not shown). The unusually large burst release from this formulation remained an anomaly as the formulation was not repeated in future studies due to its clinically irrelevant release profile.

This issue of burst release has been investigated by many groups with different strategies being adopted in an attempt to control it. Studies have investigated altering MP manufacture procedures to modify internal morphology (Igartua, 1997, Fu, 2003, Mao, 2007), altering the protein molecular weight and/or loading (Sandor, 2001), modifying protein with additives or using a bulk carrier to improve stability (Kang, 2001, Diwan, 2001) or modifying the PLGA with the addition of a hydrophilic component (Cleek, 1997, Yeo, 2004b). However, for some applications a high initial dose is not always a disadvantage as long as the level of the burst is reproducible.

A relatively straightforward answer to the issue of burst release may be to subject the MPs to a washing step to remove any surface bound material prior to the start of a release assay. A short study to monitor the burst over 24 hours for small PLGA 50:50 MPs in the 10-20 μm range indicated that 80% of the total burst occurred in the first hour, a further 7% in the next 2 hours followed by a further 6% in the next 4 hours leaving only 7% being released between 7 and 24 hours. A short wash may therefore be useful in controlling the burst, but it was decided not to incorporate it into the current protocol.

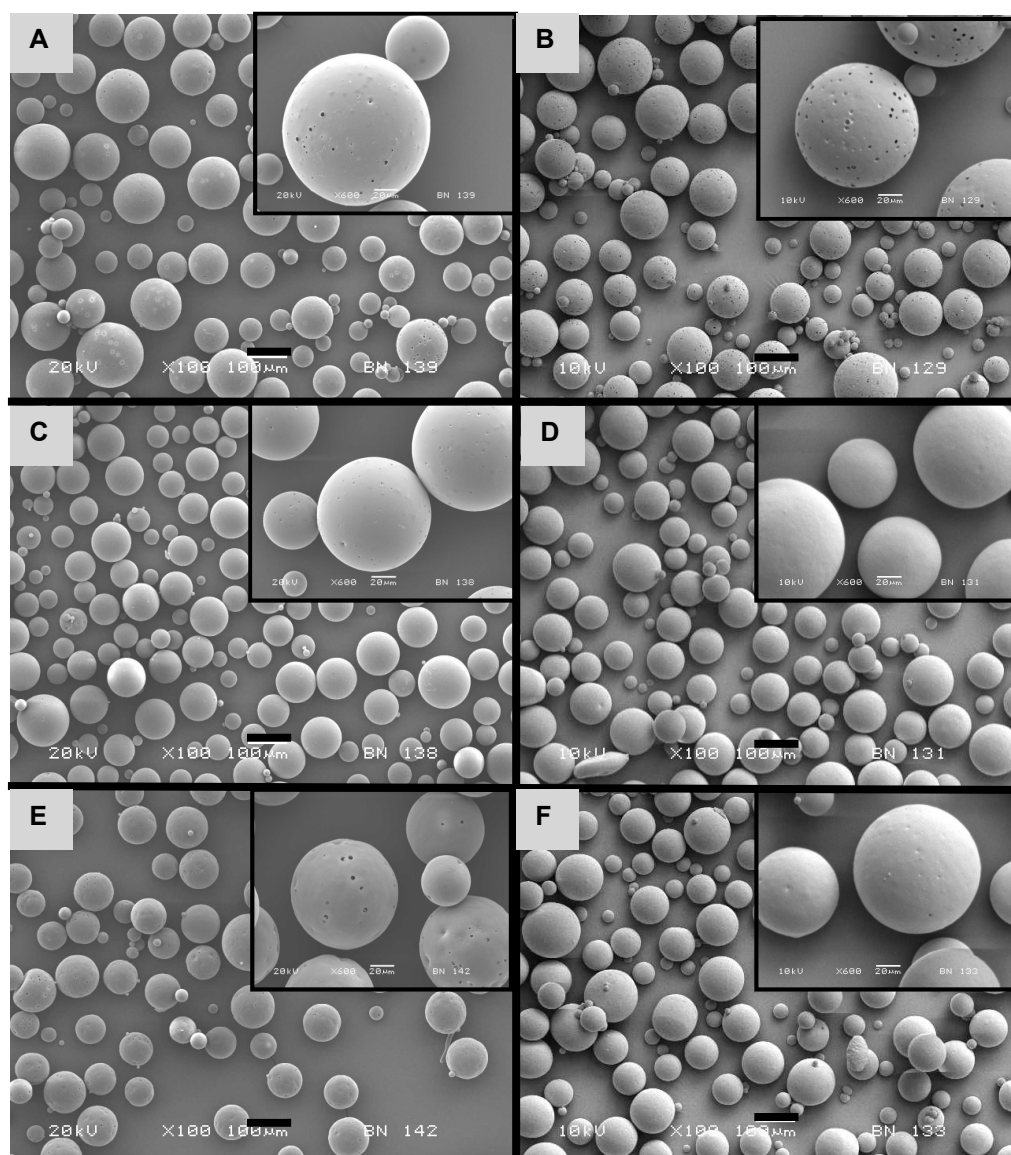


Figure 3.7: Effect on morphology of the incorporation of PLGA-PEG-PLGA triblock copolymer into PLGA microspheres. PLGA 50 50 [A, C and E] was compared with PLGA 85 15 [B, D and F]. PLGA-PEG-PLGA was incorporated into the PLGA at 0% [A and B], 10% [C and D] or 30% (w/w) [E and F] of the total mass. All microspheres were loaded with 1% HSA/lysozyme. Copolymer batch TBII-B was used.

Batches: BN 129,131,133, 138, 139 and 142

Another consideration was the effect of PLGA-PEG-PLGA triblock copolymer on the size and entrapment efficiency of the MPs. The addition of copolymer did slightly reduce the average MP size and this data is shown in Table 3.2. The average MP size for PLGA 85 15 was approximately 20% greater than that of the PLGA 50 50 MPs without copolymer and both reduced in size with the addition of copolymer. The smallest MPs were $64.57 \pm 15.87 \mu\text{m}$ (PLGA 50 50 30%_(w/w) triblock) and the largest were $95.20 \pm 31.90 \mu\text{m}$ (PLGA 85 15 0%_(w/w) triblock).

Potentially, the size differences were caused by a combination of factors. Firstly, the increased content of the triblock copolymer resulted in a reduction in the overall content of PLGA and it was shown in Chapter 2 that total PLGA concentration plays a pivotal role in MP size. Secondly, the addition of a hydrophilic component would alter the dynamics of emulsion formation resulting in smaller MPs and thirdly the difference between the size of the PLGA 50 50 and PLGA 85 15 could have been because they have slightly different molecular weights and inherent viscosities. Although the average MP size shows up the differences in the batches, the normal distribution is generally 30 % of the mean and so all of the size profiles overlap considerably (data not shown). The reduction in size due to the addition of triblock copolymer may lead to faster protein release due to the release assays being set up based on MP mass (Dawes, 2009). A higher number of small MPs would be present in a comparable mass of larger MPs resulting in larger surface area from which the protein could be released.

The entrapment efficiency results are shown in Table 3.3. The lowest values are shown in formulations without added triblock copolymer which may be tenuously linked in with the morphology as these tended to have the most

surface pores. However, all of the entrapment efficiency values were within the range 64.6 and 94.1% which was acceptable for the release studies.

Table 3.2 Average size distribution of PLGA MPs formulated with PLGA-PEG-PLGA triblock copolymer (TBII-B)

	<i>PLGA 50 50 Mwt 59 kDa</i>	<i>PLGA 85 15 Mwt56 kDa</i>
0%_(w/w) PLGA-PEG-PLGA	77.51 ± 26.19 μm	95.20 ± 31.90 μm
10%_(w/w) PLGA-PEG-PLGA	70.75 ± 20.46 μm	94.01 ± 27.60 μm
30%_(w/w) PLGA-PEG-PLGA	64.57 ± 15.87 μm	87.71 ± 24.43 μm

Table 3.3 Entrapment efficiency of PLGA MPs formulated with PLGA-PEG-PLGA triblock copolymer (TBII-B)

	<i>PLGA 50 50 Mwt 59 kDa</i>	<i>PLGA 85 15 Mwt56 kDa</i>
0%_(w/w) PLGA-PEG-PLGA	64.6 %	73.7 %
10%_(w/w) PLGA-PEG-PLGA	71.8 %	95.1 %
30%_(w/w) PLGA-PEG-PLGA	74.9 %	81.7 %

The MPs characterised in this Section were set up in a dynamic release study (gently rocking) with regular sampling points. The collected supernatants were tested for total protein using the bicinchoninic acid (BCA) assay. The cumulative release from the PLGA 50 50 MPs are shown in Figure 3.8 where there is a clear differentiation of the release profiles. All of the protein was released from the 30% _(w/w) triblock copolymer batch within 3 days. It could not be related directly to degradation because the release was so quick. Data in Figure 3.6 showed that this formulation lost approximately 50% of its mass after 20 days. Instead, it was thought that the presence of such a high hydrophilic content in the MPs caused swelling, opened up any pores and produced a hydrogel-like structure so facilitating protein release (Ghahremankhani, 2007). However, once all the protein had released, the MPs were still intact which could provide a scaffold for tissue support.

The MPs containing 10% _(w/w) triblock demonstrated a much more sustained release over the 30 day period with approximately 30-40% of the protein still available in the MPs for release. This sustained release of protein over one month was very encouraging as it overcame the triphasic release (seen in Figure 3.8) from MPs with no triblock copolymer added where a lag phase of little or no release was evident between days 2 and 11. This release from the 10% _(w/w) triblock MPs appeared to be more related to polymer degradation as this lower percentage of triblock would cause a slower rate of water ingress which would still affect the hydrolytic degradation of the MPs but at a slower rate allowing the protein to release gradually throughout what would otherwise be the lag phase.

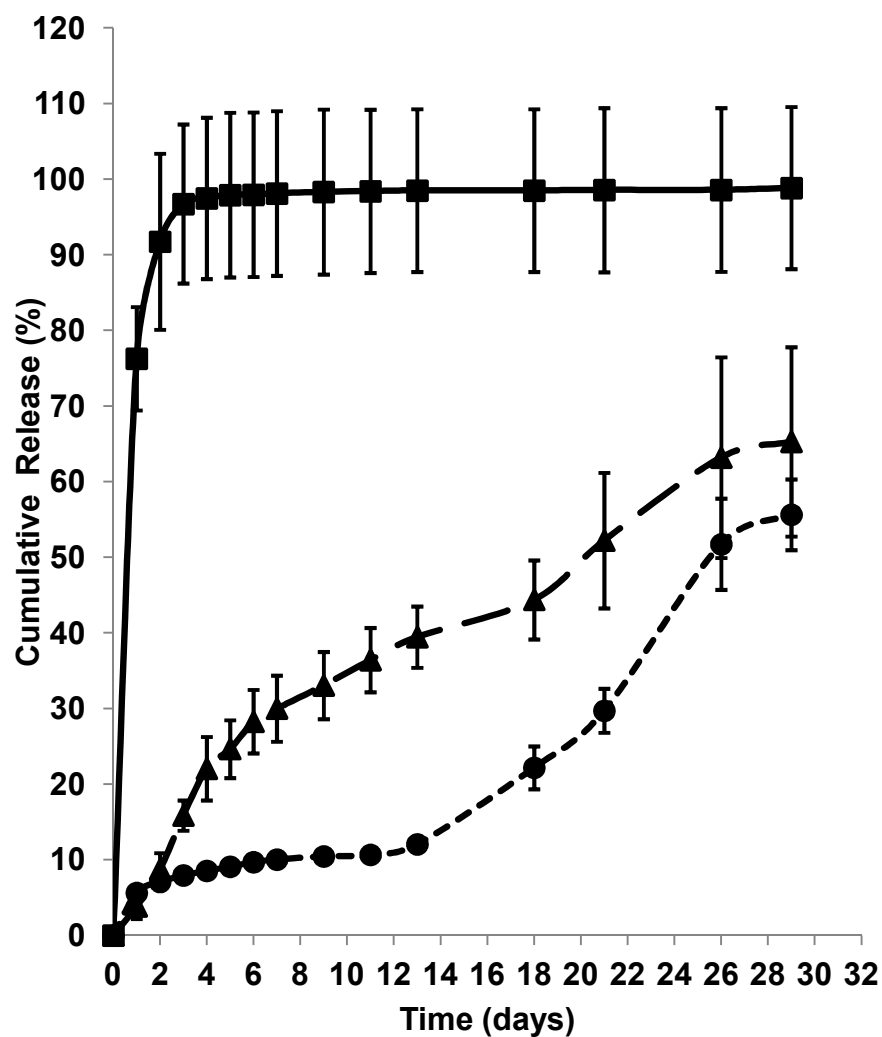


Figure 3.8: Cumulative release of HSA/lysozyme (1% loading) from PLGA 50 50 Mwt 59 KDa MPs (50-100 μm) formulated with 30% (■), 10% (▲) or 0% (●) w/w PLGA-PEG-PLGA triblock copolymer (TBII-B)

Batches: BN 123, 125 and 127

Figure 3.8 showed the effect of incorporated PLGA-PEG-PLGA triblock copolymer on the protein release profile from PLGA 50 50 MPs. Figure 3.9 shows the effect of lactide:glycolide ratio on release in conjunction with triblock copolymer. Figure 3.9A shows the comparative release profiles of 30 %_(w/w) triblock copolymer incorporated into PLGA 50 50 and PLGA 85 15, whilst Figure 3.9B shows the 10%_(w/w) triblock comparison. In both cases the PLGA 50 50 MPs release faster than their PLGA 85 15 counterparts. PLGA 85 15 has a much slower degradation rate (months rather than weeks) due to its higher lactide content. The presence of methyl side groups in lactic acid makes it more hydrophobic than the glycolic acid and hence lactic acid rich PLGA copolymers are less hydrophilic, absorb less water and subsequently degrade more slowly which explains why the release is slower than that from PLGA 50 50 (Makadia, 2011). However, the addition of 30 %_(w/w) triblock copolymer resulted in a practically zero order release for the first week of the study which meant that the release was again decoupled from the polymer degradation rate.

The addition of 10%_(w/w) triblock copolymer to PLGA 85 15 resulted in a delayed release profile (Figure 3.9B). There was very little burst release (possibly due to this batch of MPs having the most surface pores) and no release until after two weeks. Normally, this polymer would not start to degrade *in-vitro* until after 6 weeks on test (data not shown) and so the triblock was therefore still having an effect on the release rate.

All these combinations of triblock copolymer concentration and lactide:glycolide ratios has produced an interesting set of distinct release profiles which are shown together in Figure 3.10 with the error bars removed for clarity (White, 2013).

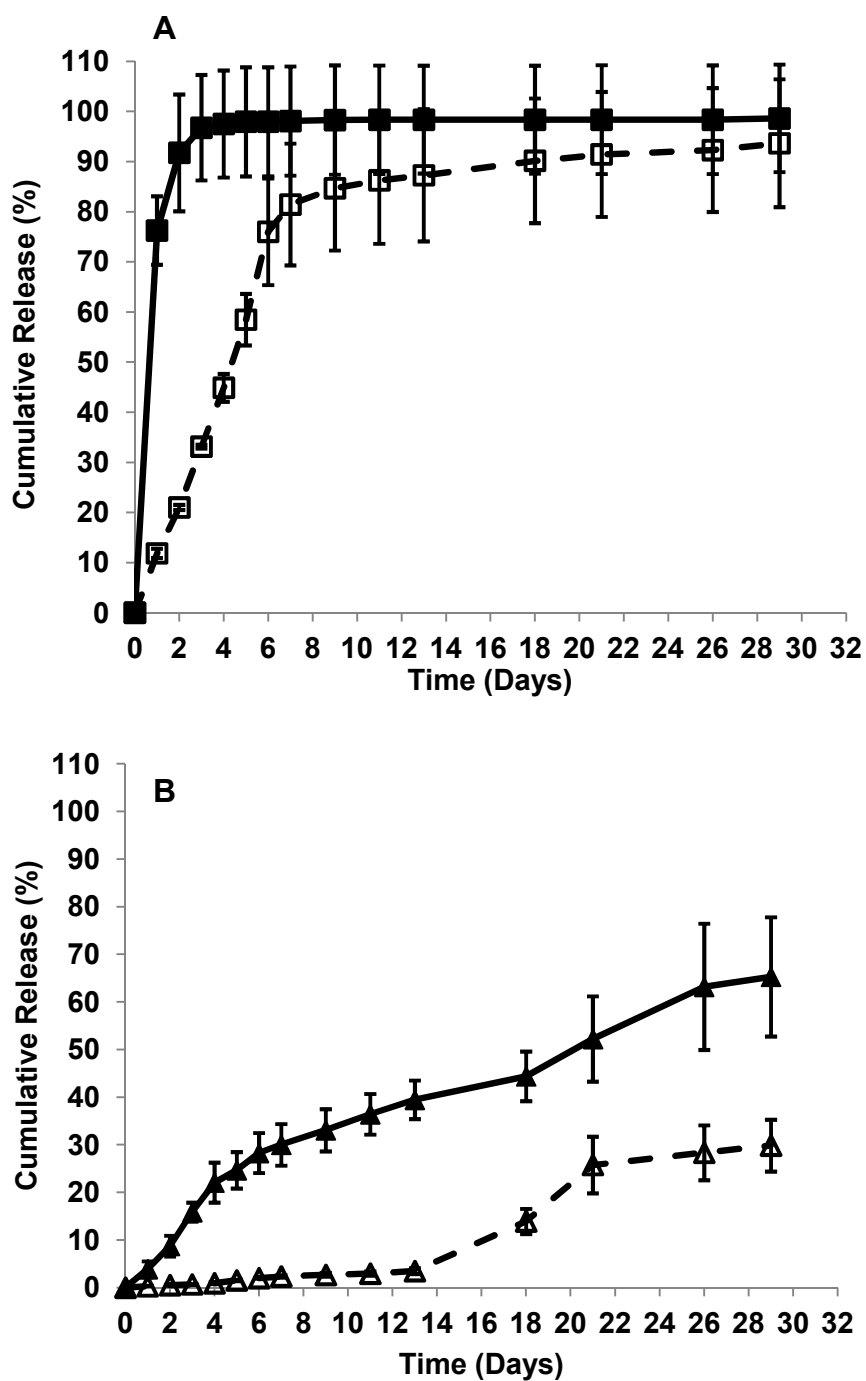


Figure 3.9: [A] Comparison of cumulative protein release from PLGA 50 50 Mwt 59 KDa (■) and PLGA 85 15 Mwt 56 KDa (□) MPs (50-100 μ m) loaded with 1% HSA/lysozyme and formulated with 30% (w/w) PLGA/PEG/PLGA triblock copolymer. [B] Comparison of cumulative protein release from PLGA 50 50 Mwt 59 KDa (▲) and PLGA 85 15 Mwt 56 KDa (△) loaded with 1% HSA/lysozyme and formulated with 10% (w/w) PLGA/PEG/PLGA triblock copolymer (TBII-B)

Batches: BN 125, 131, 127, 133.

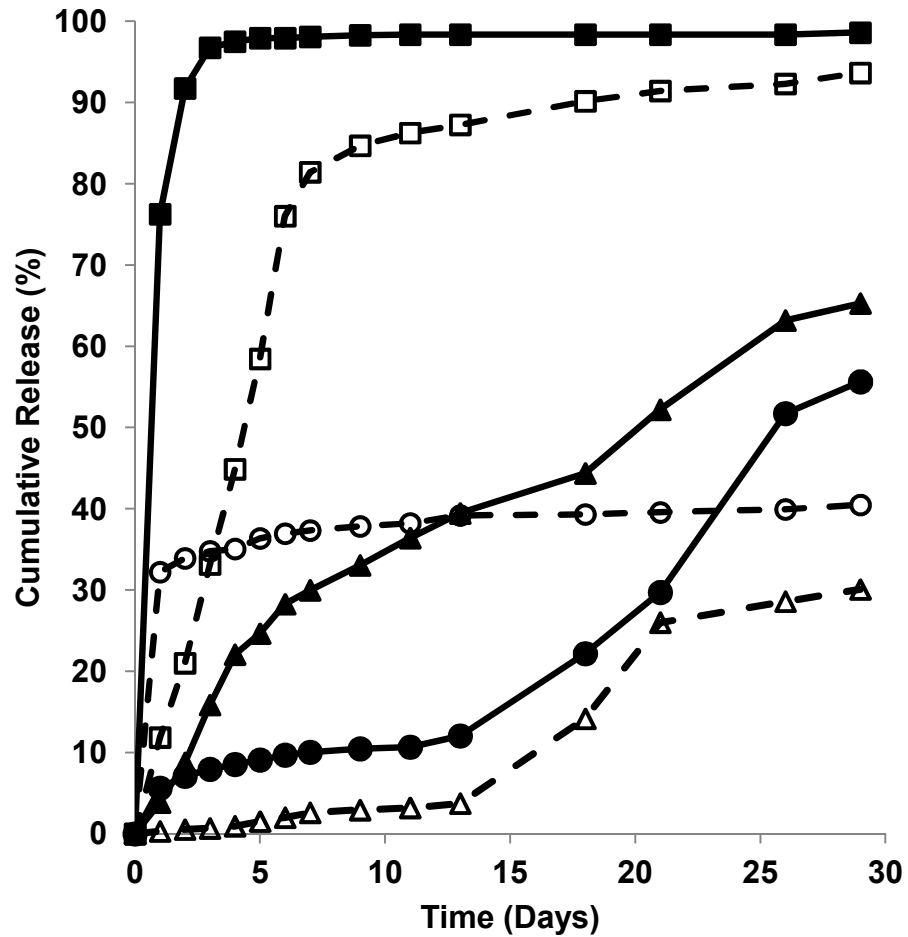


Figure 3.10 Summary of release profiles achieved in study 1 showing the effect of PLGA-PEG-PLGA concentration and Lactide:glycolide ratio. Closed symbols represent PLGA 50/50 and open symbols represent PLGA 85/15 with square being 30%, triangle being 10% and circle being 0% (w/w) PLGA-PEG-PLGA triblock copolymer (TBII-B)

Batches: BN 123, 125, 127, 131 and 133

These release profiles give a very good insight into how the incorporation of a hydrophilic copolymer will affect the protein release from PLGA MPs. However, the issue of incomplete release by the end of the 30 day period has not yet been addressed. For PLGA 85 15 MPs this is likely to be due to their longer degradation time and as shown in Figure 3.10 for each formulation the total percentage released is lower in the PLGA 85 15 formulations. However, it cannot be ignored that the PLGA 50 50 formulations with little or no modification with PLGA-PEG-PLGA triblock copolymer have also not released all of their cargo. Figure 4.6 showed that for these formulations nearly 75% of the total mass would have been lost and this was indeed observed in the release vessels.

The issue of incomplete release maybe due to a number of factors such as the properties of the release medium, the sampling method or the adsorption of the released protein either back on the PLGA matrix or the inside of the release vessel, protein aggregation or protein denaturation (Giteau, 2008, Tran, 2012). Different strategies have been applied to further understand and improve release profiles. The use of continuous flow systems (Aubert-Pouessel, 2002) negates the build up of degradation products and is more likely to replicate the *in-vivo* environment. However, previous experience showed that this method had its own problems in maintaining flow rates and subsequently led to highly variable results. Static and dynamic systems have been compared with dynamic systems such gentle rocking, stirring or shaking increasing the release rate but not altering the release profile (Hernandez, 1998). The effect of release medium will also influence the release rate adding a surfactant has been shown to increase the protein rate (Paillard-Giteau, 2010) and it is reported that lowering the pH by for example using glycine

buffer at pH 2.5 will improve lysozyme stability and avoid aggregation (Giteau, 2008). Clearly, however, this would not be a physiologically relevant model.

It is important that any system used to investigate drug release is repeated in exactly the same way for subsequent tests for the data to be comparable. A small, seemingly insignificant alteration of the protocol (for example, a small change in the volume of release medium or an alteration in the rocking speed) will undoubtedly change the dynamics of the process and potentially lead to a different release profiles being obtained. Although the *in-vitro* release profiles cannot be guaranteed to be a fully accurate prediction of what will happen *in-vivo*, they are a good starting point, especially if they are robustly performed. It was therefore important for this project that the release profiles had low inter and intra batch variability which is the subject of the next Section.

3.3.4.2 Reproducibility of release profiles

A further release study was initiated to further investigate the effect of PLGA-PEG-PLGA triblock copolymer on the release profiles of HSA/lysozyme from PLGA MPs. The schematic depicting the organisation of this study is shown in Figure 3.3B. In this case a 20 %_(w/w) loading of triblock copolymer within PLGA 50 50 was investigated along with a 1:1 combination of MPs with both a 10%_(w/w) and a 30%_(w/w) loading to determine whether an intermediate trace between the 10 and 30% profiles seen in figure 3.9 could be achieved. The first study recorded the release of triplicate samples from one batch of MPs. The second study was used as an opportunity to investigate the reproducibility of the profiles both within batches and across batches. Therefore for each formulation three separate batches of MPs were made and tested in triplicate.

The MP sizes were comparable to those achieved in the first study with the mean MPs sizes ranging from 54 μm to 90 μm depending on the copolymer concentration. The entrapment efficiencies ranged from 63% to 90% across the batches which also compared well to the first study. The results are shown in Figure 3.11 where the separate batches are highlighted by different colours. It was encouraging to see that the release profiles were similar both within batch triplicates and between batch triplicates. This gave confidence in the developed protocols and the effect of the PLGA-PEG-PLGA triblock copolymer on release.

To investigate the reproducibility of the profiles further, these results were compared retrospectively to the profiles (for the appropriate formulations) achieved in the first release study and these are shown in Figure 3.12. In general, the profiles matched up well especially for the highest concentration of PLGA-PEG-PLGA triblock copolymer (30 %_(w/w)) within PLGA 50 50. The other formulations, 30 %_(w/w) in PLGA 85 15 and 10 %_(w/w) in PLGA 50 50 as well as PLGA 50 50 alone showed slightly more variation between the studies with the release from the second study being consistently lower. Although these studies were performed using the same batch of PLGA-PEG-PLGA triblock copolymer (TBII-B), they were nearly three months apart and it may be that storage may have degraded the triblock slightly. Nevertheless, the protocols to manufacture protein loaded MPs and tailor the rate of model protein release from them were very reproducible both within batches, between batches (Figure 3.11) and moderately reproducible over time (Figure 3.12). Such robust testing of release profiles has not been cited in the literature.

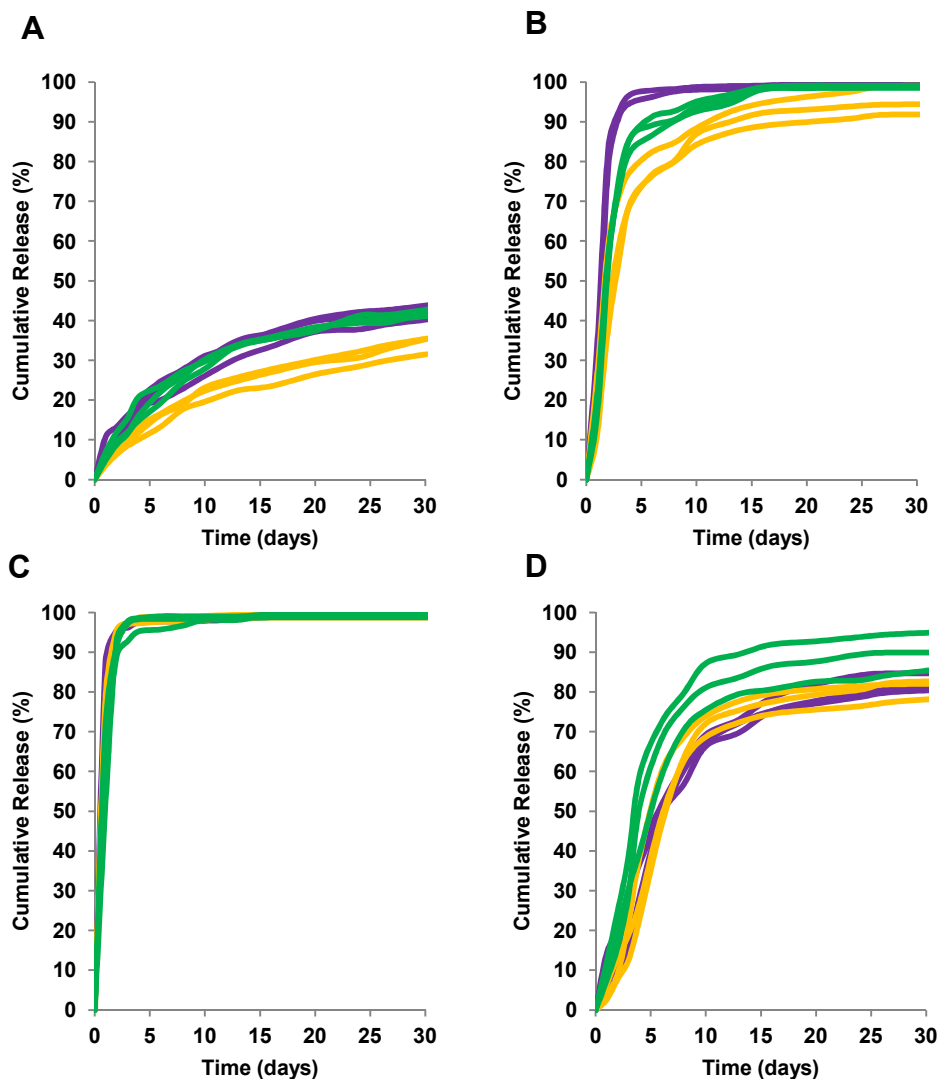


Figure 3.11: Reproducibility of cumulative release profiles. [A] Release from PLGA 50 50 Mwt 59 KDa MPs (50-100 μm) formulated with 10% (w/w) PLGA-PEG-PLGA triblock copolymer (n=9). [B] Release from PLGA 50 50 Mwt 59 KDa MPs (50-100 μm) formulated with 20% (w/w) PLGA-PEG-PLGA triblock copolymer (n=8). [C] Release from PLGA 50 50 Mwt 59 KDa MPs (50-100 μm) formulated with 30% (w/w) PLGA-PEG-PLGA triblock copolymer (n=7). [D] Release from PLGA 85 15 Mwt 56 KDa MPs (50-100 μm) formulated with 30% (w/w) PLGA-PEG-PLGA triblock copolymer (n=9). Copolymer batch TBII-B was used. Separate colours highlight triplicate traces of separate batches.

Batches: BN 135, 136, 138, 140 142, 143, 145, 147, 149, 150, 152 and 154.

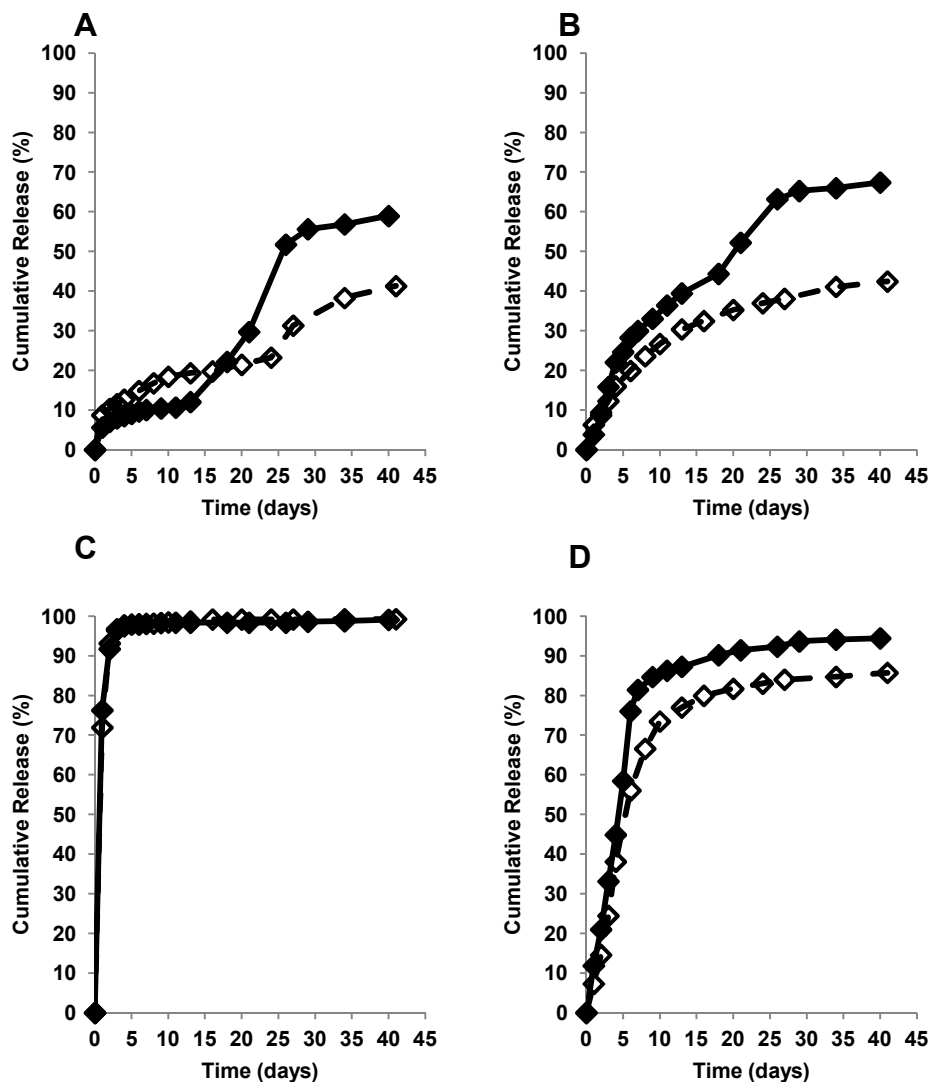


Figure 3.12 Comparison of total protein release from study 1 (closed symbols) and study 2 (open symbols) [A] PLGA 50 50 Mwt 59 KDa MPs (50-100 μm) with 0% (w/w) PLGA-PEG-PLGA triblock copolymer . [B] PLGA 50 50 Mwt 59 KDa MPs (50-100 μm) with 10% (w/w) PLGA-PEG-PLGA triblock copolymer [C] PLGA 50 50 Mwt 59 KDa MPs (50-100 μm) with 30% (w/w) PLGA-PEG-PLGA triblock copolymer [D] PLGA 85 15 Mwt 56 KDa MPs (50-100 μm) 30% (w/w) PLGA-PEG-PLGA triblock copolymer. Copolymer batch TBII-B as used in both studies.

Batches: BN 123, 125, 127, 133, 139, 146, 153, 138, 145, 152, 135, 142, 149, 140, 147 and 154

Data in Figure 3.13 again shows the release profiles from the PLGA 50 50 MPs containing 30 % and 10 % _(w/w) triblock copolymer shown in Figure 3.11 but in addition, the individual release profiles are also shown for a combination of both MP types mixed together at a 1:1 ratio before the start of the release assay. This result showed, as hypothesised, the release profile for the combination batch was in between the two other release profiles. So, the overall total protein release was dependent on some slow and some fast releasing MPs. The burst over the first 3 days was high (caused by the 30 % _(w/w) triblock MPs) and then release was slow (caused by the 10 % _(w/w) triblock MPs). The variation between the individual traces of the combination group was greater than the variation of the other two groups but this was not surprising due to their being two different MP types present.

This data gave real encouragement that a 'cocktail' of different MPs could be delivered containing different growth factors and would release their cargo at different rates within an overall sustained release profile. The great advantage of this would be that for example, angiogenic growth factors could be delivered quickly to develop vasculature followed by a slow more sustained release of osteogenic or chondrogenic factors to regenerate bone (Jeon, 2008, Strobel, 2011). Other researchers have tried different methods to achieve temporal control over release rate from biomaterials. Systems based on controlling gelatin cross-linking in multi-layered devices have been successful in delivering bone morphogenetic protein -2 (BMP-2) and insulin like growth factor-1 (IGF-1) to cells to affect their differentiation (Raiche, 2004) and more recently, PLGA microsphere scaffolds have been used to deliver IGF-1 and transforming growth factor β (TGF- β) sequentially by suppressing the burst release in some MP batches and not in others followed by fusing the MPs together with DCM vapour (Janklone 2008).

The advantage of the system presented in this project is the injectable nature of the MPs. Their potential, without any copolymer modification but co-delivered with cells (from umbilical cord blood), was shown to promote neovascularisation in ischemic peripheral artery disease when combinations of vascular endothelial growth factor, hepatocyte growth factor and Angiopoietin-1 were delivered (Saif, 2010). It would therefore be hoped that having the ability to tailor the release rate using the PLGA-PEG-PLGA copolymer and potentially deliver growth factors at different rates along with cell delivery would improve tissue regeneration when applied to *in-vivo* studies.

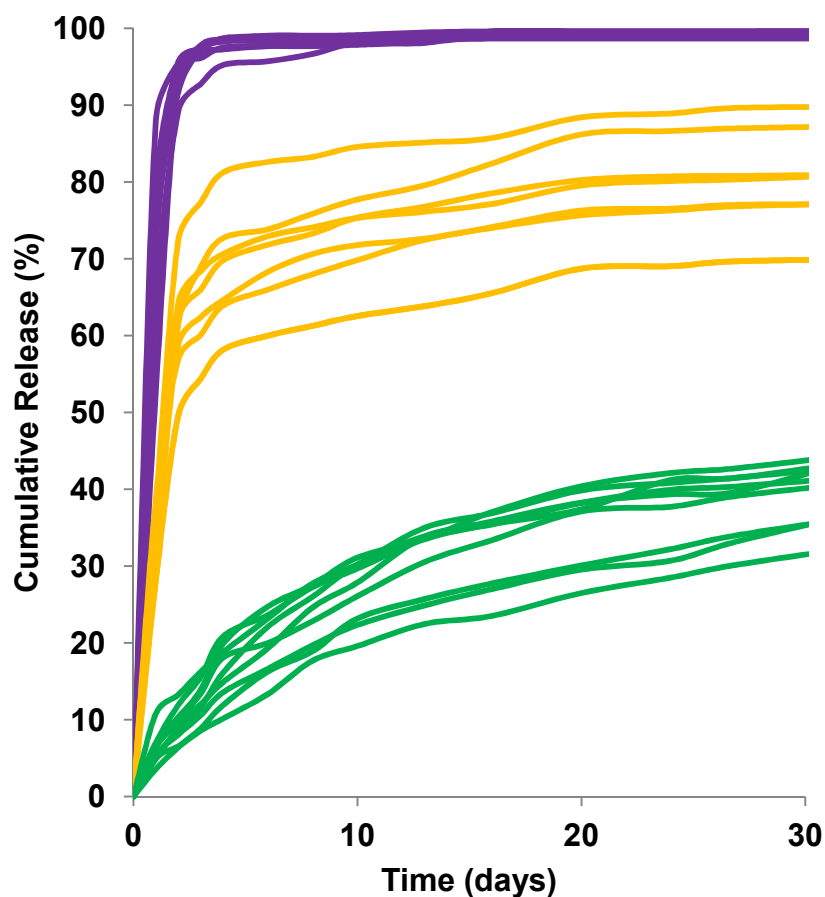


Figure 3.13: Individual cumulative protein release profiles from PLGA 50 50 Mwt 59 KDa MPs formulated with either 10 %_(w/w) PLGA-PEG-PLGA (green) or 30 %_(w/w) PLGA-PEG-PLGA (purple). In addition a release profiles were obtained by mixing the above two MP types in a 1:1 ratio (orange) Copolymer batch TBII-B was used

Batches: BN 135, 138, 142, 145, 149, 152, 160, 161 and 162

3.3.4.3 The influence of MP size on protein release profile.

All the data shown in this Chapter thus far has involved the use of 50-100 μm MPs. Smaller MPs can be made as demonstrated in Chapter 2 and may be more applicable to certain applications where for example, injection is required through a fine bore needle. Therefore, smaller MPs manufactured with a comparable HSA/lysozyme loading were compared against the 50-100 μm MPs to determine the effect on release. It was hypothesised that smaller MPs would release faster due to the increased surface to volume ratio and the result was very clear that this was apparent (Figure 3.14). This gives the potential for a further method to control release and achieve multiple growth factor delivery as rather than using a high triblock copolymer concentration, small MPs could be manufactured instead.

However, this may not be the best option, as there are drawbacks. The smallest MPs have lower entrapment efficiencies (Chapter 2) meaning much of the active molecule will be lost during their manufacture. Also, the overall porosity of a scaffold is an important parameter in promoting cell growth and differentiation, small MPs may take up free space between larger MPs and reduce the porosity. However, the 2 μm MP size range has been identified as the optimal size for some *in-vivo* applications (Sandor, 2002) and many groups use PLGA nanoparticles but generally not for orthopaedic applications (Budhian, 2008, Muthu, 2009)

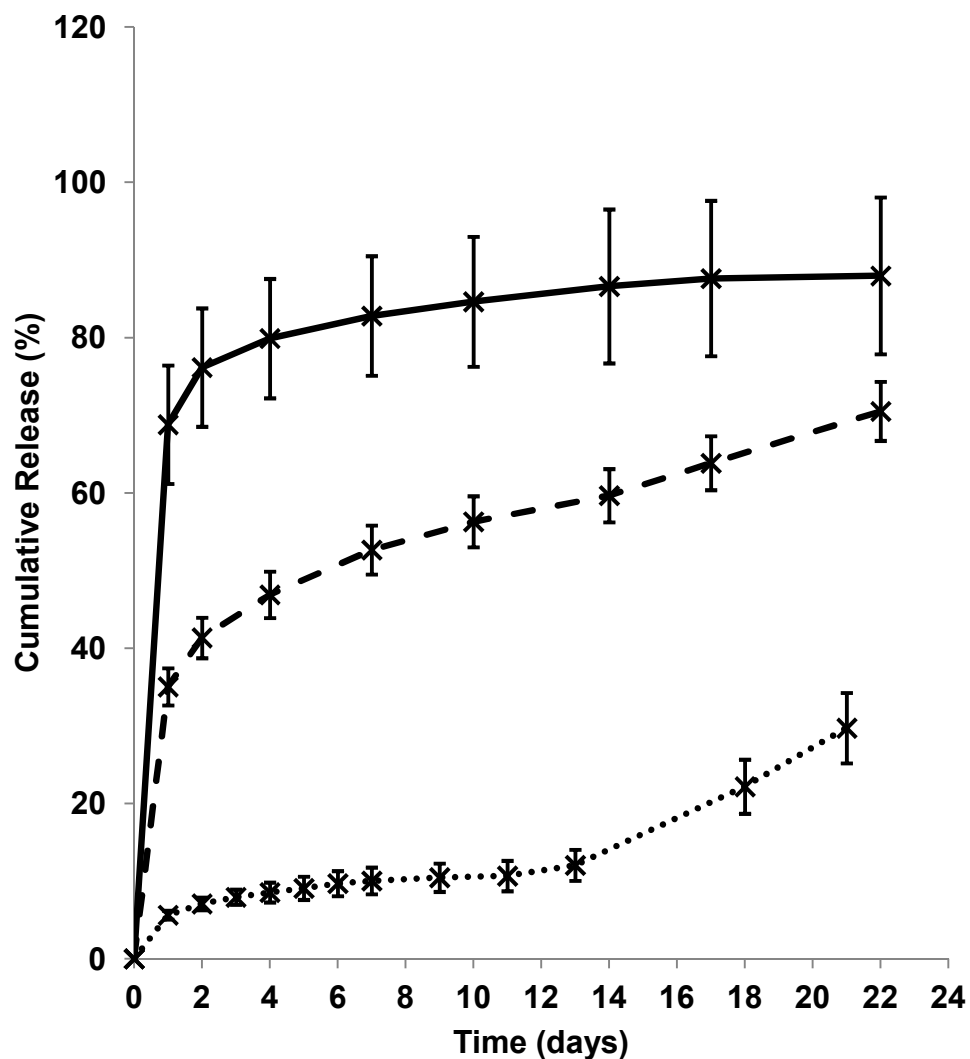


Figure 3.14: Cumulative protein release from different sizes of PLGA 50/50 Mwt 59 KDa MPs loaded with 1% (w/w) HSA/lysozyme with no PLGA-PEG-PLGA triblock modification. MPs shown are $151.3 \pm 60.7 \mu\text{m}$ (···); $13.84 \pm 7.48 \mu\text{m}$ (- -) and $2.58 \pm 0.81 \mu\text{m}$ (—) $n=3$

Batches: BN 123, 171 and 175

3.3.5 Lysozyme release from thermosensitive PLGA/PEG scaffolds

This Chapter has discussed in detail the controlled release of model protein with bulk carrier (HSA/lysozyme) from MPs manufactured from PLGA. These MPs have the advantage of being injectable but, will not spontaneously form a supportive structure and therefore as a side project, direct incorporation of lysozyme (without HSA) into thermosensitive PLGA/PEG MPs was investigated. PLGA 85/15 plasticised with low molecular weight PEG (400 Da) were milled into rough irregular shaped MPs. These MPs were mixed with lysozyme and melted at temperatures that were not destructive to the protein then re-milled to produce lysozyme containing thermosensitive MPs that could be used to make a three dimensional porous scaffold.

Scaffolds fabricated in this way were used in a release study and the profile of release is shown in Figure 3.15. The release had a significant burst followed by slow release, but it was still detectable at 60 days and only 50% of the total loading had been released. Therefore, there was still a considerable amount of lysozyme retained within the scaffold structure available for release. Figure 3.15 also shows a representative macro image and the actual SEM image of the scaffold structure prior to the release assay (Figure 3.15 B and C) where the individual MPs and the pores between them can be clearly seen. By the end of the study, the scaffold was still intact and the outer surface of the scaffold had developed a 'skin' probably due to the constant contact with the release media (Figure 3.15 D) causing degradation at the surface and it was evident that the MPs had melted into each other. This may not be the case *in-vivo* as the scaffold is likely to interdigitate with the host bone (Rahman, 2012a). The interior structure of the scaffolds remained very porous, although individual MPs could no longer be seen. The intact scaffolds had considerable

compressive strength, when manually compressed. However, the strength was not quantified using a texture analyser.

For long term delivery of growth factors with structural support, this method may have an application especially as no bulk carrier protein was needed, entrapment efficiency was high (85%) and as will be discussed later, the lysozyme remained active. These thermosensitive MPs could be used in conjunction with the growth factor loaded spherical MPs to gain the benefits of both systems namely, controlled release and structural support in an injectable format.

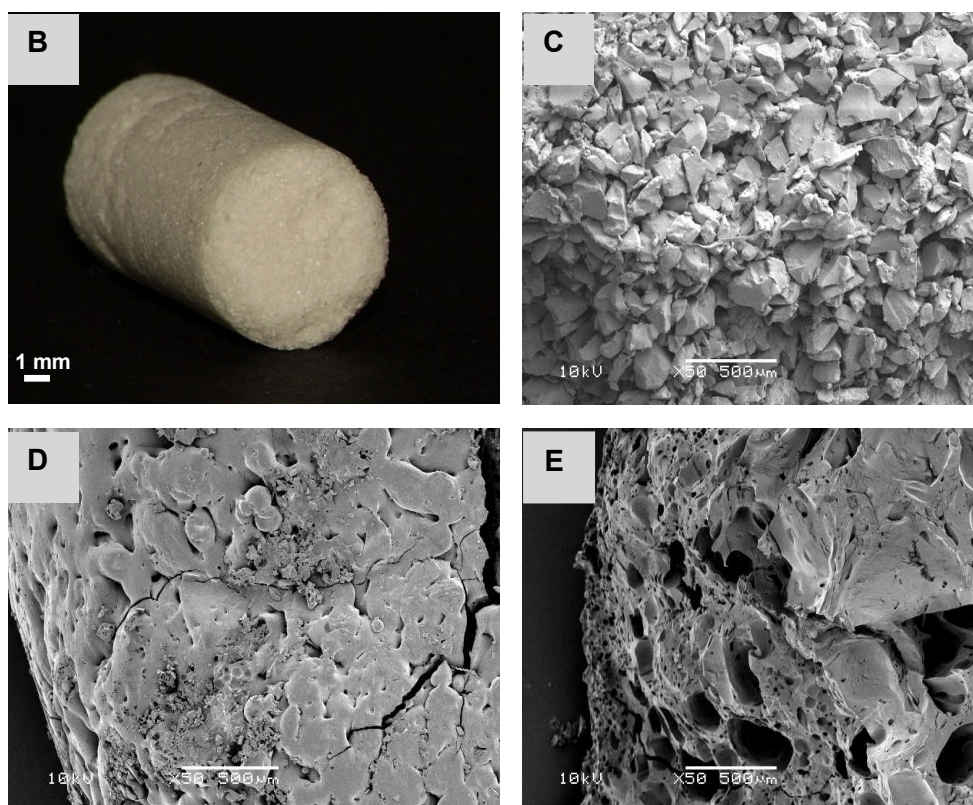
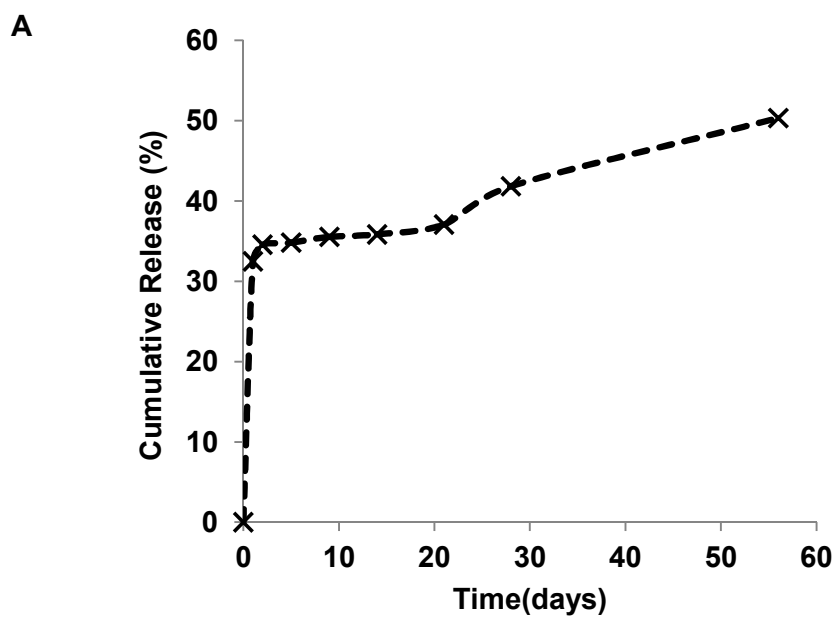


Figure 3.15 [A] Total protein release of lysozyme from thermo-sensitive PLGA/PEG scaffold. [B] A typical PLGA/PEG scaffold [C] SEM showing surface of PLGA/PEG scaffold prior to start of study [D] SEM showing surface of PLGA/PEG scaffold after 56 days in PBS [E] SEM showing the interior of a PLGA/PEG scaffold after 56 days in PBS.

3.3.6 Detection of lysozyme activity in release supernatants

The key to a successful delivery system is whether the bioactive molecule retains its activity throughout the MP manufacture and release procedures. The advantage of using lysozyme was that its activity can be monitored by its ability to lyse the bacterium *Micrococcus lysodeikticus*.

The release profiles shown in this Chapter have been constructed by measurements of total protein and as the lysozyme content was always 10% of the total with HSA being the remainder, the expected activity could be predicted by simply dividing the total protein by a factor of ten. The predicted level of activity was then compared to the actual measured lysozyme activity. The data at each collection time-point of predicted versus actual lysozyme activity for the MPs used in release study 1 (Figure 3.3A) are shown in Figure 3.16. Only up to day 13 is shown as beyond this the build up of degradation products lowered the pH in some samples and compromised the bioassay. Although activity was detected in most of the release supernatants, the correlation was not always consistent with the anticipated values and was often higher than expected.

Both the total protein assay and the activity assay have their own levels of inherent error and may not be directly comparable. On the other hand, the assumption that the lysozyme and the HSA release from the MPs at the same rate may not be true. The smaller lysozyme molecules may release faster from the polymeric matrix than the larger HSA molecules (Sandor, 2001, Zilberman, 2008). However, the positive activity results were indicative that lysozyme was not being denatured during the manufacture and release process regardless of the quantified value.

The lysozyme released from the thermosensitive scaffolds shown in Figure 3.15 was also tested for activity and the results are shown in Figure 3.17. Here, the correlation between the predicted and actual lysozyme activity was much stronger and despite release after the initial burst being low, it was detectable in both the assay systems. Lysozyme could be detected in this system up to day 28 because the degradation rate of PLGA 85 15 is slower than that of PLGA 50 50. The improved correlation may be due to the absence of a carrier protein which was not required in the melt blend encapsulation process as neither organic solvent nor water/oil interfaces were required in the protocol. However, later results will argue that the presence of the carrier protein does not stearically inhibit BMP-2 activity (Chapter 4). The thermosensitive scaffold system is an additional tool for the delivery of certain bioactive molecules that can withstand mild elevation of temperature and it has the advantage of providing considerable structural support for the newly formed tissue.

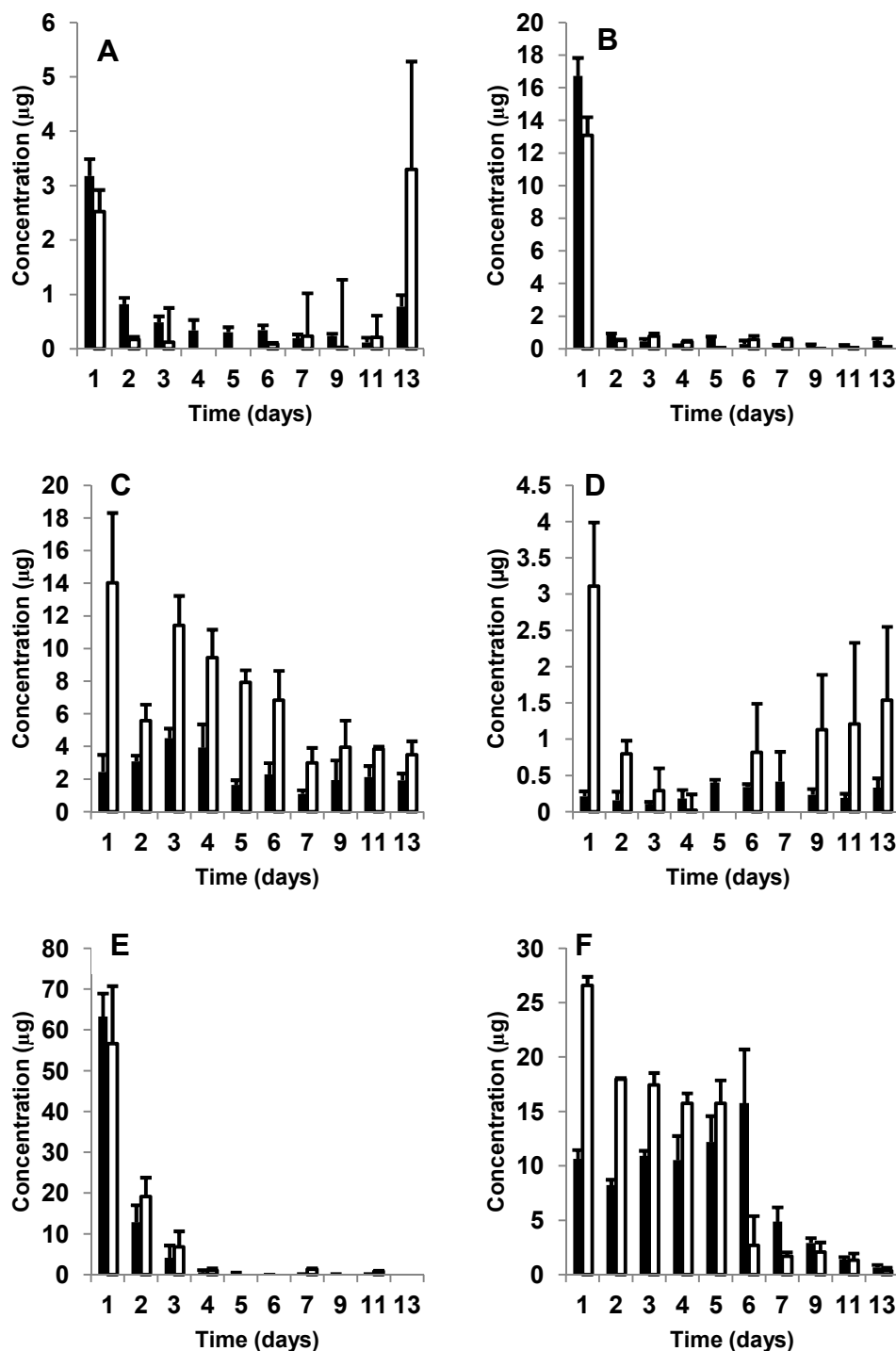


Figure 3.16: Activity of lysozyme released from 50-100 μm MPs formulated with [A] PLGA 50 50 0% (w/w) PLGA-PEG-PLGA, [C] PLGA 50 50 10% (w/w) PLGA-PEG-PLGA [E] PLGA 50 50 30% (w/w) PLGA-PEG-PLGA. [B] PLGA 85 15 0% (w/w) PLGA-PEG-PLGA [D] PLGA 85 15 10% (w/w) PLGA-PEG-PLGA and [F] PLGA 85 15 30% (w/w) PLGA-PEG-PLGA. The black bars are predicted values and the white bars are actual lysozyme activity by *M. lysodeikticus* assay. The copolymer batch was TBII-B

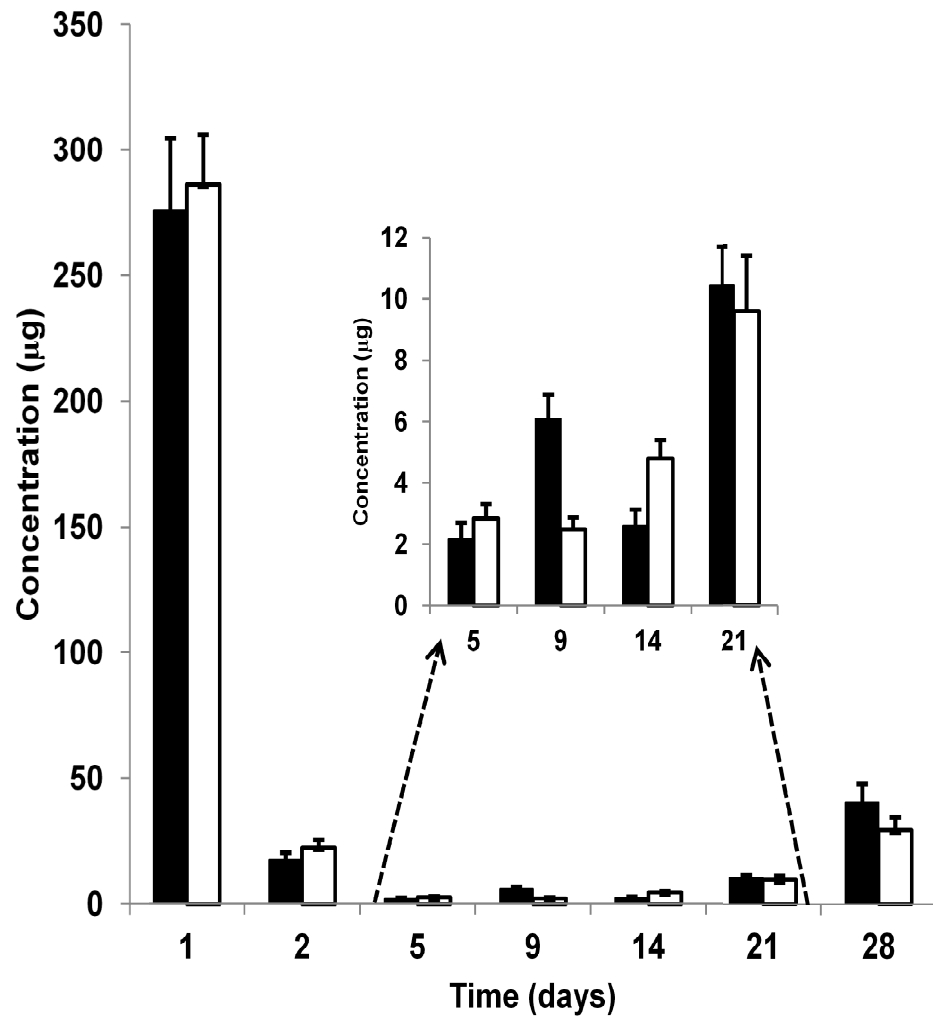


Figure 3.17: Activity of lysozyme released from PLGA/PEG scaffolds. The black bars are total protein and reflect expected lysozyme and the white bars are measurements of lysozyme activity by *M. lysodeikticus* assay.

3.3.7 Lowering total protein loading improves short term release profiles from sub 30 micron PLGA microparticles

The technology developed in this Chapter has proved to be repeatable and reliable but transferring the technology to smaller sized MPs may be problematic due to the very high burst release of around 70% seen from 2.5 μm MPs (Figure 3.14). The total protein loading was reduced, the hypothesis being that a lower mass of protein may embed more efficiently within the MP and so be more protected from the release medium and therefore the burst release may be reduced.

Figure 3.18A shows the release over 5 days from three batches of 1-5 μm MPs each with a different total protein loading. The 0.5% (w/w) and 1% (w/w) loadings gave a very high burst (approximately 70-80%) and a similar profile as seen before (Figure 3.14). However, the 0.1% (w/w) loading did result in only a 25% burst which was consistent with that achieved with 50-100 μm MPs. It was reasonable to suggest that reducing the protein content enabled the PLGA to entrap the protein more effectively. However the entrapment efficiencies of these MPs were disappointing. The 1% (w/w) loading had a 21.2% EE only to be improved to 28.0 % for the 0.5% (w/w) loading and 27.8% for the 0.1% (w/w) loading. Therefore the applications for this size of MP may be considerably limited.

Figure 3.18B shows the release profile over 5 days from 20-30 μm MPs. The burst was not as high as that from the 1-5 μm MPs with the 1% (w/w) loading being slightly higher than the 0.5% (w/w) loading. Unfortunately, release from the 0.1% (w/w) loaded MPs was undetectable and so this was repeated using 100 mg mass into 3 ml PBS. Although not directly comparable, this still

showed a lower burst of just 10%. The entrapment efficiency values for these MPs was improved over the 1-5 μm MPs and ranged from 51.4 to 58.5%. All of the profiles showed little or no release over the next 4 days which was not unexpected as with no PLGA-PEG-PLGA copolymer modification, a lag phase would have been expected. To improve the traces and avoid the lag phase, the addition of PLGA-PEG-PLGA triblock copolymer could be considered for the 20-30 μm MP size range.

It could therefore be concluded that the smallest size of MP that could potentially be manipulated to tailor release would be those in the 20-30 μm size range and future work was planned to use this size range to deliver recombinant human BMP-2. This work is the subject of the next Chapter.

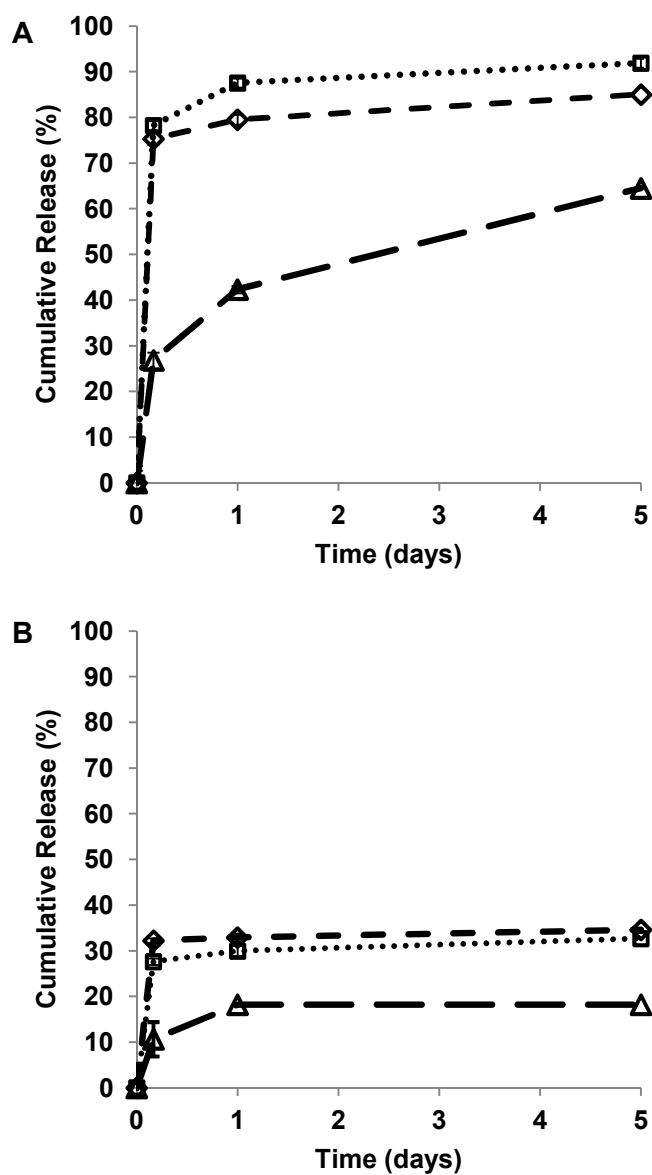


Figure 3.18. Cumulative total protein release profiles from [A] 1-5 μm PLGA 50 MPs and [B] 20-30 μm PLGA MPs. Three total protein loadings were tested 1% (— \triangle), 0.5% (- - \diamond) and 0.1% (..... \square) $n=3$

Batches: BN 179, 180, 181, 183, 184 and 185

3.4 Conclusions

The work in this Chapter has described the development of a new PLGA based microparticulate delivery system having the capability to reproducibly control the local release of the model protein lysozyme. The MPs were spherical and had few or no surface pores. The inclusion of a hydrophilic PLGA-PEG-PLGA triblock copolymer in the manufacture process altered the sub-optimal triphasic release kinetics such that they were decoupled from polymer degradation. The incorporated triblock concentration was directly related to the rate of protein released from the MPs and this was also demonstrated to be linked to glass transition temperature and the degradation rate of the PLGA MPs. The release rate from PLGA 85 15 and PLGA 50 50 could be tailored using the copolymer but the former always demonstrated a slower rate of release. The release profiles were shown to have both intra and inter batch reproducibility which would give confidence in using the system for growth factor release studies.

As well as copolymer concentration and lactide:glycolide ratio of the PLGA, the size of the manufactured MPs also affected release rate with the smallest MPs releasing their protein at the fastest rate. However, the entrapment efficiency was reduced in sub 20 micron MPs but, this could be partially overcome by reducing the overall protein loading in the MPs. A further study showed that release profiles could also be modified by mixing PLGA MPs of two different formulations and this provided another route, not previously reported, for controlling release kinetics.

Preliminary data showed the feasibility of introducing a porous hardened scaffold to support of the surrounding tissue and to prevent MP migration away from the site of delivery. The addition of these MPs would not affect the

injectability of the system and would harden in-situ to provide a three dimensional structure for tissue development.

Despite some discrepancies in the data, it was demonstrated that lysozyme remained active throughout the process of MP manufacture and after release from the MP into PBS. The correlation between lysozyme activity and predicted activity was best when the release was from thermosensitive scaffolds where no bulk carrier protein was used and no solvents were used in the manufacture process.

Some of the formulations developed within this project are potentially promising candidates for delivery of growth factors. The 10 % _(w/w) PLGA-PEG-PLGA with 50 50 PLGA that demonstrated sustained release over four weeks would be most relevant for bone morphogenetic protein -2 (BMP-2) delivery, whilst the 30% _(w/w) PLGA-PEG-PLGA with 85 15 PLGA formulation and the 30% _(w/w) PLGA-PEG-PLGA with 50 50 PLGA formulation achieved complete release after 10 and 4 days respectively and these two formulations would be more appropriated for angiogenic growth factors such as platelet derived growth factor (PDGF) and vascular endothelial growth factor (VEGF) when 50-100 µm MPs are used.

The following Chapters will focus on bone morphogenetic protein -2 and its *in-vitro* and *ex-vivo* effects on early osteogenesis. The tailored release technology will be translated to 20-30 µm MPs to achieve the required release to create a biological response.

Chapter 4: Tailored release of biologically active rhBMP-2 from biodegradable microparticles

4.1 Introduction

Bone morphogenetic proteins (BMPs) are growth factors that are members of the transforming growth factor-beta (TGF β) superfamily. Based on their structural features and amino acid sequence, the 35 mammalian members are subdivided into i) TGF-betas, ii) activins/inhibins, iii) BMPs/growth and differentiation factors (GDFs) as well as iv) a more distantly related group of glial derived neurotrophic factor (GDNF) family of ligands. The main components of the TGF β superfamily and how they are related are shown in Figure 4.1. The cytokines/growth factors with outstanding importance in control of wound healing and repair and affect both osteogenesis and chondrogenesis are TGF β , BMP-2, BMP-4 and BMP-7 and are highlighted red in Figure 4.1 (Weiskirchen, 2009).

However, BMP-2 is the most widely used growth factor to stimulate osteogenesis (Boden, 2005). It induces osteoblast differentiation via SMAD proteins which are intracellular proteins that transduce extracellular signals from ligand binding at the cell membrane to the nucleus where they activate gene transcription. A number of transcription factors Runx2/Cbfa1, Osx, Dlx5 and Msx2 work synergistically to regulate the gene expression of downstream proteins to induce osteoblasts and therefore they play a prominent role in skeletal development. See Figure 1.8 (Wu, 2008).

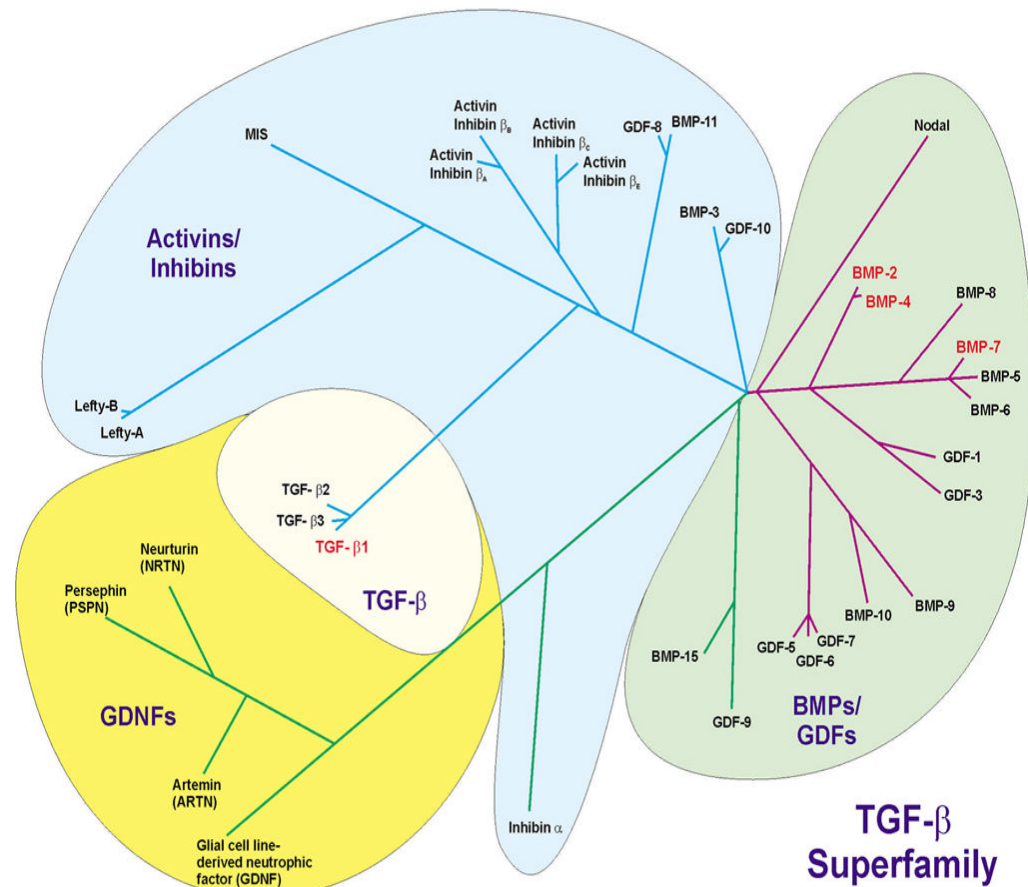


Figure 4.1 The main signalling molecules in the TGF β super family

(Weiskirchen, 2009)

BMPs have been extensively studied (Reddi, 1998, Lieberman, 2002) and rhBMP-2 (InfuseTM, Medtronic Sofamor Danek Inc.) and rhBMP-7 (OP-1TM, Stryker Biotech) were approved by regulatory bodies and marketed for the treatment of non-union bone defects, open tibial fractures and spinal fusion (De Biase, 2005, Swiontkowski, 2006, Hsu, 2008). However, delivery of BMPs is complicated by their short biological half lives, localized action and rapid clearance (Bessa, 2008). Attempts to improve the plasma half life of therapeutic proteins have been made with some success (Werle, 2006, Kontermann, 2011), but often to counteract the half life problem, high concentrations have tended to be used clinically. This resulted in some reported side effects mainly caused by

poorly controlled doses leading to overgrowth and uncontrolled bone formation, soft tissue swelling, pain, bladder retention, male infertility, osteolysis and more recently a risk of cancer when high doses were used (Zara, 2011, Carragee, 2011, Helgeson, 2011, Perri, 2007, Devine, 2012).

These implications emphasized the need for strategies to improve the efficacy and safety of recombinant growth factor delivery systems. Gradual sustained delivery of rhBMP-2 over a number of weeks could therefore harness the undoubted benefits of the molecule for bone regeneration but also mitigate the high doses and corresponding health and cost implications of supraphysiologic concentrations (Cahill, 2009). Encapsulation of the growth factor within a hydrophobic polymer microparticle (MP) will protect it from proteolytic enzymes at the target site and if formulated correctly, will allow its gradual release from the MP into the local area. This would be likely to improve the safety and reduce the side effects of growth factor delivery.

During fracture healing, BMP-2 expression is highest at the early stages to initiate and direct migration of progenitor cells for the formation of new bone, which is critical to the proper healing of damaged tissue (Bostrom, 1998, Kloen, 2003, Tsiridis, 2007). But, the delivery should then be sustained for a number of weeks to complete the repair process (Jeon, 2008). The optimum therapeutic dose of BMP-2 for bone regeneration is not well defined. Many animal studies have been performed, for example, evaluation by micro computed tomography showed that bone growth could be measured as a response to 30 – 240 ng/mm of BMP-2 in 5mm rat calvarial defects when grafted in conjunction with PLGA (Cowan, 2007). In contrast, much higher doses were used in a rat femoral segmental defect model where doses of 1-20 μg were assessed within a collagen sponge and 12 μg was declared optimum

for this model (Angle, 2012). Earlier work claimed that 0.93 μg of BMP-2 combined with PLGA could repair rat segmental defects (Lee, 1994). It is often difficult to compare results between studies due to dissimilar experimental conditions. In humans, as already alluded to, the concentration of endogenous BMPs (ng) is much lower than the amounts used clinically (μg). Improved delivery devices should allow lower, more clinically relevant doses to be administered, thus reducing the unwanted side effects.

The activity of BMPs can be determined *in-vitro* by their effect on certain cell types to alter their differentiation pathway. In particular, rhBMP-2 will inhibit the differentiation pathway of a C2C12 myoblast cell line into myotubes and drive the differentiation of the cells into an osteoblast lineage and involves cross talk with the wnt3a signalling pathway (Katagiri, 1994, Nakashima, 2005). C2C12 cells exposed to rhBMP-2 will therefore express alkaline phosphatase (ALP) activity with the levels of activity being directly proportional to rhBMP-2 concentration (Kim, 2004).

Cultures of primary osteoblasts and osteoblast cell lines will form a calcified extracellular matrix in the presence of osteogenic media although the mineral deposition can either form a nodular or diffuse pattern. Cells derived from the calvaria are heterogeneous in nature with a small percentage being osteoblasts and these are more likely to form distinct nodules *in-vitro* due to localisation of the colonies (Declercq, 2005). It has been shown by von Kossa staining that the presence of rhBMP-2 increases the mineral deposition from human mesenchymal stem cells (huMSCs) (Johnson, 2009).

To go some way to achieving an improved delivery device for rhBMP-2, the PLGA MP manufacture and formulation technology as well as the controlled

release profiles determined in the first two results Chapters of this thesis will be translated to the release of rhBMP-2. Specifically, release assays will be set up to i) compare the release of HSA/lysozyme and HSA/rhBMP-2, ii) investigate the effect of PLGA-PEG-PLGA triblock copolymer on the release using model protein from 20 – 30 μm MPs, iii) determine the scalability of the release system and iv) investigate release of rhBMP-2 from PLGA/PEG thermosensitive scaffolds. To detect the presence of released rhBMP-2 and to ensure that it remains biologically active, it will be assessed by enzyme linked immunosorbent assay (ELISA) as well as an *in-vitro* model of early osteogenesis. It will also be tested for its effect on mineralisation by primary osteoblasts as a late marker of osteogenesis.

4.2 Materials and Methods

All the laboratory equipment, consumables and chemicals used during the work for this Chapter can be sourced in Appendix I, tables A1, A2 and A3. Where MP batch numbers are stated, the details of the manufacturing parameters can be found in Appendix II.

4.2.1 Reconstitution of rhBMP-2, addition of HSA and storage

rhBMP-2 was supplied by Professor Walter Sebald (University of Wurzburg, Germany) in 5 mg lyophilised aliquots (Ruppert, 1996). It was reconstituted in 500 μl of 0.1 % $_{(w/v)}$ human serum albumin. It was then distributed into 5 x 100 μl aliquots each containing 1 mg of rhBMP-2. One of the aliquots was further diluted with 900 μl of 0.1% $_{(w/v)}$ HSA and dispensed into 100 aliquots, each aliquot containing 100 μg of rhBMP-2. A further aliquot was diluted with 400 μl of 0.1% $_{(w/v)}$ HSA and dispensed into 100 aliquots, each aliquot containing 500

µg of rhBMP-2. The reconstituted samples were stored frozen until use. Two batches of rhBMP-2 were used during the work for this project (Sept '10 and Feb '11).

The addition of HSA as a bulk carrier for MP production was performed very carefully by adding either a further 9 mg of HSA directly to the 100 µl aliquot containing 1 mg of rhBMP-2, a further 9.5 mg HSA to the 100 µl containing 500 µg rhBMP-2 or 9.9 mg to the aliquot containing 100 µg rhBMP-2. This gave 10 mg of total protein suitable for a 1% _(w/w) loading into 1 g of PLGA. Other rhBMP-2 loadings used for this work were 0.5 mg rhBMP-2 with 9.5 mg HSA and 0.1 mg rhBMP-2 with 9.9 mg HSA.

4.2.2 Manufacture of HSA/rhBMP-2 loaded PLGA MPs formulated with PLGA-PEG-PLGA triblock copolymer

PLGA MPs formulated with PLGA-PEG-PLGA triblock copolymer were fabricated the using the method previously defined in Chapter 2, Section 2.2.4.2 to prepare MPs in the 20 -30 µm or 50-100 µm size range. For controlled release batches, PLGA-PEG-PLGA triblock copolymer was added at either 10% _(w/w) or 30% _(w/w) in a total of 1g. The HSA/rhBMP-2 MPs were loaded with a total of 1% _(w/w) comprising of three different rhBMP-2 concentrations using the solutions prepared in the previous Section. Control MPs were manufactured by using 100µl of distilled water in the primary emulsion.

4.2.3 Incorporation of rhBMP-2 loaded MPs into PLGA/PEG thermosensitive scaffolds

A 1% _(w/v) solution of high viscosity carboxymethylcellulose (CMC) was made by overnight magnetic stirring of 1 g of CMC in 100 ml of distilled water. Thermosensitive PLGA/PEG MPs manufactured by hot melt blending were sieved to achieve a <100 µm fraction. These MPs were mixed at a ratio of 1:1 (50 mg: 50 mg) with PLGA MPs (20-30 µm) loaded with HSA/rhBMP-2 (1% _(w/w) loading 9.5 mg with 0.5 mg in 1 g PLGA). The high viscosity CMC (800 µl) was added to the mix of MPs to form a thick paste. The paste was transferred into a custom made PTFE 6x12 mm cylindrical mould and gently tampered down. The mould containing MPs was put in a sealable bag to maintain humidity and placed in a 37°C incubator for 30 minutes after which time the scaffold could be released from the mould for use. Acknowledgement goes to the Medical Engineering Unit at Nottingham University for manufacturing the moulds.

4.2.4 Release assays

4.2.4.1 Indirect release assays (supernatant collection)

Release assays were set up with two different masses of MPs (25 mg in 1.5 ml PBS and 50 mg in 3 ml PBS at pH 7.4). The tubes were gently rocked on a 3D shaker at 5 rpm in a humidified incubator at 37°C. At defined time intervals, the tubes were centrifuged at 3,000 rpm (MSE, Mistral 1000) for 5 minutes and the supernatant was removed and stored frozen. The MPs were resuspended in the same volume of fresh PBS and re-incubated.

In a separate study, thermosensitive PLGA/PEG scaffolds with incorporated rhBMP-2 loaded MPs were placed in 1 ml of PBS in a Bijou bottle to measure the release profile. The collected supernatants from all assays were stored frozen before being thawed and assayed for total protein content using the micro BCA assay kit as well as in an appropriate bioassay or ELISA for rhBMP-2.

4.2.4.2 Direct release assays (co-culture)

To gauge the direct *in-vitro* response of rhBMP-2 loaded MPs and to ensure there were no adverse effects caused by the MPs on the cells co-culture release assays were set up. On day zero, 30 mg of HSA/rhBMP-2 loaded MPs (1% loading 9.5 mg HSA with 0.5 mg rhBMP-2) were weighed along with 6 mg of MPs without protein loading. These were in the 20-30 μm size range. The loaded MPs were suspended into 15 ml PBS and 1 ml dispensed into 15 microcentrifuge tubes. The blank MPs were suspended into 3 ml PBS and dispensed into 3 microcentrifuge tubes. Each tube contained 2mg of MPs and were placed on a 3-D rocker at 37°C for the release study. At each time-point (1, 3, 6, 9 and 12 days) all tubes were centrifuged and supernatant carefully removed and discarded. Three of the tubes containing loaded MPs were retained and freeze dried overnight. Fresh PBS was added to the remaining tubes and they were re-incubated on the rocker. This was repeated at each time-point with the blank tubes being collected at day 12. This resulted in a collection of MPs that had been exposed to PBS for 0-1, 1-3, 3-6, 6-9 and 9-12 days and could be used in direct co-culture studies with C2C12 cell to see if they were able to elicit a pNPP response in the cells. The design of this experiment is shown schematically in Figure 2.2.

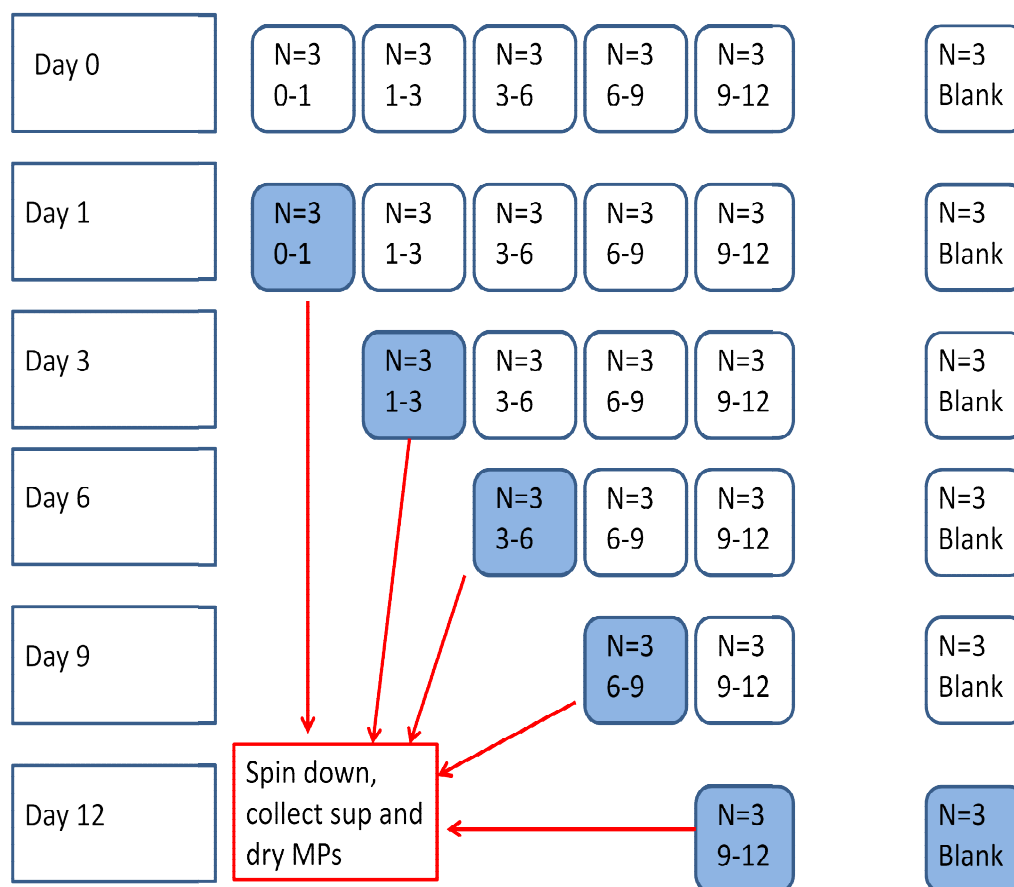


Figure 4.2 Schematic to depict the protocol required to study the release of HSA/rhBMP-2 from PLGA MPs by direct co-culture with C2C12 cells. Fifteen samples of HSA/rhBMP-2 loaded and three samples of blank MPs were incubated at 37 °C in PBS. At regular time-points, PBS was removed from all the samples, three samples were retrieved (blue box) and the remainder were re-incubated with fresh PBS. Each triplicate of MP samples would have a different exposure to PBS.

4.2.5 Detection of rhBMP-2 in release supernatants by immunoassay (ELISA)

The commercially available rhBMP-2 ELISA kit (Quantikine) was used to determine the levels of released rhBMP-2 in supernatants. Briefly, a monoclonal antibody specific for rhBMP-2 was provided pre-coated onto a micro-plate. Standards and samples were transferred to the wells and any rhBMP-2 present was bound by the immobilized antibody. The plates were washed and an enzyme-linked monoclonal antibody specific for rhBMP-2 was added to the wells. Following a further wash to remove any unbound antibody-enzyme reagent, a substrate solution was added and a colour developed in proportion to the amount of rhBMP-2 bound in the initial step. Once the reaction was stopped, the colour change could be detected at 450 nm. The detection levels for the Manufacturer's standards was 62.5 – 4000 pg/ml but the detection of the rhBMP-2 used in these studies (combined with HSA) required the standard curve in the ng/ml range (5 – 100 ng/ml).

4.2.6 Culture of C2C12 myoblasts and immortalised human mesenchymal stem cells

Both mouse C3H C2C12 muscle myoblasts (ATCC, CRL-1772) and immortalised human mesenchymal stem cells (kindly donated by Dr Hassan Rashidi, School of Pharmacy, University of Nottingham) were cultured in a complete tissue culture media consisting of Dulbecco's Modified Eagles Medium (DMEM), 10% _(v/v) foetal calf serum (FCS), 1% _(w/v) antibiotic solution (consisting of 10,000 units/ml of penicillin and 100mg/ml of streptomycin sulphate) and 2mM L-glutamine. The cultures were maintained at 37°C, 5% CO₂ in air in a humidified atmosphere in T75cm² flasks. The cells were sub

cultured when judged to be 80-90% confluent. The media was aspirated and cultures were rinsed with approximately 10 ml of PBS. The cells were then treated with a small volume (approximately 3ml) of trypsin/EDTA (0.5 g/L trypsin, 0.2 g/L EDTA) for no more than 5 minutes at room temperature. Once the cells had detached from the flask surface, a further 10 ml of complete media was added and the total contents transferred to a 15ml centrifuge tube.

The suspension was centrifuged for 5 minutes at 1,000rpm (Sigma, 2-16K). Media was then aspirated, and the pellets were usually re-suspended in 4 ml and sub-cultured at a typical ratio of 1:4 in 10 ml of complete media. Sub-culturing was required every 2 to 3 days for the C2C12 cells and every 3 to 4 days for the immortalised MSCs.

4.2.7 Measurement of rhBMP-2 activity in release supernatants by alkaline phosphatase expression in C2C12 cells and immortalised human mesenchymal stem cells

Alkaline phosphatase (ALP) is expressed as an early marker of osteogenic differentiation and when osteogenesis is induced using rhBMP-2, the levels of ALP are proportional to the BMP-2 concentration. Activity of rhBMP-2 in release supernatants was measured *in-vitro* by monitoring the level of ALP expression by C2C12 myoblast cells in the presence of rhBMP-2 (Katagiri, 1994).

The C2C12 cells (no greater than passage 12) were suspended at a concentration of 10,000 cells per ml in DMEM supplemented with 10% _(v/v) FCS and 1x antibiotic/antimycotic solution. The cell suspension (100 µl with 1000 cells) was added to a 96 well plate and incubated in a humidified environment

at 37°C 5% CO₂ overnight. The media was then replaced with either 100 µl of rhBMP-2 in complete DMEM at a concentration range of 100-1000 ng/ml to generate a standard curve or 100µl of the release supernatants in PBS. A further 100 µl of DMEM was added to the supernatants and 100 µl of PBS was added to the standards to give a final total volume of 200 µl in all wells. The expression of ALP after 5 days of culture was measured using a SigmaFAST pNPP kit. Media was aspirated from the wells and the cells carefully washed with 100 µl PBS. The pNPP solution, made to manufacturer's guidelines, was added (100µl) to the wells and any de-phosphorylated pNPP which was indicative of rhBMP-2 activity, could be detected at an absorbance of 405 nm after 1 hour of incubation at room temperature (protected from light).

In addition to using C2C12 cells, an immortalised human mesenchymal stem cell line was also used to measure rhBMP-2 activity using the same method as described above.

4.2.8 Co-culture of HSA/rhBMP-2 loaded MPs with C2C12 cells as a method for detecting rhBMP-2 activity and measuring rhBMP-2 release

The activity of released rhBMP-2 was determined by directly co-culturing C2C12 cells with HSA/rhBMP-2 loaded MPs (9.5mg HSA/0.5 mg rhBMP-2 in 1 g of PLGA). C2C12 cells were suspended at 3,000 cells per ml in complete DMEM and 1 ml was plated into each well of a 12 well plate. After 24 hours incubation, the media was replaced with media containing serially diluted suspensions of different masses (2, 1, 0.5, 0.25 and 0.125 mg) of HSA/rhBMP-2 loaded MPs or HSA/rhBMP-2 loaded MPs which had been stored during the release assay as described above in Section 4.2.4.2. The

cultures were left for 5 days before being imaged and assayed using the SigmaFAST pNPP kit.

In an alternative experiment, a range of cell concentrations (3,000, 1,500 and 750 per ml) were tested with a fixed 2 mg mass of HSA/rhBMP-2 loaded MPs.

4.2.9 Von Kossa staining for detection of mineralisation *in-vitro*

The method of staining for calcium deposition is the von Kossa method (Bancroft, 1992). It highlights deposits of calcium salt by staining cells or tissue sections with a solution of silver nitrate. Silver is deposited by replacing the calcium which is reduced by strong light. The calcium deposits are then visualized as metallic silver (Declercq, 2005).

Mouse primary calvarial cells (mPCCs) were kindly isolated and donated by Adam Taylor and Laura Sidney (PhD students, School of Pharmacy, University of Nottingham). The calvaria were dissected from CD1 neonates (supplied by the Biomedical Services Unit, Nottingham University) and digested using a solution of 1.4 mg/ml collagenase type IA and 0.5 mg/ml trypsin II S. Cells released during the first 2 populations (10 minutes each digestion) were discarded and the population of cells from the next 3 digestions were plated in tissue culture flasks at a density of 6.6×10^3 cells/cm². Cells were cultured in α MEM containing 10% FCS and 2mM L-Glutamine and 100 U/ml penicillin/100 μ g/ml streptomycin.

The mPCCs were exposed to HSA/rhBMP-2 loaded MPs (9 mg HSA/1 mg rhBMP-2) for 28 days in direct co-culture by placing 4 mg of MPs (PLGA 50 50 10% _(w/w) TBII-F, 50-100 micron) into the wells of a six well plate containing

100,000 cells per well . After incubation in a humidified atmosphere at 37°C, the cells were fixed in 10% _(v/v) paraformaldehyde for 30 minutes. A 1% _(w/v) silver nitrate solution in distilled water was added to the cells and subjected to UV light for 60 minutes. The cells were then rinsed in distilled water and treated with 5% _(w/v) sodium thiosulphate solution in distilled water for 5 minutes to remove any unreacted silver. The cells were then rinsed in distilled water and imaged. Calcium nodules appear dark brown/black.

4.2.10 Imaging of cells, cells with microparticles and scaffolds

Cultured cells were imaged using a Nikon Eclipse TS100 microscope at a magnification of x10 and polymer scaffolds were imaged by scanning electron microscopy (JSM 6060LV).

4.3 Results and Discussion

4.3.1 Comparison of model protein and growth factor release

All of the work performed on controlled release in the previous Chapters involved the use of the model protein lysozyme in conjunction with human serum albumin (HSA) as a bulk carrier protein and the release was measured from 50-100 μm sized MPs. The future direction of the project was to investigate the embryonic chick femur as a model for bone regeneration and this necessitated a smaller MP size to be studied. The size range chosen was 20-30 μm because this size of MP can be manufactured with the same PLGA concentration (20 % $_{w/v}$) as the 50-100 μm with the smaller size being achieved by an increased homogeniser speed. It was expected that tailoring of protein release kinetics using PLGA-PEG-PLGA would still be feasible with this smaller MP size especially as previous results showed there was a lag phase after the burst when the MPs had not been modified with PLGA-PEG-PLGA triblock copolymer (Chapter 3 Figure 3.18B).

The starting point was to compare rhBMP-2 release with that of the model protein lysozyme from the established 50-100 μm size range before looking at the smaller size range to ensure that the technology was transferable from model to growth factor. A batch of 50-100 μm PLGA 50 50 MPs were loaded with HSA/rhBMP-2 (9mg HSA with 1mg rhBMP-2) and were tested in a dynamic release assay and retrospectively compared with HSA/lysozyme data (Figure 4.3A). Both types of MP had been formulated with 10% $_{(w/w)}$ PLG-PEG-PLGA triblock copolymer.

Two batches of PLGA 50:50 20-30 μm also formulated with 10%_(w/w) PLGA-PEG-PLGA triblock copolymer were manufactured one containing HSA/lysozyme (9 mg HSA with 1 mg lysozyme) and one containing HSA/rhBMP-2 (9.9 mg HSA with 0.1 mg rhBMP-2) and these were also both put on a dynamic release assay. The profiles are shown in Figure 4.3B.

The release profiles for the larger MPs showed a small burst release and further sustained release over time. The profiles of the model protein and the growth factor did not overlay exactly but the study was retrospective which may account for the differences. Also, two different triblock copolymer batches were used (TBII-B and TBII-F). However, both formulations had released similar total amounts of protein over the 30 day period. The smaller MPs were fabricated with the same triblock copolymer (TBII-F) and show a better correlation between the traces but the burst release was higher than that seen with 50–100 μm MPs. This was not unexpected as previous results showed that the smallest MPs had the highest short term release (Chapter 3, Figure 3.14). These data gave confidence that HSA/rhBMP-2 release from 20–30 μm MPs could be detected and quantified especially over the first 10 days.

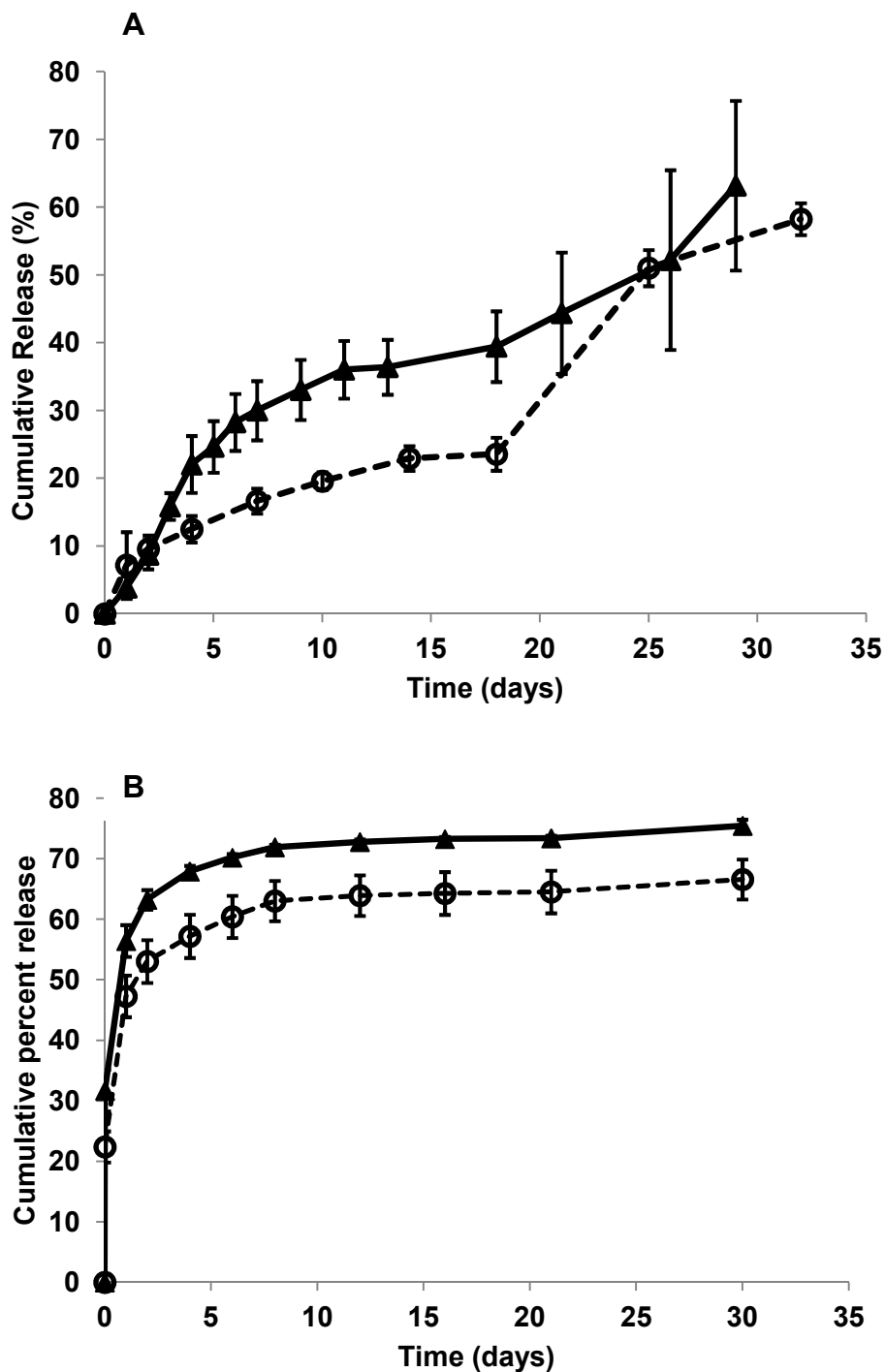


Figure 4.3. Total protein release profiles from [A] 100 mg of 50 -100 μm MPs and [B] 50 mg of 20 – 30 μm MPs comparing HSA/rhBMP2 (○) and HSA/lysozyme (▲) PLGA 50/50 MPs formulated with 10% (w/w) PLGA-PEG-PLGA triblock copolymer $n=3$

Batches: BN 344, 125, 313 and 314

4.3.2 Effect of PLGA-PEG-PLGA triblock copolymer and MP mass on the rate of protein release from PLGA MPs

The release from two different masses (25 mg and 50 mg) of MPs loaded with HSA/rhBMP-2 (0.1 mg rhBMP-2 with 9.9 mg HSA) was expressed as either cumulative protein release in μg (Figure 4.4A and 4.4B) which indicated the actual amount of protein delivered and as cumulative percentage release (Figure 4.4C and 4.4D) which showed the overall shape of the release profiles. The ratio of MP mass to release volume was kept the same for both masses. The data is shown for MPs fabricated with 10 % and 30% $_{(w/w)}$ PLGA-PEG-PLGA triblock copolymer and sized at 20-30 μm . Increasing the triblock copolymer accelerated the release and the data showed that release positively correlates with MP mass (Figure 4.4A compared to Figure 4.4B).

Over 90% of the protein load was released in the first 20 days from the 30% $_{(w/w)}$ PLGA-PEG-PLGA copolymer following a diminishing release profile, whereas only approaching 60% of the total protein was released from the 10% $_{(w/w)}$ PLGA-PEG-PLGA copolymer formulation over 30 days following a sustained release profile after the burst. The addition of PLGA-PEG-PLGA copolymer had therefore resulted in two distinctly different release profiles from these small MPs.

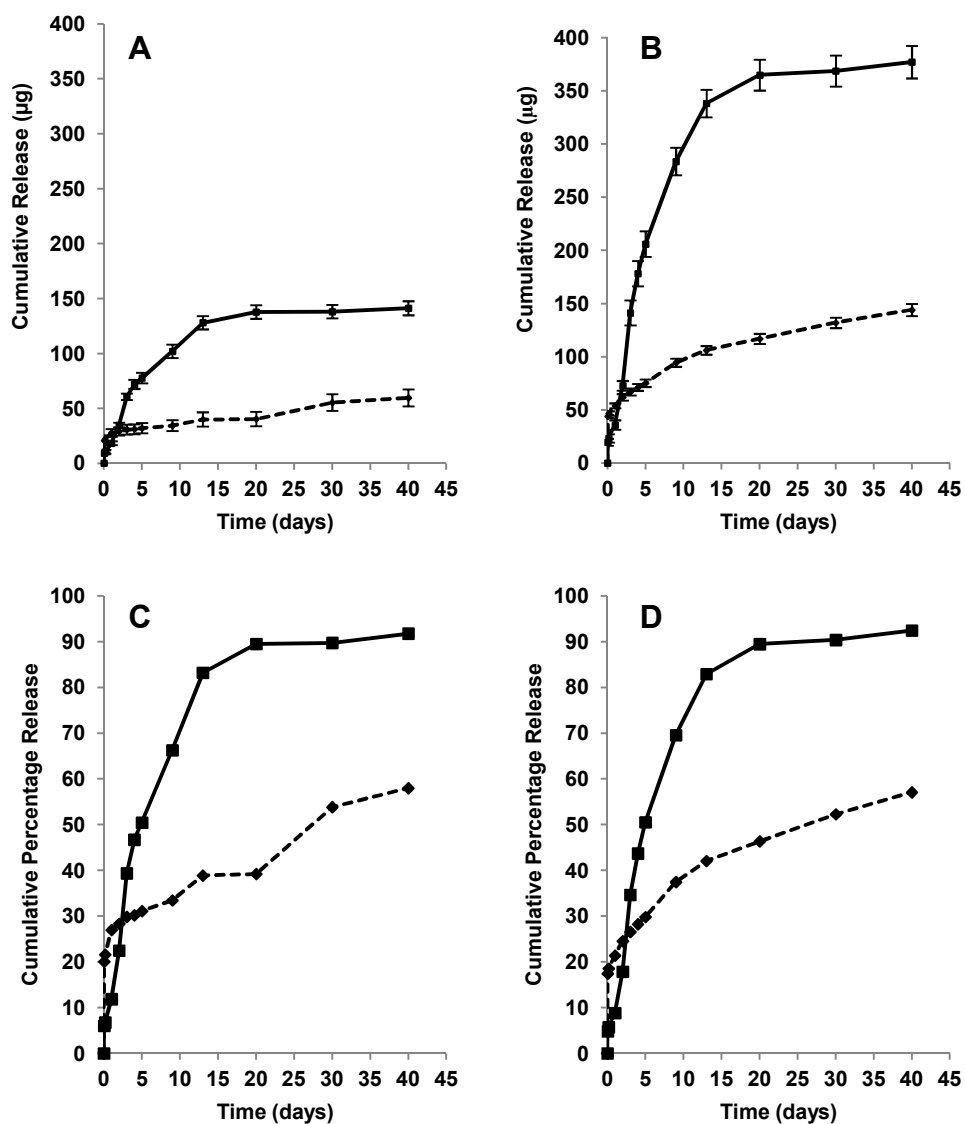


Figure 4.4. Cumulative total protein release from HSA/rhBMP-2 loaded 20 -30 μm PLGA 50 50 MPs formulated with 10% (w/w) (.....) or 30% (w/w) (—) PLGA-PEG-PEG triblock copolymer. Cumulative release is shown for two release conditions; 25 mg in 1.5 ml PBS [A, C] or 50 mg in 3 ml PBS [B, D]. Data is expressed as cumulative μg released [A and B] or cumulative percentage release [C and D]. $n=3$

Batches: BN 243 and 245

The average daily release from these MPs is shown in Table 4.1 where the estimated rhBMP-2 component of the total protein value is shown (one hundredth of the total protein) and expressed in nanograms (ng). It would be expected that many of the values shown in Table 4.1 would fall in the therapeutic range in bone regeneration applications suggested to be 1-30 nM for cell signalling (Umulis, 2009). But, the values are much lower than those used clinically and as discussed earlier in the introduction, the optimum therapeutic dose of BMP-2 for bone regeneration is not well defined.

When these supernatants were tested with C2C12 cells for ALP activity (Chapter 3), only the supernatant containing the highest concentration showed a minimal response in the assay and all of the other samples tested showed no positive response (data not shown). There may have been a number of reasons for this problem. The *in-vitro* assay was simply not sensitive enough to record rhBMP-2 activity lower than 200 ng/ml. This may have been compounded by the carrier protein (HSA) hindering the activity of rhBMP-2 at low concentrations, although, this was unlikely as the rhBMP-2 standard curve was prepared with an appropriated concentration of HSA. The more likely explanation may be that the release supernatants were stored frozen and thawed before use and this could have lead to a minor disruption of the protein structure with a direct effect on its binding capacity and activity. In particular, the PBS release medium may have had some effect on the protein structure.

To mitigate some of these issues, rhBMP-2 standard curves were prepared with and without the HSA carrier, MPs with a higher rhBMP-2 loading were also manufactured and direct co-culture of MPs and C2C12 was investigated. The results will be discussed later in this Chapter (Section 4.3.4).

Table 4.1 Estimated average daily release of rhBMP-2 (ng) calculated from the total protein release curves shown in Figure 5.4

<i>Days</i>	<i>25 mg PLGA 50 50 10% TB</i>	<i>50 mg PLGA 50 50 10% TB</i>	<i>25 mg PLGA 50 50 30% TB</i>	<i>50 mg PLGA 50 50 30% TB</i>
0-2	95.1	196.5	101.15	220.15
2-5	6.34	27.47	85.28	265.76
5-9	3.17	38.04	35.7	116.02
9-20	3.63	20.74	19.47	43.81
20-30	9.51	9.51	0.238	2.38

4.3.3 Incorporation of HSA/rhBMP-2 loaded PLGA MPs into thermosensitive scaffolds and the effect on protein release rate

It was discussed earlier in Chapter 3 that by plasticising PLGA 85/15 with 6.5 % (w/w) PEG400 the glass transition temperature could be reduced. Once milled, PLGA/6.5PEG MPs were mixed into an aqueous carrier and gently packed into a mould at 37°C, then they would firstly become cohesive, forming bridging points between MPs and then overtime, they would harden as the low molecular weight PEG leached away.

This was used as a basis to measure release of lysozyme that had been directly incorporated into the hot melt. However, many bioactive molecules would not withstand temperatures over 40 °C and so it was decided to incorporate growth factor loaded (HSA/rhBMP-2) MPs into the PLGA/6.5PEG MP scaffold by dry mixing the two types of MP in a 1:1 ratio, mixing with 0.5% CMC (to act as a lubricant for injection and as an aqueous carrier to encourage PEG leaching) and incubating at 37°C. As the rhBMP-2 MPs were sized at 20-30 µm, the PLGA/6.5PEG MPs selected were sub 100 µm.

Approximately 50% of the total protein released from the scaffold over the first two weeks (Figure 4.5A). Although the burst release in the first 24 hours was around 25% this was not dissimilar, indeed somewhat lower, than the burst achieved from HSA/rhBMP-2 MPs alone. Figure 4.5B shows a comparison of release from HSA/rhBMP-2 MPs alone and the same MPs incorporated in a scaffold. The release from the scaffold tailed off after 1 week but with 50% of the protein still within the matrix it would be expected to continue to release slowly as the scaffold degraded, but this was not investigated further. The

PLGA 85 15 used in the thermosensitive formulation has a much longer degradation time than the PLGA 50 50 used to make the loaded MPs.

To illustrate the setting and scaffold formation of these MPs, Figure 4.5C-E shows the combination of larger MPs (PLGA/6.5PEG MPs with HSA/rhBMP-2 MPs) and their morphology after sintering at 37°C. Figure 4.5E clearly shows that the thermosensitive MPs have 'melted' in to each other giving structure, whilst the growth factor loaded MPs remain spherical, not being affected at 37°C. The overall structure of the scaffold remains porous.

These scaffolds at the end of the study had considerable strength and it was difficult to crush them manually. Unpublished data (Cox, In writing) reported typical compressive strength values for PLGA/6.5PEG scaffolds of between 2 and 6 MPa after just 24 hours of incubation at 37°C. It is expected that the scaffolds would release their cargo in a controlled manner depending on the formulation of the incorporated rhBMP-2 loaded MPs. The release profile may have been improved if larger 50-100 µm spherical MPs were used but the rationale was to use smaller MPs in this study. Different ratios of the two MP types could be tested to gain the optimum combination of release and strength. However, in this instance, only one copolymer concentration one MP size and one MP mixing ratio was tested as a proof of concept for this scaffold.

The advantage of adding thermosensitive MPs is that the system will remain injectable (depending on MP size and carrier) but will strengthen *in-situ* providing support to the surrounding tissue and prevent growth factor loaded MPs migrating and will therefore keep the protein delivery vehicle local and minimise side effects.

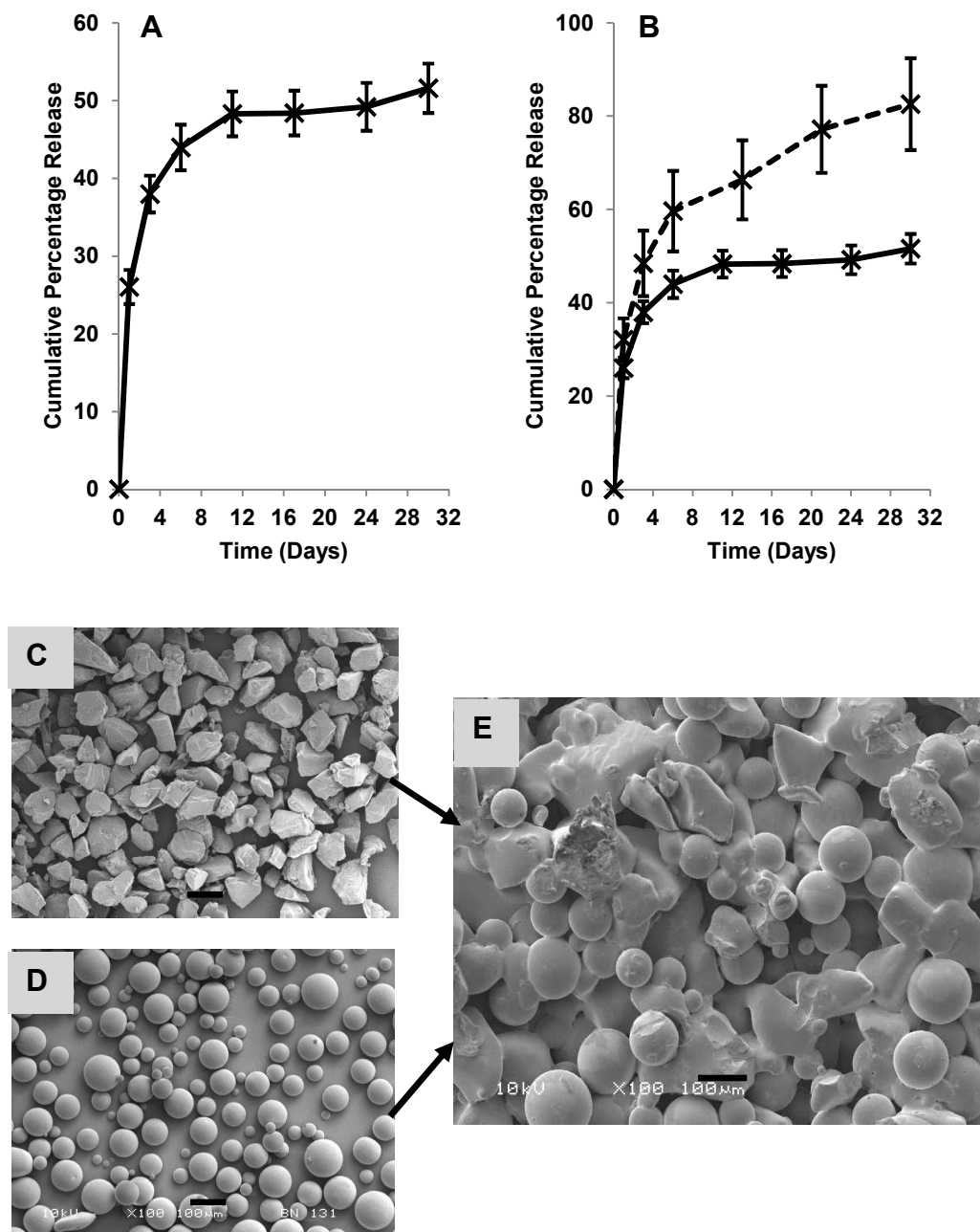


Figure 4.5 [A] Release from 50 mg HSA/bmp-2 loaded PLGA 50/50 (Mwt 56 kDa) MPs incorporated in a PLGA (85/15 Mwt 56kDa)/6.5% (w/w) PEG (Mwt 400 Da) scaffold (solid line) [B] comparison with release from 50 mg HSA/bmp-2 loaded microparticles alone (dashed line) [C] representative image of PLGA/PEG MPs manufactured by hot melt blending and milling prior to sintering. [D] representative image of PLGA MPs manufactured by double emulsion [E] scaffold showing sintered PLGA/PEG MPs and incorporated MPs. Scale bar 100 μm . Image [E] courtesy of Dan Gill (MSc student 2011)

4.3.4 Detection of rhBMP-2 and rhBMP-2 activity in release supernatants

4.3.4.1 rhBMP-2 detection: Enzyme linked immunosorbent assay (ELISA)

The initial step to detect rhBMP-2 in the release supernatants was to test them in a commercially available ELISA. The total protein release profile from these MPs is shown in Figure 4.6A. However, at the advised concentration (62.5 - 4000 pg/ml) the batch of rhBMP-2 (Sept'10) used was not detectable. This may have related to the epitope on the antibody supplied with the ELISA kit not being identical to the binding site on the rhBMP-2 used leading to a lower affinity in the immunoassay. The ELISA kit rhBMP-2 was generated through mammalian cell expression (Chinese Hamster Ovarian) whilst the rhBMP-2 used was expressed in bacterial cells (*Escherichia coli*). The different manufacturing methods may have impacted on the recognition of the growth factor by the ELISA. To counteract this issue, higher rhBMP-2 concentrations were tested (5-100 ng/ml) and these generated an appropriate standard curve (4.6B) in the range required to detect rhBMP-2 in the collected supernatants. Indeed, there was some detectable rhBMP-2 in the release supernatants but the concentration was lower than had been expected in some samples and so this assay was not appropriate for further studies (Figure 4.6C).

However, this was the first indication that rhBMP-2 had been successfully released from the MPs. Although the ELISA could be optimised for detection of growth factors in release media, the technique can only quantify the presence of the molecule and is not a measure of its biological function.

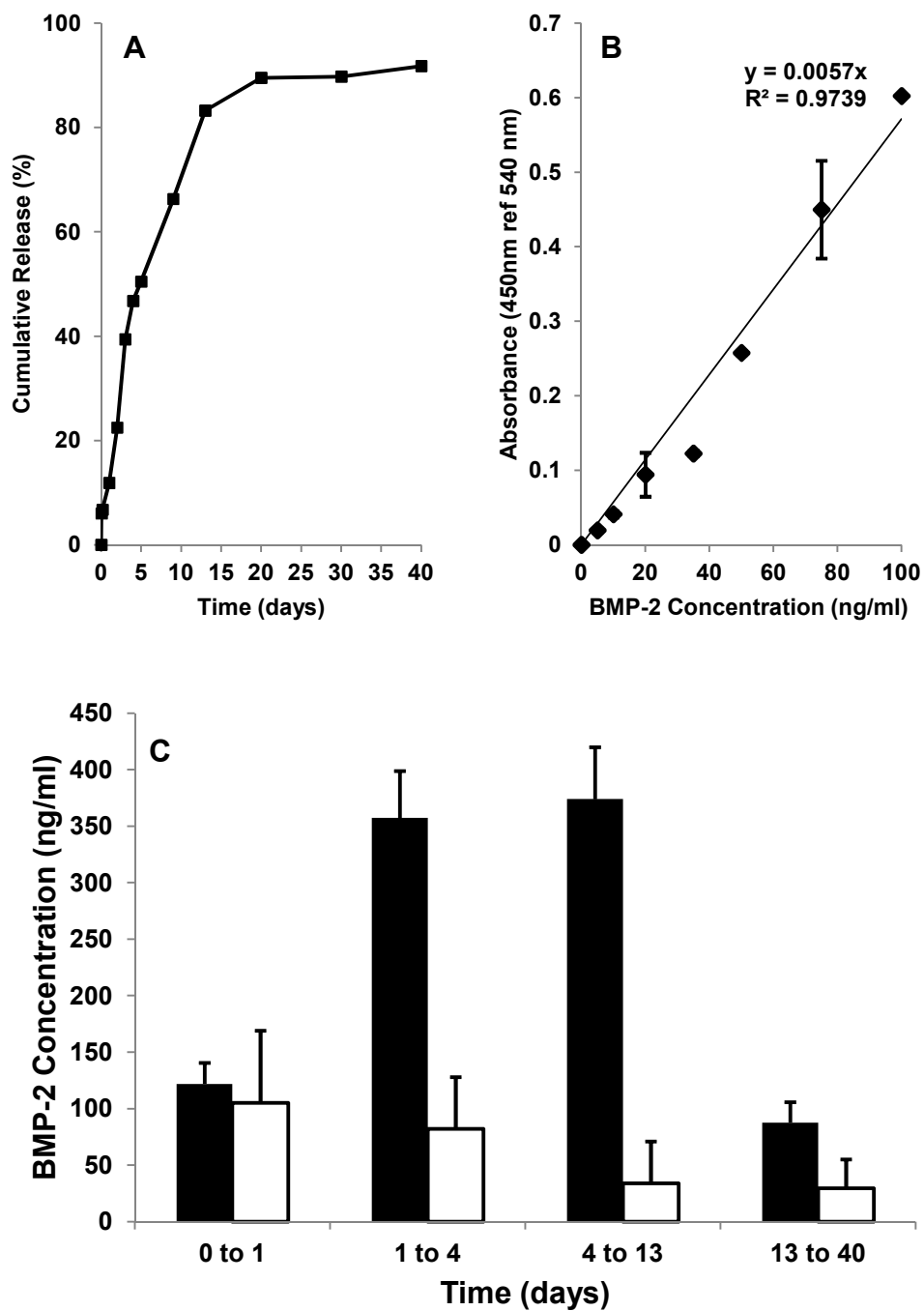


Figure 4.6: Detection of rh-BMP-2 by ELISA in supernatants collected after release from PLGA 50 50 Mwt 56 KDa MPs formulated with 30% (w/w) PLGA-PEG-PLGA copolymer loaded with 1% (w/w) HSA/rhBMP-2 over 40 days. [A] is the total protein cumulative release curve. [B] is the ELISA standard curve. [C] is the expected rhBMP-2 concentration calculated from the total protein value (black bars) and the actual concentration determined by ELISA (white bars).

BN 337

4.3.4.2 rhBMP-2 activity: Alkaline phosphatase assay

ALP is expressed as an early marker of osteogenic differentiation and when osteogenesis is induced using rhBMP-2, the levels of ALP are proportional to the BMP-2 concentration and is mediated by the induction of a wnt autocrine loop (Rawadi, 2003). Preliminary studies using ALP expression as a marker for rhBMP-2 activity in release supernatants were only positive for the burst release from the first 24 hours of release (data not shown). To improve the chance of success of the ALP bioassay, a new batch of MPs was manufactured in the 20-30 μm size range. These and were loaded with a higher concentration of rhBMP-2, but within the same total loading of 1% $_{(w/w)}$ (9.5 mg HSA, 0.5 mg rhBMP-2 in 1 g of PLGA modified with 10% $_{(w/w)}$ TBII-F).

Prior to testing any release supernatants, the feasibility of the assay to detect rhBMP-2 and the sensitivity of the assay was determined. As a preliminary study, rhBMP-2 at concentrations ranging from 50 - 1,000 ng/ml was cultured with C2C12 cells and HSA was added to the standards to mimic the carrier loading in the MPs. By day 5, there was a distinct change in the morphology of the cells. Figure 4.7A shows that C2C12 cells without rhBMP-2 become spindle-like and line up to begin the formation of myotubes. As the rhBMP-2 concentration increases, the morphology changes and the cells become more rounded or cobblestone in shape. This change in morphology is also reflected by an increase in the ALP expression which displays a good linear response between 200 and 750 ng/ml (Figure 4.7B).

Unfortunately, it was not sensitive to below 200 ng/ml which meant that in its current form, most of the rhBMP-2 in the supernatants from the release assays performed thus far (Table 4.1) would not be detectable, especially as

the samples had been stored in PBS and would need further dilution in culture medium for the *in-vitro* assay. An attempt to address this was to combine and concentrate the HSA/rhBMP-2 in the supernatants from a number of days release by using 9 kDa molecular weight filter cut off centrifuge tubes. These samples would then be re-suspended in complete culture medium (DMEM, 10% _(v/v) FCS, penicillin/streptomycin) for cell culture assays. But, this approach was not successful with little or no detection of rhBMP-2 activity in the supernatants (data not shown). It was thought that the MP manufacture and/or release process or the process of concentrating the releasate had denatured the protein or more likely, the levels in the supernatants were still below the sensitivity of the assay.

Different parameters of the C2C12 assay were investigated (for example cell number and culture plate size) to try to optimise the assay and variability within the assay was improved by removing the cell lysis step. In a further attempt to determine rhBMP-2 activity in the release supernatants, the HSA/rhBMP-2 loaded MPs (9.9 mg HSA with 0.1 mg rhBMP-2) were allowed to release their protein directly into tissue culture media (50 mg MPs in 1.5 ml DMEM + 10% _(v/v) FCS and penicillin/streptomycin). This media was then fed directly into the pNPP assay. This gave an indication of rhBMP-2 biological activity in the release supernatants (unlike the ELISA that only detected the presence of rhBMP-2) but the levels of detection were very low and considering the sensitivity of the assay and only the first day of release could be considered to be on the BMP-2 standard curve. However, this study showed that potentially, BMP-2 remained biologically active during the process of particle manufacture and release, but further improvement of the techniques were required.

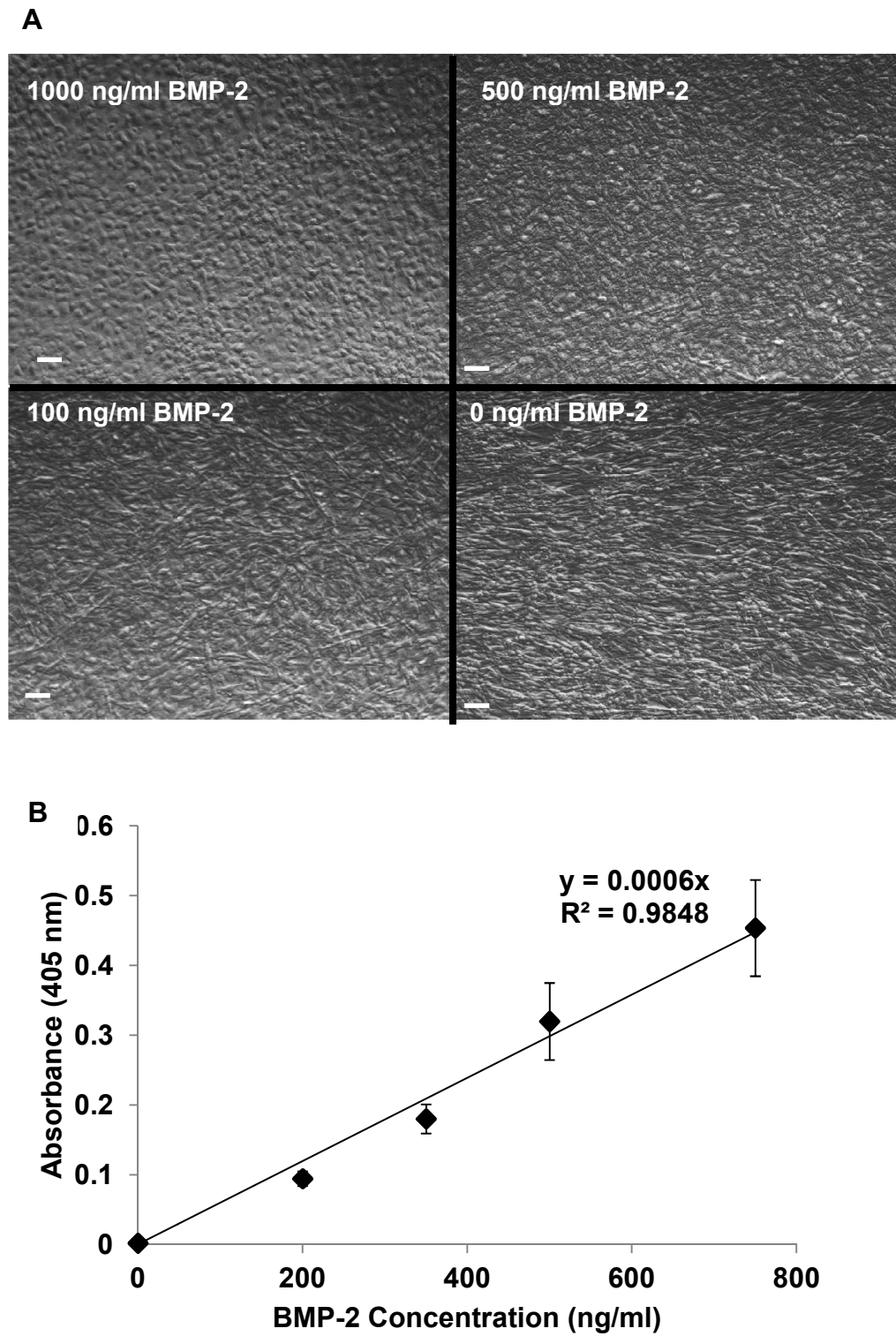


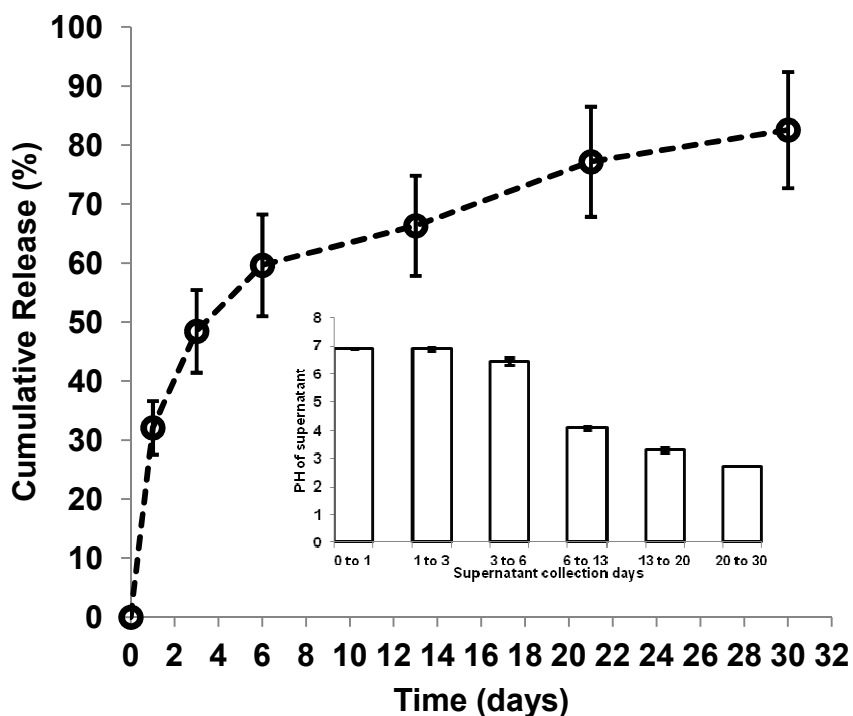
Figure 4.7 Dose dependent response of rhBMP-2 on [A] morphology (scale bar 100 μ m) [B] alkaline phosphatase expression by C2C12 myoblast cells ($n=3$).

A breakthrough in the detection of activity in release supernatants was achieved by using a new batch of MPs that had been manufactured with a fivefold higher loading of rhBMP-2 (9.5mg HSA with 0.5 mg rhBMP-2). The MPs demonstrated a sustained release rate after burst release similar to that seen before (Figure 4.3B) with approximately 80% of the total being released in 30 days (Figure 4.8A). The rhBMP-2 released from the MPs in this study were able to influence the differentiation of C2C12 cells as illustrated by the ALP expression in these cells up to 13 days (Figure 4.8B). However, the levels were up to ten times lower than what would have been predicted by the BCA total protein assay. There was no detection of rhBMP-2 activity beyond 13 days despite release still being detected by the total protein assay (Figure 4.8A) which may be due to assay sensitivity or the effect of the PLGA degradation products.

The pH of each of the supernatants was recorded and it was shown that the pH started to drop after 6 days (Figure 4.8A inset) which was earlier than seen before (Chapter 2). The reason for this may be twofold, firstly, these MPs were smaller, had thinner exterior shells so would therefore degrade faster and secondly the collection time-points are further apart so that there is more likelihood of a build up of degradation products in the supernatant.

Although the work to detect rhBMP-2 activity after release from MPs had gone some way to validating the delivery system, further work investigated different strategies to detect active rhBMP-2 from the controlled release system. Two different approaches were therefore attempted to improve the detection, firstly, an immortalised human mesenchymal stem cell line was used instead of C2C12 cells and secondly, co-culture of MPs with C2C12 cells was performed.

A



B

Days	Estimated rhBMP-2 daily activity based on total protein (ng)	Actual rhBMP-2 daily activity based on pNPP assay (ng)
------	--	--

0-1	11519.0 ± 879.1	1356.9 ± 221.5
1-3	2926.9 ± 98.4	316.1 ± 165.3
3-6	1337.7 ± 84.6	321.8 ± 80.3
6-13	350.0 ± 69.5	47.8 ± 21.7

Figure 4.8 [A] Cumulative total protein release from $27.7 \pm 14.63 \mu\text{m}$ PLGA MPs loaded with HSA/rhBMP-2 (9.5mg HSA/0.5mg rhBMP-2) formulated with 10% (w/w) PLGA-PEG-PLGA triblock copolymer. Inset shows drop in pH over time. [B] Comparison of estimated rhBMP-2 activity adjusted from total protein measurements and actual rhBMP-2 activity based on alkaline phosphatase expression and measured using pNPP assay.

Batches: BN 331, 332

4.3.5 ALP expression by immortalised human mesenchymal stem cells.

Human mesenchymal stem cells (huMSC) isolated from bone marrow have a low proliferative ability and cannot survive many passages. A population of huMSCs were kindly immortalised by Dr Hassan Rashidi by retrovirus-mediated gene transfer following the procedure published by Okamoto in 2002 (Okamoto, 2002). A combination of human telomerase reverse transcriptase with human papillomavirus E6 and E7 successfully immortalised the huMSCs without affecting their potential for adipogenic, osteogenic and chondrogenic differentiation (Rashidi, 2012).

Dilutions of HSA/rhBMP-2 (9.5 mg with 0.5 mg) were prepared with the rhBMP-2 component concentration ranging from 6.25 – 1000 ng/ml and these were tested against both C2C12 cells and the immortalised huMSC cells.

The full range of HSA/rhBMP-2 concentrations for both cell types is shown in Figure 4.9A. With concentrations of rhBMP-2 above 100 ng/ml, C2C12 cells were seen to differentiate down the osteoblast lineage. The huMSC response reached a plateau above 50 ng/ml and was dose responsive with rhBMP-2 below 50 ng/ml (Figure 4.9B), although variation and background values were both high. These cells were therefore expressing ALP without the presence of rhBMP-2 which would make using the assay routinely difficult as the actual absorbance levels, once the background was subtracted, would be very low. Use of these cells was therefore terminated and the work continued by focussing on direct co-culture of MPs and C2C12 cells.

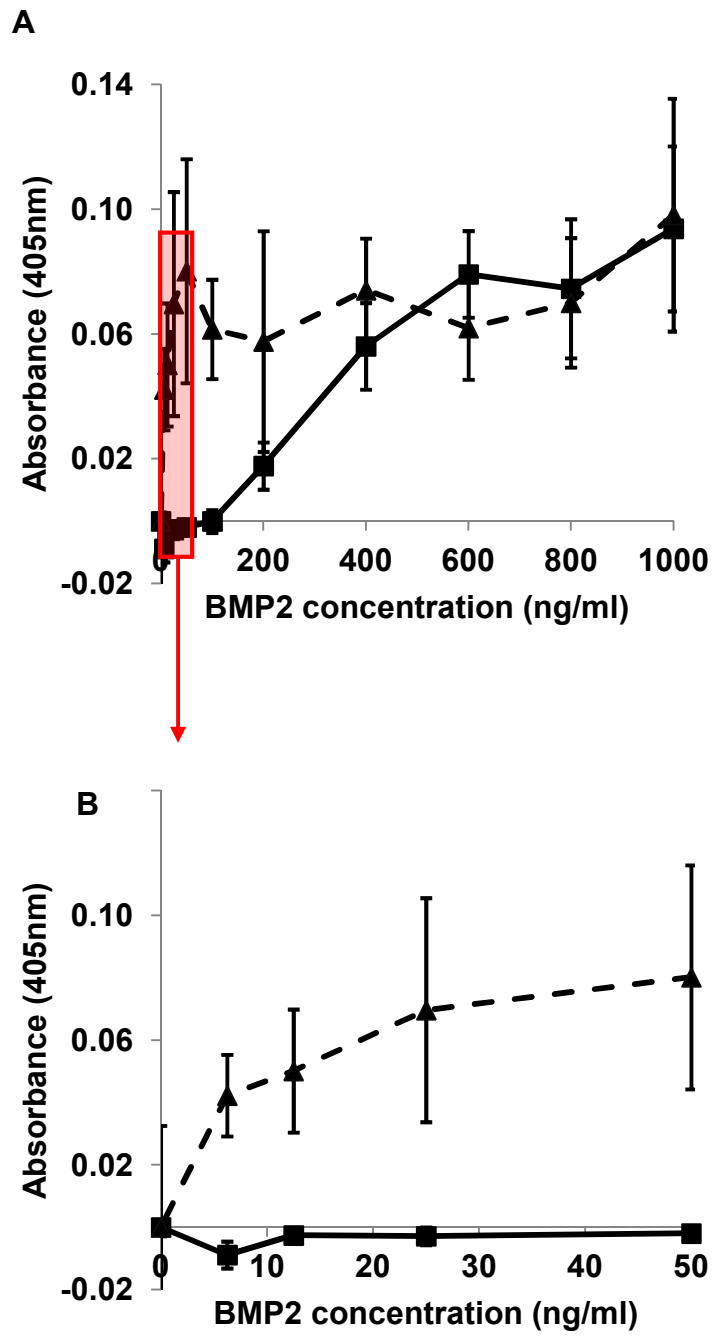


Figure 4.9: rhBMP-2 activity measured by alkaline phosphatase expression in immortalised human MSCs cells (▲) compared to C2C12 cells (■). [A] is the response up to 1000 ng/ml and [B] is the response up to 50 ng/ml

4.3.6 Direct effect of rhBMP-2 loaded MPs on C2C12 cells

It was shown in Figure 4.7 that C2C12 cells presented a myoblast morphology after 5 days of culture (Figure 4.7A 0 ng/ml rhBMP-2). The addition of blank PLGA 50 50 MPs did not adversely affect the cells (Figure 4.10A) and the cells proliferated amongst and around the MPs with no obvious cytotoxic effects after 5 days of culture. When HSA/rhBMP-2 (9.5mg with 0.5mg) loaded MPs were cultured directly with C2C12 cells there was a notable change in the cell morphology (Figure 4.10B) that was similar to the effect seen by rhBMP-2 alone on the cells (Figure 4.7A), these cells also presented a positive response for ALP expression (Figure 4.10C).

These results proved that rhBMP-2 released from PLGA MPs could elicit a biological response on the surrounding cells. To confirm further that the response was directly related to the rhBMP-2 concentration, a number of different masses of rhBMP-2 loaded MPs were cultured with a fixed number of C2C12 cells. Using 2 mg of MPs and below, there was an excellent correlation with MP mass and rhBMP-2 concentration as determined by ALP expression (Figure 4.11). As an additional study, 2 mg of rhBMP-2 loaded MPs were cultured with a range of cell concentrations and data illustrated that the ALP response was related to cell number (Figure 4.12).

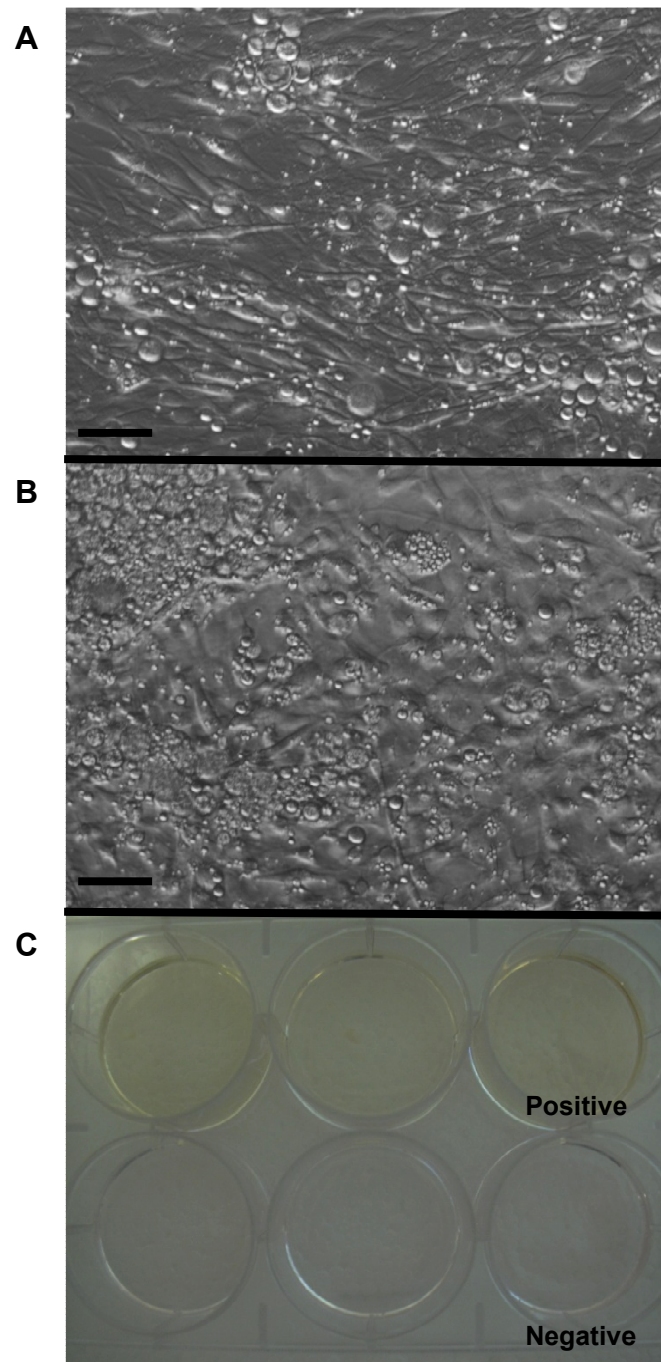


Figure 4.10: Co-Culture for 5 days of C2C12 cells with [A] blank PLGA 50/50 (Mwt 56 KDa) MPs and [B] HSA/rhBMP-2 loaded PLGA 50/50 MPs (9.5 mg HSA/0.5 mg rhBMP-2) showing the difference in morphology. [C] Positive alkaline phosphatase expression in C2C12 cells cultured with HSA/rhBMP-2 loaded PLGA 50/50 MPs. Scale bar 500 μ m

Batches: BN 331 and 332

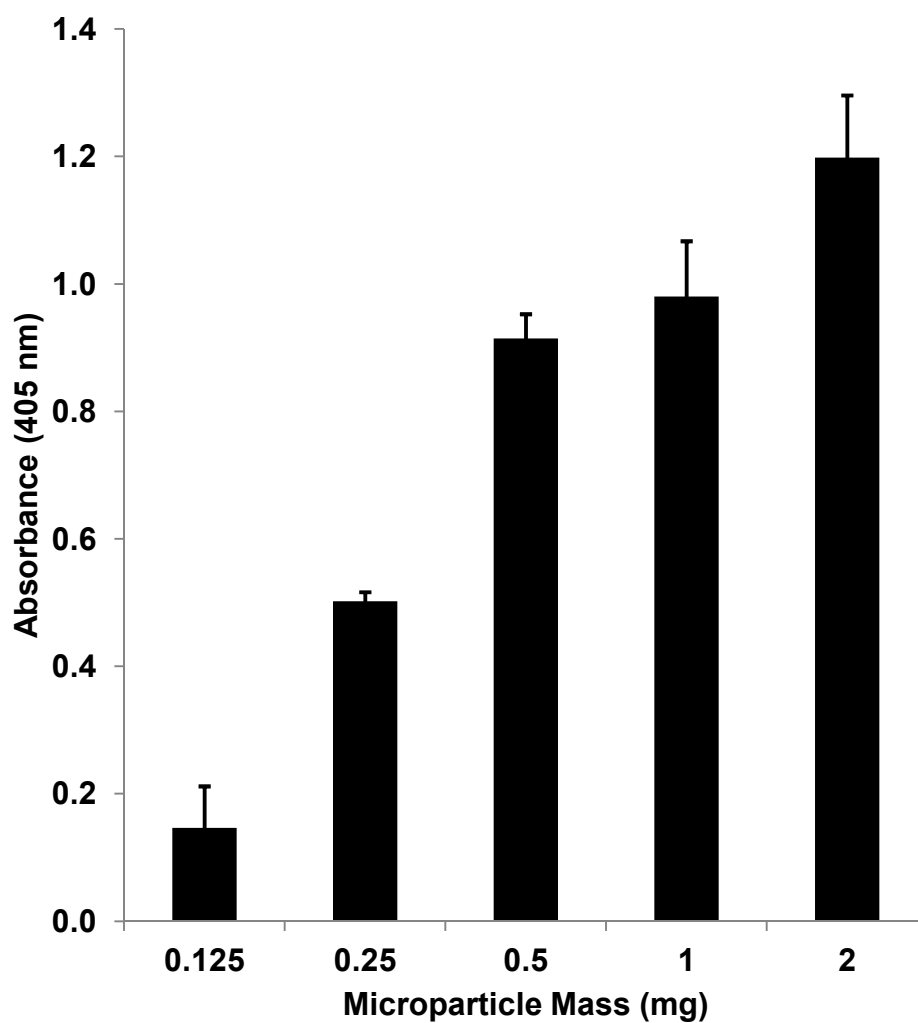


Figure 4.11 Effect of mass of HSA/rhBMP-2 loaded PLGA 50 50 10% (w/w) PLGA-PEG-PLGA MPs on alkaline phosphatase expression in C2C12 cells (n=4)

Batch: BN337

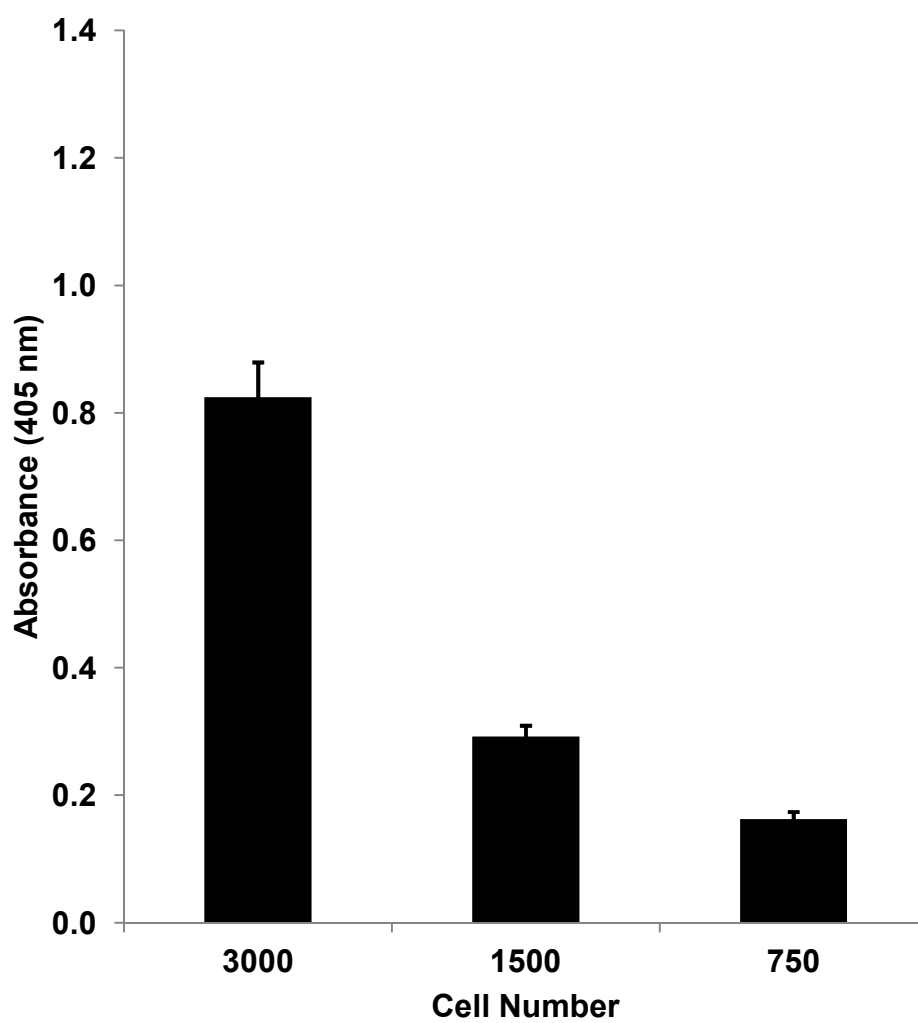


Figure 4.12 Effect of C2C12 cell number when cultured with 2 mg of HSA/rhBMP-2 loaded PLGA 50 50 10% (w/w) PLGA-PEG-PLGA MPs (n=4) Batch: BN337

The rhBMP-2 loaded MPs had now been shown to elicit a biological response when co-cultured with C2C12 cells but the concentration of released rhBMP-2 had not been quantified as the conventional assay was only sensitive at >100 ng/ml and the supernatants from 2 mg of MPs would be below detection limits. However, by knowing the initial loading (9.5mg HSA with 0.5mg rhBMP-2 per g PLGA), the entrapment efficiency of the batch ($51.47 \pm 4.38\%$) and the release curve of these MPs (4.8A), it could be estimated that the 2 mg of MPs would have released approximately 50 ng of rhBMP-2 per day after the initial burst. It was encouraging that these levels were potentially sufficient to have a biological effect as it correlated with some of the published data (Cowan, 2007, Umulis, 2009). However, as discussed earlier, the optimal clinical concentration is not well defined. The advantage of the microparticulate delivery system is that the growth factor delivery cannot only be tailored by formulation of the MPs but also by the mass of the MPs administered.

4.3.7 Sustained rhBMP-2 release determined by direct co-culture of HSA/rhBMP-2 loaded MPs with C2C12 cells

The direct co-culture of HSA/rhBMP-2 loaded MPs with C2C12 cells showed that rhBMP-2 was being released from the MP and was able to drive the differentiation of the cells towards an osteogenic lineage. But, the MPs would have already released 20-30% of their load in the first 24 hours and it may be just the effect of this burst released protein that was causing the cells to differentiate.

To show that rhBMP-2 remaining entrapped in the MPs after the initial burst was still being released in sufficient quantities to exert a biological effect on the C2C12 cells, a release study was set up as described in Section 4.2.4.2

with a schematic shown in Figure 4.2. Individual samples of HSA/rhBMP-2 loaded MPs were exposed to PBS for different times before being recovered, dried and used in a direct culture C2C12 ALP assay. Figure 4.13 shows the morphology of C2C12 cells after 5 days of culture with HSA/rhBMP-2 MPs that had pre-released some of their payload. After 12 days of release prior to incubating the MPs with the cells, the MPs still caused a biological response in the cells (demonstrated by a change in morphology), despite approximately 60% of their protein load (estimated from release curve Figure 4.8A) having already been released.

To consolidate the morphological changes seen the ALP assay was performed on the C2C12 cells. The ALP response, as measured by absorbance at 405 nm, was substantial for the rhBMP-2 loaded MPs compared to the blank MPs up to day 9. The response then tailed off between days 9 and 12 which was consistent with a typical diminishing release profile. The raw data is shown in Table 4.2. Unfortunately it was not possible to quantify these values due to conventional standard curves only being sensitive >200 ng/ml.

The MPs were now proven to encapsulate and release rhBMP-2 in a controlled manner and could be used in further studies into mineralisation and bone repair forming the basis of the work in Chapter 5.

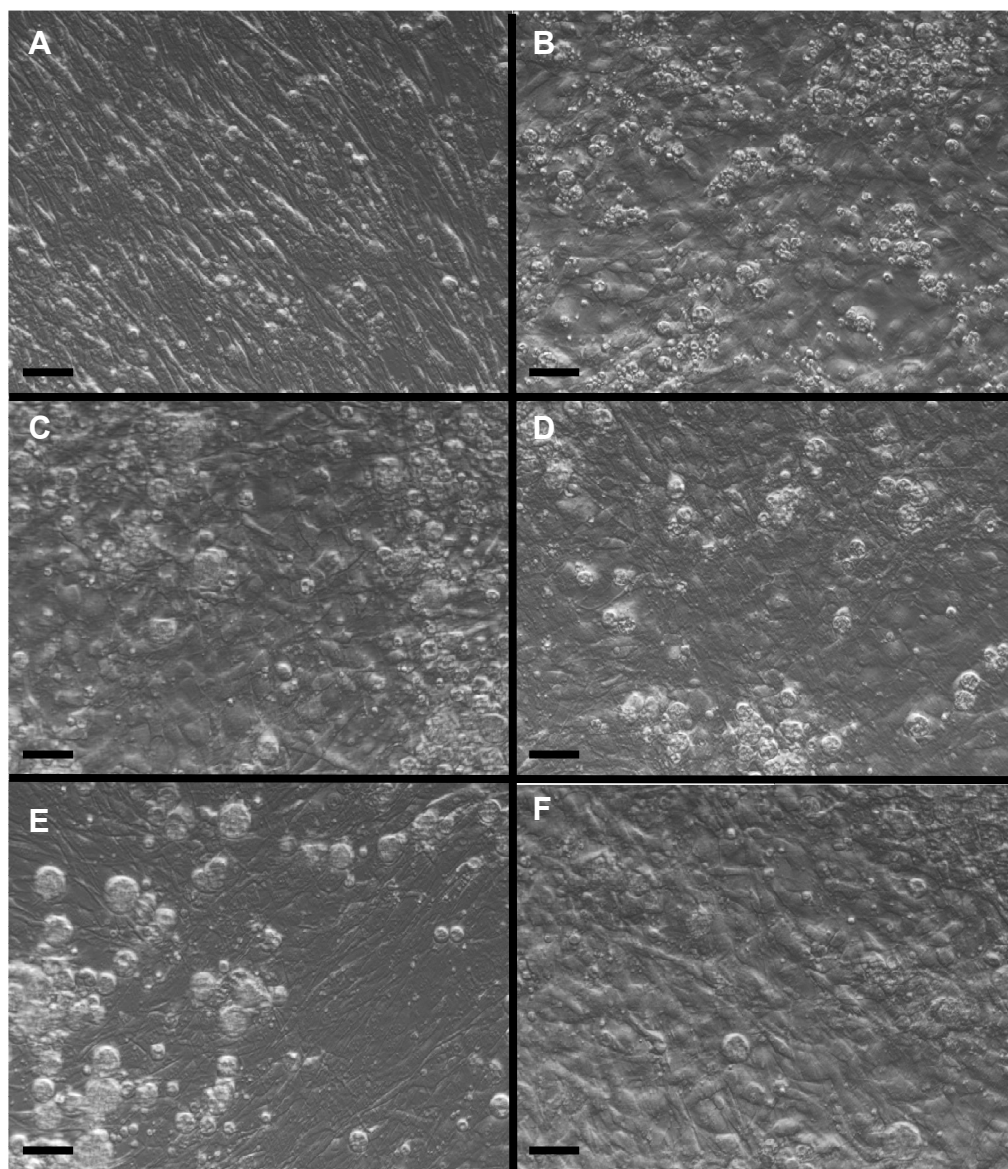


Figure 4.13 Morphology of C2C12 cells after 5 days of culture with [A] no MPs and with PLGA 50 50 MPs loaded with 1% _(w/w) HSA/rhBMP-2 (9.5 mg/0.5 mg) that have been allowed to release into phosphate buffered saline for [B] 1 day, [C] 3 days, [D] 6 days, [E] 9 days and [F] 12 days followed by drying. Scale bar 20 μ m.

BN337

Table 4.2 Alkaline phosphatase expression (determined by absorbance at 405 nm) by C2C12 cells after incubation with HSA/rhBMP-2 MPs that had pre-released their protein load into PBS for different time periods.

<i>Number of days MPs exposed to PBS</i>	<i>50 mg PLGA 50 50 10% PLGA-PEG-PLGA TBII-F (9.5 mg HSA 0.5 mg BMP-2)</i>
<i>Absorbance measured at 405nm</i>	
0	0.308 ± 0.05
1	0.266 ± 0.051
3	0.214 ± 0.034
6	0.312 ± 0.127
9	0.314 ± 0.030
12	0.181 ± 0.082
Blank MPs	0.089 ± 0.006

4.3.8 Von Kossa staining for calcium deposits

To further confirm that the HSA/rhBMP-2 loaded MPs could induce osteogenesis by releasing bioactive rhBMP-2, a 21 day direct culture study was performed using mouse primary calvarial cells (mPCCs). The HSA/rhBMP-2 (PLGA 50 50/ 30%_{w/w} TBII-F 50 -100 µm) loaded MPs were dispensed amongst the adhered cells and remained throughout the 21 day culture period in basal media. Due to the longer culture period for this assay, it was decided to use 50-100 µm MPs to avoid the expected build up of degradation products

from the 20-30 μm which may have adversely affected the viability of the cells. Figure 4.14 shows the von Kossa staining achieved. The opaque MPs are clearly visible as well as their effect on the surrounding cells.

Acknowledgement goes to Dr Lisa White (School of Pharmacy, University of Nottingham) for providing the data.

The mPCCs cultured with blank (no HSA/rhBMP-2) MPs showed a weak diffuse staining with no nodular formation when compared to the HSA/rhBMP-2 loaded MPs which gave a good strong staining with the presence of nodules. The cells with no MPs showed no staining for calcium deposits. The data suggests that the presence of PLGA MPs caused a low level osteoinductive effect and other researchers have investigated PLGA alone for its osteogenic potential on human mesenchymal stem cells (Kruger, 2011). However, the response is greatly enhanced by the release of rhBMP-2 from the PLGA MPs.

The nodular deposition of calcium by primary calvarial cells has been reported before and is thought that the heterogeneous nature of the primary calvarial cell population localises the calcification (Declercq, 2005). Due to the large number of MPs in the culture, it was difficult to define whether the calcification was localised around individual MPs or whether it was due to the overall level of rhBMP-2 released. But, it was clear that calcium deposits were evident and this result gave further evidence as to the osteogenic potential of these MPs.

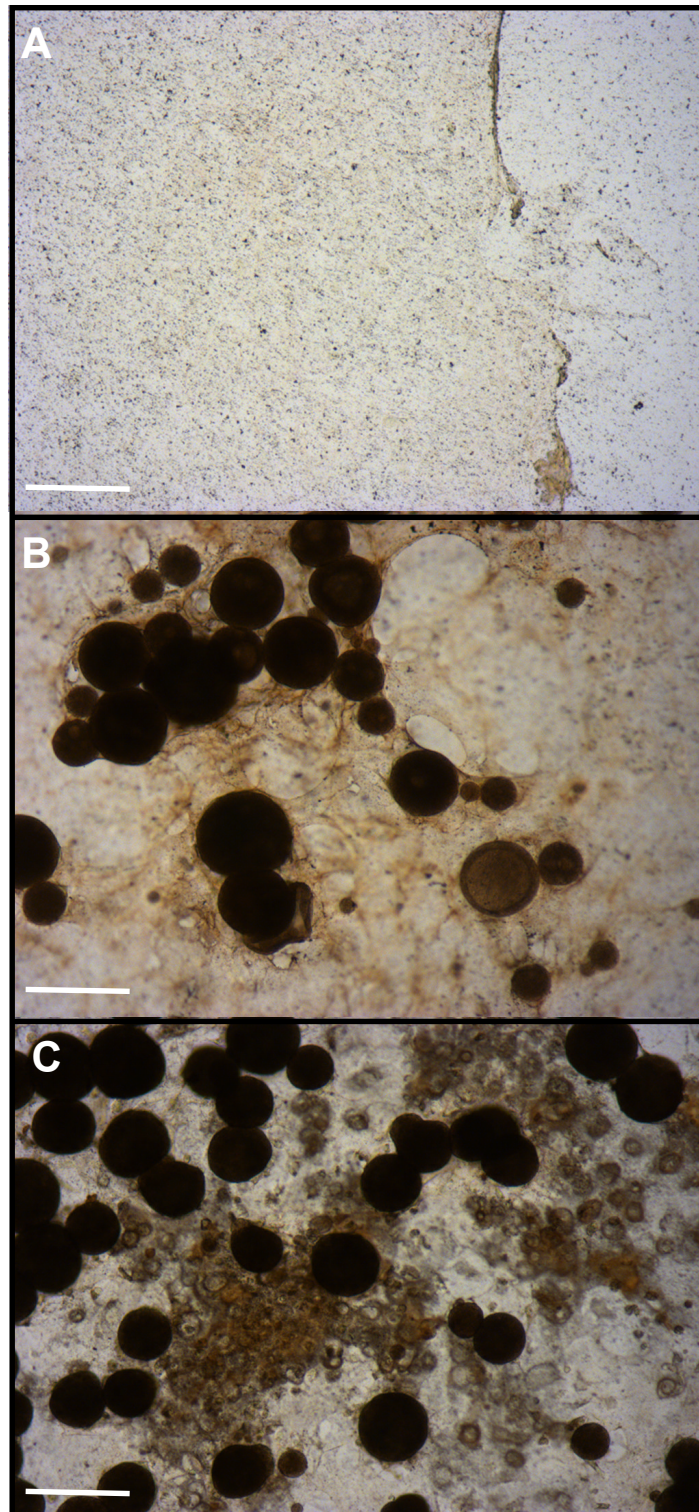


Figure 4.14 Von Kossa staining for calcium deposits by mouse primary calvarial cells after 21 days of culture with [A] no MPs, [B] blank PLGA 50 50 30%_(w/w) TBII-F 50 -100 μ m MPs and [C] HSA/rhBMP-2 loaded (9 mg HSA/1 mg rhBMP-2 in 1 g) PLGA 50 50 30%_(w/w) TBII-F 50 -100 μ m MPs. Scale bar 100 μ m. Images courtesy of Dr Lisa White BN 346

4.4 Conclusions

This Chapter has focussed on transferring the controlled release technology for a model protein developed in Chapters 2 and 3 to the release of rhBMP-2. A smaller MP size was used (20-30 μm as opposed to 50-100 μm) and despite the burst release being higher for these MPs, release could still be controlled by using PLGA-PEG-PLGA triblock copolymer within the polymer formulation. The addition of thermosensitive PLGA/PEG MPs to the rhBMP-2 releasing MPs will still allow the delivery device to be injectable, but will enable the scaffold to harden *in-situ* thus giving support to the surrounding tissue and providing a scaffold for new tissue growth whilst localising growth factor delivery to the injection site. Results showed that the release of growth factor after the initial burst is likely to be sustained over a period of months rather than days as the MPs are trapped in a solid structure which degrades slowly.

Detection of active rhBMP-2 after release from MPs was paramount to the delivery device being successful and this proved to be a considerable challenge. The C2C12 cells provided a good tool to detect rhBMP-2 activity but it was only sensitive >100 ng/ml for the rhBMP-2 used. The expected levels of rhBMP-2 in the release supernatants were lower than this detection and so MPs with higher rhBMP-2 content were manufactured and these gave more encouraging results. Using co-culture techniques, the rhBMP-2 released from the MPs were shown to be active against C2C12 cells in low masses and therefore low concentrations of rhBMP-2. Longer term effects were demonstrated by positive staining for calcium deposits showing that the MPs had caused mineralisation occur. These rhBMP-2/HSA MPs could now be progressed to use in an *ex-vivo* model of bone repair which is the subject of the following Chapter.

Chapter 5: The development of an ex-ovo chick femur as a model to investigate the effects of rhBMP-2 loaded microparticles on bone regeneration and repair

5.1 Introduction

During the development of pharmaceutical products and medical devices including drug delivery systems, a reliable *ex-vivo* model to screen candidate materials and formulations prior to embarking on large scale pre-clinical models would be advantageous. This is particularly relevant for models of skeletal repair as *in-vivo* models tend to involve large, skeletally mature animals such as sheep meaning only a relatively small animal numbers are usually possible in a study. We have utilised the chick embryo to investigate bone growth and repair as supply is plentiful and cost effective (Rashidi, 2009). The embryonic development of the chick is well documented with the seminal work being performed by Hamburger and Hamilton who described the forty six chronological stages of chick development over the 21 day gestation period and more recent work using ultrasound imaging and micro computed tomography to monitor development has been used (Hamburger, 1951, Schellpfeffer, 2007, Kanczler, 2012). A pictorial guide to *in-ovo* chick development is shown in Figure 5.1.

Although the chick embryo is a good candidate as a tool to study the effects of growth factors on development, one potential problem is that growth can be affected by a number of variables such as incubation temperature, delay between laying and incubation and breed of hen (Oviedo-Rondon, 2008). In particular, the skeletal development can be affected by temperature having a positive correlation (Brookes, 1972) and so incubation time, humidity and

temperature control must be taken into careful consideration when planning studies.

When chick femurs are dissected from day 13 embryos and cultured *in-vitro* for 10 to 15 days, they produce new osteoid from skeletal stem cells present in the perichondrium (Roach, 1996). Therefore, organ culture of small whole bones may provide a niche for studies of scaffolds and/or growth factors with or without cells. Tissue culture of the bones at the air/liquid interface is the preferred method as the higher oxygen concentration is more likely to favour osteogenic differentiation (Roach, 1997). This method of culture will be described in this thesis as organotypic culture.

If the femur is removed after 11 days of incubation at 37°C and is cultured organotypically for a further 10 days, it continues to develop *in-vitro*. The first 2 days have been described as the adaptation period characterised by release of intracellular enzymes, followed by a period of steady growth during which skeletal cells proliferate and secrete bone and cartilage matrix (Roach, 1990). Although the bones grow, they do not follow normal endochondral ossification because there is no vasculature present. The chorioallantoic membrane (CAM) model has been used as an *ex-vivo* model to test the angiogenic properties of a tissue or explants and has been used to culture bones and investigate fracture healing (Takahashi, 1991, Roach, 1998) and has been described as a preferred model due to the lack of vasculature in *in-vitro* culture (Kachi, 2008) but the CAM assay is not in the scope of the current work. The disadvantage of the CAM assay is that it gives very variable results, is technically difficult to perform and the results are open to different interpretation.

Endochondral ossification involves a series of precisely controlled events leading to a cartilaginous template being converted to a highly organised bone structure. The cellular and molecular events leading to cartilage and bone formation have been thoroughly studied (von der Mark, 1977, Cancedda, 2000) and involve mesenchymal stem cells proliferating and differentiating into chondroblasts, which secrete a cartilagenous matrix and progressively become embedded chondrocytes. The chondrocytes undergo hypertrophy and the matrix is calcified as oxygen, nutrients and cellular wastes can no longer diffuse through the matrix. The chondrocytes degenerate and leave behind a scaffolding of calcified cartilage. Blood vessels invade and both osteoprogenitor and hemopoietic cells enter the cartilage model. The hemopoietic cells will form bone marrow and bone matrix is laid down on scaffolding of calcified cartilage by osteoblasts. The sequential aspect of this process is highlighted by the distinct zones from the epiphysis to the diaphysis, these being resting chondrocytes, proliferative chondrocytes, hypertrophic chondrocytes and the calcified zone and positional cues are important (Caplan, 1983). The changes in chondrocyte behaviour are tightly regulated by both systemic factors and locally secreted factors, which act on receptors to effect intracellular signalling and activation of chondrocyte-selective transcription factors (Mackie, 2008).

Due to its potential to remodel, bone has inherent regenerative capacity and therefore any animal model must ensure that the defects created are of critical size and will not heal spontaneously. It is of utmost importance that any animals used have reached skeletal maturity and that the model should mimic the clinical situation as closely as possible which is why large animals are usually used for preclinical studies (Buma, 2004). However, these studies have high cost implications and the embryonic chick femur can potentially be

used to bridge the gap between *in-vitro* and large animal *in-vivo* studies. The whole bone organotypic culture has not been widely used but was compared directly with chorioallantoic membrane culture was shown to grow well *in-vitro* (Kachi, 2008) and has been used more recently to investigate the effect of parathyroid hormone and parathyroid related hormone on bone formation (Smith, 2012).

The aim of this Chapter is to develop an *ex-vivo* model of defect bone repair which can be used to screen a number of delivery devices containing scaffolds, cells and growth factors to give a higher chance of success in future animal studies. The preliminary work is to observe the normal growth of the chick femur and compare it with organotypic growth using histological techniques. The cultured bones can be fixed, wax embedded, sectioned then stained with alcian blue which will stain cartilage matrix and picrosirius red stain along with phosphomolybdic acid as a mordant which will stain collagen highlighting the ossified areas of the bone and thus the bone development.

The project will then aim to create defects in the embryonic bone and fill them with BMP-2 growth factor loaded microparticles (MPs) developed in the early phase of this project. Any effects of the MPs on the tissue will be determined by histological techniques. This *ex-ovo* culture method to investigate critical defect repair is novel and the development of the technique is the subject of this thesis chapter.



Figure 5.1 Normal chick development during the gestational period.

Taken from www.cob-vantress.com

5.2 Materials and Methods

All the laboratory equipment, consumables and chemicals used during the work for this Chapter can be sourced in Appendix I, tables A1, A2 and A3.

Where MP batch numbers are stated, the details of the manufacturing parameters can be found in the Appendix II. The reagents for tissue processing and histological staining are shown in Appendix III

5.2.1 Dissection of embryonic chick femurs

Fertile hen eggs (Henry Stewart, Dekalb white) were placed in a 37°C humidified incubator on the day of arrival. If incubation needed to be delayed, the eggs were stored in a fridge set at 10-18°C (any colder would compromise the viability of the embryos). After incubation (usually 11 days) the embryos were sacrificed and the femur bones were dissected out by isolating the leg and carefully rolling on a piece of sterile filter paper to remove the musculature. Once dissected, the bones were placed in pairs in PBS to keep them hydrated prior to use. The procedure for dissection out the bones is shown in Figure 5.2

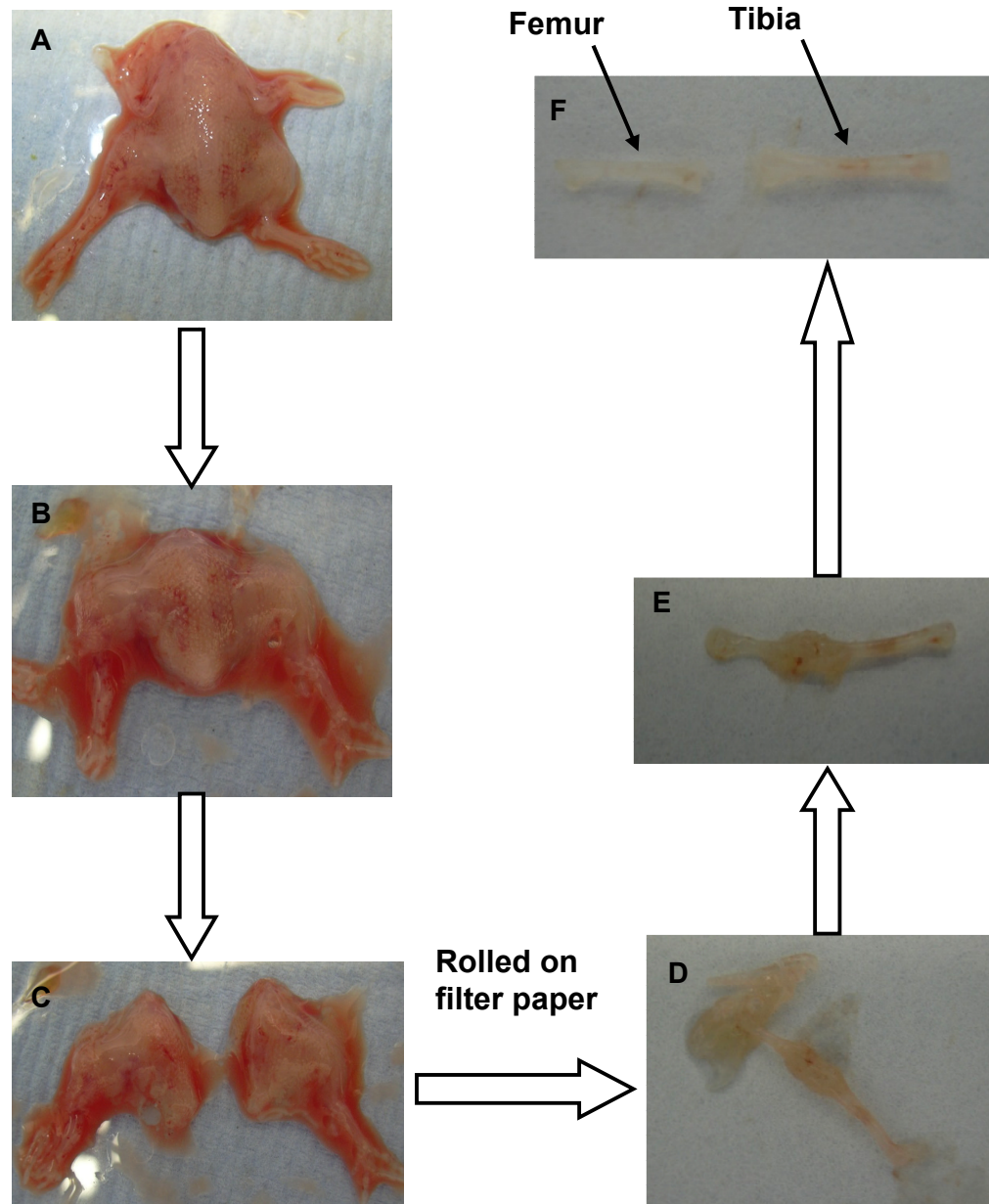


Figure 5.2 Schematic showing the technique to dissect out femur bones from 11 day chick embryos. Firstly, the embryos is laid in the prone prone position [A] and a horizontal cut made midway across the abdomen [B]. A vertical cut then separates the legs [C]. Each leg is carefully trimmed of musculature and then rolled on filter paper [D] to continue the process. As the limb is rolled, the position of the bones becomes clear [E]. The tibia and femur are carefully separated [F] and the bones can be used for experimentation.

5.2.2 Creating critical sized defects in the diaphysis and epiphysis

5.2.2.1 Wedge defects

A freshly dissected day 11 femur was placed in a Petri dish under a stereomicroscope and held carefully with fine forceps. A wedge of bone collar was carefully cut out of the diaphysis using a fine scalpel blade. Images of these defects are shown in Figure 5.7.

5.2.2.2 Drill defects

A Day 11 femur was placed on a piece of sterile filter paper under a stereomicroscope and carefully rolled to dry it. Fine forceps were used to carefully hold the bone in place with minimal pressure, whilst a 300 μm drill bit was manually used to create a defect by rotating the drill between the fingers with gentle pressure on the bone to create a hole. The drill bit was then removed leaving behind the defect. These drill defects were made in both the diaphysis and epiphysis and images are shown in Figures 5.7 - 5.9.

5.2.2.3 Non-union defects

In order to create a non-union defect model, a freshly dissected day 11 chick femur was simply cut cleanly with a sharp scalpel blade and the two pieces were cultured at set distances apart on Millicell inserts. Images of these defects are shown in Figure 5.10.

5.2.3 Filling the defects with HSA/rhBMP loaded microparticles

5.2.3.1 Defect filling using femtoject injector

The PLGA MPs to be loaded were suspended in a small volume of PBS to give a concentrated solution (actual mass/volume not recorded). A pulled glass capillary was attached to the Femtojet injector and the MPs drawn up under capillary pressure. The capillary was placed in the defect hole in the bone and the injection was set to deliver in 0.1 seconds under approximately 90 Pa of pressure using the foot pedal.

5.2.3.2 Defect filling using microspatulas

A small dry mass of MPs to be loaded into the defect were used. A bone, with defect, was dried thoroughly on filter paper and placed under a stereomicroscope with the gentle support of fine forceps. The 100 μm microspatula was dipped in the MPs and the attached MPs were transferred to the defect. If necessary, more MPs were added until the hole was filled and a larger spatula was used to gently tamper down the MPs. This process requires a moderate degree of technical skill to avoid further damage to the bone by handling. Generally, diaphyseal defects were easier to fill than epiphyseal defects due to the harder composition of the diaphysis.

5.2.4 Filling non-union defects with huMSCs in alginate

The alginate was prepared aseptically by dissolving 1.5 g of alginate in 100 ml PBS and the resulting solution was left under UV light for 30 minutes.

Immortalised hMSCs were added into 1 ml of the alginate solution (1.5×10^6 per

ml) and were mixed by gentle trituration. The alginate/cell solution was added dropwise into a calcium chloride solution (100 mM) to act as a cross linker. The calcium chloride solution was later replaced with complete culture medium. Chick bones were isolated as described earlier and cut in middle to form a non union defect. The alginate/cell construct was placed between two parts. The bones were cultured organotypically for 10 days (described below) before being fixed with 4% _(w/v) PFA overnight and processed for histology.

5.2.5 Organotypic culture of chick femurs

The femurs, after treatment, were carefully placed onto the membrane of a Millicell insert which was subsequently placed into the well of a 6 well non treated tissue culture plate (Kanczler, 2012). 1 ml of alpha minimal essential medium (α MEM) supplemented with penicillin/streptomycin and ascorbic acid was added into the well underneath the filter. The media must only be supplemented with ascorbic acid (50 μ M) just before use and so a small volume should be prepared as required. The media was carefully removed by aspiration and replaced with fresh on a daily basis throughout the ten day culture period in a humidified atmosphere at 37°C. This method is advantageous for non-union defects and for bones where MPs would be likely to disperse if submerged in media.

5.2.6 Tissue processing, embedding and sectioning

After the ten day culture period, the bones were carefully removed from the Millicell insert and if necessary, imaged. The bones were transferred to labelled wax embedding cassettes. An automated tissue processor was used

to dehydrate and infiltrate the samples in wax. Details of the reagents and incubation times used are in Appendix III.

On completion of the program, the cassettes were transferred to a wax embedder and the sample orientated in the desired plane before embedding in wax. Sections (10 µm) were cut using a Microtome, stretched on a water bath at 60°C and mounted on Superfrost™ plus microscope slides which were dried on a hot plate at 50°C overnight.

5.2.7 Histology staining: picrosirius red and alcian blue

The sections were first de-waxed in histoclear and rehydrated through a series of increasing ethanol concentrations. Cell nuclei were stained with Weigerts haematoxylin and following treatment with acid/alcohol to reduce the pH, the sections were stained with alcian blue to stain the cartilagenous matrix. After thorough washing in tap water the slides were treated with phosphomolybdic acid followed by picrosirius red to stain collagen deposition. Finally the slides were dehydrated through a series of decreasing ethanol concentrations and coverslips applied with DPX mounting medium. After drying, the slides were imaged using brightfield microscopy. The details for the preparation of the reagents and the ethanol concentration used are shown in Appendix III

5.3 Results and Discussion

5.3.1 Normal chick femur growth

The gestation period of a chick is 21 days and the rate of skeletal development beyond eight days is remarkably rapid. In order to recreate an

ex-vivo developmental niche for the study of bone growth and development and repair it was important to standardise the *in-ovo* incubation time. Figure 5.3 is an image of a chick embryo at 12 days of incubation showing how advanced the development is with the legs and wings clearly formed.



Figure 5.3 A close-up image of a chick embryo after 12 days of in-ovo incubation at 37°C.

Taken from <http://php.med.unsw.edu.au/embryology>

To investigate the natural growth rate of the chick femur during embryogenesis, eggs were removed from incubation daily from day 8 to day 15 and the femurs were carefully dissected from the embryo. After imaging, they were processed in preparation for histological analysis and stained with picro-sirius red and alcian blue to highlight the osteogenic and chondrogenic areas within the bone.

Figure 5.4 shows the scale of growth and thickening of these bones over this development period by endochondral ossification. At day 8 they are very fragile and approximately 3 mm in length. By day 15, they are approaching 10 mm in length and much stronger. Dissection from the surrounding musculature was more difficult. The increasing vascularisation during development can be seen by the reddening of the diaphysis over time.

Figure 5.5 shows sections of these bones after picro-sirius red/alcian blue staining. The process of the conversion of cartilage to bone by endochondral ossification is described in more detail Section 1.3 of Chapter 1. Briefly, primary ossification occurs in the diaphysis and bone collar forms followed by cavity formation and vascularisation. As blood vessels, osteoclasts, and osteocytes continue to invade, the medullary cavity is formed and the diaphysis continues to lengthen during embryonic development. The histology shown in Figure 5.5 confirms the progression of this process and the efficacy of the staining procedure. The day eight femur was practically all cartilage and consequently stained blue. By day ten, primary ossification had begun in the diaphysis and was shown by the picro-sirius red staining. As time progressed, the picro-sirius red staining became more extensive and progressed towards the epiphysis. By day fifteen, only the epiphysis was still cartilaginous and the diaphysis had a recognised cancellous bone structure. If bones had been dissected at later gestation times, secondary ossification centres in the epiphysis would have completed the transformation of cartilage to bone leaving just articular cartilage at epiphyseal plates to allow to continued growth of the bird after hatching.

This work on using the developing chick femur as a model to research bone repair and regeneration is of a collaborative nature with a number of other groups working on different aspects of the model. It was important to standardise the *in-ovo* incubation and it was agreed that day 11 would be suitable for the majority of studies. The relatively the early stage of endochondral ossification gives optimum opportunity and scope to i) re-create the natural *in-ovo* development outside the egg by culturing the bones, ii) alter the natural development by looking at the effects of rhBMP-2 and iii) use the bone as a model for critical defect repair.



Figure 5.4: Images of chick femurs dissected on each day between day 8 and day 15 ex-ovo. Imaged by bright field microscope (x10) (two images stitched together)

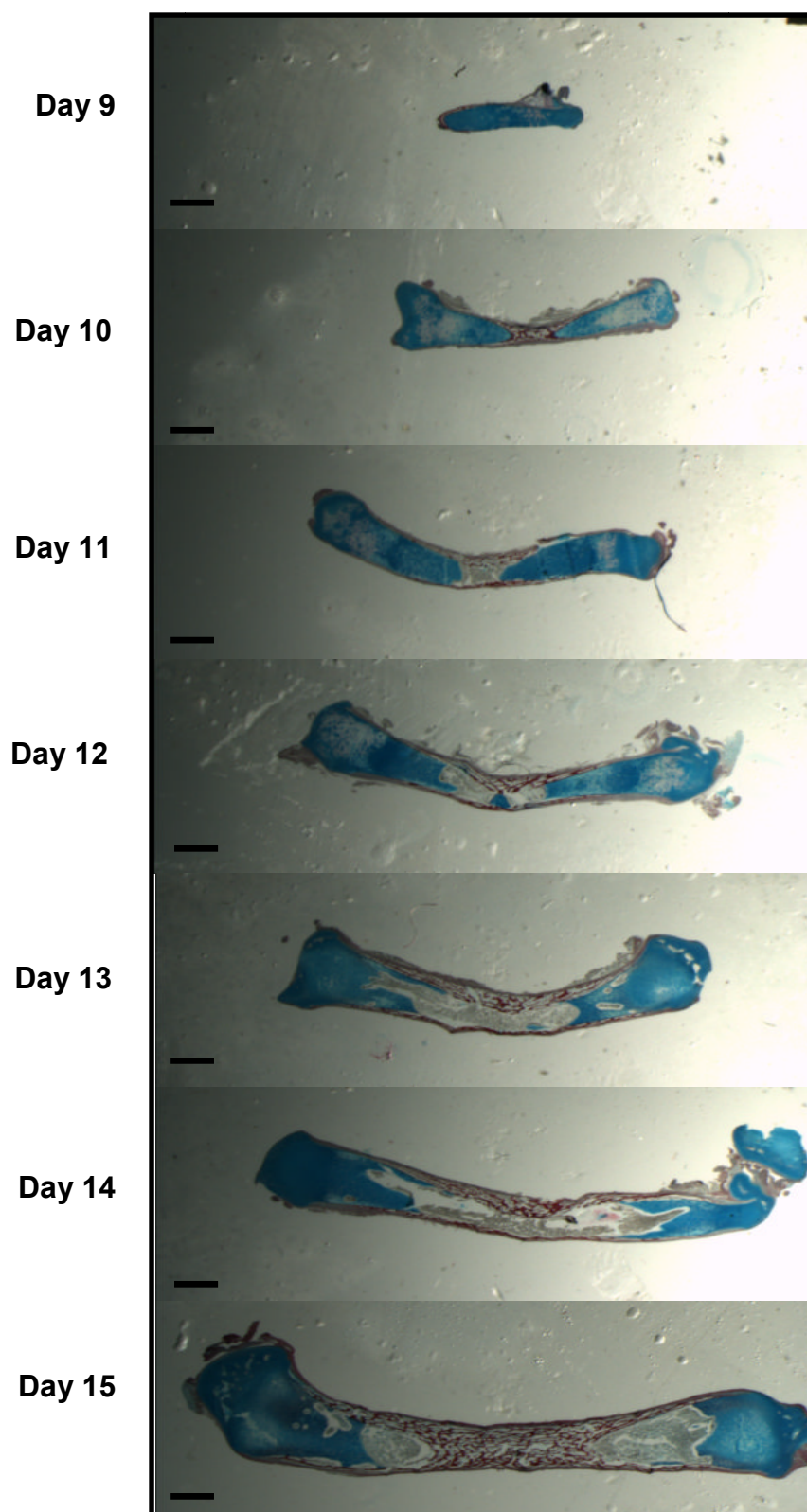


Figure 5.5: Alcian blue and picrosirius red staining of chick femurs dissected from the embryo between days 8 and 15 of incubation at 37°C.

Scale bars 1 mm

5.3.2 Chick femur growth during organotypic culture

The chick femurs dissected from the day 11 embryos were in most cases treated in pairs. For example, either one femur would be treated with growth factor releasing MPs whilst the other would be treated with blank MPs and then they would be both cultured organotypically, or one femur would be fixed whilst its pair would be cultured.

To demonstrate the growth of the embryonic bones in tissue culture, one femur was fixed in 4%_(w/v) paraformaldehyde immediately after dissection whilst its pair was cultured for 10 days on a Millicell insert with daily changes of culture medium supplemented with ascorbic acid. Figure 5.6A shows the extent of the bone growth over the ten day period. The non-cultured femur was approximately 6 mm in length whilst the cultured paired femur was approximately 10 mm in length. Although this is significant growth, it is more like the *in-ovo* growth seen from day 11 to day 14 rather than mimicking the gestation as the chick would normally hatch on day 21. However, this growth in culture gives a good opportunity and scope to study the developmental process. Day 11 chick femurs were also cultured submerged in the media throughout the 10 day culture period. These femurs also grew well (data not shown) but this method was not preferred as any addition of MPs to the exterior surfaces of the bones would be lost in the media.

A potential drawback with this work is the delicate nature of the bones and very careful handling that is needed to avoid damage to the bone. Figure 5.6B shows another pair of femurs, again, one was fixed upon dissection and the other was cultured. It is clear that the bone in culture has not grown normally *in-vitro*. The diaphysis looks narrower and the epiphyses appear bigger than expected. This was probably the result of mishandling the bone whilst setting

up the culture thus disturbing the normal growth processes. The manual dexterity required to handle the bones is a procedure which improved with practice. But, it is very important that anomalies in bone morphology that may have been caused by handling are not mistaken for a response caused by experimentation with growth factors.

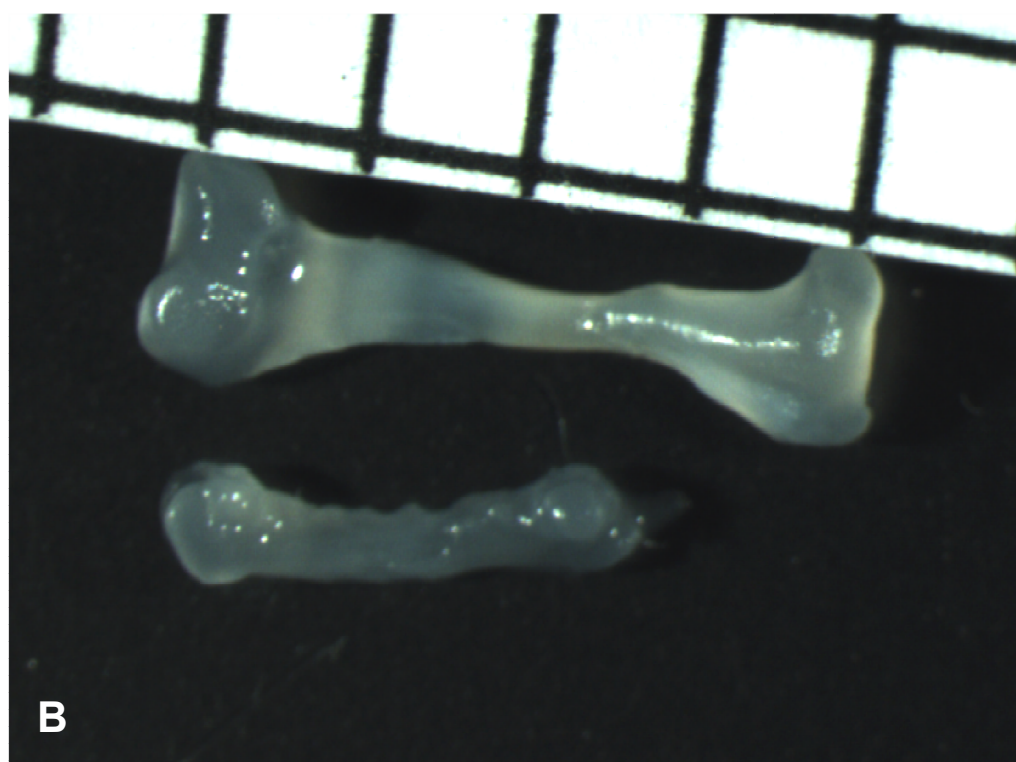
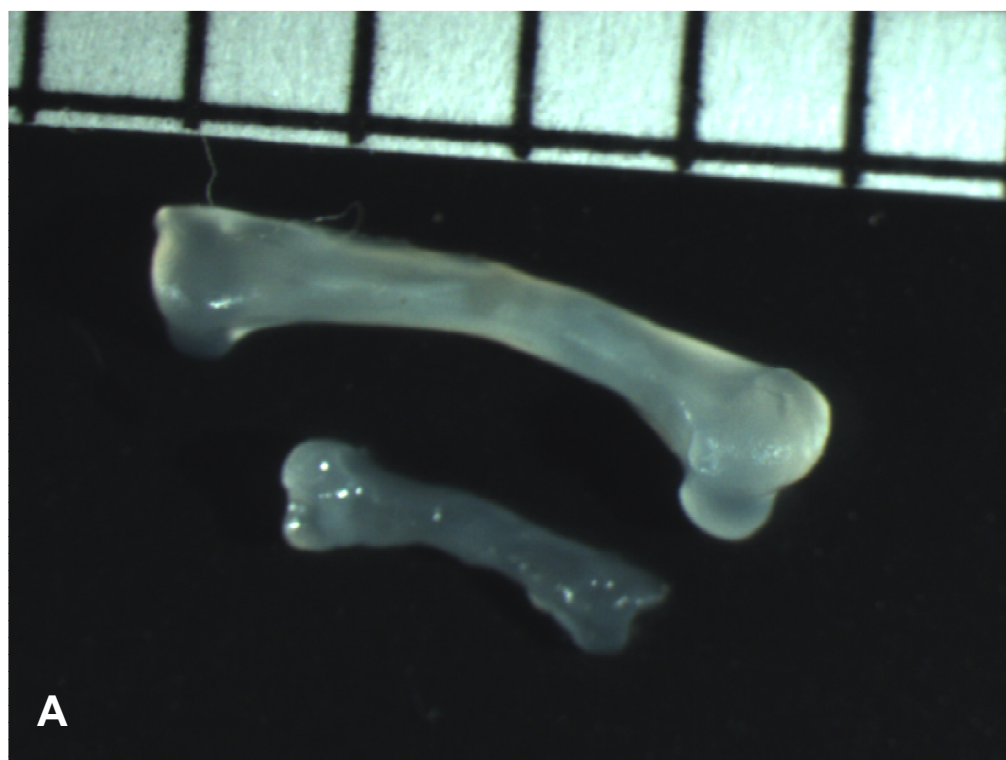


Figure 5.6: [A] Growth of a chick femur over a 10 day organotypic culture period. [B] shows the effect of damage caused by handling on the femur growth. Grid is 2 mm square

5.3.3 Critical sized defects in chick femur

The aim was to use the embryonic chick femur as a model to investigate the potential of BMP-2 loaded MPs to influence the surrounding developing tissue. MPs could be either injected directly into the femur in a minimally invasive manner, or defects could be made and the MPs used to fill them. The latter seemed a more appropriate method to research the regeneration and repair. There is no literature available on the use of chick femur defects and a number of different techniques were attempted.

5.3.3.1 Wedge defects

Before the ability of growth factor loaded MPs to affect bone repair could be tested, reproducible critical sized defects in the bone needed to be established. The first attempt was, under a stereomicroscope, to use a fine scalpel blade to cut a wedge out of the diaphysis. Two different methods were attempted, firstly, to take out and remove a completely diaphyseal wedge (Figure 5.7A) and secondly, to cut a wedge but leave some of the bone collar intact (Figure 5.7B). The reason for this was to potentially use the flap of bone collar to hold the MPs in place after administration. The difficulty in using this method as a model was the inability to cut reproducible wedges as well as the damage caused by forceps whilst handling the bone. Despite handling the bones becoming less damaging with practice, it was decided not to use a scalpel to make the defect as the size and shape could not be guaranteed from bone to bone.

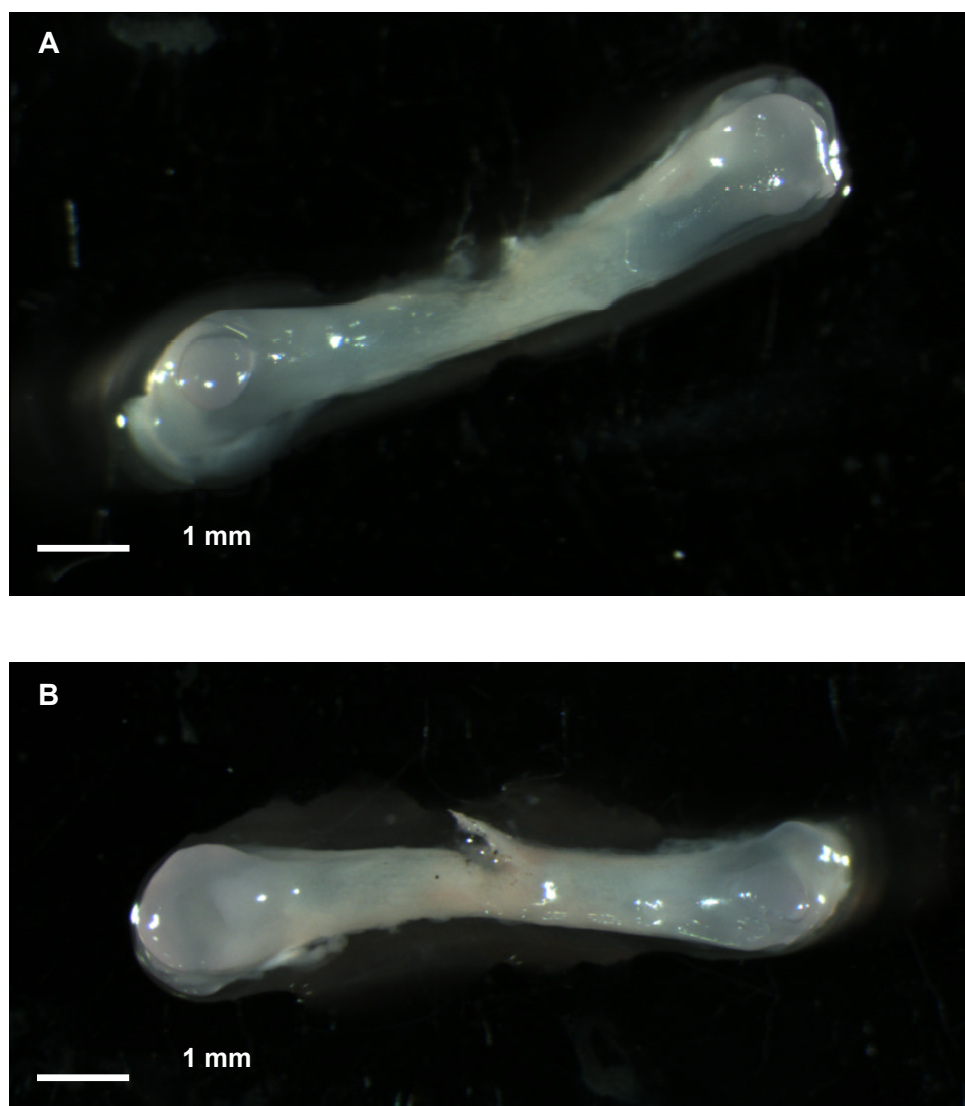


Figure 5.7 Demonstration of two different wedge defects cut using a fine scalpel blade. [A] bone collar removed. [B] bone collar partially intact.

5.3.3.2 Drill defects

The wedge defect model was not chosen for study due to the size and shape of the defect not being reproducible. Precision micron sized drills were sourced and used to manually create holes in the bones. The advantage to the drill was that the diameter of the hole would always be the same and with careful rotation of the drill, the material inside the hole could be removed. This was a very skilful process requiring dexterity to create defects without causing further damage to the bone. Unpublished work (Hassan Rashidi) showed that the chick femur could self heal defects under 200 micron in size whereas a 300 micron defect did not repair over the ten day culture period.

The 300 micron drill bit was therefore used as the standard to create the defects for use in bone repair studies. Figure 5.8 shows the drill being used on a day 11 femur. The precision of this drill meant that if required, multiple defects could be made on a single femur. Figure 5.9 shows a drilled diaphyseal defect and picro-sirius red/alcian blue staining after ten days of organotypic culture post defect of the same femur. An intact femur is shown for comparison and the staining clearly shows the extent of the ossification at this level of development. It is clear that the defect has not healed. Instead, it seems that the cells of the bone collar may have migrated into the defect to form a thin layer of bone inside sealing off the defect. This observation was not seen in all defects created during the course of this work but possible migration of cells during the creation of the defect and during tissue culture will be discussed later.

The advantage of using the drill was that defects could also be created in the epiphyses. This chondrogenic area of the bone could play a key role in the

study of rhBMP-2 release especially if the cells could be driven prematurely down an osteogenic path by the action of released rhBMP-2. The problem with creating epiphyseal defects was that the tissue is very soft and it was i) easy to cause unintentional damage and ii) difficult to see the defect once it had been created due to the tissue appearing to 'fill' back into the hole. A successful epiphyseal defect is shown in Figure 5.10. The bone was carefully blotted dry to aid visualisation of the defect. The histology shown in Figure 5.10D is not of the same bone but representative slide. Good histological sections of the epiphyseal defect were not often easy to achieve mainly due to the orientation of the bone embedded in the wax. The section shown in Figure 5.10D still appears to have some tissue in the defect but it has not stained.

The epiphysis has a number of different zones where cells are in different stages of development. Some are in a resting phase whilst some are proliferative. It was not possible to accurately predict when the defect was made what cell types were being disturbed which may have led to some of the biological variability in the model.

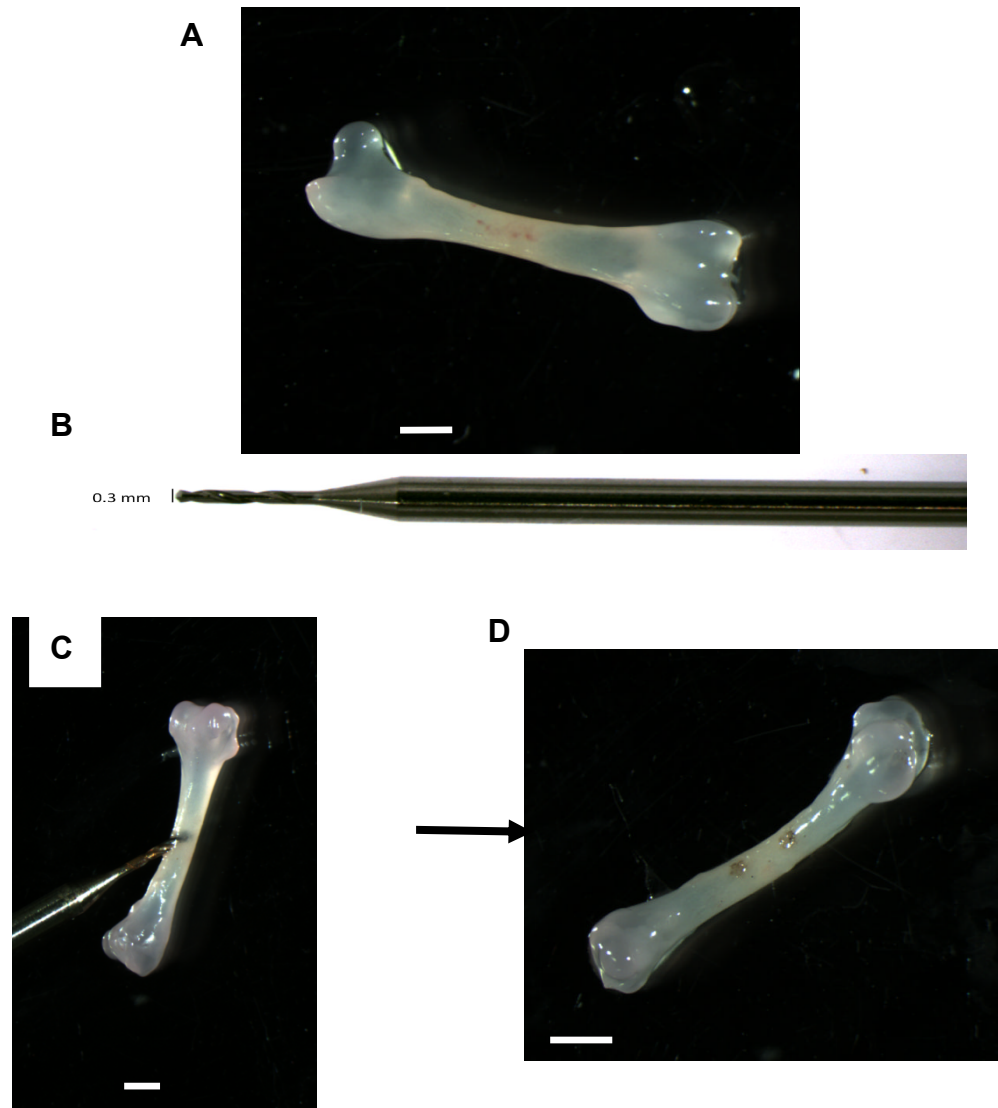


Figure 5.8: [A] shows a day 11 intact chick femur. [B] is the 300 micron drill used to create critical sized defects [C] shows the drill entering the bone [D] shows two defects made in the same bone with a small amount of ink to highlight the holes (scale bar 1 mm)

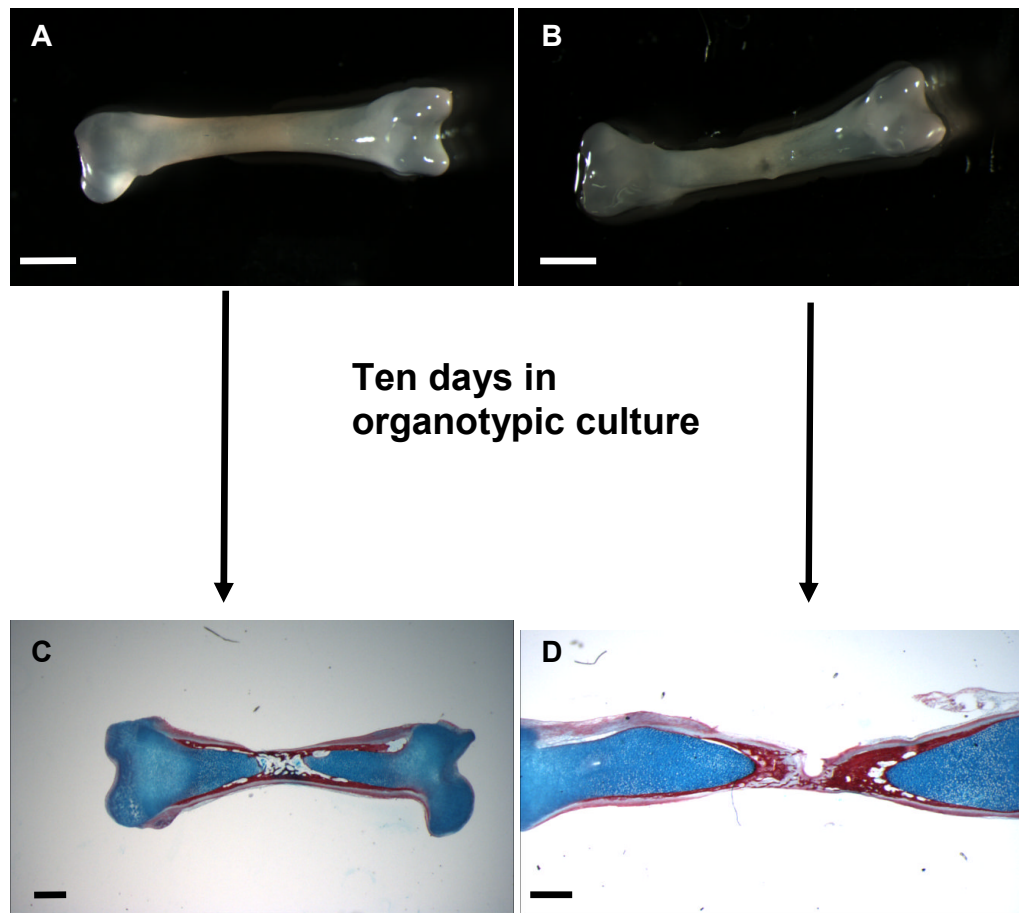


Figure 5.9: [A] An intact femur from an 11 day old chick embryo and [B] a similar femur shown with a 300 micron drill hole in the diaphysis. [C] is the intact femur after ten days of culture and stained with alcian blue/picro-sirius red staining. [D] shows the critical sized defect that has not repaired during the culture period. Scale bars 1 mm

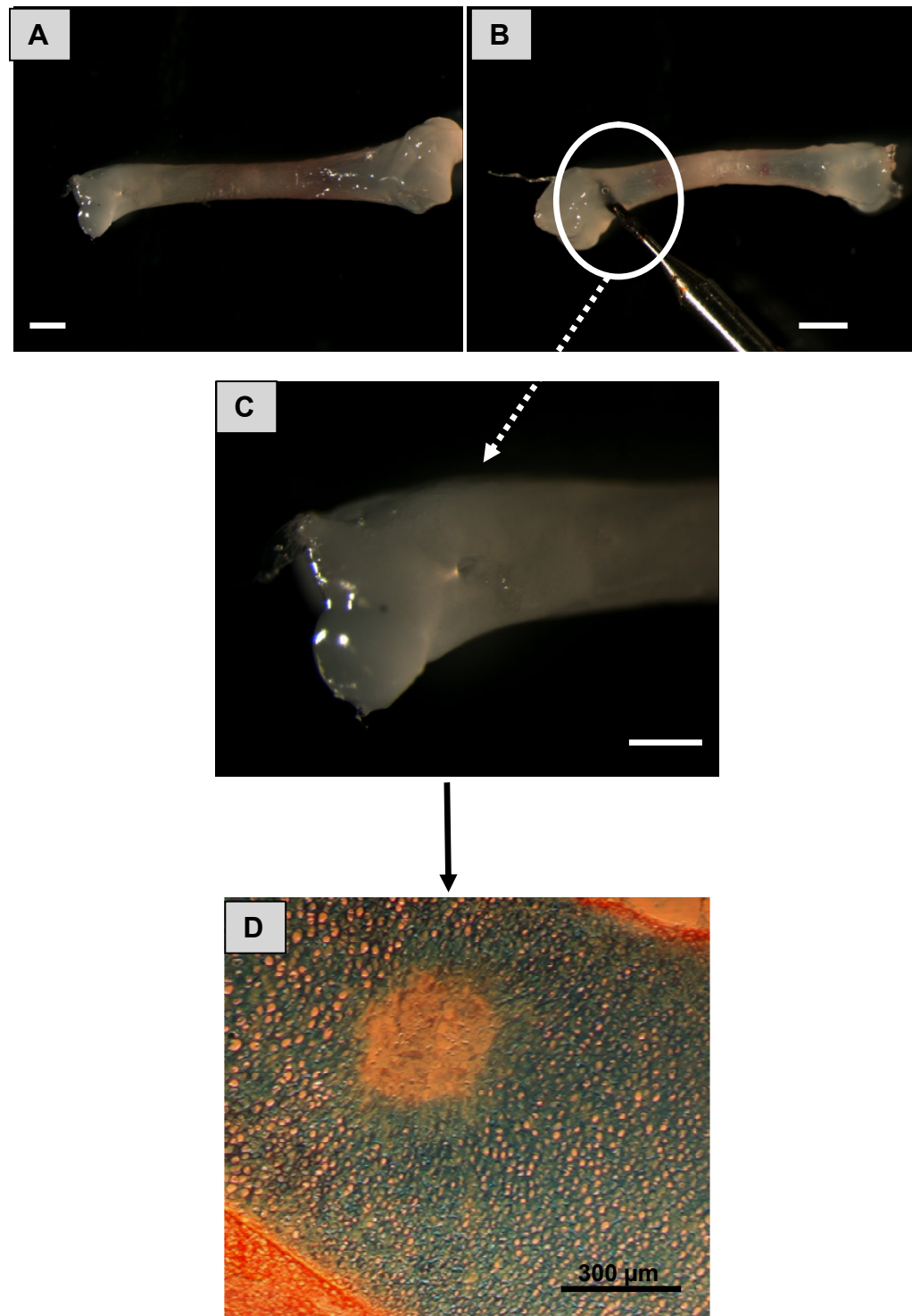


Figure 5.10: [A] An intact femur from an 11 day old chick embryo and [B] a similar femur shown with a 300 micron drill causing a defect in the epiphysis. [C] shows the defect and the cartillagenous nature of the tissue. [D] shows an epiphyseal defect after staining with alcian blue/picro-sirius red staining. Scale bars 1 mm unless otherwise stated.

5.3.3.3 Non-union defects

Fractures that do not heal over several months are described as non-union. There can be a number of causes such as excessive motion at the fracture site, invasion of muscular tissue, too much distance between the fractured ends, infection, inadequate blood supply or bone diseases. Although the drill defects mentioned earlier would go some way to modelling this, bones were cut and cultured apart to more closely model non-union.

Figure 5.11 shows that the femur has little capacity to re-grow in culture over ten days when the two ends were set at over 1 mm apart. This is confirmed by the Alcian blue/picro-sirius red staining of the sections shown in Figure 5.12. The histology confirms the clean cut across the diaphysis with no discernable growth of the bone within the diaphysis. However, at 1 mm apart there may be evidence of some growth into the gap in one bone over ten days as shown by the light images in Figure 5.11 but unfortunately, the sectioning and staining of this femur was not successful. Despite little or no growth along the diaphysis, the epiphyses of the cut bones seemed to have continued to grow normally over the culture period.

Cutting the bone further along the diaphysis where there were more likely to be proliferating cells may have provided a different result regarding grow-back, but using the diaphysis cut in the middle potentially provided a good model to model the non-union fracture. Strategies for bridging the gap between the two pieces of bone will be discussed later (Section 5.3.4.3).

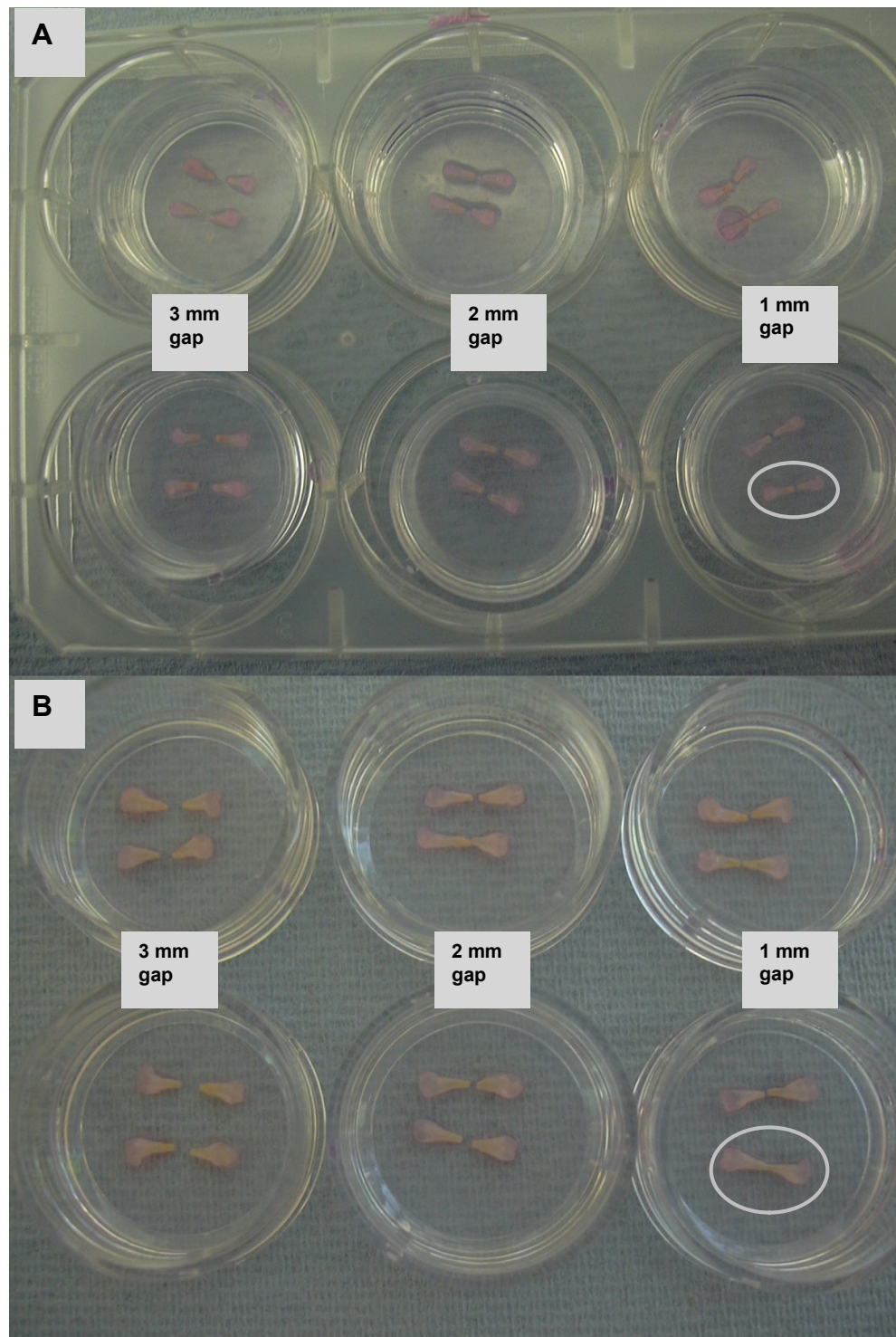


Figure 5.11: Non union defect model at [A] day 1 and [B] day 10 of organotypic culture. Bones were cleanly cut and placed on the membrane apart. The single femur highlighted in a circle shows some evidence of bone re-growth

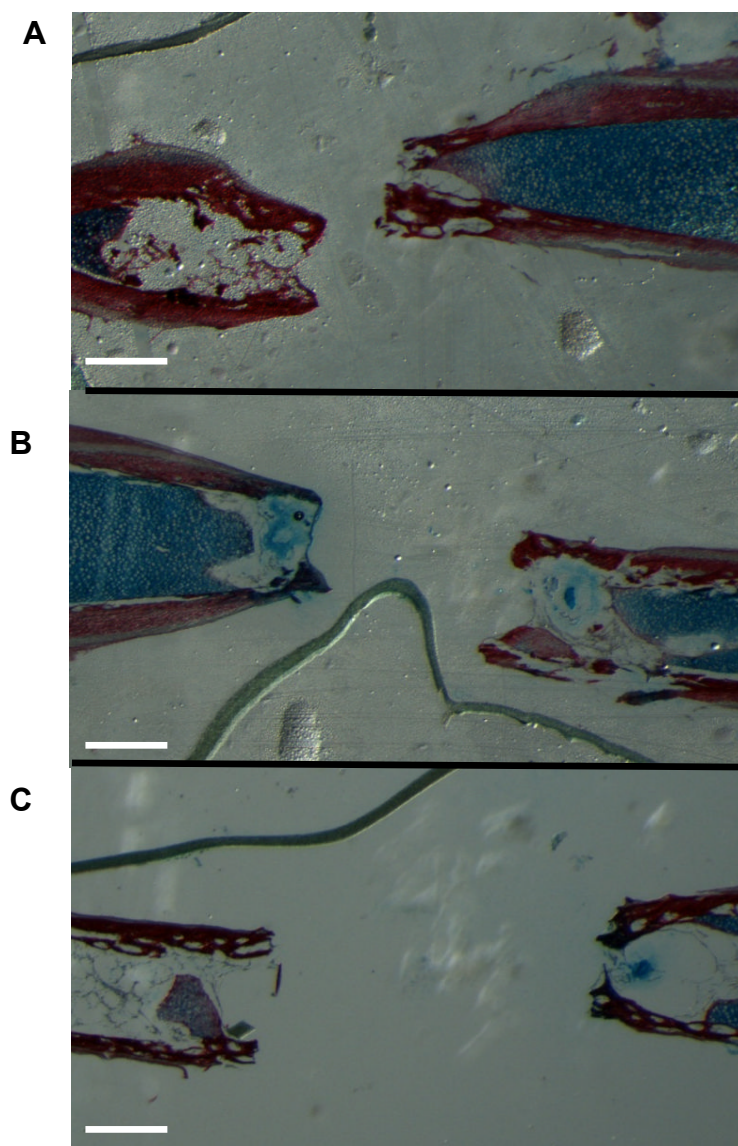


Figure 5.12. Alcian blue/picro-sirius red staining of the non union defect model after 10 days of organotypic culture showing [A] 1 mm, [B] 2 mm and [C] 3 mm defect. Scale bar 1 mm

5.3.4 Filling the defects with microparticles

Once sufficient a defect had been created, the challenge was to fill it with rhBMP-2 loaded MPs. An micro-injector system was available for use as well as microspatulas. Both methods were assessed in the performance of these studies.

5.3.4.1 Injection method

The Femtojet injector had been used in a separate project to deposit growth factor loaded MPs into the developing chick femur to cause minimal damage to the surrounding tissue. In this case, fine pulled capillaries often used in embryology and *in-vitro* fertilisation techniques, were used for injection. This injection technique was adapted by using a wider bore capillary to fill the femoral defects and non growth factor loaded PLGA MPs were used for preliminary studies.

Two problems became apparent with using the injector. The MPs had to be administrated in solution (PBS) and this was loaded by capillary action. Quite often, too few MPs were taken up into the capillary with the PBS being preferably loaded. Once sufficient MPs had been loaded (visually judged, no quantification) they were ejected into the defect. The problems were that in some cases, surface tension caused the volume injected to remain on the surface of the bone with few MPs entering the defect (Figure 5.13A) and in other cases, the injected MPs spilled out of the defect completely (Figure 5.13B). It was thought that the reason for these problems was the force of the injection and the fact that no surrounding tissue was holding the MPs in place which would not be the case if a minimally invasive injection technique was being used. Being able to successfully administer MPs into the defect,

preferably a known mass, was a key factor in this project and thus far was proving problematic.

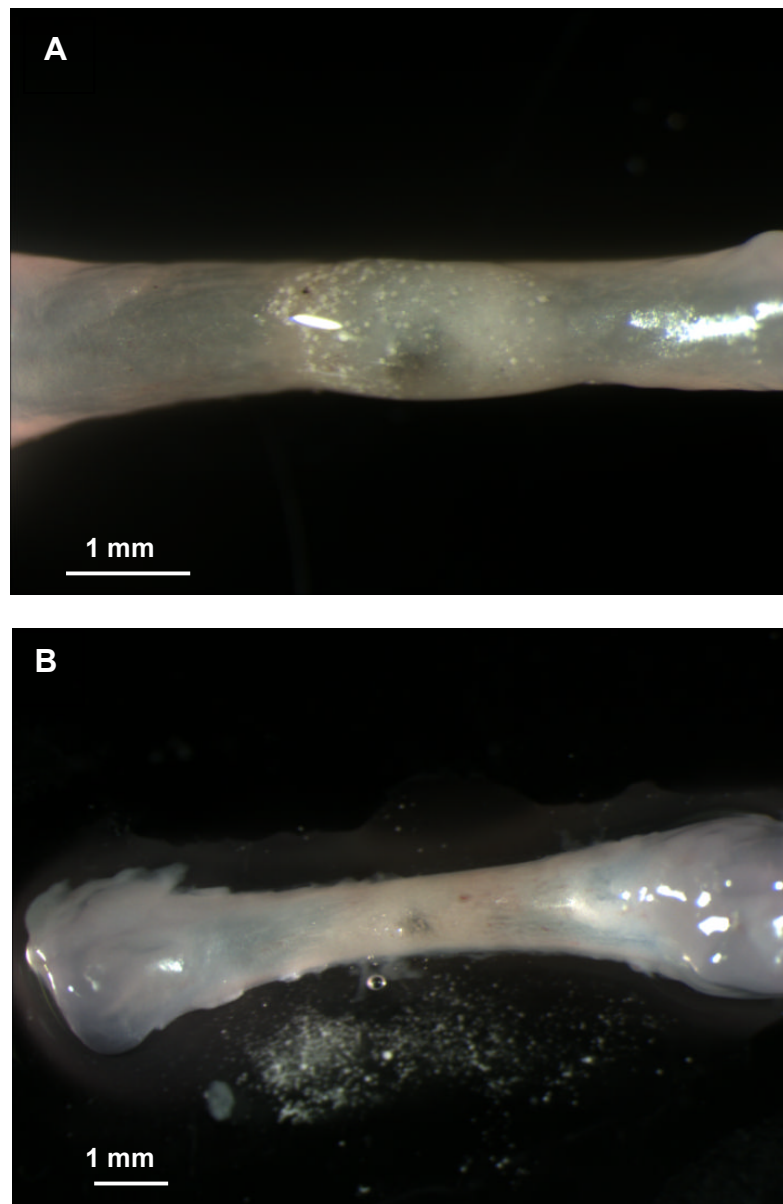


Figure 5.13 Injection of blank PLGA microparticles into day 11 diaphyseal chick femur drill defects. [A] shows that surface tension is causing the microparticles not to enter the defect and [B] shows an unsuccessful injection where the microparticles are lying next to the bone

BN 332

5.3.4.2 Microspatula method

The issues surrounding the injection method of MP administration prompted the use of microspatulas to fill the day 11 chick femoral defects. The first attempts to apply a thick paste of MPs in a small volume of PBS to diaphyseal and epiphyseal defects showed limited success. Figure 5.14A is a stereomicroscope image showing a pair of femurs after 0 and 10 days of culture with blank MPs administered by spatula. The MPs are in the defect and on the surface of the bone but not localised enough to warrant good delivery of growth factors.

To improve the administration technique, dry MPs were used. It was discovered that dry MPs would adhere to a 100 micron spatula. The bone and defect area were thoroughly dried by rolling on filter paper and the MPs on the spatula were transferred to the defect. Remaining moisture within the defect would attract the MPs into the defect and this was a much more effective way of filling the defect. Figure 5.14B shows a close-up light microscope image of MPs successfully transferred into the diaphyseal defect.

Once the methods to create and fill critical sized defects in day 11 chick embryonic femurs had been established, they could be applied to growth factor loaded MPs and any effects on bone repair established through morphology changes and histology.

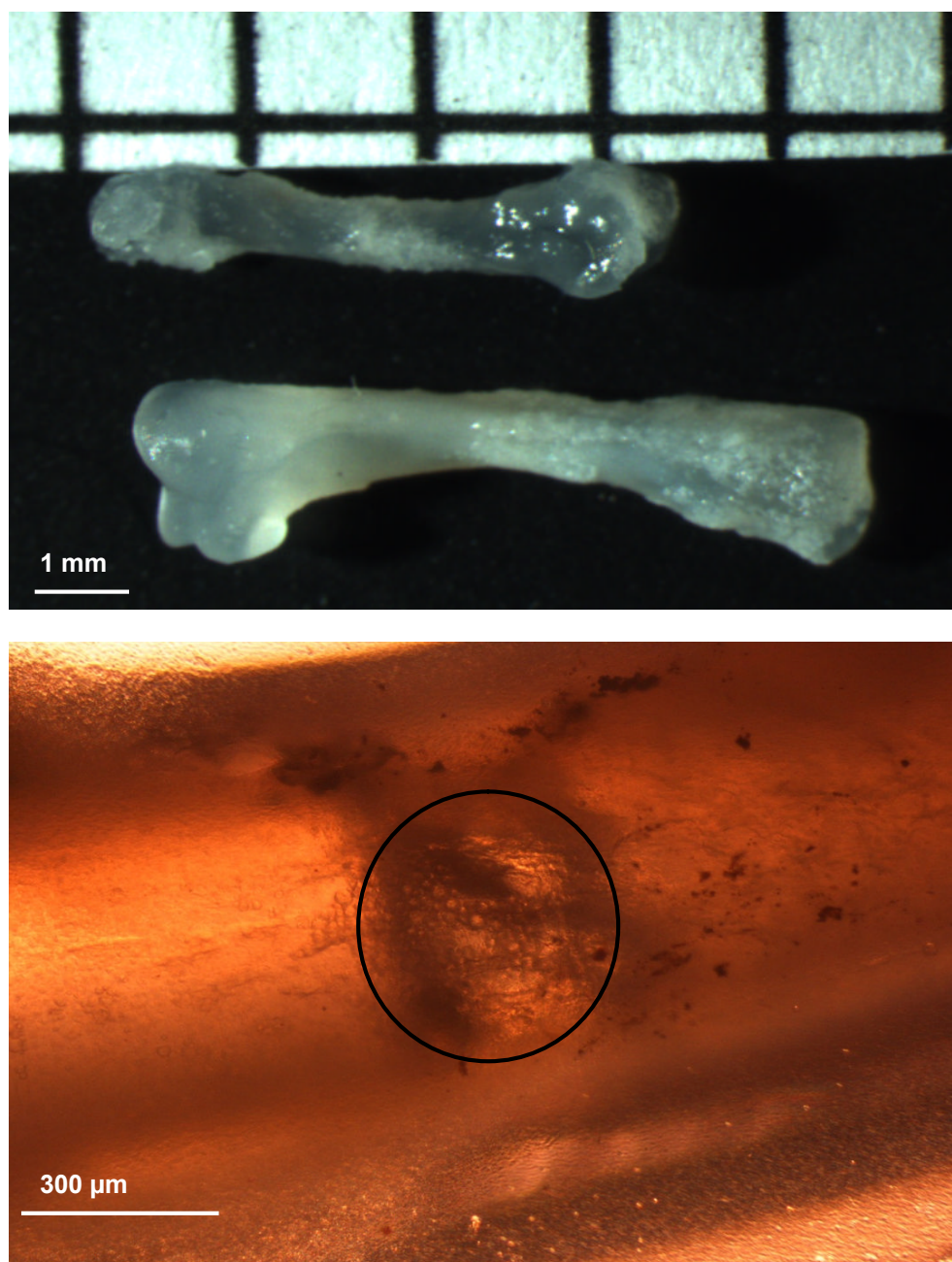


Figure 5.14 Microparticles applied to the bone defects by microspatula. [A] shows the microparticles applied as a paste to a pair of femurs. One was cultured for 10 days. Grid is 2 mm [B] shows an improved method using dry microparticles to localise them in the defect. Circle shows area of defect.

BN 332

Using hexane rather than the more commonly used xylene in the preparation of the femurs for sectioning meant that PLGA MPs in the main, could survive the tissue processing without being dissolved and therefore could be visualised within the defects after sectioning.

A good level of filling in diaphyseal defects using the microspatula was usually observed although results could be quite variable. Figure 5.15 shows multiple cross sections up through a drill defect. The images A to D depict the bottom to the top of the defect. The defect does appear to enlarge as the surface is approached. This may be due to the drill not being removed cleanly from the hole or what seems to be the case in Figure 5.15D, the section was taken very near to the bone surface (hence the very thick bone collar) and MPs were dispersed on the surface.

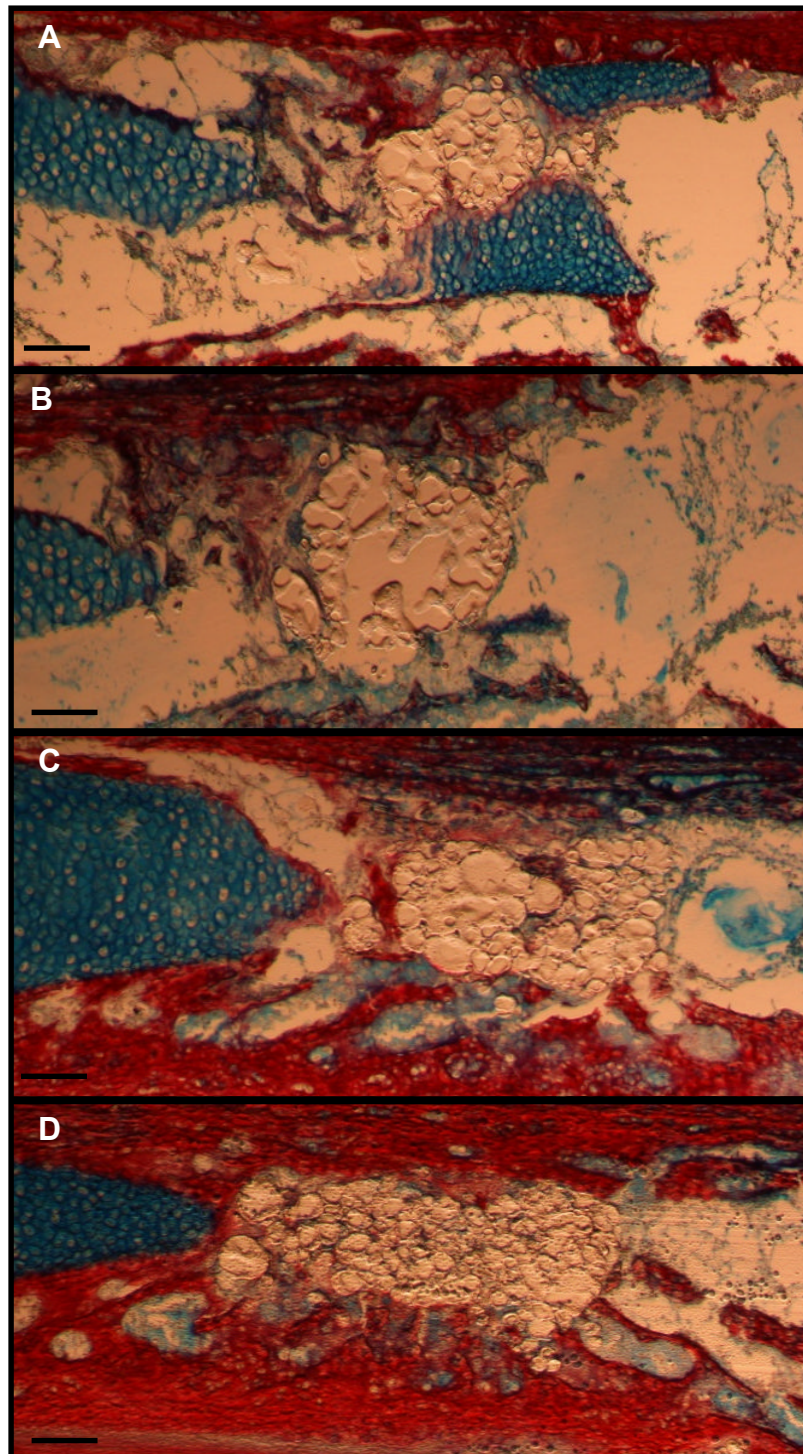


Figure 5.15 Cross sections through drill defect filled with blank PLGA microparticles using a micrspatula showing the presence of microparticle throughout the defect. [A] is the base of the defect with [B], [C] and [D] showing sections toward the surface of the defect. Scale bar 100 μm

BN 332

5.3.4.3 Filling the non-union defect

Bridging the gap in the non-union defect model is difficult to do due to there being nothing to hold the MPs in place during organotypic culture. A combination of growth factor loaded MPs with the temperature sensitive (PLGA/PEG400) MPs presented as being a solution to the problem but preliminary studies were not successful. Although work was not continued with this model in combination with temperature sensitive scaffolds, there is much scope for future work potentially with pre-formed scaffolds containing mesenchymal stem cells and growth factors made specifically with dimensions to bridge the two cut bones.

Another strategy to bridge the gap was performed by a Dr Hassan Rashidi who kindly permitted the use of some of his results. An alginate gel was prepared and seeded with immortalised human mesenchymal stem cells (MSC) (as used for rhBMP-2 detection studies in Chapter 4). The alginate was used as an inert component to hold the cells in place between the two bone pieces so that any response was due to the cells. Figure 5.16A shows the gel containing MSCs in contact with both ends of the bone despite leakage of the gel from the site. The bone was cultured on a Millicell insert for the standard 10 days and prepared for alcian blue/picrosirius red staining which is shown in Figure 5.16B.

This result showed the MSCs still in place around the ends of the bone and there appears to be a layer of bone formed at the edge of the cut on both sides of the bone. If this micrograph is compared to those in Figure 5.12 then the difference becomes clear. The cells may therefore be playing a positive role on bone growth.

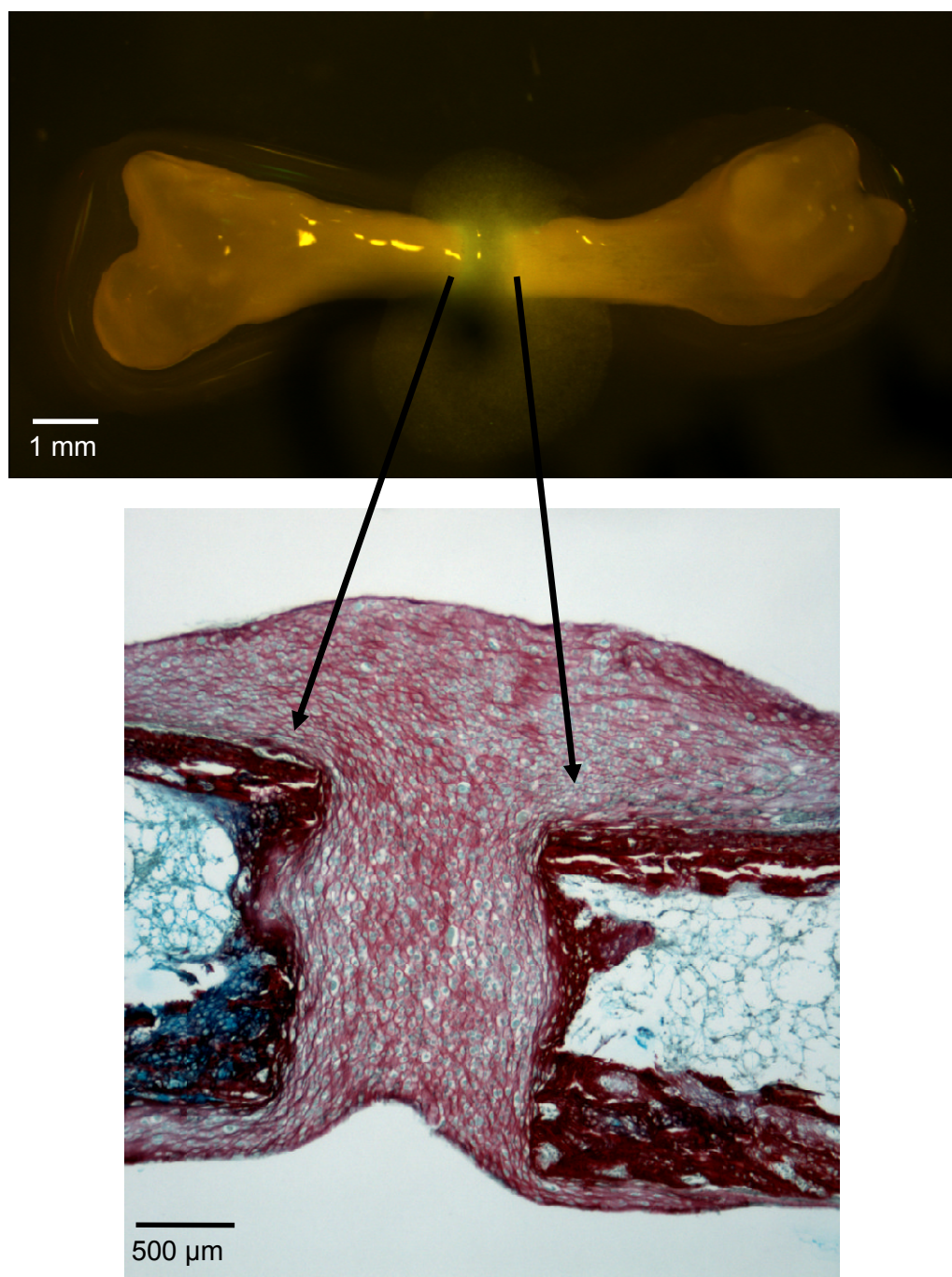


Figure 5.16 A non-union defect in a day 11 ex-ovo chick femur filled with mesenchymal stem cells seeded in alginate. [A] shows the bone immediately after administration of the cells and [B] shows the alcian blue/picrosirius red staining after ten days of culture

5.3.5 Potential pitfalls in histological analysis

Artefacts can be commonplace in histological images and as such they must always be viewed with caution and interpreted carefully. The embedding of these small bones into wax was often problematic and ensuring a level plane was difficult. The chick femurs are not a simple uniform shape, the condyles protrude at each end of the bone and the angle at which they are sectioned can give different, sometimes anomalous results. Figure 5.17 attempts to depict the issues faced with sectioning with just a simple tube shape. If identical sections are taken from identical shapes, the results can be drastically different from each other simply because of the orientation of the shapes. For the femurs often horizontal sections would make the epiphysis appear detached from the diaphysis simply because they were not on the horizontal plane. Another issue to be wary of was thickened bone collars due to near surface sectioning. It is important to take many sections from one bone, thoroughly inspect the sections and draw conclusions carefully.

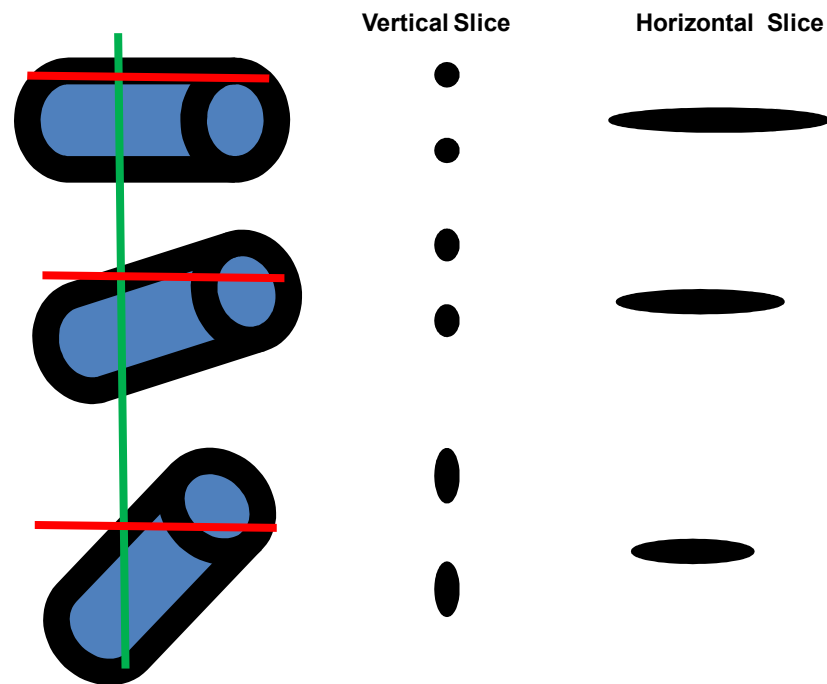


Figure 5.17 Representation showing how identical shapes can give different results due to their orientation when being sectioned in exactly the same way

5.3.6 Effect of HSA/rhBMP-2 loaded microparticles on chick femur growth and repair

After 11 days of incubation, primary ossification was well underway in the embryonic chick femur and the diaphysis had a mineralised bony structure. Once the technique was optimised, filling diaphyseal defects was relatively easy due to the hole having a structure that could support the MPs. Figure 5.18 shows both blank MPS (Figure 5.18A) and MPs loaded with HSA/rhBMP-2 (Figure 5.18B) successfully loaded into diaphyseal defects. The sections are at an approximate 90 degree different plane to the sections shown in Figure 5.17. In this case the defect is cut through vertically rather than horizontally. In both examples in Figure 5.18, the defect is clearly defined, the MPs are visible and the defect is completely filled albeit with some overspill at the bone surface. In both examples, the tissue surrounding the defect is not necrotic and indeed in some places, the MPs appear integrated with the tissue.

However, there does not appear to be any discernable effect of the rhBMP-2 released from the MPs on the tissue, the two micrographs look very similar. This is not a surprising result as although rhBMP-2 is a potent inducer of osteogenesis, the diaphysis has already undergone the ossification process. These diaphyseal studies provide proof of concept that PLGA MPs can be used to fill a critical sized defect. It may be possible to deliver MPs loaded with potent chondrogenic growth factors into these diaphyseal defects to see a response. It is more sensible to deliver rhBMP-2 MPs to the epiphyseal regions of the bone to determine an osteogenic effect

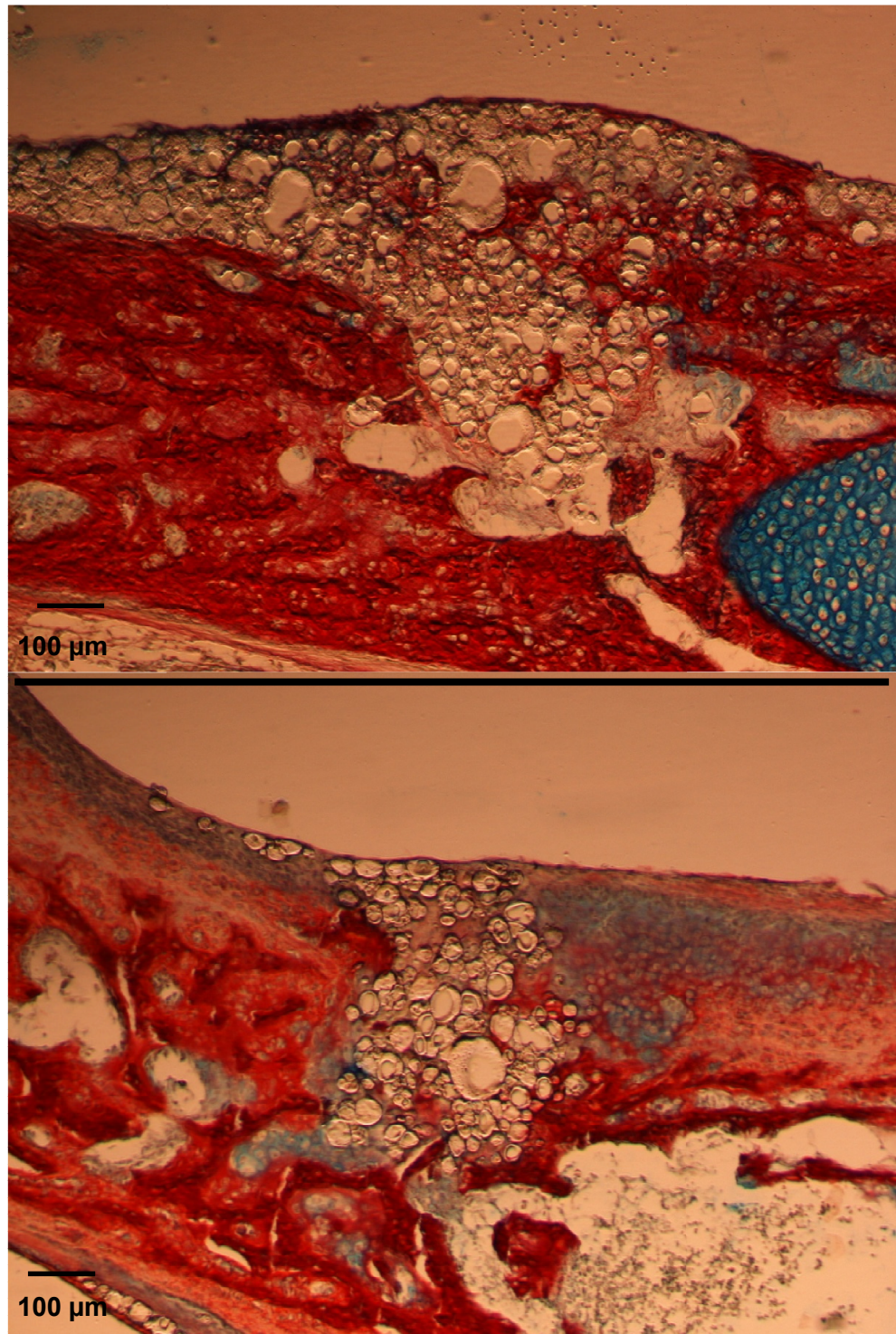


Figure 5.18: The effect of filling PLGA microparticles into a diaphyseal drill defect in a day 11 embryonic chick femur. The bones had been cultured for 10 days. [A] shows blank microparticles and [B] shows microparticles loaded with HSA/rhBMP-2 (1% loading 9.5 mg HSA/0.5 mg rhBMP-2)

Batch BN331 BN 332

Although the epiphyseal defects were more likely to show effects caused by rhBMP-2, they were more difficult to create and fill. This was due to their cartilaginous nature, making it difficult to microscopically manipulate the spatula containing the MPs into the defect without causing further damage. Figure 5.19A shows a vertical section through an epiphyseal defect loaded with blank PLGA MPs. Only a few MPs are visible (highlighted by arrows) but the outline of the defect is clear. Despite a faint red staining, around the edge of the defect, there is no apparent effect of the MPs. It is feasible that the red staining may be due to osteogenic cells from the thin bone collar being pushed into the defect by the drill. On many control slides of blank MPs, there was evidence of positive picosirius red staining (collagen) either surrounding the defect or at the base of the defect. However, the effects were generally very weak when compared to the rhBMP-2 positive MPs.

Figure 5.19B shows a vertical section through an epiphyseal defect loaded with rhBMP-2 MPs. This was the first of a few very interesting results. Despite the defect not being clearly defined, there was a distinct increase in picosirius red staining around the rhBMP-2 MPs that were clearly visible and artefacts in sectioning were ruled out. The morphology changes of the chondrocytes at the base of the defect may have been an indicator of tissue damage or more likely a response to the released rhBMP-2 as similar morphological changes can be seen in the surrounding chondrocytes in Figure 5.20.

By carrying out repeats tests on a number of femurs it became credible that the rhBMP-2 entrapped with the PLGA MPs was releasing after administration to the defect and the the released rhBMP-2 was affecting the surrounding chondrocytes encouraging them to begin to express collagen. It must be mentioned that not all femurs gave positive results but the issues mainly

surrounded problems with embedding, sectioning and visualising the defects and MPs adequately, especially after the difficulties in loading the MPs into the defects.

Figure 5.20 gave the clearest indication of these MPs affecting the surrounding tissue. The image shows a horizontal section through an epiphyseal defect and quite clearly there was an affect of the MPs on the local tissue. This was exceedingly encouraging to see the PLGA MPs re-directing the differentiation of the surrounding cells. The alcian blue/picrosirius red staining is a clear indicator of chondrogenic and osteogenic areas in the bone but for further evidence of the effect of the MPs immunostaining would be a useful tool. This will be discussed in Chapter 6 under future work.

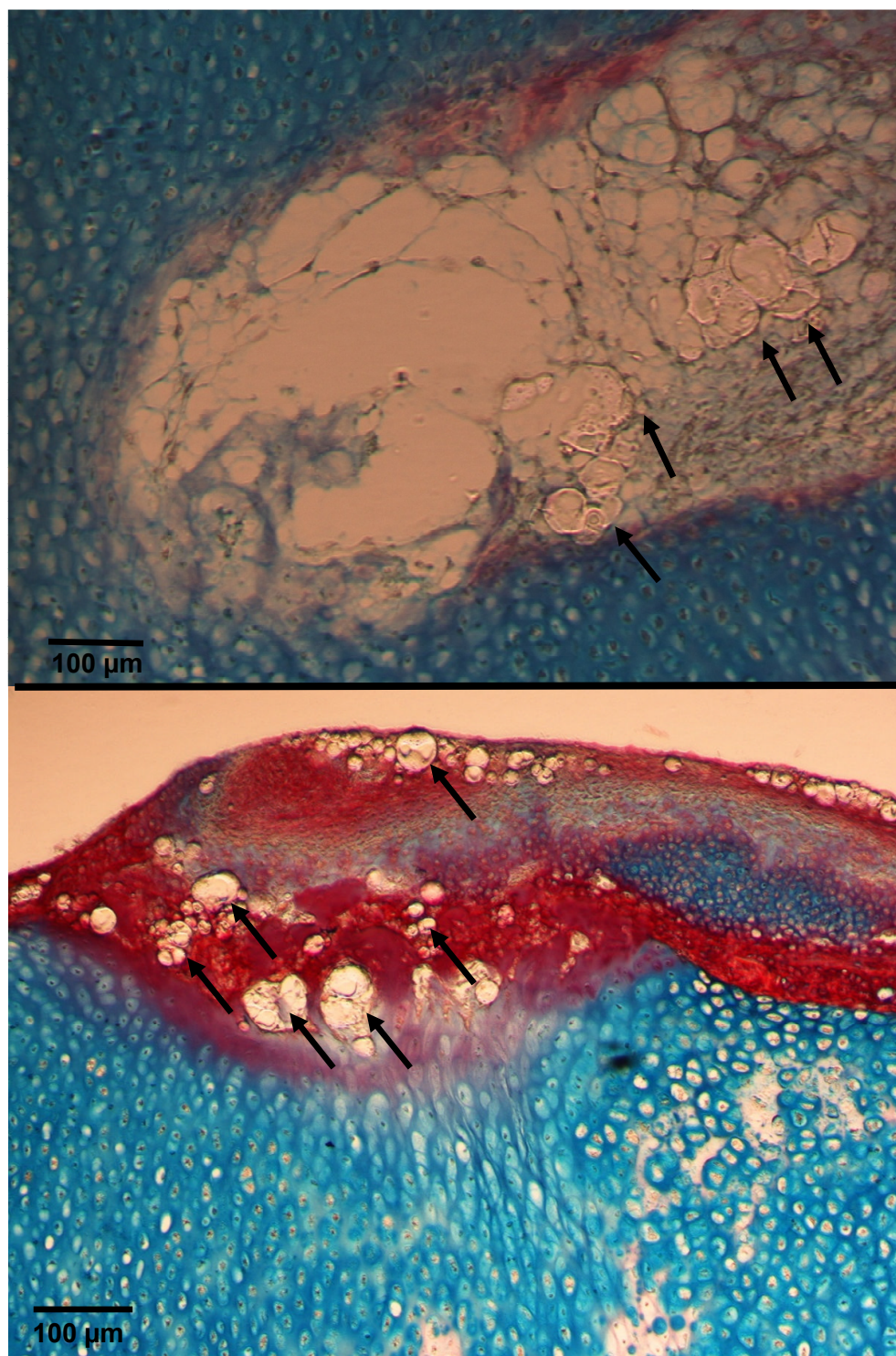


Figure 5.19: The effect of filling PLGA microparticles into an epiphyseal drill defect in a day 11 embryonic chick femur. The bones had been cultured for 10 days. [A] shows blank microparticles highlighted by arrows and [B] shows microparticles loaded with HSA/rhBMP-2 (1% loading 9.5 mg HSA/0.5 mg rhBMP-2)

BN 336 BN 337

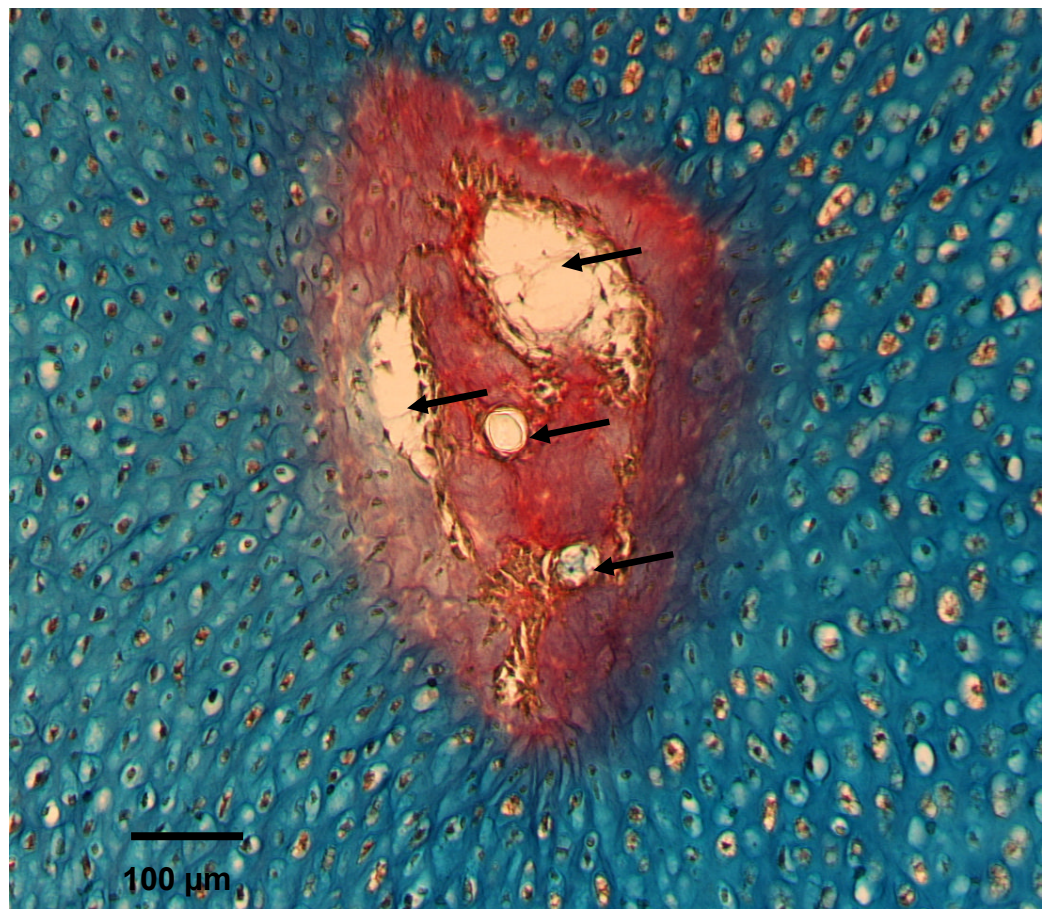


Figure 5.20 The epiphyseal region of an 11 day ex-ovo chick femur following 10 days of organotypic culture in basal media. A 300 μm drill defect was made prior to culture and filled with rhBMP-2 loaded PLGA microparticles (1% $_{(w/w)}$ total loading 9.5 mg HSA/0.5 mg rhBMP-2). Femurs were processed and stained with alcian blue (glycosaminoglycans in cartilage) and picosirius red (collagen in bone). Position of microparticles highlighted through cross section of defect are highlighted (\blacktriangleright) showing localised picosirius red staining around the microparticles.

BN 337

5.4 Conclusions

The developing chick embryo has been used as an *ex-vivo* model to investigate the effects of rhBMP-2 loaded MPs on the repair of bone. The rate of osteogenesis within the chick femur is relatively quick with the total gestational period being 21 days. Choosing the mid-point of day 11 gave femurs undergoing primary ossification and was optimal for studies with MPs. As with many *ex-vivo* biological systems, this model had issues with variability from study to study but these could be improved through training and practice to improve the level of skill required.

Defects in the bones could be reproducibly made using a micro-drill bit, but filling the defects could only be successfully achieved using micro-spatulas as micro-injection techniques proved unsuccessful. For non-union defects, the rhBMP-2 loaded MPs could be delivered in an alginate gel. However, the diffusion rate of the rhBMP-2 into alginate is unknown and work to investigate the release into the alginate would have to be performed. Preliminary work with immortalised mesenchymal stem cells showed the potential of using the alginate gel as a scaffold and there may be further potential to use the PLGA/PEG thermosensitive scaffold to bridge the gap.

Importantly, the same batches of HSA/rhBMP-2 MPs that were used in *in-vitro* assays of early osteogenesis (Chapter 4) were also used for the investigations into bone repair (BN 331 and BN 337).

The data in this Chapter showed that these MPs could be loaded into a critical sized defect and exerted an osteogenic effect on the cartilage rich areas of the bone. These results were encouraging and give confidence that these MPs could be used in other models of bone development (e.g. direct injection of

MPs into the epiphysis with minimal damage to surrounding tissue) and indeed some positive data has been produced (Rashidi, unpublished). Now the protocols for MPs production and tailoring of release profiles are in place, the future work would be to produce MPs with different growth factors and establish whether synergistic effects of growth factors on bone repair are possible. Eventually these biodegradable MPs could be candidates as bone void fillers in large animal critically sized defect studies.

Chapter 6: Summary and future direction

The work in this thesis was performed to begin to address some of the limitations currently preventing optimal performance of protein therapies, by combining tissue engineering strategies for designing biocompatible scaffolds with drug delivery strategies for localised growth factor release. The project was focussed on therapies relating to bone repair applications but could be applied to other areas of regenerative medicine.

The aim was to develop a microparticulate system to achieve localised delivery of biologically active proteins with control over their rate of release in a three dimensional structure. The ideal biomaterial needed to meet a range of requirements that included being biodegradable, osteoconductive, integrative, mechanically compatible with native bone and ideally osteoinductive. The synthetic polymer PLGA was the chosen as the biomaterial for use as it has been used extensively for research into controlled release as it can be tailored to degrade at different rates and it has a good track record for safety. The versatility of PLGA allows the fabrication of devices with a wide range of mechanical, degradation and drug release properties.

In Chapter 2, the emulsion techniques cited in the literature for microparticle manufacture were developed and improved to enable the reproducible manufacture of PLGA microparticles loaded with the model protein lysozyme. The water-in-oil-in water technique was the preferred method over the solid-in-oil-in-water technique due to the superior entrapment efficiency results achieved. The higher the entrapment efficiency meant there was less wastage of the bioactive molecule during the manufacture process leading to a commercially more cost effective product.

The use of a homogeniser with control at low speeds, meant batches of PLGA microparticles could be reproducibly made in distinct size ranges within 1 to 100 μm and so had the versatility for different potential applications. The microparticle manufacture technique was thoroughly interrogated to understand the impact of the variables within the emulsion technique on size, morphology and entrapment efficiency.

Entrapment efficiency was directly proportional to microparticle size. Values of over 50% were usually achieved for microparticles over 10 μm in size up to 90% for microparticles sized around 100 μm . Entrapment efficiency was inversely proportional to total protein loading and a 1% _(w/w) total loading was chosen as optimal. Human serum albumin was used as a bulk carrier protein to potentially protect the lysozyme from the water-oil interface and to allow the level of lysozyme to be altered within a constant total protein loading.

The degradation rate of PLGA was investigated by measuring its pH and mass loss over time as well as the long term effect on the morphology of the microparticles. The findings agreed with published work and showed that PLGA 85 15 degraded slower than PLGA 50 50 and the degradation rate was temperature sensitive.

Chapter 3 concerned controlling the rate of protein release from PLGA microparticles by the addition of a PLGA-PEG-PLGA triblock copolymer at the point of microparticle manufacture. The triblock copolymer acted as a plasticiser and changed the viscoelastic properties of PLGA by reducing the glass transition temperature which in turn affected the release rate of the entrapped protein.

The hydrophilic nature of the PLG-PEG-PLGA copolymer increased water ingress into the PLGA microparticles and increased the hydrolytic degradation, allowing the entrapped protein to be released in a gradual manner, thus overcoming the lag phase normally associated with release from PLGA delivery systems. The higher concentrations of the copolymer accelerated the protein release over and above the rate of polymer degradation leaving a three dimensional structure in place to support ongoing tissue growth. The mechanical properties of the scaffold could be improved by using thermosensitive PLGA microparticles plasticised with low molecular weight PEG which form bridging points between the microparticles that harden as the PEG leaches away.

The model protein used was lysozyme as its biological activity could be detected by its action on the bacterial cell wall of *Micrococcus lysodeikticus*. Positive lysozyme activity in the release supernatants indicated that the protein had retained its conformation throughout the manufacture of the microparticles and after subsequent release. The correlation between released lysozyme and its activity was improved when the lysozyme was directly melt blended into plasticised PLGA microparticles.

Once the optimisation assays were complete, the technology was transferred to the growth factor rhBMP-2 and a single polymer formulation (PLGA 50 50 with 10% _(w/w) triblock copolymer) and microparticle size (20-30 μm) was chosen to give a sustained release over a one month period. If these microparticles were mixed with thermosensitive PLGA/PEG microparticles, then an *in-situ* scaffold could be formed to localise the release. The formation of the scaffold, immobilised the microparticles, prevented unwanted migration and slowed the release of rhBMP-2.

Cumulative release curves based on total protein were used to predict the expected level of rhBMP-2 in the release supernatants. The expression of alkaline phosphatase in C2C12 myoblast cells was used as a tool to detect rhBMP-2 activity in the release supernatants. However, the assay was not sensitive enough to detect the rhBMP-2 in the samples.

An alternative was to co-culture C2C12 cells directly with HSA/rhBMP-2 loaded microparticles and detect the effect of released rhBMP2 on the morphology and ALP expression of the cells. The response was directly proportional to microparticle mass. In addition, the response could still be detected by microparticles that had pre-released a proportion of rhBMP-2 prior to testing against C2C12 cells. This showed that the release of active rhBMP-2 was sustained for over 12 days. The same rhBMP-2 loaded microparticles also caused deposition of calcium by murine primary calvarial cells after 21 days of culture as determined by von Kossa staining. These results gave confidence that the released rhBMP-2 had retained its structure and remained active after release from the microparticles.

Finally, the rhBMP-2 loaded microparticles were used in an *ex-vivo* study of bone repair using the chick embryonic femur as the model. The femurs were dissected at day 11 of gestation and grown organotypically for 10 days *in-vitro*. Once normal growth was established, defects were made in the bones and filled with rhBMP-2 loaded microparticles. The effect of the microparticles was determined by histological analysis. The microparticles caused the chondrogenic cells of the epiphysis to stain positive for collagen which was an indication that the cells were being driven locally through ossification and that the microparticles were having a biological effect on the tissue.

The work presented in this thesis has laid down the technology for further research into the effect of a range of different growth factors. The immediate future work to confirm the results of the histological staining would be to perform immunostaining on the sections for collagen I. *In-situ* hybridisation techniques could be performed to determine the success of the cell signalling and gene transcription within the cells.

Different polymer formulations could be selected to manufacture microparticles with different release characteristics for delivery of growth factors with different kinetics. A similar progression of research could be performed for each key growth factor until a specially formulated 'cocktail' of microparticles could be delivered in a large animal critical sized femoral defect model for optimal tissue repair. The addition of thermosensitive microparticles would localise the microparticles and give mechanical support to the structure.

Sterilisation of the material is an important factor in the development of a new medical device. There are a number of sterilisation techniques including gamma, electron beam and ultraviolet irradiation as well as ethylene oxide treatment and these may affect the material especially with regard to chain scission and a reduction in molecular weight. Studies to understand the change in material characteristics and effect on release profiles would need to be performed post sterilisation prior to the material entering *in-vivo* studies.

The techniques developed during the course of work for this thesis would enable the fabrication of growth factor loaded microparticles that could be applied to a range of regenerative medicine applications and are an exciting tool to have in the Tissue Engineer's 'tool box'.

Chapter 7: References

- AKIZUKI, S., TAKIZAWA, T, HORIUCHI, H. 2003. Fixation of a hydroxyapatite-tricalcium phosphate-coated cementless knee prosthesis. *The journal of bone and joint surgery*, 85, 1123-1127.
- AL-AZZAM, W., PASTRANA, EA & GRIEBENOW, K 2002. Co-lyophilization of bovine serum albumin (BSA) with poly(ethyleneglycol) improves efficiency of BSA encapsulation and stability in polyester microspheres by a solid-in-oil-in-oil technique. *Biotechnology letters*, 24, 1367-1374.
- ALLISON, S. 2008a. Analysis of initial burst in PLGA microparticles. *Expert opinion drug delivery*, 5, 615-28.
- ALLISON, S. 2008b. Effect of structural relaxation on the preparation and drug release behavior of poly(lactic-co-glycolic)acid microparticle drug delivery systems. *Journal of Pharmaceutical Sciences*, 97, 2022-35.
- ANDERSON, J., SHIVE, MS. 1997. Biodegradation and biocompatibility of PLA and PLGA microspheres. . *Advanced drug delivery reviews*, 28, 5-24.
- ANGLE, S., SENA, K,SUMNER, DR, VIRKUS, WW, VIRDI, AS. 2012. Healing of rat femoral segmental defect with bone morphogenetic protein-2: a dose response study. *Journal musculoskeletal neuronal interactions*, 12, 28-37.
- ARRINGTON , E., SMITH, WJ, CHAMBERS HC, BUCKNELL, AL, DAVINO NA 1996. Complications of iliac crest bone harvesting. *Clinical orthopaedic and related research*, 329, 300-309.
- ASLAN, M., SIMSEK, G, DAYI, E. 2006. The effect of hyaluronic acid-supplemented bone graft in bone healing: experimental study in rabbits. *Journal of biomaterial applications*, 20, 209-20.
- ASO, Y., YOSHIOKA, S,LI WAN PO, A, TERAQ,T 1994. Effect of temperature on mechanisms of drug release and matrix degradation of poly (D,L-lactide) microspheres. *Journal of controlled release*, 31, 33-39.
- AUBERT-POUESSEL, A., BIBBY, DC, VENIER-JULIENNE, MCL, HINDRE, F, BENOIT, JP. 2002. A novel in vitro delivery system for assessing the biological integrity of protein upon release from PLGA microspheres. *Pharmaceutical research*, 19, 1046-1051.
- BAJADA, S., HARRISON, PE, ASHTON, BA, CASSAR-PULLICINO, VN, ASHAMMAKHI, N RICHARDSON, JB 2007. Succesful treatment of refractory tibial nonunion using calcium sulphate and bone marrow stromal cell implantation. *Journal of bone and joint surgery*, 89-B, 1382-6.
- BALMAYOR, E., FEICHTINGER, GA, AZEVEDO, HS, VAN GRIENSVEN, M, REIS, RL. 2009. Starch-poly-epsilon-caprolactone microparticles reduce the needed amount of BMP-2. *Clinical orthopaedic and related research*, 467, 3138-48
- BANCROFT, J., STEVENS, A 1992. Theory and practice of histological techniques 3rd Edition. *Churchill Livingstone*, Edinburgh, London Melbourne and New York.
- BATYCKY, R., HANES, J, LANGER, R, EDWARDS, DA. 1996. A theoretical model of erosion and macromolecular drug release from biodegrading microspheres. *Journal of pharmaceutical Sciences*, 86, 1464-1477.
- BEHREND, O., AX, K, SCHUBERT, H. 2000. Influence of continuous phase viscosity on emulsification by ultrasound. *Ultrasonics sonochemistry*, 7, 77-85.

- BELLUCCI, D., S OLA, A, CANNILLO, V. 2011. A Revised Replication Method for Bioceramic Scaffolds. *Bioceramics development and applications*, 1, 1-8.
- BESSA, P., CASAL, M, REIS, RL. 2008. Bone morphogenetic proteins in tissue engineering: the road from laboratory to clinic, part II (BMP delivery). *Journal of tissue engineering and regenerative medicine*, 2-3, 81-96.
- BHAT, S., KUMAR, A. 2012. Cell proliferation on three-dimensional chitosan-agarose-gelatin cryogel scaffolds for tissue engineering applications. *Journal of biosciences and bioengineering*, 114, 663-70.
- BHATT, Y., SHAH, D. 2012. Influence of additives on fabrication and release from protein loaded PLGA microparticles. *Journal of chemical and pharmaceutical research*, 4, 1708-1715.
- BIBLE, E., CHAU, DY, ALEXANDER, MR, PRICE, J, SHAKESHEFF, KM, MODO, M. 2009. Attachment of stem cells to scaffold particles for intra-cerebral transplantation. *Nature protocols*, 4, 1440-53.
- BIRNBAUM, D., KOSMALA, JD, KOSMALA JD, HENTHORN, DB, BRANNON-PEPPAS, L. 2000. Controlled release of beta-estradiol from PLGA microparticles: the effect of organic phase solvent on encapsulation and release. *Journal of controlled release*, 65, 375-387.
- BLACKWOOD, K., BOCK, N, DARGAVILLE, TR, WOODRUFF, MA. 2012. Scaffolds for growth factor delivery as applied to bone tissue engineering. *International journal of polymer science*, 2012, 1-25.
- BODEN, S. 2005. The ABCs of BMPs. *Orthop Nurs*, 24, 49-52.
- BOERCKEL, J., KOLAMBKAR, YM, DUPONT, KM, UHRIG, BA, PHELPS, EA, STEVENS, HY, GARCIA, AJ, GULDBERG, RE. 2011. Effects of protein dose and delivery system on BMP-mediated bone regeneration. *Biomaterials*, 32, 5241-51.
- BORNEMANN, R., KOCH, E. M, WOLLNY, M. AND PFLUGMACHER, R. 2013. Treatment options for vertebral fractures an overview of different philosophies and techniques for vertebral augmentation. *European journal of orthopaedic surgery and traumatology*, 16.
- BOSTROM, M. 1998. Expression of bone morphogenetic proteins in fracture healing. *Clinical orthopaedic and related research*, 355 sup, s116-23.
- BRAUN, C. 1992. Autogenously vascularised bone allografts. Experimental model of a new bone-muscle composite graft. *Archives of orthopaedic and trauma surgery*, 111, 5.
- BROOKES, M., MAY, KU. 1972. The influence of temperature on bone growth in the chick. *Journal of Anatomy*, 111, 351-363.
- BUDHIAN, A., SIEGEL, SJ, WINEY, KI. 2008. Controlling the in vitro release profiles for a system of haloperidol-loaded PLGA nanoparticles. *International journal of pharmaceuticals*, 346, 151-9.
- BUMA, P., SCHREURS, W, VERDONSCHOT, N. 2004. Skeletal tissue engineering—from in vitro studies to large animal models. *Biomaterials*, 25, 1487-1495.
- BURDAN, F., SZUMILO, J, KOROBOWICZ, A, FAROOQUEE, R, PATEL, S, ANKIT, DAVE, A, SZUMILO, M, SOLECKI, M, KLEPACZ, R, DUDKA, J. 2009. Morphology and physiology of the epiphyseal growth plate. *Folia Histochemica and cytobiologica*, 47, 5-16.
- BURGE, R., DAWSON-HUGHES, B, SOLOMON, DH, WONG, JB, KING, A, TOTESON, A. 2007. Incidence and economic burden of osteoporosis related fractures in the United States, 2005-2025. *Journal of bone and mineral research*, 22, 465-475.
- BUTSCHER, A. B., M, ROTH, C, ERNSTBERGER, A, HEUBERGER, R, DOEBELIN, N VON ROHR, P. R, MULLER, R. 2012. Printability of calcium phosphate powders for three-dimensional printing of tissue engineering scaffolds. *Acta Biomateriala*, 8, 373-85.
- CAHILL, K., CHI, JH, DAY, A, CLAUS, EB. 2009. Prevalence, complications, and hospital charges associated with use of bone-morphogenetic

- proteins in spinal fusion procedures. *Journal of the American medical association*, 302, 58-66.
- CANCEDDA, R., CASTAGNOLA, P, CANCEDDA, FD, DOZIN, B, QUARTO, R. 2000. Developmental control of chondrogenesis and osteogenesis. *International journal of developmental biology*, 44, 707-714.
- CAPLAN, A., SYFTESTAD, G, OSDOBY, P. 1983. The development of embryonic bone and cartilage in tissue culture. *Clinical orthopaedics and related research*, 174, 243-63.
- CARRAGEE, E., HURWITZ, EL, WEINER, BK. 2011. A critical review of recombinant human bone morphogenetic protein-2 trials in spinal surgery: emerging safety concerns and lessons learned. *Spine*, 11, 471-91.
- CASTELLANOS, L., CARRASQUILLO, KG, LOPEZ, JD, ALVAREZ, M, GRIEBENOW, K. 2001. Encapsulation of bovine serum albumin in poly(lactide-co-glycolide) microspheres by the solid-in-oil-in-water technique. *Journal of pharmacy and pharmacology*, 53, 167-78.
- CHEN, S., PIEPER, R, WEBSTER, DC, SINGH, J. 2005. Triblock copolymers: synthesis, characterization, and delivery of a model protein. *International journal of pharmaceuticals*, 288, 207-18.
- CHISTIYAKOV, D. 2012. Liver regenerative medicine: advances and challenges. *Cells, tissues, organs*, 196, 291-312.
- CHUN, K., YOO, HS, YOON, JJ, PARK, TG. 2004. Biodegradable PLGA microcarriers for injectable delivery of chondrocytes: effect of surface modification on cell attachment and function. *Biotechnology progress*, 20, 1797-1801.
- CIRILLO, V., GUARINO, V, AMBROSIO, L. 2012. Design of bioactive electrospun scaffolds for bone tissue engineering. *Journal of applied biomaterials and functional materials*, 10, 223-228.
- CLEEK, R., TING, K, ESKIN, G, MIKOS, A 1997. Microparticles of poly(DL-lactic-co-glycolic acid)/poly(ethylene glycol) blends for controlled drug delivery. *Journal of controlled release*, 48.
- COHEN, S., YOSHIOKA, T, LUCARELLI, M, HWANG, LH, LANGER, R. 1991. Controlled delivery systems for proteins based on poly(lactic/glycolic acid) microspheres. *Pharmaceutical Research*, 8, 13-20.
- COLLINS, M., BASSETT, BS, BO WEN, H, GERVAIS, C, LOMICKA, M, PAPANICOLAOU S. 2012. Trabecular metal dental implants: overview of design and developmental research. *Copyright Zimmer Dental Inc.*
- COWAN, C., AGHALOO, T, CHOU, YF, WALDER, B, ZHANG, X, SOO, C, TING, K, WU, B. 2007. MicroCT evaluation of three-dimensional mineralization in response to BMP-2 doses in vitro and in critical sized rat calvarial defects. *Tissue engineering* 13, 501-12.
- COX, H., DHILLON, A, MCLAREN JS, RAHMAN, CV, QUIRK RA, SHAKESHEFF KM In writing. A novel injectable scaffold for bone repair applications.
- CROCKETT, J., ROGERS, MJ, COXON, FP, HOCKING, LJ, HELFRICH, MH. 2011. Bone remodelling at a glance. *Journal of cell science*, 124, 991-998.
- CUI, X., ZHAO, D, ZHANG, B, GAO, Y. 2009. Osteogenesis mechanism of chitosan-coated calcium sulfate pellets on the restoration of segmental bone defects. *Journal of craniomaxillofacial surgery*, 20, 1445-50.
- DANIEL, M., CHESSMAN, R, AL-ZAHID, S, RICHARDS, B, RAHMAN, C, ASHRAF, W, MCLAREN, J, COX, H, QUTACHI, O, FORTNUM, H, FERGIE, N, SHAKESHEFF, K, BIRCHALL, JP, BAYSTON, RR. 2012. Biofilm eradication with biodegradable modified-release antibiotic pellets: a potential treatment for glue ear. *Archives of otolaryngology: head and neck Surgery*, 138, 942=9.

- DANILCHENKO, S., KALINKEVICH OV, POGORELOV, MV, KALINKEVICH, AN, SKLYAR, AM, KALINICHENKO, TG, ILYASHENKO, VY, STARIKOV, VV, BUMEYSTER, V, SIKORA, VZ, SUKHODUB, LF. 2011. Characterization and in vivo evaluation of chitosan-hydroxyapatite bone scaffolds made by one step coprecipitation method. *Journal Biomedical materials research part A* 96, 639-47.
- DAWES, G., FRATILA-APACHITEI, LE, MULIA, K, APACHITEI, I, WITKAMP, GJ, DUSZCZYK, J. 2009. Size effect of PLGA spheres on drug loading efficiency and release profiles. *Journal of materials science: Materials in medicine*, 20, 1089-94.
- DAWES, G., FRATILA-APACHITEI, LE, NECULA, BS, APACHITEI, I, WHITCAMP, GJ, DUSZCZYK, J 2010. Release of PLGA-encapsulated dexamethasone from microsphere loaded porous surfaces. *Journal of materials science: Materials in Medicine*, 21, 215-21.
- DAWSON, J., OREFFO, RO. 2008. Bridging the regeneration gap: stem cells, biomaterials and clinical translation in bone tissue engineering. *Archives of biochemistry and biophysics*, 473, 124-31.
- DE BIASE, P., CAPANNA, R. 2005. Clinical applications of BMPs. *Injury*, 36, S43-6.
- DECLERCQ, H., VERBEECK, RM, DE RIDDER, LI, SCHACHT, EH, CORNELISSEN, MJ. 2005. Calcification as an indicator of osteoinductive capacity of biomaterials in osteoblastic cell cultures. *Biomaterials*, 26, 4964-74.
- DEMERS, C., HAMDY, CR, CORSI, K, CHELLAT, F, TABRIZIAN, M YAHIA, L. 2002. Natural coral exoskeleton as a bone graft substitute: a review. *Biomedical materials and engineering*, 12, 15-35.
- DENG, M., NAIR, LS, NUKAVARAPU, SP, JIANG, T, KANNER, W.A, LI, X, KUMBAR, SG, WEIKEL, AL, KROGMAN, NR, ALLCOCK, HR, LAURENCIN, CT. 2010. Dipeptide-based polyphosphazene and polyester blends for bone tissue engineering. *Biomaterials*, 31, 4898-908.
- DEVINE, J., DETTORI, JR, FRANCE, JC, BRODT, E, MCGUIRE, RA. 2012. The use of rhBMP in spine surgery: is there a cancer risk? *Evidence based spine care j*, 3, 35-41.
- DEVIRIM, B., BOZKIR, A, CANEFE, K 2011. Preparation and evaluation of PLGA microparticles as carrier for the pulmonary delivery of rhIL-2 : I. Effects of some formulation parameters on microparticle characteristics. *Journal of Microencapsulation*, 28, 582-94.
- DHAKAR, R., MAURYA, SD, SAGAR, BPS, BHAGAT, S, PRAJAPATI, SK, JAIN, CP 2010. Variables influencing the drug entrapment efficiency of microspheres: A pharmaceutical review. *Der Pharmacia Lettre*, 2, 102-116.
- DHILLON, A., SCHNEIDER, P, KUHN, G, REINWALD, Y, WHITE, L. J, LEVCHUK, A, ROSE, F. R, MULLER, R, SHAKESHEFF, KM, RAHMAN, CV. 2011. Analysis of sintered polymer scaffolds using concomitant synchrotron computed tomography and in situ mechanical testing. *J Materials Science: Materials in medicine*, 22, 2599-605.
- DI MARTINO, A., SITTINGER, M, RISBUD, MV. 2005. Chitosan: a versatile biopolymer for orthopaedic tissue-engineering. *Biomaterials*, 26, 5983-90.
- DING, S., SHIE, MY, WEI, CK. 2011. In vitro physicochemical properties, osteogenic activity, and immunocompatibility of calcium silicate-gelatin bone grafts for load-bearing applications. *ACS Applied material interfaces*, 10, 4142-53.
- DIWAN, M., PARK, TG. 2001. Pegylation enhances protein stability during encapsulation in PLGA microspheres. *Journal of controlled release*, 73, 233-244.

- EL HAJ, A., CARTMELL, SH. 2010. Bioreactors for bone tissue engineering. *Proceedings of the institute of mechanical engineers H*, 224, 1523-32.
- EVEN, J., ESKANDER, M. AND KANG, J. 2012. Bone morphogenetic protein in spine surgery: current and future uses. *Journal of the American academy of orthopaedic surgeons*, 20, 547-52.
- FLINT, A. 2007. A textbook of human physiology Version 2.
- FRIESS, W., SCHLAPP, M 2002. Release mechanisms from gentamicin loaded poly(lactic-co-glycolic acid) (PLGA) microparticles. *Journal of pharmaceutical sciences*, 91, 845-855.
- FU, K., HARRELL, R, ZINSKI, K, UM, C, JAKLENEC, A, FRAZIER, J, LOTAN, N, BURKE, P, KLIBANOV, AM, LANGER, R. 2003. A potential approach for decreasing the burst effect of protein from PLGA microspheres. *Journal of pharmaceutical Sciences*, 92, 1582-91.
- FU, K., KLIBANOV, AM, LANGER, R. 2000. Protein stability in controlled-release systems. *Nature Biotechnology*, 18, 24-25.
- GAGLIARDI, R., CESCUT, A, GAMBOZ, C, RUGOLO, F. 1986. Bacterial lysis by lysozyme. *Boll Ist seiroter milan* 65, 112-7.
- GALESKA, I., KIM, TK, PATIL, SD, BHARDWAJ, U, CHATTOPADHYAY, D, PAPANIMITRAKOPOULOS, F, BURGESS, DJ. 2005. Controlled release of dexamethasone from PLGA microspheres embedded within polyacid-containing PVA hydrogels. *The academy of pharmaceutical sciences Journal*, 7, 22.
- GHAHREMANKHANI, A., DORKOOSH, F, DINARVAND, R 2007. PLGA-PEG-PLGA tri-block copolymers as an in-situ gel forming system for calcitonin delivery. *Polymer bulletin*, 59, 637-646.
- GHALANBOR, Z., KORBER, M, BODMEIER, R. 2010. Improved lysozyme stability and release properties of poly(lactide-co-glycolide) implants prepared by hot-melt extrusion. *Pharmaceutical research*, 27, 371-9.
- GITEAU, A., VENIER-JULIENNE, MC, AUBERT-POUESSEL, A, BENOIT, JP. 2008. How to achieve sustained and complete protein release from PLGA-based microparticles? *International journal of pharmaceuticals*, 350, 14-26.
- GIUNCHEDI, P., ALPAR, HO, CONTE, U. 1998. PDLLA microspheres containing steroids: spray-drying, o/w and w/o/w emulsifications as preparation methods. *Journal of microencapsulation*, 15, 185-195.
- GIUNCHEDI, P., CONTI, B, GENTA, I, CONTE, U, PUGLISI, G. 2001. Emulsion spray-drying for the preparation of albumin-loaded PLGA microspheres. *Drug development and industrial pharmacy*, 7, 745-750.
- GUERROUANI, N., BALDO, A, BOUFFIN, A, DRAKIDES, C, GUIMON, M, MAS, A 2007. Allylamine plasma-polymerisation on PLLA surface evaluation of the biodegradation. *Journal of applied polymer science*, 105, 1978-1986.
- GUNATILLAKE, P., ADHIKARI, R. 2006. Biodegradable synthetic polymers for tissue engineering. *Biotechnology annual review*, 12, 301-47.
- HAMBURGER, V., HAMILTON, HL. 1951. A series of normal stages in the development of the chick embryo. *Journal of morphology*, 88, 49-92.
- HAMISHEKHAR, E., J, NAJAFABADI, AR, NAJAFABADI, AR, GILANI, K, MINAIYAN, M, MAHDAVI, H, NOKHODCHI, A. 2009. The effect of formulation variables on the characteristics of insulin-loaded poly(lactic-co-glycolic acid) microspheres prepared by a single phase oil in oil solvent evaporation method. *Colloids and surfaces B: Biointerfaces*, 74, 340-349.
- HE, J., FENG, M, ZHOU, X, MA, S, JIANG, Y, WANG, Y, ZHANG, H. 2011. Stabilization and encapsulation of recombinant human erythropoietin into PLGA microspheres using human serum albumin as a stabilizer. *International journal of pharmaceuticals*, 416, 69-76.

- HELGESON, M., LEHMAN, RA JR., PATZKOWSKI, JC, DMITRIEV, AE, ROSNER, MK, MACK, AW. 2011. Adjacent vertebral body osteolysis with bone morphogenetic protein use in transforaminal lumbar interbody fusion. *Spine*, 11, 507-10.
- HENCH, L. L. 2006. The story of Bioglass. *Journal of material sciences: Materials in medicine*, 17, 967-78.
- HENCH, L. L. 2009. Genetic design of bioactive glass. *Journal of the European Ceramic Society*, 29, 1257-1265.
- HENSLEE, A., GWAK, DH, MIKOS, AG, KASPER, FK. 2012. Development of a biodegradable bone cement for craniofacial applications. *Journal of biomedical materials research part A*, 100, 2252-9.
- HERNANDEZ, R., IGARTUA, M, GASCON, A, CALVO, B, PEDRAZ, J 1998. Influence of shaking and surfactants on the release of bsa from plga microspheres. *European congress of biopharmaceutics and pharmacokinetics*, 23, 272.
- HIEMSTRA, C., ZHONG, Z, VAN STEENBERGEN, MJ, HENNINK, WE, FEIJEN, J. 2007. Release of model proteins and basic fibroblast growth factor from in situ forming degradable dextran hydrogels. *Journal of controlled release*, 122, 71-78.
- HOROWITZ, R., MAZOR, Z, FOITZIK, C, PRASAD, H, ROHRER, M, PALTI, A 2009. Beta tri-calcium phosphate as bone substitute material: properties and clinical applications. *Titanium*, 1, 2-11.
- HOU, Q., CHAU, DY, PRATOOMSOOT, C, TIGHE, PJ, DUA, HS, SHAKESHEFF, KM, ROSE, FR 2008. In situ gelling hydrogels incorporating microparticles as drug delivery carriers for regenerative medicine. *J Pharmaceutical sciences*, 97, 3972-80.
- HOU, Q., DE BANK, PA, SHAKESHEFF, M. 2004. Injectable scaffolds for tissue regeneration. *Journal of materials chemistry*, 14, 1915.
- HOWARD, D., BUTTERY, LD, SHAKESHEFF, KM, ROBERTS, SJ. 2008. Tissue engineering: strategies, stem cells and scaffolds. *Journal of anatomy*, 213, 66-72.
- HSU, W., WANG, JC. 2008. The use of bone morphogenetic protein in spine fusion. *Spine*, 3, 419-25.
- HUBER, A., PICKETT, A, SHAKESHEFF, KM. 2007. Reconstruction of spatially orientated myotubes in vitro using electrospun, parallel microfibre arrays. *European cells and materials journal*, 14, 56-63.
- IANNITTI, T., ROTTIGNI, V, PALMIERI, B. 2012. A pilot study to compare two different hyaluronic acid compounds for treatment of knee osteoarthritis. *International journal of immunopathol and pharmacology*, 25, 1093-8.
- IGARTUA, M., HERNANDEZ, RM, ESQUISABEL, A, GASCON, AR, CALVO, MB, PEDRAZ, JL. 1997. Influence of formulation variables on the in-vitro release of albumin from biodegradable microparticulate systems. *Journal of microencapsulation*, 14, 349-356.
- JAHAGIRDAR, R., SCAMMELL, BE. 2009. Principles of fracture healing and disorders of bone union. *Surgery*, 27, 63-69.
- JAIN, J. 2000. The manufacturing techniques of various drug loaded biodegradable poly(lactide-co-glycolide) (PLGA) devices. *Biomaterials*, 21, 2475-2490.
- JAKLENEC, A., HINCKFUSS, A, BILGEN, B, CIOMBOR, DM, AARON, R, MATHIOWITZ, E. 2008. Sequential release of bioactive IGF-I and TGF-beta 1 from PLGA microsphere-based scaffolds. *Biomaterials*, 29, 1518-25.
- JEON, O., SONG, SJ, YANG, HS., BHANG, SH, KANG, SW, SUNG, MA, LEE, JH, KIM, BS. 2008. Long-term delivery enhances in vivo osteogenic efficacy of bone morphogenetic protein-2 compared to short-term delivery. *Biochemical and biophysical research communications*, 369, 774-80.

- JEONG, S., JEON, O, KREBS, MD, HILL, MC, ALSBERG, E. 2012. Biodegradable photo-crosslinked alginate nanofibre scaffolds with tuneable physical properties, cell adhesivity and growth factor release. *European cells and materials journal*, 24, 331-43.
- JIANG, G., WOO, BH, KANG, F, SINGH, J, DELUCA, PP. 2002. Assessment of protein release kinetics, stability and protein polymer interaction of lysozyme encapsulated poly(D,L-lactide-co-glycolide) microspheres. *Journal of controlled release*, 79, 137-145.
- JOHNSON, M. R., LEE, HJ, BELLAMKONDA, RV, GULDBERG, RE. 2009. Sustained release of BMP-2 in a lipid-based microtube vehicle. *Acta Biomaterialia*, 5, 23-8.
- JONES, J., EHRENFRIED, LM, HENCH, LL. 2006. Optimising bioactive glass scaffolds for bone tissue engineering. *Biomaterials*, 27, 964-73.
- KACHI, M., SUGIYAMA, T, KUSUHARA, S 2008. Endochondral ossification of chick embryonic femora invitro and on chorioallantoic membrane. *Journal of poultry science*, 45, 51-56.
- KALAM, M., HUMANYUN, M, PARVEZ, N, YADAV, S, GARG, A, AMIN, S, SULTANA, Y, ALI, A 2007. Release kinetics of modified pharmaceutical dosage forms: A review. *Continental journal of pharmaceutical sciences*, 1, 30-35.
- KALARIA, D., SHARMA, G, BENIWAL, V, RAVI KUMAR, MNV. 2009. Design of biodegradable nanoparticles for oral delivery of doxorubicin in vivo pharmacokinetics and toxicity studies in rats. *Pharmaceutical research*, 26, 492-501.
- KALLROT, M., EDLUND, U, ALBERTSSON, AC. 2006. Surface functionalization of degradable polymers by covalent grafting. *Biomaterials*, 27, 1788-96.
- KANCZLER, J., BARRY, J, GINTY, P, HOWDLE, SM, SHAKESHEFF, KM, OREFFO, R. O. 2007. Supercritical carbon dioxide generated vascular endothelial growth factor encapsulated poly(DL-lactic acid) scaffolds induce angiogenesis in vitro. *Biochemical and biophysical research communications*, 352, 135-41.
- KANCZLER, J., SMITH, EL, ROBERTS, CA, OREFFO, ROC. 2012. A novel approach for studying the temporal modulation of embryonic skeletal development using organotypic bone cultures and microcomputed tomography. *Tissue Engineering Part C*, 18, 747-760.
- KANDEL, R., GRYPAS, M, PILLIAR, R, LEE, J, WANG, J, WALDMAN, S, ZALZAL, P, HURTIG, C. 2006. Repair of osteochondral defects with biphasic cartilage-calcium polyphosphate constructs in a sheep model. *Biomaterials*, 27, 4120-31.
- KANG, F., JIANG, GE, HINDERLITER, A, DELUCA, PP, SINGH, J. 2002. Lysozyme stability in primary emulsion for PLGA microsphere preparation: effect of recovery methods and stabilizing excipients. *Pharmaceutical Research*, 19, 629-633.
- KANG, F., SINGH, J. 2001. Effect of additives on the release of a model protein from PLGA microspheres. *AAPS PharmSciTech*, 2, 1-7.
- KANG, Y., WU, J, YIN, G, HUANG, Z, YAO, Y, LIAO, X, CHEN, A, PU, X, LIAO, L. 2008. Preparation, characterization and in vitro cytotoxicity of indomethacin-loaded PLLA/PLGA microparticles using supercritical CO₂ technique. *European Journal of Pharmaceutics and Biopharmaceutics*, 70, 85-97.
- KATAGIRI, T., YAMAGUCHI, A, KOMAKI, M, ABE, E, TAKAHASHI, N, IKEDA, T, ROSEN, V, WOZNEY, JM, FUJISAWA-SEHARA, A, SUDA, T. 1994. Bone morphogenetic protein-2 converts the differentiation pathway of C2C12 myoblasts into the osteoblast lineage. *Journal of cell biology*, 127, 1755-66.
- KAYAL, R., TSATSAS, D, BAUER, MA, ALLEN, B, AL-SEBAEI, MO, KAKAR, S, LEONE, CW, MORGAN, EF, GERSTENFELD, LC, EINHORN, TA,

- GRAVES, DT 2007. Diminished bone formation during diabetic fracture healing is related to the premature resorption of cartilage associated with increased osteoclast activity. *Journal of bone and mineral research*, 22, 560-8.
- KELPKE, S., ZINN, KR, RUE, LW, THOMPSON, JA. 2004. Site-specific delivery of acidic fibroblast growth factor stimulates angiogenic and osteogenic responses in vivo. *Journal of biomedical materials Research A*, 71, 316-25.
- KEMP, P. 2006. History of regenerative medicine: looking backwards to move forwards.
- KEMPEN, D., LU, L, HEIJINK, A, HEFFERAN, TE, CREEMERS, L B, MARAN, A, YASZEMSKI, MJ, DHERT, WJ. 2009. Effect of local sequential VEGF and BMP-2 delivery on ectopic and orthotopic bone regeneration. *Biomaterials*, 30, 2816-25.
- KEMPEN, D. C., LB, ALBLAS, J, LU, L, VERBOUT, AJ, YASZEMSKI, MJ, DHERT, WJ. 2010. Growth factor interactions in bone regeneration. *Tissue Engineering Part B*, 16, 551-66.
- KENAWY, E., BOWLIN, GL, MANSFIELD, K, LAYMAN, J, SIMPSON, DG, SANDERS, EH, WNEK, GE. 2002. Release of tetracycline hydrochloride from electrospun poly(ethylene-co-vinylacetate), poly(lactic acid), and a blend. *Journal of controlled release*, 81, 57-64.
- KHAN, S., LANE, JM. 2004. Spinal fusion surgery: animal models for tissue-engineered bone constructs. *Biomaterials*, 25, 1475-1485.
- KIM, Y., LEE, MH, WOZNEY, JM, CHO, JY, RYOO, HM. 2004. Bone morphogenetic protein-2-induced alkaline phosphatase expression is stimulated by Dlx5 and repressed by Msx2. *Journal of Biological Chemistry*, 279, 50773-80.
- KIRBY, G., WHITE, LJ, RAHMAN, CV, COX, HC, QUTACHI, O, ROSE, FRAJ, HUTMACHER, DW, SHAKESHEFF, KM, WOODRUFF, MA. 2011. PLGA-Based Microparticles for the Sustained Release of BMP-2. *Polymers*, 3, 571-586.
- KLOEN, P., DI PAOLA, M, BORENS, O, RICHMOND, J, PERINO, G, HELFET, DL, GOUMANS, MJ. 2003. BMP signaling components are expressed in human fracture callus. *Bone*, 33, 362-71.
- KLOSE, D., DELPLACE, C, SIEPMANN, J. 2011. Unintended potential impact of perfect sink conditions on PLGA degradation in microparticles. *International Journal of Pharmaceutics*, 404, 75-82.
- KLOSE, D., SIEPMANN, F, ELKHARRAZ, K, KRENZLIN, S, SIEPMANN, J. 2006. How porosity and size affect the drug release mechanisms from PLGA-based microparticles. *International journal of Pharmaceutics*, 314, 198-206.
- KLUIN, O., VAN DER MEI, HC, BUSSCHER, HJ, NEUT, D. 2013. Biodegradable vs non-biodegradable antibiotic delivery devices in the treatment of osteomyelitis. *Expert opinion drug delivery*.
- KONTERMANN, R. 2011. Strategies for extended serum half-life of protein therapeutics. *Current Opinion in biotechnology*, 22, 868-76.
- KORBER, M. 2010. PLGA erosion: solubility- or diffusion-controlled? *Pharmaceutical research*, 27, 2414-20.
- KOUSTENI, S., BILEZIKIAN, JP. 2008. The cell biology of parathyroid hormone in osteoblasts. *Current Osteoporosis Reports* 6, 72-76.
- KRUGER, E., IM, DD, BISCHOFF, DS, PEREIRA, CT, HUANG, W, RUDKIN, GH, YAMAGUCHI, DT, MILLER, TA. 2011. In vitro mineralization of human mesenchymal stem cells on three-dimensional type I collagen versus PLGA scaffolds: a comparative analysis. *Plast Reconstr Surg*, 127, 2301-11.
- KUMAR, N., LANGER, RS, DOMB, AJ. 2002. Polyanhydrides: an overview. *Advanced drug delivery reviews*, 54, 889-910.

- KUNG, M., YUKATA, K, O'KEEFE, RJ, ZUSCIK, MJ 2012. Aryl hydrocarbon receptor-mediated impairment of chondrogenesis and fracture healing by cigarette smoke and benzo(a)pyrene. *Journal of cell physiology*, 227, 1062-70.
- LAKSHMI, S., KATTI, DS, LAURENCIN, CT. 2003. Biodegradable polyphosphazenes for drug delivery applications. *Advanced drug delivery reviews*, 55, 467-482.
- LAM, C., HUTMACHER, D W, SCHANTZ, JT, WOODRUFF, MA, TEOH, SH. 2009. Evaluation of polycaprolactone scaffold degradation for 6 months in vitro and in vivo. *Journal of biomedical materials research A*, 90, 906-19.
- LANGER, R., CIMA, LG, TAMADA, JA, WINTERMANTEL, E. 1990. Future directions in biomaterials. *Biomaterials*, 11, 738-45.
- LARSSON, S., BAUER, TW. 2002. Use of injectable calcium phosphate cement for fracture fixation: a review. *Clinical orthopaedic and related research*, 395, 23-32.
- LARSSON, S., HANNINK, G. 2011. Injectable bone-graft substitutes: current products, their characteristics and indications, and new developments. *Injury*, 42 Suppl 2, S30-4.
- LE GUEHENNEC, L., LAYROLLE P, DACULSI, G. 2004. A review of bioceramics and fibrin sealant. *European cells and materials*, 8, 1-11.
- LEE, S., SHEA, M, BATTLE, MA, KOZITZA, K, RON, E, TUREK, T, SCHAUB, RG, HAYES, WC. 1994. Healing of large segmental defects in rat femurs is aided by RhBMP-2 in PLGA matrix. *Journal of biomedical materials research* 28, 1149-56.
- LI, X., DENG, X, HUANG, Z. 2001. In vitro protein release and degradation of poly-dl-lactide-poly(ethylene glycol) microspheres with entrapped human serum albumin: quantitative evaluation of the factors involved in protein release phases. *Pharmaceutical research*, 18, 117-124.
- LIEBERMAN, J., DALUISKI, A, EINHORN, TA. 2002. The role of growth factors in the repair of bone. Biology and clinical applications. *Journal of bone and joint surgery Am*, 84-A, 1032-1044.
- LINDBERG, K., BADYLAK, SF. 2001. Porcine small intestinal submucosa (SIS): a bioscaffold supporting in vitro primary human epidermal cell differentiation and synthesis of basement membrane proteins. *Burns*, 27, 254-266.
- LIU, J. Y. 2011. Fabrication and characterization of polycaprolactone/calcium sulfate whisker composites. *Express Polymer Letters*, 5, 742-752.
- LIU, Y., GHASSEMI, AH, HENNINK, WE, SCHWENDEMAN, SP. 2012. The microclimate pH in poly(d,l-lactide-co-hydroxymethyl glycolide) microspheres during biodegradation. *Biomaterials*, 33, 7584-93.
- LOPEZ-HEREDIA, M., PATTIPEILOHY, J, HSU, S, GRYKIEN, M, VAN DER WEIJDEN, B, LEEUWENBURGH, SCG, SALMON, P, WOLKE, JGC, JANSEN, JA. 2013. Bulk physicochemical, interconnectivity, and mechanical properties of calcium phosphate cements-fibrin glue composites for bone substitute applications. *Journal of biomedical materials research A*, 101, 478-90.
- MACKIE, E., AHMED, YA, TATARCZUCH, L, CHEN, KS, MIRAMS, M. 2008. Endochondral ossification: how cartilage is converted into bone in the developing skeleton. *International journal of biochemistry and cell biology*, 40, 46-62.
- MAHBOUBIAN, A., HASEMEIN, SK, MOGHADAM, S, ATYABI, F, DINARVAND, R. 2010. Preparation and in-vitro evaluation of controlled release PLGA microparticles containing triptoreline. *Iranian journal of pharmaceutical research*, 9, 369-378.

- MAKADIA, H., SIEGEL, SJ. 2011. Poly Lactic-co-Glycolic Acid (PLGA) as Biodegradable Controlled Drug Delivery Carrier. *Polymers*, 3, 1377-1397.
- MALLICK, K., COX, SC. 2013. Biomaterial scaffolds for tissue engineering. *Frontiers of Bioscience (Elite Ed)*, 1, 341-60.
- MANDAL, B., GRINBERG, A, GIL, ES, PANILAITIS, B, KAPLAN, DL.. 2012. High-strength silk protein scaffolds for bone repair. *Proceedings of the national academy of sciences, USA* 20, 7699-704.
- MAO, S., XU, J, CAI, C, GERMERSHAUS, O, SCHAPER, A, KISSEL, T. 2007. Effect of WOW process parameters on morphology and burst release of FITC-dextran loaded PLGA microspheres. *International journal of pharmaceuticals*, 334, 137-48.
- MARTINO, S., D'ANGELO, F, ARMENTANO, I, KENNY, JM, ORLACCHIO, A. 2012. Stem cell-biomaterial interactions for regenerative medicine. *Biotechnological advances*, 30, 338-51.
- MCMAHON, L., PRENDERGAST, PJ, CAMPBELL, VA. 2008. A comparison of the involvement of p38, ERK1/2 and PI3K in growth factor-induced chondrogenic differentiation of mesenchymal stem cells. *Biochemical and biophysical research communication*, 368, 990-5.
- MEHTA, M., SCHMIDT-BLEEK, K, DUDA, GN, MOONEY, D J. 2012. Biomaterial delivery of morphogens to mimic the natural healing cascade in bone. *Advanced drug delivery reviews*, 64, 1257-76.
- MERRILL, J., HARRISON, JH, MURRAY, J, GUILD, WR 1954. Successful homotransplantation of the kidney in an identical twin. *Trans Am Clin Climatol Assoc*, 67, 166-173.
- MERRILL, J., MURRAY, JE, HARRISON, JH, GUILD, WR. 1984. Landmark article Jan 28, 1956: Successful homotransplantation of the human kidney between identical twins. By John P. Merrill, Joseph E. Murray, J. Hartwell Harrison, and Warren R. Guild. *Journal of the American medical association*, 251, 2566-71.
- MICROMERITICS, T. W. 2000. Particle sizing by static laser light scattering. http://www.particletesting.com/docs/primer_particle_sizing_laser.pdf.
- MIDDLETON, J., TIPTON, AJ. 2000. Synthetic biodegradable polymers as orthopedic devices. *Biomaterials*, 21, 2335-2346.
- MORITA, T., HORIKIRI, Y, SUZUKI, T, YOSHINO, H. 2001. Applicability of various amphiphilic polymers to the modification of protein release kinetics from biodegradable reservoir-type microspheres. *European Journal of Pharmaceutics and Biopharmaceutics*, 51, 45-53.
- MORITA, T., HORIKIRI, Y, YAMAHARA, H, SUZUKI, T, YOSHINO, H. 2000a. Formation and isolation of spherical fine protein microparticles through lyophilization of protein-poly(ethylene glycol) aqueous mixture. *Pharmaceutical research*, 17, 1367-1373.
- MORITA, T., SAKAMURA, Y, HORIKIRI, Y, SUZUKI, T, YOSHINO, H. 2000b. Protein encapsulation into biodegradable microspheres by a novel S/O/W emulsion method using poly(ethylene glycol) as a protein micronization adjuvant. *Journal of controlled release*, 69, 435-444.
- MORLOCK, M., KISSEL, T, LI, YX, KOLL, H, WINTER, G. 1996. Erythropoietin loaded microspheres prepared from biodegradable LPLG-PEO-LPLG triblock copolymers: protein stabilization and in-vitro release properties. *European journal of pharmaceuticals and biopharmaceutics*, 43, 29-36.
- MUGGLI, D., BURKOTH, A K, ANSETH, KS. 1999. Crosslinked polyanhydrides for use in orthopedic applications: degradation behavior and mechanics.
- MUNSTER, A. M. 1996. Cultured skin for massive burns. A prospective, controlled trial. *Annals of Surgery*, 224, 372-377.

- MURPHY, S., ATALA, A. 2012. Organ engineering - combining stem cells, biomaterials, and bioreactors to produce bioengineered organs for transplantation. *Bioessays*.
- MUTHU, M. 2009. Nanoparticles based on PLGA and its co-polymer: An overview. *Asian Journal of Pharmaceutics*, 3, 266.
- NAKAMURA, S., KUBO, T, IJIMA, H. 2012. Heparin-conjugated gelatin as a growth factor immobilization scaffold. . *Journal of biosciences and bioengineering*
- NAKASHIMA, A., KATAGIRI, T, TAMURA, M. 2005. Cross-talk between Wnt and bone morphogenetic protein 2 (BMP-2) signaling in differentiation pathway of C2C12 myoblasts. *Journal of biological chemistry*, 280, 37660-8.
- NAMUR, J., CABRAL-ALBUQUERQUE, EC, QUINTILIO, W, SANTANA, MH, POLITI, MJ, DE ARAUJO, PS, LOPES, AC, DA COSTA, MH. 2006. Poly-lactide-co-glycolide microparticle sizes: a rational factorial design and surface response analysis. *Journal of nanosciences and nanotechnology*, 6, 2403-7.
- NOBLE, J., BAILEY, JA 2009. Quantitation of protein. *Methods in enzymology*, 463, 73-95.
- NYKAMP, G., CARSTENSEN, U, MULLER, BW. 2002. Jet milling--a new technique for microparticle preparation. *International journal of pharmaceutics*, 242, 79-86.
- ODA, H., NAKAMURA, K, MATSUSHITA, T, YAMAMOTO, S, ISHIBASHI, H, YAMAZAKI, T, MORIMOTO, S. 2006. Clinical use of a newly developed calcium phosphate cement (XSB-671D). *Journal of Orthopaedic Sciences*, 11, 167-74.
- OKAMOTO, T., AOYAMA, T, NAKAYAMA, T, NAKAMATA, T, HOSAKA, T, NISHIJO, K, NAKAMURA, T, KIYONO, T, TOGUCHIDA, J. 2002. Clonal heterogeneity in differentiation potential of immortalized human mesenchymal stem cells. *Biochemical and biophysical research communication*, 295, 354-61.
- OVIEDO-RONDON, E., SMALL, J, WINELAND, MJ, CHRISTENSEN, VL, MOZDZIAK, PS, KOCI, MD, FUNDERBURK, SVL, ORT, DT, MANN, KM. 2008. Broiler embryo bone development is influenced by incubator temperature, oxygen concentration and eggshell conductance at the plateau stage in oxygen consumption. *British Poultry Science*, 49, 666-676.
- OZBOLAT, I., YU, Y. 2013. Bioprinting towards Organ Fabrication: Challenges and Future Trends. *Transactions on biomedical engineering*, ahead of print.
- PAILLARD-GITEAU, A., TRAN, VT, THOMAS, O, GARRIC, X, COUDANE, J, MARCHAL, S, CHOURPA, I, BENOIT, JP, MONTERO-MENEI, CN, VENIER-JULIENNE, MC. 2010. Effect of various additives and polymers on lysozyme release from PLGA microspheres prepared by an s/o/w emulsion technique. *European journal of pharmaceutics and biopharmaceutics*, 75, 128-36.
- PARK, G., PATTISON, MA, PARK, K, WEBSTER, TJ. 2005. Accelerated chondrocyte functions on NaOH-treated PLGA scaffolds. *Biomaterials*, 26, 3075-82.
- PASSERINI, N., CRAIG, DQ. 2001. An investigation into the effects of residual water on the glass transition temperature of polylactide microspheres using modulated temperature DSC. *Journal of controlled release*, 73, 111-5.
- PATEL, R., PATEL, MP, SUTHAR, AM 2009. Spray drying technology: an overview. *Indian journal of science and technology*, 2, 44-47.

- PEREZ, C., DE JESUS, P, GRIEBENOW, K. 2002. Preservation of lysozyme structure and function upon encapsulation and release from poly(lactic-co-glycolic) acid microspheres prepared by the water-in-oil-in-water method. *International Journal of Pharmaceutics*, 248, 193-206.
- PERRI, B., COOPER, M, LAURYSSSEN, C, ANAND, N. 2007. Adverse swelling associated with use of rh-BMP-2 in anterior cervical discectomy and fusion: a case study. *Spine*, 7, 235-9.
- PILLIAR, R., KANDEL, RA, GRYPNPAS, MD, HU, Y. 2013. Porous calcium polyphosphate as load-bearing bone substitutes: In vivo study. *Journal of biomedical materials research B: Applied biomaterials*, 101.
- PILLIAR, R., KANDEL, RA, GRYPNPAS, MD, ZALZAL, P, HURTIG, M. 2007. Osteochondral defect repair using a novel tissue engineering approach: sheep model study. *Technology and health care*, 15, 47-56.
- PORTER, J., RUCKH, TT, POPAT, KC 2009. Bone tissue engineering: a review in bone biomimetics and drug delivery strategies. *Biotechnological progress*, 25, 1539-60.
- POUNTOS, I., GIANNOUDIS, PV. 2005. Biology of mesenchymal stem cells. *Injury*, 36 Suppl 3, S8-S12.
- RAHMAN, C., BEN-DAVID, D, DHILLON, A, KUHN, G, GOULD, TWA, MULLER, R, ROSE, FRAJ, SHAKESHEFF, KM, LIVNE, E. 2012a. Controlled release of BMP-2 from a sintered polymer scaffold enhances bone repair in a mouse calvarial defect model. *Journal of tissue engineering and regenerative medicine*.
- RAHMAN, C., KUHN, G, WHITE, LJ, KIRBY, GTS, VARGHESE, OP, MCLAREN, JS, COX, H C, ROSE, F R, MÜLLER, R, HILBORN, J, SHAKESHEFF, KM. 2013. PLGA/PEG-hydrogel composite scaffolds with controllable mechanical properties. *Journal of Biomedical Materials Research Part B: Applied Biomaterial*.
- RAHMAN, C., SAEED, A, WHITE, LJ. GOULD, TWA, KIRBY, GTS, SAWKINS, MJ, ALEXANDER, C, ROSE, FRAJ, SHAKESHEFF, KM. 2012b. Chemistry of Polymer and Ceramic-Based Injectable Scaffolds and Their Applications in Regenerative Medicine. *Chemistry of Materials*, 24, 781-795.
- RAICHE, A., PULEO, DA. 2004. Cell responses to BMP-2 and IGF-I released with different time-dependent profiles. *Journal of biomedical materials Research A*, 69, 342-50.
- RASHIDI, H., SOTTILE, V. 2009. The chick embryo: hatching a model for contemporary biomedical research. *Bioassays*, 31, 459-65.
- RASHIDI, H., STROHBUECKER, S, JACKSON, L, KALRA, S, BLAKE, AJ, FRANCE, L, TUFARELLI, C, SOTTILE, V. 2012. Differences in the pattern and regulation of mineral deposition in human cell lines of osteogenic and non-osteogenic origin. *Cells Tissues Organs*, 195, 6.
- RAWADI, G., VAYSSIERE, B, DUNN, F, BARON, R, ROMAN-ROMAN, S. 2003. BMP-2 controls alkaline phosphatase expression and osteoblast mineralization by a Wnt autocrine loop. *Journal of bone and mineral research*, 18, 1842-53.
- RECKLING, F., DILLON, W L. 1977. The bone-cement interface temperature during total joint replacement. *Journal of bone and joint surgery American volume*, 59, 80-2.
- REDDI, A. 1998. Role of morphogenetic proteins in skeletal tissue engineering and regeneration. *Nature biotechnology*, 16, 247-252.
- RENIER, M., KOHN, DH. 1997. Development and characterization of a biodegradable polyphosphate. *Journal of Biomedical Materials Research*, 34, 95-104.

- REZWAN, K., CHEN, QZ, BLAKER, JJ, BOCCACCINI, AR. 2006. Biodegradable and bioactive porous polymer/inorganic composite scaffolds for bone tissue engineering. *Biomaterials*, 27, 3413-31.
- RIZZINO, A., KUSZYNSKI, C, RUFF, E, TIESMAN, J. 1988. Production and utilization of growth factors related to fibroblast growth factor by embryonal carcinoma cells and their differentiated cells. *Developmental biology*, 129, 61-71.
- ROACH, H. 1990. Long-term organ culture of embryonic chick femora: a system for investigating bone and cartilage formation at an intermediate level of organization. *Journal of bone and mineral research*, 5, 85-100.
- ROACH, H. 1997. New aspects of endochondral ossification in the chick: chondrocyte apoptosis, bone formation by former chondrocytes, and acid phosphatase activity in the endochondral bone matrix. *Journal of bone mineral research*, 5, 795-805.
- ROACH, H., BAKER, JE, CLARKE, NM. 1998. Initiation of the bony epiphysis in long bones: chronology of interactions between the vascular system and the chondrocytes. *Journal of bone mineral research*, 6, 950-961.
- ROACH, H., ERENPREISA, J. 1996. The phenotypic switch from chondrocytes to bone-forming cells involves asymmetric cell division and apoptosis. *Connect tissue research*, 35, 85-91.
- ROSAS, J., HERNANDEZ, RM, GASCON, AR, IGARTUA, M, GUZMAN, F, PATARROYO, ME, PEDRAZ, JL. 2001. Biodegradable PLGA microspheres as a delivery system for malaria synthetic peptide SPf66. *Vaccine*, 19, 4445-4451.
- ROSCA, I., WATARI, F. UO, M. 2004. Microparticle formation and its mechanism in single and double emulsion solvent evaporation. *Journal of controlled release*, 99, 271-80.
- RUMPEL, E., WOLF, E, KAUSCHKE, E, BIENENGRABER, V, BAYERLEIN, T, GEDRANGE, T, PROFF, P. 2006. The biodegradation of hydroxyapatite bone graft substitutes in vivo. *Folia Morphologica (Warsz)*, 65, 43-48.
- RUPPERT, R., HOFFMANN, E, SEBALD, W. 1996. Human bone morphogenetic protein 2 contains a heparin-binding site which modifies its biological activity. *European journal of biochemistry*, 237, 295-302.
- SAH, H. 1997. A new strategy to determine the actual protein content of poly(lactide-co-glycolide) microspheres. *Journal of pharmaceutical sciences*, 86, 1315-1318.
- SAH, H. 1999. Protein behavior at the water/methylene chloride interface. *Journal of Pharmaceutical sciences*, 88, 1320-1325.
- SAIF, J., SCHWARZ, TM, CHAU, DY, HENSTOCK, J, SAMI, P, LEICHT, SF, HERMANN, PC, ALCALA, S, MULERO, F, SHAKESHEFF, KM, HEESCHEN, C, AICHER, A. 2010. Combination of injectable multiple growth factor-releasing scaffolds and cell therapy as an advanced modality to enhance tissue neovascularization. *Arteriosclerosis Thrombosis and vascular biology*, 30, 1897-904.
- SAINT-BLANCARD, J., CHUZEL, P, MATHIEU, Y, PERROT, J, JOLLES, P. 1970. Influence of pH and ionic strength of the lysis of *Micrococcus lysodeikticus* cells by six human and four avian lysozymes. *Biochimica and biophysica acta*, 220, 300-306.
- SANDOR, M., ENSCORE, D, WESTON, P, MATHIOWITZ, E. 2001. Effect of protein molecular weight on release from micron-sized PLGA microspheres. *Journal of controlled release*, 76, 296-311.
- SANDOR, M., HARRIS, J, MATHIOWITZ, E. 2002. A novel polyethylene depot device for the study of PLGA and P(FASA) microspheres in vitro and in vivo. *Biomaterials*, 23, 4413-4423.

- SANDUSKY, G., LANTZ, GC, BADYLAK, SF. 1995. Healing comparison of small intestine submucosa and ePTFE grafts in the canine carotid artery. *Journal of surgical research*, 58, 415-421.
- SANTOVENA, A., ALVAREZ-LORENZO, C, CONCHEIRO, A, LLABRES, M, FARINA, JB. 2004. Rheological properties of PLGA film-based implants: correlation with polymer degradation and SPf66 antimalaric synthetic peptide release. *Biomaterials*, 25, 925-31.
- SASAKI, T., WATANABE, C. 1995. Stimulation of osteoinduction in bone wound healing by high-molecular hyaluronic acid. *Bone*, 16, 9-15.
- SCHELLPFEFFER, M., BOLENDER, DL, KOLESARI, GL. 2007. High frequency ultrasound imaging of the growth and development of the normal chick embryo. *Ultrasound in medicine and bioogyl*, 33, 751-761.
- SCHNEIDER, T., KB, KOHL, B, SAUTER, T, KRATZ, K, LENDLEIN, A, ERTEL, W, SCHULZE-TANZIL, G. 2012. Influence of fiber orientation in electrospun polymer scaffolds on viability, adhesion and differentiation of articular chondrocytes. *Clinical hemorheology and Microcirculation*, 52, 325-336.
- SEITZ, H. R., W, IRSEN, S, LEUKERS, B, TILLE, C. 2005. Three-dimensional printing of porous ceramic scaffolds for bone tissue engineering. *Journal of biomedical materials research B: Applied biomaterials*, 74, 782-8.
- SEPULVEDA, P., JONES, JR, HENCH, L L. 2001. Bioactive sol-gel foams for tissue repair.
- SHAFIEI-SARVESTANI, Z., ORYAN, A, BIGHAM, AS, MEIMANDI-PARIZI, A. 2012. The effect of hydroxyapatite-hPRP, and coral-hPRP on bone healing in rabbits: radiological, biomechanical, macroscopic and histopathologic evaluation. *International journal of surgery*, 10, 96-101.
- SHARMA, G., SRIKANTH, MV, UHUMWANGHO, MU, PHANI, KUMAR KS. RAMANA, MURTHY KV. 2010. Recent trends in pulsatile drug delivery systems - A review. *International journal of drug delivery*, 2, 200-212.
- SIMON, L., STELLA, VJ, CHARMAN, WN, CHARMAN, SA. 1999. Mechanisms controlling diffusion and release of model proteins through and from partially esterified hyaluronic acid membranes. *Journal of controlled release* 62, 267-279.
- SINGHAL, S., LOHAR, VK, ARORA, V. 2011. Hot melt extrusion technique. *Science*, 2.
- SMITH, E., KANCZLER, JM, ROBERTS, CA, OREFFO, ROC. 2012. Developmental Cues for Bone Formation from Parathyroid Hormone and Parathyroid Hormone-Related Protein in an Ex Vivo Organotypic Culture System of Embryonic Chick Femora. *Tissue Engineering Part C*, 18, 984-994.
- SOHIER, J., VLUGT, TJ, CABROL, N, VAN BLITTERSWIJK, C, DE GROOT, K, BEZEMER, JM. 2006. Dual release of proteins from porous polymeric scaffolds. *Journal of controlled release*, 111, 95-106.
- SOKOLSKY-PAPKOV, M., AGASHI, K, OLAYE, A, SHAKESHEFF, K, DOMB, AJ. 2007. Polymer carriers for drug delivery in tissue engineering. *Advanced drug delivery reviews*, 59, 187-206.
- STROBEL, C., BORMANN, N, KADOW-ROMACKER, A, SCHMIDMAIER, G, WILDEMANN, B. 2011. Sequential release kinetics of two (gentamicin and BMP-2) or three (gentamicin, IGF-I and BMP-2) substances from a one-component polymeric coating on implants. *Journal of controlled release*, 156, 37-45.
- SUCIATI, T., HOWARD, D, BARRY, J, EVERITT, NM, SHAKESHEFF, KM, ROSE, FR. 2006. Zonal release of proteins within tissue engineering scaffolds. *Journal of material science materials in medicine*, 17, 1049-56.

- SWIONTKOWSKI, M., ARO, HT, DONELL, S, ESTERHAI, JL, GOULET, J, JONES, A, KREGOR, PJ, NORDSLETTEN, L, PAIEMENT, G, PATEL, A. 2006. Recombinant human bone morphogenetic protein-2 in open tibial fractures. A subgroup analysis of data combined from two prospective randomized studies. *Journal of bone and joint surgery American version*, 86, 1258-65.
- TABATA, M., SHIMODA T, SUGIHARA, K, OGOMI, D, SERIZAWA, T, AKASHI, M 2003. Osteoconductive and hemostatic properties of apatite formed on/in agarose gel as a bone-grafting material. *Journal of biomedical materials research B: Applied biomaterials*, 67, 680-688.
- TAI, H., MATHER, ML, HOWARD, D, WANG, W, WHITE, LJ, CROWE, JA, MORGAN, SP, CHANDRA, A, WILLIAMS, DJ, HOWDLE, SM, SHAKESHEFF, KM. 2007. Control of pore size and structure of tissue engineering scaffolds produced by supercritical fluid processing. *European cells and materials*, 14, 64-77.
- TAKAHASHI, K., SHANAHAN, MD, COULTON, LA, DUCKWORTH, T. 1991. Fracture healing of chick femurs in tissue culture. *Acta Orthopaedica Scandnidaica*, 62, 352-5.
- TAMURA, M., NEMOTO, E, SATO, MM, NAKASHIMA, A, SHIMAUCHI, H. 2010. Role of the Wnt signaling pathway in bone and tooth. *Frontiers of Biosciences (Elite Ed)*, 2, 1405-13.
- TERPE, K. 2006. Overview of bacterial expression systems for heterologous protein production: from molecular and biochemical fundamentals to commercial systems. *Applied Microbiology and biotechnology*, 72, 211-222.
- THOMSON, J., ITSKOVITZ-ELDOR, J, SHAPIRO, SS, WAKNITZ, MA, SWIERGIEL, JJ, MARSHALL, VS, JONES, J. M. 1998. Embryonic stem cell lines derived from human blastocysts. *Science*, 282, 1145-1147.
- TIEN, L., GIL, ES, PARK, SH, MANDAL, BB, KAPLAN, DL. 2012. Patterned silk film scaffolds for aligned lamellar bone tissue engineering. *Macromolecular bioscience*, 12, 1671-9.
- TRAN, V., KARAM, JP, GARRIC, X, COUDANE, J, BENOIT, JP, MONTERO-MENEI, CN, VENIER-JULIENNE, MC. 2012. Protein-loaded PLGA-PEG-PLGA microspheres: a tool for cell therapy. *European journal of pharmaceutical science*, 45, 128-37.
- TRIVEDI, P., VERMA, A, GARUD, N. 2008. Preparation and characterisation of aceclofenac microspheres. *Asian journal of pharmaceuticals*, 2, 110-115.
- TSIRIDIS, E., UPADHYAY, N, GIANNOUDIS, P. 2007. Molecular aspects of fracture healing: which are the important molecules? *Injury*, 38, S11-25.
- UMULIS, D., O'CONNOR, MB, BLAIR, SS. 2009. The extracellular regulation of bone morphogenetic protein signaling. *Development*, 136, 3715-28.
- VAN DE WEERT, M., HENNINK, WE, JISKOOT, W. 2000a. Protein instability in poly(lactic-co-glycolic acid) microparticles. *Pharmaceutical research*, 10, 1159-67.
- VAN DE WEERT, M., HOECHSTETTER, J, HENNINK, WE, CROMMELIN, DJ. 2000b. The effect of a water/organic solvent interface on the structural stability of lysozyme. *Journal of controlled release*, 68, 351-359.
- VARGAS, G., MESONES, RV, BRETCANU, O, LOPEZ, JM. BOCCACCINI, AR, GORUSTOVICH, A. 2009. Biocompatibility and bone mineralization potential of 45S5 Bioglass-derived glass-ceramic scaffolds in chick embryos. *Acta Biomateriala*, 5, 374-80.
- VENKATESAN, J., KIM, SK. 2010. Chitosan composites for bone tissue engineering--an overview. *Marine drugs*, 8, 2252-66.

- VERRIER, S., PALLU, S, BAREILLE, R, JONCZYK, A, MEYER, J, DARD, M, AMEDEE, J. 2002. Function of linear and cyclic RGD-containing peptides in osteoprogenitor cells adhesion process. *Biomaterials*, 23, 585-596.
- VISWANATHAN, N., THOMAS, PA, THOMAS, PA, PANDIT, JK, KULKARNI, MG, MASHELKAR, RA. 1999. Preparation of non-porous microspheres with high entrapment efficiency of proteins by a (water-in-oil)-in-oil emulsion technique. *Journal of controlled release*, 58, 9-20.
- VON DER MARK, K., VON DER MARK, H. 1977. The role of three genetically distinct collagen types in endochondral ossification and calcification of cartilage. *Journal of bone and joint surgery Br*, 59-B, 458-64.
- WALSTRA, P. 1993. Principles of emulsion formation. *Chemical engineering science*, 48, 333-349.
- WANG, S., LU, L, YASZEMSKI, MJ. 2006. Bone-tissue-engineering material poly(propylene fumarate): correlation between molecular weight, chain dimensions, and physical properties. *Biomacromolecules*, 7, 1976-82.
- WEBB, J., SPENCER, RF. 2007. The role of polymethylmethacrylate bone cement in modern orthopaedic surgery. *Journal of bone and joint surgery* 89, 851-7.
- WEI, L., GELLYNCK, K, NG, YL, GULABIVALA, K, BUXTON, P. 2011. The influence of a bisphosphonate on bone generation determined using a chick-femur model. *International Endodontic journal*, 44, 550-9.
- WEISKIRCHEN, R., MEURER, SK, MEURER SK, GRESSNER, OA, HERRMANN, J, BORKHAM-KAMPHORST, E, GRESSNER, AM. 2009. BMP-7 as antagonist of organ fibrosis. *Frontiers of bioscience*, 14, 4992-5012.
- WELLS, L., SHEARDOWN, H. 2007. Extended release of high pI proteins from alginate microspheres via a novel encapsulation technique. *European journal of pharmaceutics and biopharmaceutics*, 65, 329-335.
- WENG, L., CHEN, X, CHEN, W. 2007. Rheological characterization of in situ crosslinkable hydrogels formulated from oxidized dextran and N-carboxyethyl chitosan. *Biomacromolecules*, 8, 1109-15.
- WERLE, M., BERNKOP-SCHNURCH, A. 2006. Strategies to improve plasma half life time of peptide and protein drugs. *Amino Acids*, 30, 351-67.
- WHITE, L., KIRBY, GTS, COX, HC, QODRATNAMA, R, QUTACHI, O, ROSE, FRAJ, SHAKESHEFF, KM. 2013. Accelerating protein release from microparticles for regenerative medicine applications. *Materials science and engineering: C*, in press.
- WISCHKE, C., SCHWENDEMAN, SP. 2008. Principles of encapsulating hydrophobic drugs in PLA/PLGA microparticles. *International journal of pharmaceutics*, 364, 298-327.
- WU, C., LU, H 2008. Smad signal pathway in BMP-2-induced osteogenesis - a mini review. *Journal dental science* 3, 13-21.
- WU, G., LIU, Y, IIZUKA, T, HUNZIKER, EB. 2010. The effect of a slow mode of BMP-2 delivery on the inflammatory response provoked by bone-defect-filling polymeric scaffolds. *Biomaterials*, 31, 7485-93.
- WU, X., WANG, N 2001. Synthesis, characterisation, biodegradation and drug delivery application of biodegradable lactic/glycolic acid polymers. Part II: Biodegradation. *Journal of biomaterials science: Polymer edition*, 12, 21-34.
- WU, Y., SHAW, SY, LIN, HR, LEE, TM, YANG, CY. 2006. Bone tissue engineering evaluation based on rat calvaria stromal cells cultured on modified PLGA scaffolds. *Biomaterials*, 27, 896-904.
- XIONG, Y., ZHU, JX, FANG, ZY, ZENG, CG, ZHANG, C, QI, GL, LI, MH, ZHANG, W, QUAN, DP, WAN, J. 2012. Coseeded Schwann cells myelinate neurites from differentiated neural stem cells in neurotrophin-3-loaded PLGA carriers. *International journal of nanomedicine*, 7.

- YAMAMOTO, N., AKIYAMA, S, KATAGIRI, T, NAMIKI, M, KUROKAWA, T, SUDA, T. 1997. Smad1 and smad5 act downstream of intracellular signalings of BMP-2 that inhibits myogenic differentiation and induces osteoblast differentiation in C2C12 myoblasts. *Biochemical and biophysical research communication*, 238, 574-80.
- YANG, S., KIM, J, RYU, J. H, OH, H, CHUN, CH, KIM, BJ, MIN, BH, CHUN, JS. 2010. Hypoxia-inducible factor-2alpha is a catabolic regulator of osteoarthritic cartilage destruction. *Nature medicine*, 16, 687-93.
- YANG, Y., CHIA, HH, CHUNG, TS. & CHUNG, T. S. 2000. Effect of preparation temperature on the characteristics and release profiles of PLGA microspheres containing protein fabricated by double-emulsion solvent extraction/evaporation method. *Journal of controlled release*, 69, 81-96.
- YANG, Y., CHUNG, TS, NG, NP. 2001. Morphology, drug distribution, and in vitro release profiles of biodegradable polymeric microspheres containing protein fabricated by double-emulsion solvent extraction/evaporation method. *Biomaterials*, 22, 231-241.
- YE, M., KIM, S, PARK, K. 2010. Issues in long-term protein delivery using biodegradable microparticles. *Journal of controlled release*, 146, 241-60.
- YEO, Y., CHEN, AU, BASARAN, OA, PARK, K 2004a. Solvent exchange method: a novel microencapsulation technique using dual microdispensers. *Pharmaceutical Research*, 21, 1419-1427.
- YEO, Y., PARK, K. 2004b. Control of encapsulation efficiency and initial burst in polymeric microparticle systems. *Archives of Pharmaceutical Research*, 27, 1-12.
- YILGOR, P., HASIRCI, N, HASIRCI, V. 2010. Sequential BMP-2/BMP-7 delivery from polyester nanocapsules. *Journal of biomedical materials research A*, 93, 528-36.
- YOON, S., KIM, SH, HA, HJ, KO, YK, SO, JW, KIM, MS, YANG, YL, KHANG, G, RHEE, JM, LEE, HB. 2008. Reduction of inflammatory reaction of poly(d,l-lactic-co-glycolic Acid) using demineralized bone particles. *Tissue Engineering part A*, 14, 539-47.
- YU, N., SCHINDELER, A, LITTLE, DG, RUYS, AJ. 2010. Biodegradable poly(alpha-hydroxy acid) polymer scaffolds for bone tissue engineering. *Journal of biomedical materials research B: Applied biomaterials*, 93, 285-95.
- ZARA, J., SIU, RK, ZHANG, X, SHEN, J, NGO, R, LEE, M, LI, W, CHIANG, M, CHUNG, J, KWAK, J, WU, BM, TING, K, SOO, C. 2011. High doses of bone morphogenetic protein 2 induce structurally abnormal bone and inflammation in vivo. *Tissue Engineering Part A*, 17, 1389-99.
- ZENTNER, G., RATHI, R, SHIH, C, MCREA, JC, SEO, MH, OH, H, RHEE, BG, MESTECKY, J, MOLDOVEANU, Z, MORGAN, M, WEITMAN, S. 2001. Biodegradable block copolymers for delivery of proteins and water-insoluble drugs. *Journal of controlled release*, 72, 203-215.
- ZHAI, P., CHEN, XB, SCHREYER, DJ. 2013. Preparation and characterization of alginate microspheres for sustained protein delivery within tissue scaffolds. *Biofabrication*, 5.
- ZHANG, H., MIGNECO, F, LIN, CY, HOLLISTER, SJ. 2010. Chemically-conjugated bone morphogenetic protein-2 on three-dimensional polycaprolactone scaffolds stimulates osteogenic activity in bone marrow stromal cells. *Tissue Engineering Part A*, 16, 3441-8.
- ZHANG, Q., HE, QF, ZHANG, TH, YU, XL, LIU, Q, DENG, FL. 2012. Improvement in the delivery system of bone morphogenetic protein-2: a new approach to promote bone formation. *Biomedical materials*, 7, 1-11.

- ZHOU, Y., HUTMACHER, DW, VARAWAN, SL, MENG, LT. 2007. In vitro bone engineering based on polycaprolactone and polycaprolactone-tricalcium phosphate composites. *Polymer International*, 56, 333-342.
- ZHU, L., LI, Y, ZHANG, Q, WANG, H, ZHU, M. 2009. Fabrication of monodisperse, large-sized, functional biopolymeric microspheres using a low-cost and facile microfluidic device. *Biomedical microdevices*, 12, 169-177.
- ZILBERMAN, M., GRINBERG, O. 2008. HRP-loaded bioresorbable microspheres: effect of copolymer composition and molecular weight on microstructure and release profile. *Journal of biomaterials applications*, 22, 391-407.
- ZIMMERMANN, G., MOGHADDAM, A. 2011. Allograft bone matrix versus synthetic bone graft substitutes. *Injury*, 42 Suppl 2, S16-21.

Appendix I: Equipment, consumables and materials

The equipment, consumables and materials used to perform all of the studies described in this thesis are detailed in Tables A1 (equipment), A2 (consumables) and A3 (chemicals/reagents) along with manufacturer, model number, supplier and primary use.

Table A1 Laboratory equipment inventory

Equipment	Manufacturer/ Model Number	Supplier	Use
3D rocker	Gyrotwister	Fisher Scientific UK, Ltd	Release assay
Automatic tissue processor	Leica TP1020	Leica Microsystems (UK) Ltd	Tissue prep
Balance	Mettler Toledo AB-5	Fisher Scientific UK, Ltd	General
Centrifuge	MSE Mistral 1000	Scientific Laboratory Supplies Ltd	General
Centrifuge	Sigma 2-16K	Scientific Laboratory Supplies Ltd	Cell culture
Safety cabinet	Class II Biomat 2	Thermo Electron Corporation	Cell culture
Freeze drier	Edwards Modulyo D	IMA Edwards, UK	MP Preparation
Freezer	LabCold	Fisher Scientific UK, Ltd	Storage
Fume hood	Mach-Aire Classic FC	Mach-Aire Ltd	MP Preparation
GPC	PL-GPC-120	Polymer labs	MP Mwt
High shear mixer	Silverson L5M	Silverson machines, UK	MP Preparation
Hotplate	Yellow line MST Basic C	Fisher Scientific UK, Ltd	General
Incubator	Sanyo MCO-17A1C	Scientific Laboratory Supplies Ltd	Cell culture
Injector	Eppendorf Femtojet	VWR International	Defect filling
Magnetic stirrer - multiway	Variomag	Thermo Scientific, Uk	MP preparation
Magnetic stirrer - single	IKA Big squid	Fisher Scientific UK, Ltd	General
Microcentrifuge	Spectrafuge 24D Labnet Inc	Scientific Laboratory Supplies Ltd	Release assay
Microscope	Nikon EclipseTS100	Nikon	Imaging cells
Microtome	Leica RM2165	Leica Microsystems (UK) Ltd	Sectioning
Mill	Krups 75	Amazon.co.uk	MP preparation

Equipment	Manufacturer/ Model Number	Supplier	Use
Orbital shaker	IKA MTS 4	Scientific Laboratory Supplies Ltd	General
Oven	Binder	Scientific Laboratory Supplies Ltd	General
Particle sizer	Coulter LS230	Beckman Coulter, UK	MP sizing
pH meter	Mettler Toledo Seven easy	Scientific Laboratory Supplies Ltd	pH readings
Plate reader	Tecan Infinite M200	Tecan UK Ltd, UK	Assay reading
Refrigerator	LabCold	Fisher Scientific UK, Ltd	Storage
Refrigerator for eggs	Liebherr Profiline	Leibherr GB Ltd	Eggs storage
Rheometer	Physica MCR 301	Anton Paar, UK	Tg determination
Scanning electron microscope	JSM 6060LV	Jeol, UK	MP imaging
Sputter coater	SCD 030	Balzars, Lichtenstein	MP gold coating
Steromicroscope	Leica M216F	Leica Microsystems (UK) Ltd	Bone imaging
Camera	Qimaging Q17837		
Vacuum packer	Orvid VM03	Scientific Laboratory Supplies Ltd	General
Vacuum pump	Charles Austin B100 SEC	Scientific Laboratory Supplies Ltd	General
Vortex mixer	Stuart Scientific SA8	Scientific Laboratory Supplies Ltd	General
Wax embedder	Leica EG1160	Leica Microsystems (UK) Ltd	Embedding
Woven mesh sieves	100, 200 micron	Scientific Laboratory Supplies Ltd	Sieving

Table A2 Consumables inventory

Consumables	Specification/ Catalogue Number	Supplier	Use
Beakers	20 -500 ml	Fisher Scientific UK, Ltd, UK	General
Bijou bottles (7 ml)	CON 7524	Scientific Laboratory Supplies Ltd	General
Centrifuge tubes (15/50 ml)	15 ml 188261 50 ml 227270	Greiner Bio One	Release assays
Filter paper (Grade 1)	Z240095	Scientific Laboratory Supplies Ltd	Femur dissection
Filter units (0.2 µm)	FIL6570	Scientific Laboratory Supplies Ltd	MP preparation
Fine forceps	Dumont Size 5	Scientific Laboratory Supplies Ltd	Femur dissection
Glass followers (50 mm)	FB55626	Fisher Scientific UK, Ltd, UK	MP preparation
Glass scintillation vials	VGA-050-300P	Fisher Scientific UK, Ltd, UK	MP preparation
Laboratory blue roll	CMC 790-011L	Fisher Scientific UK, Ltd, UK	General/MP prep
Micro drill bit (300 µm)	Guhring 300 µm	Cromwell	Femur defect
Micro spatulas (0.1-1 mm)	FB70365	Fisher Scientific UK, Ltd, UK	Filling defect
Microcentrifuge tubes (1.6 ml)	72.690	Sarstedt Ltd	Release assays
Millicell inserts	Millipore FDR-541-020X	Fisher Scientific UK, Ltd, UK	Femur culture
Multichannel pipette (20-200 µl)	F14401	Scientific Laboratory Supplies Ltd	BCA assays
Parafilm	SEL0400030P	Fisher Scientific UK, Ltd, UK	General
Pasettes (3 ml)	FB55348	Scientific Laboratory Supplies Ltd	Release assays
Pipette filler	FB69000	Fisher Scientific UK, Ltd, UK	General
Pipette tips (all sizes)	FR1200/1250/1015	Alpha Laboratories	General
Pipettes (20-200, 100- 1000 µl)	S1122-18301/8810C	Starlab (UK) Ltd	General
Pipettes glass (5 ml)	12314388	Fisher Scientific UK, Ltd, UK	DCM pipetting
Pipettes plastic (5, 10 ml)	TVK-671- 040Q/050N	Fisher Scientific UK, Ltd, UK	General
PTFE scaffold moulds	Mechanical engineering unit. University of Nottingham		Scaffold preparation
PTFE screw cap jar	FB58832	Fisher Scientific UK, Ltd, UK	MP preparation
PTFE sheet	Bako-glide	Amazon UK	MP preparation
Pulled capillaries	Supplied by Human Development Unit. University of Nottingham		Micro-injection

Consumables	Specification/ Catalogue Number	Supplier	Use
Scalpel	SCA-310-150A	Fisher Scientific UK, Ltd, UK	Chick dissection
Sealable bags	BAG 1018/20/26/28	Scientific Laboratory Supplies Ltd	General storage
Syringes	SZR 150-041H	Fisher Scientific UK, Ltd, UK	General
Tissue culture flasks	Nunc178905/178883	Fisher Scientific UK, Ltd, UK	Cell culture
Tissue culture plates	Nunc 96/24/6 well	Fisher Scientific UK, Ltd, UK	Cell assays
Wax embedding cassettes and base moulds	380308E – base 14039441100 - cassette	Leica Microsystems	Wax embedding

Table A3 Chemical/reagents inventory

Chemical/ Reagent	Specification/ Catalogue Number	Supplier	Use
Acetone	A/0560/17	Fisher Scientific UK, Ltd, UK	General
Alcian blue 8G	400460100	Acros Organics	Staining
Alpha MEM	BE12-169F	Sigma-Aldrich, UK	Femur culture
Antibiotic antimycotic solution	A5955 – 100 ml	Sigma-Aldrich, UK	Cell culture
Ascorbic acid	A4403	Sigma-Aldrich, UK	Femur culture
Bicinchoninic assay kit	Pierce 23235	Fisher Scientific UK, Ltd, UK	Protein assay
BMP-2 ELISA kit	DBP-200	R and D Systems Europe Ltd, UK	BMP-2 detection
rhBMP-2	Professor Walter Sebald (University of Wurzburg, Germany)		Growth factor
Collagenase type 1A	C5894	Sigma-Aldrich, UK	mPCC isolation
Dichloromethane	D/1856/17	Fisher Scientific UK, Ltd, UK	MP preparation
Dimethylsulphoxide	D-5879	Sigma-Aldrich, UK	Protein assay
Distilled water	In-house supply		General
DL Lactide	9026	Lancaster Synthesis	TB Preparation
DMEM	VX42430025	Sigma-Aldrich, UK	Cell culture
DPX mountant	D/5319/05	Fisher Scientific UK, Ltd, UK	Slide preparation
Ethanol	E/0650DF/17	Fisher Scientific UK, Ltd, UK	Histology
FCS			Cell culture
Fertile eggs	Dekalb White	Henry Stewart (Medegg)	Embryo development
L-Glutamine	G7513	Sigma-Aldrich, UK	mPCC isolation
Glycolide	Purasorb G	Purac, Netherlands	TB preparation
Hexane	H/0406/17	Fisher Scientific UK, Ltd, UK	Histology
Histoclear	717969-1	Scientific Laboratory Supplies Ltd	Histology
Human serum albumin	A9511	Sigma-Aldrich, UK	MP preparation
Industrial methylated spirits	M/4400/17	Fisher Scientific UK, Ltd, UK	Cleaning general
Liquid nitrogen	Cryospeed	BOC Industrial gases	Snap freezing MPs
Lysozyme	L-6876	Sigma-Aldrich, UK	Model protein
Micrococcus lysodekticus	M-3770	Sigma-Aldrich, UK	Lysozyme activity
Paraformaldehyde	158127	Sigma-Aldrich, UK	Tissue fixing

Chemical/ Reagent	Specification/ Catalogue Number	Supplier	Use
Penicillin/Streptomycin	Invitrogen VX15070063	Fisher Scientific UK, Ltd, UK	Femur culture
Phosphate buffered saline	BPE9739-1	Fisher Scientific UK, Ltd, UK	Release assay
Phosphmolybdic acid	221856	Sigma-Aldrich, UK	Histology
Poly (DL lactic-co- glycolic) acid 50 50	LX00279-133 Mw 59 kDa IV 0.45 dL/g LX00195-63 Mw 62kDa IV 0.46 dL/g LX00414-125 Mw 56 KDa IV 0.44 dL/g	Evonik Industries, Birmingham, Al, USA	MP preparation
Poly (DL lactic-co- glycolic) acid 85 15	LP421 Mw 53 kDa IV 0.40 dL/g LX00195-135 Mw 56 KDa IV 0.43 dL/g LP546 Mw 52 KDa IV 0.40 dL/g LP671 Mw 50 KDa IV 0.40 dL/g		
Poly vinyl alcohol (87- 89% hydrolysed)	363170	Sigma-Aldrich, UK	MP preparation
Polyethylene glycol 400	PEG400	Clariant SE, UK	MP preparation
Polyethylene glycol 1500	81210	Sigma-Aldrich, UK	TB preparation
Polyethylene glycol 6000	81260	Sigma-Aldrich, UK	Micronisation
SigmaFast pNPP kit	N-2770	Sigma-Aldrich, UK	ALP activity
Silver nitrate	S-6506	Sigma-Aldrich, UK	Von Kossa
Sirius red	365548	Sigma-Aldrich, UK	Staining
Sodium carboxymethylcellulose	C4888	Sigma-Aldrich, UK	Scaffold preparation
Sodium dodecyl sulphate	L-3771	Sigma-Aldrich, UK	Protein assay
Sodium hydroxide	467176	Sigma-Aldrich, UK	Protein assay
Stannous octoate/Tin (II) 2-ethylhexanoate	S-3252	Sigma-Aldrich, UK	TBP preparation
Sodium thiosulphate	13481	Sigma-Aldrich, UK	Von Kossa
Trypsin II	T7409	Sigma-Aldrich, UK	mPCC isolation
Trypsin/EDTA			Cell culture
Weigerts haematoxylin	HT1079	Sigma-Aldrich, UK	Histology

Appendix II: MP Batch manufacturing record

<i>BATCH NO</i>	<i>PLGA Type (Lot No)</i>	<i>Triblock</i>	<i>Protein</i>	<i>PLGA %</i>	<i>Homogeniser Speed (rpm)</i>	<i>Vortex Speed</i>
BN 01	85 15 lp421	none	none	20	9000	N/A
BN 02	85 15 lp421	none	none	20	9000	N/A
BN 03	85 15 lp421	none	none	20	9000	N/A
BN 04	85 15 lp421	none	none	20	19000	N/A
BN 05	85 15 lp421	none	none	20	19000	N/A
BN 06	85 15 lp421	none	none	20	19000	N/A
BN 07	85 15 lp421	none	none	20	9000	N/A
BN 08	85 15 lp421	none	none	20	9000	N/A
BN 09	85 15 lp421	none	none	20	9000	N/A
BN 10	85 15 lp421	none	none	20	19000	N/A
BN 11	85 15 lp421	none	none	20	19000	N/A
BN 12	85 15 lp421	none	none	20	19000	N/A
BN 13	85 15 lp421	none	none	2	19000	N/A
BN 14	85 15 lp421	none	none	2	19000	N/A
BN 15	85 15 lp421	none	none	2	19000	N/A
BN 16	85 15 lp421	none	none	2	N/A	2000
BN 17	85 15 lp421	none	none	2	N/A	2000
BN 18	85 15 lp421	none	none	20	N/A	2000
BN 19	85 15 lp421	none	none	20	N/A	2000
BN 20	85 15 lp421	none	none	20	500	N/A
BN 21	85 15 lp421	none	none	20	500	N/A
BN 22	85 15 lp421	none	none	20	1000	N/A
BN 23	85 15 lp421	none	none	20	1000	N/A
BN 24	85 15 lp421	none	none	20	2000	N/A
BN 25	85 15 lp421	none	none	20	2000	N/A
BN 26	85 15 lp421	none	none	20	1000	N/A
BN 27	85 15 lp421	none	none	20	2000	N/A
BN 28	85 15 lp421	none	none	20	3000	N/A
BN 29	85 15 lp421	none	none	20	9000	N/A
BN 30	85 15 lp421	none	none	2	24000	N/A
BN 31	85 15 lp421	none	none	2	24000	N/A
BN 32	85 15 lp421	none	none	2	24000	N/A
BN 33	85 15 lp421	none	none	2	24000	N/A
BN 34	85 15 lp421	none	none	2	24000	N/A
BN 35	85 15 lp421	none	none	2	24000	N/A
BN 36	85 15 lp421	none	none	2	11000	N/A
BN 37	85 15 lp421	none	none	2	11000	N/A
BN 38	85 15 lp421	none	none	2	11000	N/A
BN 39	50 50 lx195-63	none	1% HSA	18	4000/2000	N/A
BN 40	50 50 lx195-63	none	2% HSA	18	4000/2000	N/A
BN 41	50 50 lx195-63	none	1% HSA	20	9000/9000	N/A
BN 42	50 50 lx195-63	none	2% HSA	20	9000/9000	N/A
BN 43	50 50 lx195-63	none	1% HSA	10	4000/9000	N/A
BN 44	50 50 lx195-63	none	2% HSA	10	4000/9000	N/A
BN 45	50 50 lx195-63	none	1% HSA	10	9000/9000	N/A
BN 46	50 50 lx195-63	none	2% HSA	10	9000/9000	N/A
BN 47	50 50 lx195-63	none	1% HSA	2	4000/9000	N/A
BN 48	50 50 lx195-63	none	1% HSA	2	4000/9000	N/A
BN 49	50 50 lx195-63	none	1% HSA	2	9000/9000	N/A
BN 50	50 50 lx195-63	none	2% HSA	2	9000/9000	N/A
BN 51	50 50 lx195-63	none	1% HSA	20	9000/19000	N/A
BN 52	50 50 lx195-63	none	2% HSA	20	9000/19000	N/A
BN 53	85 15 lp421	none	none	2	N/A	N/A
BN 54	85 15 lp421	none	none	2	N/A	N/A
BN 55	85 15 lp421	none	none	2	9000	N/A
BN 56	85 15 lp421	none	none	2	9000	N/A
BN 57	85 15 lp421	none	none	2	9000	N/A
BN 58	85 15 lp421	none	none	2	24000	N/A
BN 59	85 15 lp421	none	none	2	24000	N/A
BN 60	85 15 lp421	none	none	2	24000	N/A
BN 61	50 50 lx195-63	none	0%	2	9000/9000	N/A
BN 62	50 50 lx195-63	none	1% HSA	2	9000/9000	N/A
BN 63	50 50 lx195-63	none	0.9% HSA 0.1% Lyso	2	9000/9000	N/A
BN 64	50 50 lx195-63	none	0%	2	9000/9000	N/A
BN 65	50 50 lx195-63	none	10% HSA	2	9000/9000	N/A
BN 66	50 50 lx195-63	none	0.9% HSA 0.1% Lyso	2	9000/9000	N/A
BN67	85 15 lp421	none	none	20	9000	N/A
BN68	85 15 lp421	none	none	15	9000	N/A

Appendices

BATCH NO	PLGA Type (Lot No)	Triblock	Protein	PLGA %	Homogeniser Speed (rpm)	Vortex Speed
BN69	50 50 lx195-63	none	5% lyso/6k PEG	20	2000	N/A
BN70	50 50 lx195-63	none	5% lyso/6k PEG	20	2000	N/A
BN71	50 50 lx195-63	none	5% lyso/6k PEG	20	2000	N/A
BN72	50 50 lx195-63	none	5% lyso/6k PEG	20	2000	N/A
BN73	50 50 lx195-63	30% TB2-B	5% lyso/6k PEG	20	2000	N/A
BN74	50 50 lx195-63	none	5% lyso/6k PEG	18	9000	N/A
BN75	50 50 lx195-63	none	5% lyso/6k PEG	18	9000	N/A
BN76	50 50 lx195-63	30% TB2-B	5% lyso/6k PEG	18	9000	N/A
BN77	85 15 LP421	none	6KPEG only	10	9000	N/A
BN78	85 15 LP421	none	6KPEG only	15	2000	N/A
BN79	50 50 lx279-133	none	6KPEG only	20	N/A	2000
BN80	50 50 lx279-133	none	5% lyso/6k PEG	20	N/A	2000
BN81	50 50 lx279-133	none	5% lyso/6k PEG	20	N/A	2000
BN82	50 50 lx279-133	none	6KPEG only	20	2000	N/A
BN83	50 50 lx279-133	none	5% lyso/6k PEG	20	2000	N/A
BN84	50 50 lx279-133	none	5% lyso/6k PEG	20	2000	N/A
BN85	50 50 lx195-63	none	5% lyso/6k PEG	20	N/A	2000
BN86	50 50 lx195-63	none	6KPEG only	20	N/A	2000
BN87	50 50 lx195-63	none	1% lyso/4% HSA/ PEG	20	N/A	2000
BN88	50 50 lx195-63	none	6KPEG only	20	N/A	2000
BN89	50 50 lx195-63	10% TB2-B	5% lyso/6k PEG	20	N/A	2000
BN90	50 50 lx195-63	10% TB2-B	6KPEG only	20	N/A	2000
BN91	50 50 lx195-63	none	none (H2O)	20	2000/2000	N/A
BN92	50 50 lx195-63	none	1% Lysozyme	20	2000/2000	N/A
BN93	50 50 lx195-63	none	none (H2O)	20	4000/2000	N/A
BN94	50 50 lx195-63	none	1% Lysozyme	20	4000/2000	N/A
BN95	50 50 lx195-63	none	none (H2O)	20	4000/2000	N/A
BN96	50 50 lx195-63	none	5% lysozyme	20	4000/2000	N/A
BN97	50 50 lx279-133	none	48mg HSA 0.8mg Lyso 268 mg PEG	20	2000	N/A
BN98	50 50 lx279-133	none	50 mg HSA 0.85 mg Lyso 280 mg PEG	20	2000	N/A
BN99	50 50 lx279-133	none	49 mg HSA 1 mg Lyso 400 mg PEG	20	2000	N/A
BN100	50 50 lx279-133	none	50 mg lyso 60 mg PEG	20	2000	N/A
BN101	50 50 lx279-133	none	50 mg lyso 400 mg PEG	20	2000	N/A
BN102	50 50 lx279-133	none	50 mg HSA 400 mg PEG	20	2000	N/A
BN103	50 50 lx279-133	none	400 mg PEG	20	2000	N/A
BN104	50 50 lx279-133	none	48mg HSA 0.8mg Lyso 268 mg PEG	20	2000	N/A
BN105	50 50 lx279-133	none	50 mg HSA 0.85 mg Lyso 280 mg PEG	20	2000	N/A
BN106	50 50 lx279-133	none	49 mg HSA 1 mg Lyso 400 mg PEG	20	2000	N/A
BN107	50 50 lx279-133	none	50 mg lyso 60 mg PEG	20	2000	N/A
BN108	50 50 lx279-133	none	50 mg lyso 400 mg PEG	20	2000	N/A
BN109	50 50 lx279-133	none	50 mg HSA 400 mg PEG	20	2000	N/A
BN110	50 50 lx279-133	none	400 mg PEG	20	2000	N/A
BN111	85 15 lp225	0.3 g	50 mg Lyso and 60 mg PEG	20	2000	N/A
BN112	85 15 lp225	0.1g	50 mg Lyso and 60 mg PEG	20	2000	N/A
BN113	85 15 lp225	0.3 g	50 mg Lyso and 60 mg PEG	20	2000	N/A
BN114	85 15 lp225	0.1 g	50 mg Lyso and 60 mg PEG	20	2000	N/A
BN115	50 50 lx279-133	none	none (H2O)	20	4000/2000	N/A
BN116	50 50 lx279-133	none	0.9% HSA 0.1% Lyso	20	4000/2000	N/A
BN117	50 50 lx279-133	none	4.5% HSA 0.5% Lyso	20	4000/2000	N/A
BN118	50 50 lx279-133	none	none (H2O)	20	4000/2000	N/A
BN119	50 50 lx279-133	none	5% Lyso	20	4000/2000	N/A
BN120	50 50 lx279-133	none	4.5% HSA 0.5% Lyso	20	4000/2000	N/A
BN121	50 50 lx279-133	none	none (H2O)	20	4000/2000	N/A
BN122	50 50 lx279-133	none	none (H2O)	20	4000/2000	N/A
BN123	50 50 lx279-133	none	0.9% HSA 0.1% Lyso	20	4000/2000	N/A
BN124	50 50 lx279-133	10% TB2-B	none (H2O)	20	4000/2000	N/A
BN125	50 50 lx279-133	10% TB2-B	0.9% HSA 0.1% Lyso	20	4000/2000	N/A
BN126	50 50 lx279-133	30% TB2-B	none (H2O)	20	4000/2000	N/A
BN127	50 50 lx279-133	30% TB2-B	0.9% HSA 0.1% Lyso	20	4000/2000	N/A
BN128	85 15 lx195-135	none	none (H2O)	20	4000/2000	N/A
BN129	85 15 lx195-135	none	0.9% HSA 0.1% Lyso	20	4000/2000	N/A
BN130	85 15 lx195-135	10% TB2-B	none (H2O)	20	4000/2000	N/A
BN131	85 15 lx195-135	10% TB2-B	0.9% HSA 0.1% Lyso	20	4000/2000	N/A
BN132	85 15 lx195-135	30% TB2-B	none (H2O)	20	4000/2000	N/A
BN133	85 15 lx195-135	30% TB2-B	0.9% HSA 0.1% Lyso	20	4000/2000	N/A

Appendices

BATCH NO	PLGA Type (Lot No)	Triblock	Protein	PLGA %	Homogeniser Speed (rpm)	Vortex Speed
BN134	50 50 lx279-133	30% TB2-B	0.9% HSA 0.1% Lyso	20	4000/2000	N/A
BN135	50 50 lx279-133	30% TB2-B	0.9% HSA 0.1% Lyso	20	4000/2000	N/A
BN136	50 50 lx279-133	20% TB2-B	0.9% HSA 0.1% Lyso	20	4000/2000	N/A
BN137	50 50 lx279-133	10% TB2-B	0.9% HSA 0.1% Lyso	20	4000/2000	N/A
BN138	50 50 lx279-133	10% TB2-B	0.9% HSA 0.1% Lyso	20	4000/2000	N/A
BN139	50 50 lx279-133	none	0.9% HSA 0.1% Lyso	20	4000/2000	N/A
BN140	85 15 lx195-135	30% TB2-B	0.9% HSA 0.1% Lyso	20	4000/2000	N/A
BN141	50 50 lx279-133	30% TB2-B	0.9% HSA 0.1% Lyso	20	4000/2000	N/A
BN142	50 50 lx279-133	30% TB2-B	0.9% HSA 0.1% Lyso	20	4000/2000	N/A
BN143	50 50 lx279-133	20% TB2-B	0.9% HSA 0.1% Lyso	20	4000/2000	N/A
BN144	50 50 lx279-133	10% TB2-B	0.9% HSA 0.1% Lyso	20	4000/2000	N/A
BN145	50 50 lx279-133	10% TB2-B	0.9% HSA 0.1% Lyso	20	4000/2000	N/A
BN146	50 50 lx279-133	none	0.9% HSA 0.1% Lyso	20	4000/2000	N/A
BN147	85 15 lx195-135	30% TB2-B	0.9% HSA 0.1% Lyso	20	4000/2000	N/A
BN148	50 50 lx279-133	30% TB2-B	0.9% HSA 0.1% Lyso	20	4000/2000	N/A
BN149	50 50 lx279-133	30% TB2-B	0.9% HSA 0.1% Lyso	20	4000/2000	N/A
BN150	50 50 lx279-133	20% TB2-B	0.9% HSA 0.1% Lyso	20	4000/2000	N/A
BN151	50 50 lx279-133	10% TB2-B	0.9% HSA 0.1% Lyso	20	4000/2000	N/A
BN152	50 50 lx279-133	10% TB2-B	0.9% HSA 0.1% Lyso	20	4000/2000	N/A
BN153	50 50 lx279-133	none	0.9% HSA 0.1% Lyso	20	4000/2000	N/A
BN154	85 15 lx195-135	30% TB2-B	0.9% HSA 0.1% Lyso	20	4000/2000	N/A
BN155	50 50 lx279-133	30% TB2-B	none (H2O)	20	4000/2000	N/A
BN156	50 50 lx279-133	20% TB2-B	none (H2O)	20	4000/2000	N/A
BN157	50 50 lx279-133	10% TB2-B	none (H2O)	20	4000/2000	N/A
BN158	50 50 lx279-133	none	none (H2O)	20	4000/2000	N/A
BN159	85 15 lx195-135	30% TB2-B	none (H2O)	20	4000/2000	N/A
BN160	50 50 lx279-133	combined				
BN161	50 50 lx279-133	combined				
BN162	50 50 lx279-133	combined				
BN163	50 50 lx414-125	20% TB2-B	0.9% HSA 0.1% BMP-2	20	4000/2000	N/A
BN164	50 50 lx414-125	20% TB2-B	none (H2O)	20	4000/2000	N/A
BN165	85 15 lx195-135	30% TB2-B	0.9% HSA 0.1% BMP-2	20	4000/2000	N/A
BN166	85 15 lx195-135	30% TB2-B	none (H2O)	20	4000/2000	N/A
BN167	50 50 lx414-125	none	0.9% HSA 0.1% Lyso	20	4000/9000	N/A
BN168	50 50 lx414-125	none	none (H2O)	20	4000/9000	N/A
BN169	50 50 lx414-125	none	0.9% HSA 0.1% Lyso	5	4000/9000	N/A
BN170	50 50 lx414-125	none	none (H2O)	5	4000/9000	N/A
BN171	50 50 lx414-125	none	0.9% HSA 0.1% Lyso	15	4000/9000	N/A
BN172	50 50 lx414-125	none	none (H2O)	15	4000/9000	N/A
BN173	50 50 lx414-125	none	0.9% HSA 0.1% Lyso	10	4000/9000	N/A
BN174	50 50 lx414-125	none	none (H2O)	10	4000/9000	N/A
BN175	50 50 lx414-125	none	0.9% HSA 0.1% Lyso	5	4000/9000	N/A
BN176	50 50 lx414-125	none	none (H2O)	5	4000/9000	N/A
BN177	50 50 lx414-125	none	0.9% HSA 0.1% Lyso	2	4000/9000	N/A
BN178	50 50 lx414-125	none	none (H2O)	2	4000/9000	N/A
BN179	50 50 lx414-125	none	0.9% HSA 0.1% Lyso	20	4000/9000	N/A
BN180	50 50 lx414-125	none	0.45% HSA 0.05% Lyso	20	4000/9000	N/A
BN181	50 50 lx414-125	none	0.09% HSA 0.01% Lyso	20	4000/9000	N/A
BN182	50 50 lx414-125	none	none (H2O)	20	4000/9000	N/A
BN183	50 50 lx414-125	none	0.9% HSA 0.1% Lyso	5	4000/9000	N/A
BN184	50 50 lx414-125	none	0.45% HSA 0.05% Lyso	5	4000/9000	N/A
BN185	50 50 lx414-125	none	0.09% HSA 0.01% Lyso	5	4000/9000	N/A
BN186	50 50 lx414-125	none	none (H2O)	5	4000/9000	N/A
BN187	50 50 lx414-125	none	none (H2O)	20	4000/2000	N/A
BN188	50 50 lx414-125	none	0.045% HSA 0.005% Lyso	20	4000/2000	N/A
BN189	50 50 lx414-125	none	0.09% HSA 0.01% Lyso	20	4000/2000	N/A
BN190	50 50 lx414-125	none	0.45% HSA 0.05% Lyso	20	4000/2000	N/A
BN191	50 50 lx414-125	none	0.9% HSA 0.1% Lyso	20	4000/2000	N/A
BN192	50 50 lx414-125	none	1.8% HSA 0.2% Lyso	20	4000/2000	N/A
BN193	50 50 lx414-125	none	2.7% HSA 0.3% Lyso	20	4000/2000	N/A
BN194	50 50 lx414-125	none	3.6% HSA 0.4% Lyso	20	4000/2000	N/A
BN195	50 50 lx414-125	none	4.5% HSA 0.5% Lyso	20	4000/2000	N/A
BN201	50 50 lx414-125	10% TB2-B	none (H2O)	20	4000/2000	N/A
BN202	85 15 lx195-135	10% TB2-B	0.9% HSA 0.1% Lyso	20	4000/2000	N/A
BN203	85 15 lx195-135	10% TB2-B	0.5% HSA 0.5% Lyso	20	4000/2000	N/A
BN204	85 15 lx195-135	10% TB2-B	0.99% HSA 0.01% Lyso	20	4000/2000	N/A
BN205	85 15 lx195-135	10% TB2-B	no protein	20	4000/2000	N/A
BN216	50 50 lx 414-125	none	0.99% HSA 0.01% Lyso	5	4000/9000	N/A
BN217	50 50 lx 414-125	none	no protein	5	4000/9000	N/A
BN230	50 50 lx 414-125	10% TB2-C	no protein	20	4000/9000	N/A
BN231	50 50 lx 414-125	10% TB2-C	0.9 % HSA and 0.1% lyso	20	4000/9000	N/A

<i>BATCH NO</i>	<i>PLGA Type (Lot No)</i>	<i>Triblock</i>	<i>Protein</i>	<i>PLGA %</i>	<i>Homogeniser Speed (rpm)</i>	<i>Vortex Speed</i>
BN232	50 50 lx 414-125	20% TB2-C	no protein	20	4000/9000	N/A
BN233	50 50 lx 414-125	20% TB2-C	0.9 % HSA and 0.1% lyso	20	4000/9000	N/A
BN234	50 50 lx 414-125	30% TB2-C	no protein	20	4000/9000	N/A
BN235	50 50 lx 414-125	30% TB2-C	0.9 % HSA and 0.1% lyso	20	4000/9000	N/A
BN236	85 15 lx195-135	10% TB2-C	0.9% HSA 0.1% Lyso	20	4000/2000	N/A
BN237	85 15 lx195-135	10% TB2-C	0.99% HSA 0.01% Lyso	20	4000/2000	N/A
BN238	85 15 lx195-135	10% TB2-C	no protein	20	4000/2000	N/A
BN242	50 50 lx 414-125	20% TB2-C	no protein	20	4000/9000	N/A
BN243	50 50 lx 414-125	10% TB2-C	0.99% HSA 0.01% BMP-2	20	4000/9000	N/A
BN244	50 50 lx 414-125	30% TB2-C	no protein	20	4000/9000	N/A
BN245	50 50 lx 414-125	30% TB2-C	0.99% HSA 0.01% BMP-2	20	4000/9000	N/A
BN246	50 50 lx 414-125	20% TB2-C	no protein	20	4000/2000	N/A
BN247	50 50 lx 414-125	20% TB2-C	0.99% HSA 0.01% Lyso	20	4000/2000	N/A
BN248	85 15 lx195-136	30% TB2-C	no protein	20	4000/2000	N/A
BN249	85 15 lx195-136	30% TB2-C	0.99% HSA 0.01% Lyso	20	4000/2000	N/A
BN250	50 50 lx 414-125	20% TB2-C	no protein	20	4000/2000	N/A
BN258	85 15 lx195-136	10% TB2-C	0.9 % HSA and 0.1% BMP	20	4000/2000	N/A
BN259	85 15 lx195-136	10% TB2-C	no protein	20	4000/2000	N/A
BN260	50 50 lx 414-125	10% TB2-C	0.9 % HSA and 0.1% BMP	20	4000/2000	N/A
BN261	50 50 lx 414-125	10% TB2-C	no protein	20	4000/2000	N/A
BN271	85 15 LP546	none	no protein	25	4000/2000	
BN272	85 15 LP546	none	no protein	20	4000/2000	
BN273	85 15 LP546	none	no protein	25	N/A	2500
BN274	85 15 LP546	none	no protein	20	N/A	2500
BN275	85 15 LP546	none	no protein	25	N/A	2500
BN276	85 15 LP546	none	no protein	25	N/A	2500
BN277	85 15 LP546	none	no protein	25	N/A	2500
BN278	85 15 LP546	none	no protein	25	N/A	2500
BN279	50 50 lx 414-125	10% TB2-C	0.99 % HSA 0.01% BMP-2	20	4000/2000	N/A
BN280	50 50 lx 414-125	10% TB2-C	0.995 % HSA 0.005% BMP	20	4000/2000	N/A
BN281	50 50 lx 414-125	10% TB2-C	0.9975 HSA 0.0025% BMP	20	4000/2000	N/A
BN282	50 50 lx 414-125	10% TB2-C	no protein	20	4000/2000	N/A
BN288	85 15 LP546	none	no protein	20	N/A	2500
BN297	85 15 LP546	none	no protein	20	N/A	2500
BN298	50 50 lx 414-125	none	no protein	20	4000/2000	N/A
BN299	50 50 lx 414-125	none	4.5% HSA 0.5% Lyso	20	4000/2000	N/A
BN312	50 50 lx 414-125	10% TB2-F	no protein	20	4000/9000	N/A
BN313	50 50 lx 414-125	10% TB2-F	0.9% HSA 0.1% Lyso	20	4000/9000	N/A
BN314	50 50 lx 414-125	10% TB2-F	0.99% HSA 0.01% BMP-2	20	4000/9000	N/A
BN315	50 50 lx 414-125	30% TB2-F	None	20	9000	N/A
BN331	50 50 lx 414-125	10% TB2-F	0.95% HSA 0.05% BMP-2	20	4000/9000	N/A
BN332	50 50 lx 414-125	10% TB2-F	no protein	20	4000/9000	N/A
BN337	50 50 lx 414-125	10% TB2-F	0.95% HSA 0.05% BMP-2	20	4000/9000	N/A
BN341	50 50 lx 414-125	10% TB2-F	no protein	20	4000/9000	N/A
BN342	85 15 LP671	20% TB2-F	0.9% HSA 0.1% BMP-2	20	4000/2000	N/A
BN343	85 15 LP671	20% TB2-F	no protein	20	4000/2000	N/A
BN344	50 50 lx 414-125	10% TB2-F	0.9% HSA 0.1% BMP-2	20	4000/2000	N/A
BN345	50 50 lx 414-125	10% TB2-F	no protein	20	4000/2000	N/A
BN346	50 50 lx 414-125	30% TB2-F	0.9% HSA 0.1% BMP-2	20	4000/2000	N/A
BN347	50 50 lx 414-125	30% TB2-F	no protein	20	4000/2000	N/A
BN348	50 50 lx 414-125	10% TB2-F	0.95% HSA 0.05% BMP-2	20	4000/9000	N/A
BN349	50 50 lx 414-125	30% TB2-F	Blank	20	4000/2000	N/A

Appendix III: Reagents for tissue processing and histological stainingAutomated tissue processor reagents and incubation times

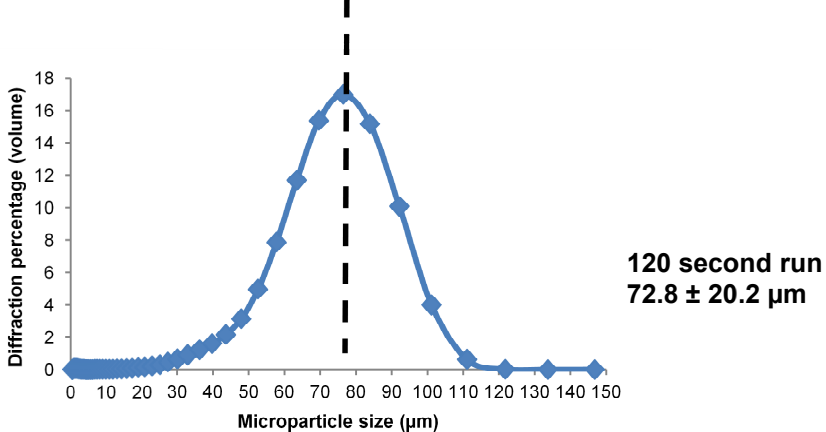
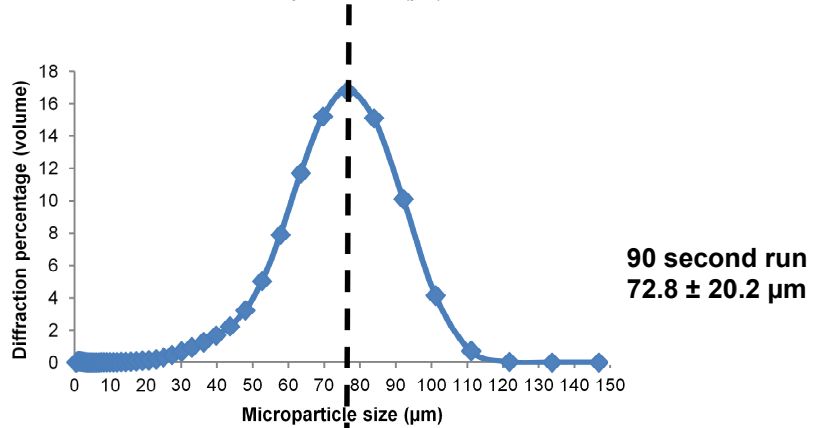
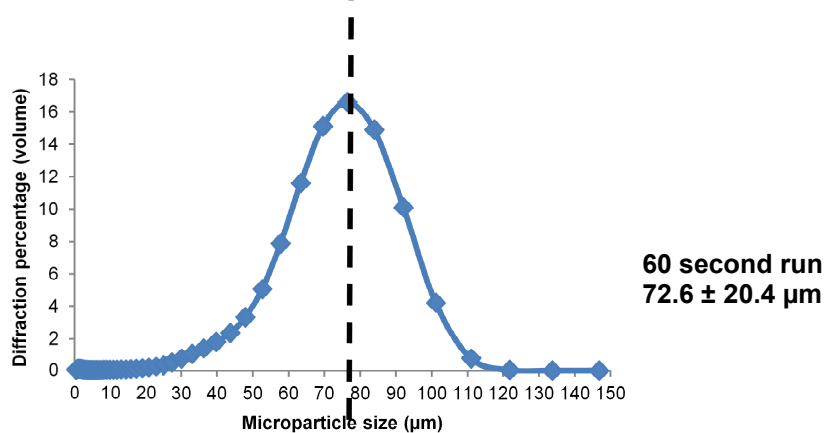
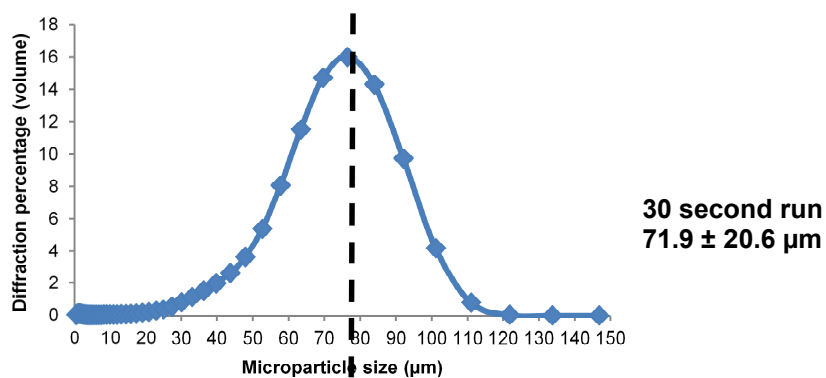
1:	25 % Ethanol in H ₂ O	1 hr 5 min
2:	50 % Ethanol in H ₂ O	1 hr 5 min
3:	75 % Ethanol in H ₂ O	1 hr 5 min
4:	96 % Ethanol in H ₂ O	1 hr 5 min
5:	100% Ethanol	1 hr 5 min
6:	100% Ethanol	1 hr 5 min
7:	Hexane	2 hr
8:	Hexane	2 hr
9:	Paraffin wax	2 hr
10:	Paraffin wax	2 hr

Manufacture of reagents required for alcian blue and picrosirius red staining

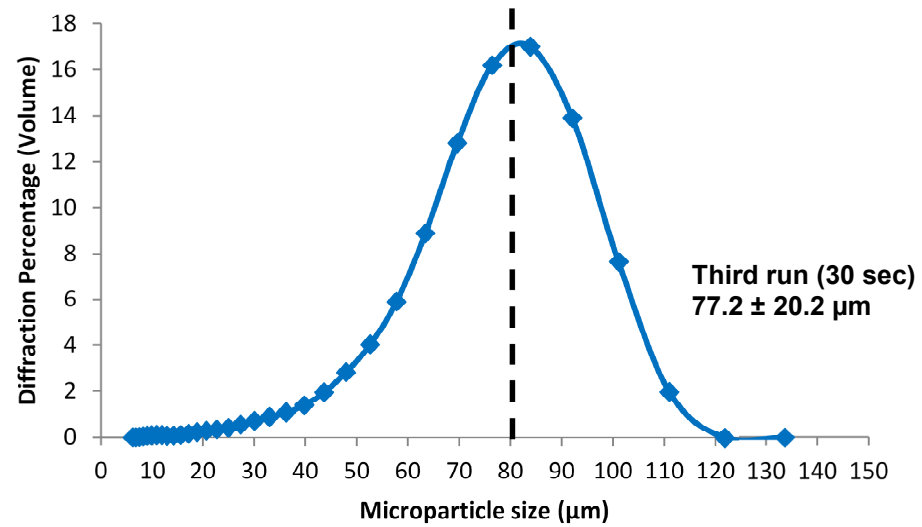
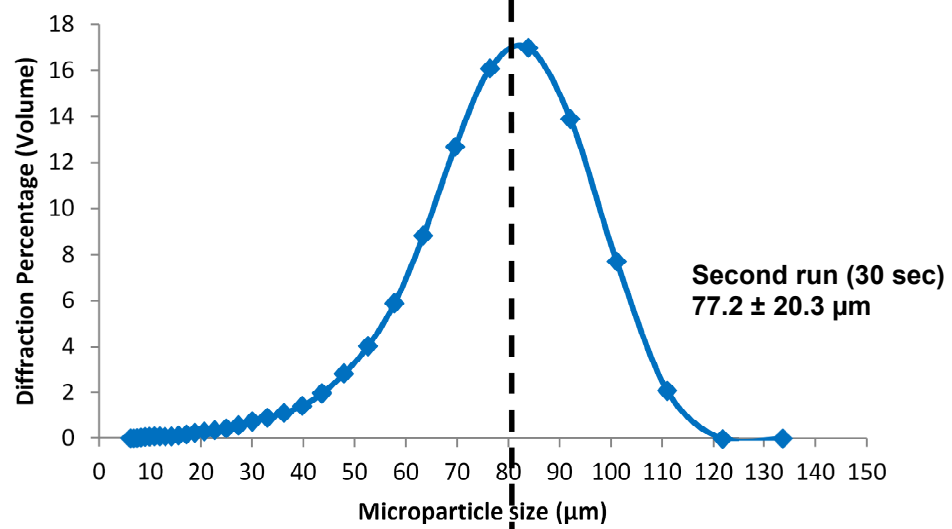
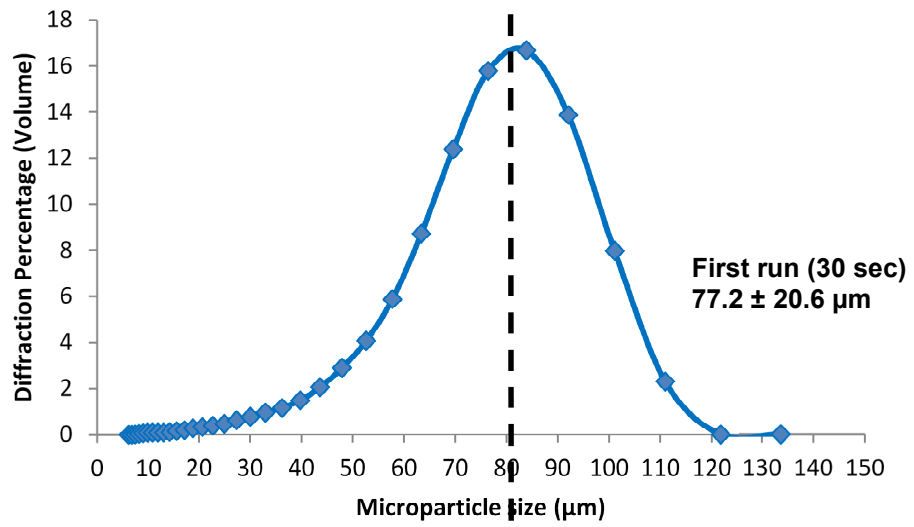
Alcian Blue	1.5 g alcian blue 8G 300 ml distilled water 3 ml acetic acid
Phosphomolybdic acid	3 g Phosphomolybdic acid 300 ml distilled water
Picrosirius red F3B	0.3 g picrosirius red F3B 100 ml saturated picric acid 200 ml distilled water 300 ml methanol (50% v/v) 3 ml hydrochloric acid

Appendix IV: Optimisation of MP size analysis (Coulter L5M)

A. Effect of run time on MPs size



B. Variability between multiple runs



All Coulter measurements in this thesis were shown as one 30 second measurement

Appendix V: Gel permeation chromatography (GPC) and nuclear magnetic resonance (NMR) for triblock copolymers

All analyses performed by Natasha Birkin, School of Chemistry, University of Nottingham

Cirrus GPC Sample Injection Report

04 March 2011 13:14

Batch Name: Lisa

Acquired: 04/03/2011 12:16:15

Sample Name: Triblock B

Workbook: C:\Cirrus Workbooks\GPC 120 - THF ONLY - 24-JAN-2011\GPC 120 - THF ONLY -

Filename: C:\Cirrus Workbooks\GPC 120 - THF ONLY - 24-JAN-2011\lisa-0002.cgrm

Eluent: THF

Flow Rate: 1.00 ml/min

Analysis Using Method: GPC 120 - THF ONLY - 24-JAN-2011

Comments:

Results File: C:\Cirrus Workbooks\GPC 120 - THF ONLY - 24-JAN-2011\lisa-0002.rst

Calibration Used: 26/01/2011 11:35:22

Calibration Type: Narrow Standard

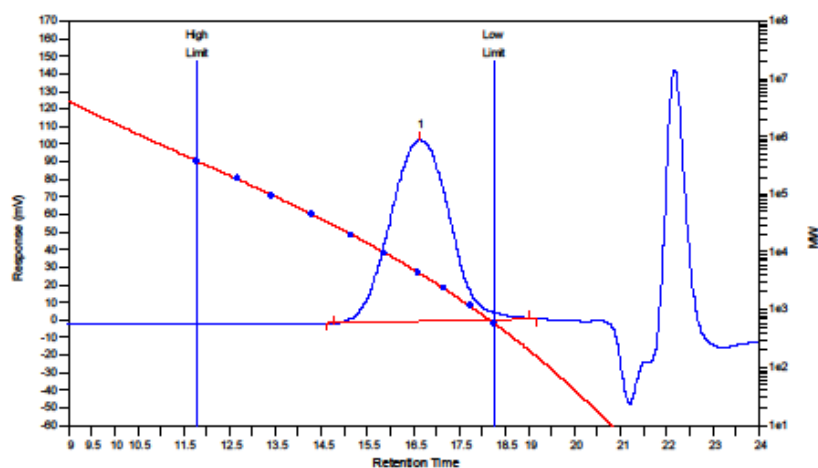
Curve Fit Used: 3

High Limit MW RT: 11.78 mins

Low Limit MW RT: 18.25 mins

High Limit MW: 381479

Low Limit MW: 588



MW Averages

Peak No	Mp	Mn	Mw	Mz	Mz+1	Mv	PD
1	4250	3317	5202	7328	9610	4915	1.56828

Processed Peaks

Peak No	Name	Start RT (mins)	Max RT (mins)	End RT (mins)	Pk Height (mV)	% Height	Area (mV.secs)	% Area
1		14.77	16.65	19.03	102.961	0	9190.78	100

Cirrus GPC Sample Injection Report

04 March 2011 13:15

Acquired: 04/03/2011 12:43:13

Batch Name: Lisa

Sample Name: Triblock C

Workbook: C:\Cirrus Workbooks\GPC 120 - THF ONLY - 24-JAN-2011\GPC 120 - THF ONLY -

Filename: C:\Cirrus Workbooks\GPC 120 - THF ONLY - 24-JAN-2011\lisa-0003.cgrm

Eluent: THF

Flow Rate: 1.00 ml/min

Analysis Using Method: GPC 120 - THF ONLY - 24-JAN-2011

Comments:

Results File: C:\Cirrus Workbooks\GPC 120 - THF ONLY - 24-JAN-2011\lisa-0003.rst

Calibration Used: 26/01/2011 11:35:22

Calibration Type: Narrow Standard

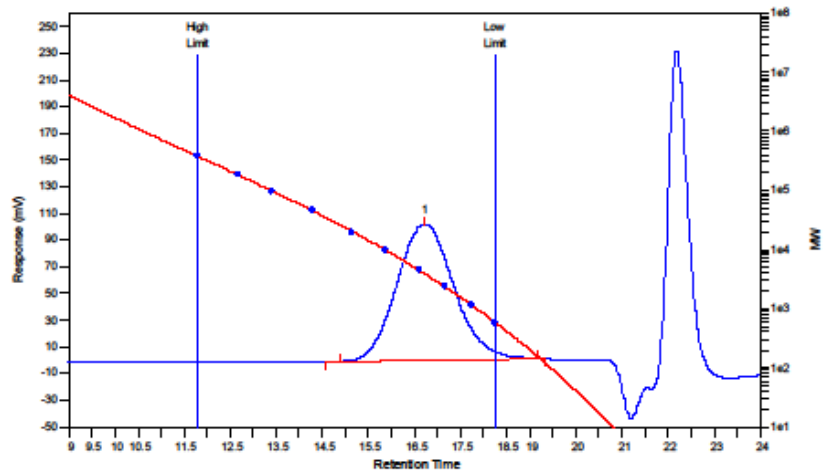
Curve Fit Used: 3

High Limit MW RT: 11.78 mins

Low Limit MW RT: 18.25 mins

High Limit MW: 381479

Low Limit MW: 588



MW Averages

Peak No	Mp	Mn	Mw	Mz	Mz+1	Mv	PD
1	3942	2861	4590	6432	8390	4338	1.60433

Processed Peaks

Peak No	Name	Start RT (mins)	Max RT (mins)	End RT (mins)	Pk Height (mV)	% Height	Area (mV.secs)	% Area
1		14.90	16.72	19.17	102.26	100	8788.59	100

Cirrus GPC Sample Injection Report

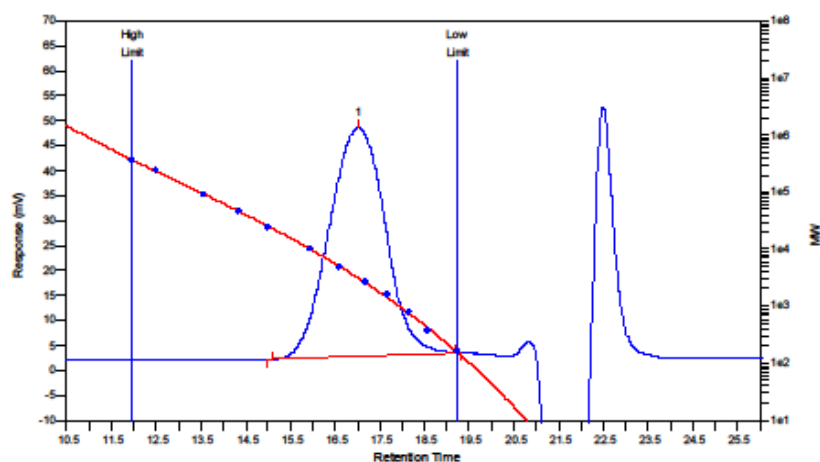
23 June 2011 12:16

Batch Name: Imported
Sample Name: F

Acquired: 23/06/2011 12:12:25

Workbook: C:\Cirrus Workbooks\Natasha Birkin 2011\Natasha Birkin 2011.plw
 Filename: C:\Cirrus Workbooks\Natasha Birkin 2011\imported-0087.cgm
 Eluent: THF Flow Rate: 1.00 ml/min
 Analysis Using Method: PS Standards
 Comments:

Results File: C:\Cirrus Workbooks\Natasha Birkin 2011\imported-0087.rst
 Calibration Used: 11/03/2011 14:17:08
 Calibration Type: Narrow Standard Curve Fit Used: 3
 High Limit MW RT: 11.95 mins Low Limit MW RT: 19.23 mins
 High Limit MW: 375508 Low Limit MW: 154



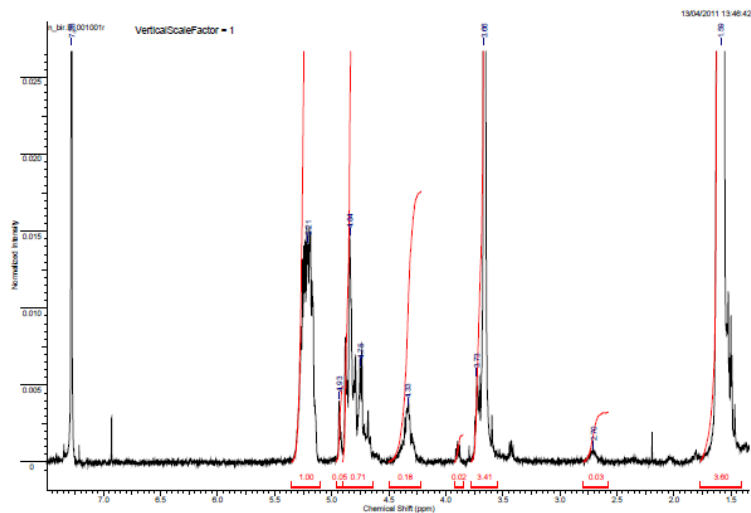
MW Averages

Peak No	Mp	Mn	Mw	Mz	Mz+1	Mv	PD
1	3133	2576	3980	5592	7367	3742	1.53727

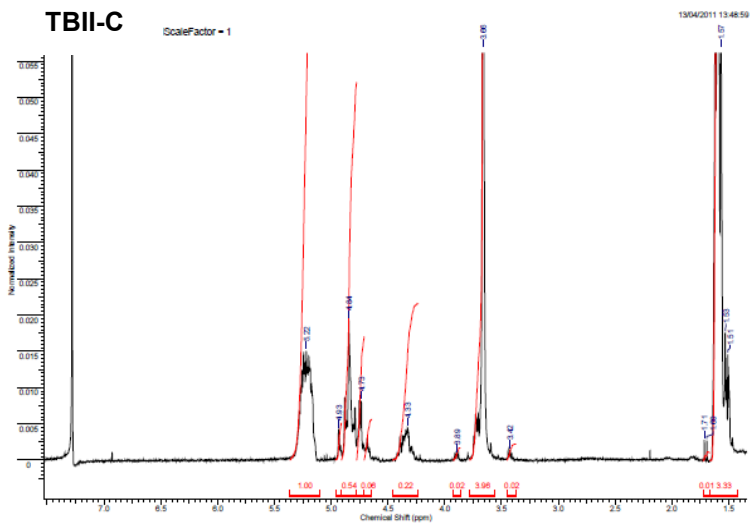
Processed Peaks

Peak No	Name	Start RT (mins)	Max RT (mins)	End RT (mins)	Pk Height (mV)	% Height	Area (mV.secs)	% Area
1		15.08	17.02	19.18	45.8197	100	3972.77	100

TBII-B



TBII-C



TBII-F

